Preparation and Characterization of Polymeric Composite Materials Using Natural Fibers in Bangladesh Environment

A Thesis Submitted to the Department of Applied Chemistry and Chemical Engineering, University of Dhaka, in Partial Fulfilment of the Requirements for the Degree of Doctor of Philosophy (PhD)

May, 2023

SUBMITTED BY

MOST. AFROZA KHATUN

Registration Number: 68/2015-2016, (Re) 105/2019-2020

SUPERVISED BY

DR. HUSNA PARVIN NUR
Ex-Director
BCSIR Laboratories,
Dr. Qudrat-I-Khuda Road,
Dhanmondi, Dhaka-1205.

PROF. DR. A. M. SARWARUDDIN CHOWDHURY
Professor (Grade-1) & Ex-Chairman
Department of Applied Chemistry
and Chemical Engineering,
Faculty of Engineering and Technology,
University of Dhaka, Dhaka 1000.

I dedicate this thesis to my parents and family

CANDIDATE'S DECLARATION

I, Most. Afroza Khatun, Department of Applied Chemistry and Chemical Engineering, University of Dhaka, declare that the research work which is being presented in the PhD thesis, entitled, "**Preparation and Characterization of Polymeric Composite Materials Using Natural Fibers in Bangladesh Environment**" is my own work and carried out by me under the supervision of Prof. Dr. A. M. Sarwaruddin Chowdhury, Professor (Grade-I), Department of Applied Chemistry and Chemical Engineering, Faculty of Engineering and Technology, University of Dhaka, Dhaka-1000, and Dr. Husna Parvin Nur, Ex-Director, Bangladesh Council of Scientific and Industrial Research (BCSIR), Dr. Qudrat-I-Khuda Road, Dhanmondi, Dhaka-1205. The matter embodied in this thesis has not been submitted for the award of any other Degree or Diploma of the university or other institute of higher learning.

…….....

(Most. Afroza Khatun)

SUPERVISOR'S CERTIFICATE

This is to certify that the thesis entitled, "**Preparation and Characterization of Polymeric Composite Materials Using Natural Fibers in Bangladesh Environment**" is being submitted by **Most. Afroza Khatun** to the University of Dhaka, Dhaka-1000 for examination in fulfillment of the requirements for the award of the degree of Doctor of philosophy (PhD) in Applied Chemistry and Chemical Engineering, embodies the original research work carried out by him, registration number: 105/2019-2020 under our joint supervisions and guidance and has not been submitted in part or full for any degree of this or any other university. The work presented in this thesis is true and original.

It is also certified that the candidate **Most. Afroza Khatun** fulfills all the requirements as laid down by the University for the purpose of submission of PhD thesis.

(DR. HUSNA PARVIN NUR)
Ex-Director
BCSIR Laboratories,
Dr. Qudrat-I-Khuda Road,
Dhanmondi, Dhaka-1205.

(PROF. DR. A. M. SARWARUDDIN CHOWDHURY)
Professor (Grade-1) & Ex-Chairman
Department of Applied Chemistry
and Chemical Engineering,
Faculty of Engineering and Technology,
University of Dhaka, Dhaka 1000.

ACKNOWLEDGEMENTS

Acknowledgements

First and foremost, I want to express my gratitude to Almighty Allah, who has always provided me with the assistance I needed. I would like to express my deepest sense of gratitude to my reverend supervisor, Dr. A. M. Sarwaruddin Chowdhury, Professor (Grade-I), Department of Applied Chemistry and Chemical Engineering, Faculty of Engineering and Technology, University of Dhaka, Dhaka-1000. I am grateful to him for choosing me to be a PhD student under his scholastic supervision and for providing great support with his constant guidance, ideas and inspiration for my research work.

I am thankful to my co-supervisor Dr. Husna Parvin Nur, Ex-Director, Bangladesh Council of Scientific and Industrial Research, Dhanmondi, Dhaka-1205, for permitting me to perform my research work in her laboratory. Her guidance and time to time valuable suggestions throughout my study is incomparable.

I would like to sincerely thank to the Chairman of the department and all of the teachers for their excellent ideas and encouragements to make the research work better and more palatable. Thanks to concern authority of University of Dhaka. I am grateful to the Bangladesh University Grant Commission for awarding me the UGC Ph. D fellowship. I am also thankful to Dr. Ruhul Amin Khan, Director, IPRT, Bangladesh Atomic Energy Commission, Savar, Dhaka, for his assistance to do research works. I would like to thank to all members of University of Dhaka, and IPRT Laboratory, Bangladesh Atomic Energy Commission, Savar, Dhaka for their cooperation.

I want to express my gratitude to Shahin Sultana, Principal Scientific Officer, Zahidul Islam, Scientific Officer, Fiber & Polymer Research Division, BCSIR Laboratories, Dhaka, and all other members of Fiber & Polymer Research Division Laboratory (BCSIR), Dhaka in particular for their kind cooperation in completing this research work quickly. If I have forgotten anyone, I apologize.

I am also very indebted to my parents, brothers, husband and beloved son for their cordial cooperation throughout the entire research work.

Finally, I would like to thank to all of my friends, colleagues and well-wishers for their unending inspiration during this dissertation.

……..…….....

(Most. Afroza Khatun)

ABSTRACT

Abstract

Natural fibers have drawn a lot of interest for the use of reinforcing materials in composites as a sustainable and renewable resource. By adopting a compression molding technique and varying fiber contents (5, 10, 15, 20 and 25 wt%), short date palm mat (DPM) fiber reinforced HDPE and polystyrene (PS) composites were prepared. Physical, mechanical, structural, thermal, morphological, and biodegradation properties were examined. 10% DPM fiber reinforced composites exhibited optimum mechanical properties. The DPM fibers were subjected to different percentages of NaOH treatment to enhance the fiber-matrix adhesion. The maximum value of mechanical properties was attained for the composites treated with 5% NaOH. ZnO nanoparticles as nano filler was also used to improve the mechanical properties of the composites. The composites with 3% ZnO nanoparticles showed highest mechanical properties. The produced optimized samples were exposed to various gamma radiation doses, and the results for all types of composites were best when exposed to 5 kGy of gamma radiation. Further, three fire retardant additives namely, monosodium phosphate, monoammonium phosphate and magnesium hydroxide were used in the composites and monoammonium phosphate displayed best fire retardant properties. A biodegradable composite was developed using various percentages of DPM fiber and polylactic acid (PLA). 10% DPM fiber reinforced PLA composite presented highest results. A hybrid composite was made using date palm mat (DPM) and palmyra palm fruit (PPF) fiber with HDPE matrix. A hybrid composite with 5% fiber content achieved better properties. Crystalline nanocellulose were extracted from DPM fibers and used to prepare nanocomposite films. 9% crystalline nanocellulose containing nanocomposite films revealed highest mechanical properties. The characteristics of these newly created composites indicate potential applications in various fields.

Keywords: Date Palm Mat (DPM), High Density Polyethylene (HDPE), Polystyrene (PS), Composite, Gamma radiation, Crystalline nanocellulose.

LIST OF ABBREVIATIONS

DPM	Date Palm Mat
PPF	Palmyra Palm Fruit
HDPE	High Density Polyethylene
PS	Polypropylene
PLA	Polylactic Acid
PVA	Polyvinyl Alcohol
PVP	Polyvinylpyrrolidone
FTIR	Fourier-transform Infrared Spectroscopy
ATR	Attenuated Total Reflectance
SEM	Scanning Electron Microscopy
TGA	Thermo Gravimetric Analysis
DSC	Differential Scanning Calorimetry
MSP	Monosodium Phosphate
MAP	Monoammonium Phosphate
MH	Magnesium Hydroxide
CNC	Crystalline nanocellulose

CONTENTS

CONTENTS

LIST OF TABLES

LIST OF TABLES

Page

LIST OF FIGURES

LIST OF FIGURES

CHAPTER 1

Introduction

1.1 Introduction

Rapid progress in manufacturing industries has directed to the necessity for the improvement of materials with respect to strength, stiffness, density, and lower cost with enriched sustainability. Composite materials are considered as one of the materials with such improvement in characteristics showing their potentiality in numerous fields of applications [1]. Composite material is defined as the combination of two or more materials and the final material possess superior properties to the properties of individual component of the materials. In the composite materials discontinuous phases which are called the reinforcement or reinforcing material dispersed in continuous phases are called the matrix [2]. The reinforcing materials are held together by a matrix, which functions as an adhesive. This matrix also distributes the applied load to the reinforcing components. Moreover, it holds the reinforcing materials firmly in place and protects against the composite damaging its surroundings. Contrarily, the reinforcing materials in the composite transfer the load on the structure, which give the material strength and stiffness [3]. On the basis of matrix, composite materials are classified into three categories, namely metal, ceramic and polymer composite materials. Among these three categories, polymer composite materials have received much attention owing to their light weight and strength [4]. Usually, polymers are of two types namely, thermoplastic and thermosetting [3]. Thermoplastic softens and melts when heat is applied and hardens on cooling. It is possible to re-melt and reformulate thermoplastics. Acrylonitrile butadiene styrene, nylon, polyethylene, polypropylene, polystyrene, polyvinyl chloride and polyethylene terephthalate are typical examples of thermoplastic polymers. Thermosetting polymers harden permanently when heated and once hardened it does not melt for reshaping. Epoxy, polyester, phenol formaldehyde, and polyurethane are a few common examples of thermosetting polymers. Thermoplastic polymers are most frequently employed in engineering applications owing to their exceptional chemical resistance, low shrinkage rate, improved mechanical properties, etc [5,6]. Several reinforcements, either natural or synthetic, are used to make composites [7]. Numerous synthetic fibers such as glass, kevlar, and carbon fibers are used as reinforcing material for polymers. However, synthetic fiber based polymer composites have been used significantly in various

advanced engineering applications. These composite materials are heavy and toxic to human. Moreover, society's concern about the environment has gradually increased through the last few decades [8].

The increasing environmental awareness and community interest, the new environmental guidelines and unmaintainable depletion of petroleum, led to think about the utilization of environmentally friendly materials. Natural fibers which are treated as one of the environmental friendly materials with good properties compared to traditional synthetic fiber [9]. Natural fibers have noteworthy advantages over synthetic fibers, making them competitive in the modern industrial applications. The advantages of using natural fibers as reinforcing materials are low density, light weight, renewability, biodegradability, cheap, good insulation properties, eco-friendly, non-abrasive, and machine wear [10-12]. The use of natural fiber composites has extended greatly during the last few years. Natural fiber composites are widely used in numerous applications such as building and construction, automobile, aerospace, biomedical, sports, marine, textile and packaging industry [9,13,14]. The Mercedes Benz A-class model utilized coconut fibers reinforced rubber latex composites for the seats, while the E-class model employed flax-sisal fiber mat reinforced epoxy composites as door panels. There are three types of natural fibers, namely animal, mineral and plant fibers. Among these, plant fiber has received the most attention and is also a widely used reinforcing agent. Plant fibers come in six main categories, including seed fiber, bast fiber, leaf fiber, fruit fiber, and straw fiber [3]. Extensive research has been carried out to develop the polymer composites using natural fibers. The natural fibers such as jute, bamboo, sisal, banana, coir, pineapple, flax, hemp, sugar cane bagasse, oil palm empty fruit bunch are used for the preparation of composites and the outcomes signified that natural fibers can be used as potential reinforcing materials [15-24].

A crucial factor in determining the properties of composites is the selection of an appropriate matrix. In conclusion, choosing a thermoplastic or thermoset polymeric composite is an important decision. The potential benefits of thermoplastic composites over thermosets include enhanced toughness, potential recyclability, and shorter cycle times [5]. The utilization of natural fiber reinforced thermoplastic matrix-based composites is much more widespread, as demonstrated by several research works and applications in a variety of sectors [25].

Despite their growing popularity, the main shortcomings of natural fibers are their hydrophilic nature and poor incompatibility between fiber and matrix. One of the main factors contributing to the high mechanical characteristics of composites is the adhesion between fibers and matrix, which also plays a significant role in the transfer of loads from matrix to fibers. Weak or inefficient interactions between fibers and matrix are mostly caused by poor surface adhesion [22, 26]. A variety of approaches have been used to overcome the shortcomings of natural fibers and to enhance the properties of composites [24, 27,28].

Date palm (*Phoenix sylvestris*) and Palmyra palm (*Borassus flabellifer*) trees are grown abundantly in Bangladesh. These trees produce a lot of fibers every year. Various portions such as leaves, naturally woven mat or leaf sheath and fruit stalks from date palm and palmyra palm fruits are easily converted to fiber. At present, the fibers from date palm mat (DPM) and palmyra palm fruit (PPF) are not used as resources designed for materials in a systematized way. Actually, these fibers are thought as an agricultural waste and utilized as fuel in the rural area. The use of these renewable and green source of reinforcing materials in polymer composite which can be low cost and ecofriendly. Therefore, the fibers have been transformed into short fibers for polymer reinforcing materials.

In this work, we have attempted to develop, characterize and optimize DPM fiber reinforced composites with thermoplastic matrices. The physical, mechanical, thermal, morphological, and biodegradation properties of the composites are investigated to determine their potentiality for a variety of applications within the environmental legal outline. In order to improve the quality of the composite, chemical treatment, nano filler, gamma irradiation, a different matrix material (PLA), and fire retardant additives are used. We also tried to develop a novel hybrid composite by the combination of two reinforcing fibers (DPM and PPF) into a single matrix (HDPE). Crystalline nano cellulose also extracted and used as reinforcement for the preparation of nanocomposite films. The physical, mechanical, and morphological properties are examined in order to assess the composites' potential for use in a range of applications.

1.2 Objectives

The objectives of this investigation are to use DPM and PPF fibers as sustainable reinforcing materials in thermoplastic matrix and to prepare, evaluate and optimize the properties of composites. The objectives of this study are outlined below:

- To prepare new biodegradable and partially biodegradable fiber reinforced composites with thermoplastics. Chemical modification of fibers, incorporation of ZnO nano fillers and gamma radiation are used to enhance the properties of composites.
- To develop and characterize fire retardant composites using fire retardant additives.
- To fabricate and characterize hybrid composites using DPM and PPF fibers with thermoplastic matrix.
- To prepare and examine crystalline nano-cellulose reinforced PVA, and PVP blended nanocomposite films. Extraction of crystalline nanocellulose from DPM fiber is essential for achieving this goal.

1.3 References

1. Gowda, T.G. Y.; Sanjay, M.R.; Bhat, K. S.; Madhu, P.; Senthamaraikannan, P.; Yogesha, B. Polymer matrix-natural fiber composites: An overview, *Cogent Eng.*, **2018,** 5(1). DOI: 10.1080/23311916.2018.1446667
2. Hsissou, R.; Seghiri, R.; Benzekri, Z.; Hilali M.; Rafik, M.; Elharfi, A. Polymer composite materials: A comprehensive review, *Composite Struct.*, **2021**, 262, 113640, ISSN 0263-8223. https://doi.org/10.1016/j.compstruct.2021.113640.
3. Mishra, T.; Mandal, P.; Rout, A.K.; Sahoo, D. A state-of-the-art review on potential applications of natural fiber-reinforced polymer composite filled with inorganic nanoparticle, *Compos. Part C: Open Acc.*, **2022**, 9, 100298, ISSN 2666-6820. https://doi.org/10.1016/j.jcomc.2022.100298.
4. Nurazzi, N.M.; Asyraf, M.R.M.; Khalina, A.; Abdullah, N.; Aisyah, H.A.; Rafiqah, S.A.; Sabaruddin, F.A.; Kamarudin, S.H.; Norrrahim, M.N.F.; Ilyas, R.A.; Sapuan, S.M. A Review on Natural Fiber Reinforced Polymer Composite for Bullet Proof and Ballistic Applications, *Polymers*, **2021,** 13. https://doi.org/10.3390/polym13040646
5. Jain, P.; Jariwala, H. A comprehensive review on natural fiber reinforced polymer composites and its applications, *Trends in Appl. of Polym. and Polym. Compos.*, edited by

V. K. Patel, R. Kant, P. S. Chauhan, and S. Bhattacharya (AIP Publishing, Melville, New York), **2022,** 4-1–4-32.

6. Ramachandran, A. R.; Rangappa, S. M.; Kushvaha, V.; Khan, A.; Seingchin, S.; . Dhakal, H. N. Modification of Fibers and Matrices in Natural Fiber Reinforced Polymer Composites: A Comprehensive Review, *Macromol. Rapid Commun*., **2022,** 43. https://doi.org/10.1002/marc.202100862
7. Singh, M. K.; Tewari, R.; Zafar, S.; Rangappa, S. M.; Siengchin, S. A comprehensive review of various factors for application feasibility of natural fiber-reinforced polymer composites, *Results in Mater.*, **2023**, 17, 100355, ISSN 2590-048X. https://doi.org/10.1016/j.rinma.2022.100355.
8. Kamarudin; Hasnah, S.; Basri, M. M.S.; Rayung, M.; Abu, F.; Ahmad, S.; Norizan, M. N.; Osman, S.; Sarifuddin, N; Desa, M. S. Z. M.; Abdullah, U. H.; Tawakkal, I. S. M. A.; Abdullah. L. C. A Review on Natural Fiber Reinforced Polymer Composites (NFRPC) for Sustainable Industrial Applications, *Polymers*, **2022,** 14(17), 3698**.** https://doi.org/10.3390/polym14173698
9. Mohammed, L.; Ansari, M. N. M.; Pua, G.; Jawaid, M.; Islam M. S. A Review on Natural Fiber Reinforced Polymer Composite and Its Applications, *Int. J. of Polym. Sci.*, **2015**. https://doi.org/10.1155/2015/243947
10. Nguong, C. W. S.; Lee, N. B.; Sujan. D. A Review on Natural Fibre Reinforced Polymer Composites, *Int. J. of Chem. Mater. and Biomol. Sci*,, **2013,** 6.0(1). https://doi.org/10.5281/zenodo.1332600
11. Bongarde, U.S.; Shinde, V.D. Review on natural fiber reinforcement polymer composites, *Int. J. of Eng. Sci. and Innov. Technol. (IJESIT)*, **2014**, 3(2), 431-436, ISSN: 2319-5967 ISO 9001:2008.
12. Rabbi, M.; Islam, M. Jute Fiber-Reinforced Polymer Composites: A Comprehensive Review, *Int. J. of Mech. and Product. Eng. Res. and Develop.* (IJMPERD), **2020**, 10(3), 3053–3072, ISSN (P): 2249–6890; ISSN (E): 2249–8001.
13. kumar, G. R.; Seshadri, S. A.; Devnani, G.L.; Sanjay, M.R.; Suchart Siengchin, Maran, J. P.; Al-Dhabi, N. A.; Karuppiah, P.; Mariadhas, V. A.; Sivarajasekar, N.; Anuf, A. R. Environment friendly, renewable and sustainable poly lactic acid (PLA) based natural fiber

reinforced composites – A comprehensive review, *J. of Cleaner Prod.*, **2021**, 310, 127483, ISSN 0959-6526. https://doi.org/10.1016/j.jclepro.2021.127483.

14. Sonkar, D.; Singh, P. Impact, Hardness and Water Absorption Properties of Natural Fibres (Banana, Hemp and Sisal) Hybrid Composite Material, *Int. J. of Sci. Res. in Sci., Eng. and Technol.*(IJSRSET), **2019,** 6(4), 63-72.
15. Ahamed, B.; Hasan, M.; Azim, A. Y. M. A.; Saifullah, A.; Alimuzzaman S.; Dhakal, H. N.; Sarker, F. High performance short jute fibre preforms for thermoset composite applications, *Compos. Part C: Open Acc.*, **2022**, 9, 100318, ISSN 2666-6820. https://doi.org/10.1016/j.jcomc.2022.100318.
16. Chakkour, M.; Moussa, M. O.; Khay, I.; Balli, M.; Zineb, T. B. Effects of humidity conditions on the physical, morphological and mechanical properties of bamboo fibers composites, *Ind. Crops and Prod.*, **2023**, 192, 116085, ISSN 0926-6690. https://doi.org/10.1016/j.indcrop.2022.116085.
17. Tesfay, D.; Balakrishnan, S,; Ashine, F.; Sivaprakasam, P. Sisal fibre / polypropylene composites properties by plunger injection moulding, *Mater. Today: Proc.*, **2022**, 62(2), 448-453, ISSN 2214-7853. https://doi.org/10.1016/j.matpr.2022.03.565.
18. Ernest, E. M., Peter, A. C. Application of selected chemical modification agents on banana fibre for enhanced composite production, *Cleaner Mater.*, **2022**, 5, 100131, ISSN 2772-3976. https://doi.org/10.1016/j.clema.2022.100131.
19. Kumar, S.; Shamprasad, M.S.; Varadarajan, Y.S.; Sangamesha, M.A. Coconut coir fiber reinforced polypropylene composites: Investigation on fracture toughness and mechanical properties, *Mater. Today: Proc.*, **2021**, 46(7), 2471-2476, ISSN 2214-7853. https://doi.org/10.1016/j.matpr.2021.01.402.
20. Singh, T.; Pruncu, C. I.; Gangil, B.; Singh, V.; Fekete, G. Comparative performance assessment of pineapple and Kevlar fibers based friction composites, *J. of Mater. Res. and Technol.*, **2020**, 9(2), 1491-1499, ISSN 2238-7854. https://doi.org/10.1016/j.jmrt.2019.11.074.
21. Mohammed, A.; Rao, D. K. N. Investigation on mechanical properties of flax fiber/expanded polystyrene waste composites, *Heliyon*, **2023**, 9(3), e13310, ISSN 2405-8440. https://doi.org/10.1016/j.heliyon.2023.e13310.

22. Bollino, F.; Giannella, V.; Armentani, E.; Sepe, R. Mechanical behavior of chemically-treated hemp fibers reinforced composites subjected to moisture absorption, *J. of Mater. Res. and Technol.*, **2023,** 22, 762-775, ISSN 2238-7854. https://doi.org/10.1016/j.jmrt.2022.11.152.
23. Cerqueira, E.F.; Baptista, C.A.R.P.; Mulinari, D.R. Mechanical behaviour of polypropylene reinforced sugarcane bagasse fibers composites, *Procedia Eng.*, **2011**,10, 2046-2051, ISSN 1877-7058. https://doi.org/10.1016/j.proeng.2011.04.339.
24. Ramlee, N. A.; Jawaid, M.; Zainudin, E. S.; Yamani, S. A. K. Tensile, physical and morphological properties of oil palm empty fruit bunch/sugarcane bagasse fibre reinforced phenolic hybrid composites, *J. of Mater. Res. and Technol.*, **2019**, 8(4), 3466-3474, ISSN 2238-7854. https://doi.org/10.1016/j.jmrt.2019.06.016
25. Agunsoye, J.O.; Aigbodion, V.S. Bagasse filled recycled polyethylene bio-composites: Morphological and mechanical properties study, *Results in Phys.*, **2013**, 3, 187-194, ISSN 2211-3797. https://doi.org/10.1016/j.rinp.2013.09.003.
26. Bartos, A.; Utomo, B. P.; Kanyar, B.; Anggono, J.; Soetaredjo, F. E.; Móczó, J.; Pukánszky, B. Reinforcement of polypropylene with alkali-treated sugarcane bagasse fibers: Mechanism and consequences, *Compos. Sci. and Technol.*, **2020**, 200, 108428, ISSN 0266-3538. https://doi.org/10.1016/j.compscitech.2020.108428.
27. Jotiram, G. A.; Palai, B. K.; Bhattacharya, S.; Aravinth, S.; Gnanakumar, G.; Subbiah, R.; Chandrakasu, M. Investigating mechanical strength of a natural fibre polymer composite using SiO2 nano-filler, *Mater. Today: Proc.*, **2022**, 56(3), 1522-1526, ISSN 2214-7853. https://doi.org/10.1016/j.matpr.2022.01.176.
28. Kumar, V.; Gulati, K.; Lal, S.; Arora, S. Effect of gamma irradiation on tensile and thermal properties of poplar wood flour-linear low density polyethylene composites, *Rad. Phys. and Chem.*, **2020**, 174, 108922, ISSN 0969-806X. https://doi.org/10.1016/j.radphyschem.2020.108922.

CHAPTER 2

Literature Survey

2.1 Literature Survey

The earliest known applications of composite materials were credited to Egyptians and Mesopotamians around 1500 B.C. They utilized a mixture of mud and straw to build tough and long-lasting structures. Straw was used to reinforce ancient composite items like mud bricks, pottery and boats. The first composite bow was created around 1200 AD, by the Mongols. Wood, bamboo, bone, cattle tendons, horns, bamboo and silk combined with natural pine resin to create these bows.

Scientists' discovery of plastics marked the start of the contemporary era of composites. Plastics including vinyl, polyester, polystyrene, and phenolic were created during the beginning of the 1900s. Leo Baekeland produced Bakelite from synthetic chemicals in 1907 and outperformed in various applications. Owens Corning developed fiberglass in 1935. By mixing fiberglass and a plastic polymer, a remarkably durable and light structure was produced and started the development of fiber reinforced polymer composite [1,2].

Advanced engineering applications have made extensive use of synthetic fiber-based polymer composites. These composite materials are hazardous to humans [3]. The use of ecologically friendly materials has come into consideration as a result of rising public concern for the environment, increased environmental regulations, and the relentless depletion of petroleum. Natural fibers are light weight, low density, renewable, biodegradable, cheap, good insulation property, eco-friendly. Researchers are paying attention on the use of natural fiber because of their several advantages. Many studies have been carried out to develop the polymer matrix based composites using natural fibers [4].

Sayeed et al. [5] prepared jute, kenaf, and pineapple leaf fiber reinforced polypropylene composites by varying weight percentages of fibers and suggested that pineapple leaf fiber polypropylene composite exhibited superior mechanical characteristics than other composites. The mechanical characteristics of the composites improved considerably for all composites with various fiber contents in comparison to the pure polypropylene matrix.

Neher et al. [6] developed and characterized banana fiber reinforced HDPE composites with different fiber contents. They made composites with 5%, 10%, 15% and 20% fiber content. They concluded that 20% banana fiber HDPE composites had superior mechanical qualities including

tensile strength. 20% banana fiber HDPE composites also exhibited more thermal stability when compared to others.

Zhao et al. [7] reported the influence of fiber content, compatibilizer and manufacturing process on the sisal fiber reinforced high density polyethylene composite. The mechanical characteristics improved with increasing fiber content. Maleic anhydride grafted HDPE (MAPE) as compatibilizer considerably improved fiber-matrix adhesion. The composites prepared by pre-impregnation offer greater mechanical properties than those created through simultaneous blending.

Bukar et al. [8] studied the preparation and examination of coconut fiber reinforced low density composite. The best tensile and impact strength were found for the composites with 30 and 20% fiber content compared to the composites with 40% fiber content .

According to Tungjitpornkull et al. [9], wood polymer composites prepared by compression molding offers superior mechanical characteristic than extrusion and injection molding. Authors also demonstrated that the compression moulding technique reduced shearing stress contributed to less heat degradation of the matrix and less fiber breakage when compared to the twin-screw extrusion procedure.

Numerous investigations have been conducted to create composite materials with polymer matrices using natural fibers such as coir, oil palm, hemp, sisal, bamboo, flax, banana , rice husk, sugarcane bagasse, jute, kenaf [10-14]. However, there is very little study on date palm fiber-based polymer composites. In light of this, the current research work was carried out with the intention of investigating the potential of date palm mat fiber polymer composites and characterizing various composites from a physical, mechanical, thermal, and morphological standpoint.

2.2 References

1. Mar-Bal Incorporated Home page, https://www.mar-bal.com/language/en/applications/history-of-composites/.
2. ThoughtCo. Homepage, https://www.thoughtco.com/history-of-composites-820404.

3. Ayalew, A. A.; Wodag, A, F. Characterization of Chemically Treated Sisal Fiber/Polyester Composites, *J. of Eng.*, **2022,** https://doi.org/10.1155/2022/8583213
4. Azman, M. A.; Asyraf, M. R. M.; Khalina, A.; Petru, M.; Ruzaidi, C. M.; Sapuan, S. M.; Nik, W. B. W.; Ishak, M. R.; Ilyas, R. A.; Suriani, M. J. Natural Fiber Reinforced Composite Material for Product Design: A Short Review. *Polymers*. 2021. 13. 1-24. 10.3390/polym13121917.
5. Sayeed, M.M.A.; Sayem, A.S.M.; Haider, J.; Akter, S.; Habib, M.M.; Rahman, H.; Shahinur, S. Assessing Mechanical Properties of Jute, Kenaf, and Pineapple Leaf Fiber-Reinforced Polypropylene Composites: Experiment and Modelling. *Polymers* **2023**, *15*, 830. https://doi.org/10.3390/polym15040830
6. Neher, B.; Rakib, H.; Fatima, K.; Gafur, M.A.; Ahmed, F. Study of the Physical, Mechanical and Thermal Properties of Banana Fiber Reinforced HDPE Composites. *Mater. Sci.and Appl.*, **2020**. 11. 245-262. 10.4236/msa.2020.114017.
7. Zhao, X.; Li, K.Y. R.; Bai, S. Mechanical properties of sisal fiber reinforced high density polyethylene composites: Effect of fiber content, interfacial compatibilization, and manufacturing process. *Compos. Part A: Appl.Sci. and Manuf.*, **2014,** 65, 169–174. doi:10.1016/j.compositesa.2014.06.017
8. Bukar, A. M.; El-Jummah, A. M.; Hammajam, A. A. Development and Evaluation of the Mechanical Properties of Coconut Fibre Reinforced Low Density Polyethylene Composite. *Open J. of Compo. Mater.*, **2022** 12, 83-97. doi: 10.4236/ojcm.2022.123007
9. Tungjitpornkull, S.; Sombatsompop, N. Processing technique and fiber orientation angle affecting the mechanical properties of E-glass fiber reinforced wood/PVC composites, *J. Mater. Process. Technol.*, **2009**, 209(6), 3079-3088 https://doi.org/10.1016/j.jmatprotec.2008.07.021
10. Adeniyi, A. G.; Onifade, D. V.; Ighalo, J. O.; Adeoye, A. S. A review of coir fiber reinforced polymer composites, *Compos. Part B: Eng.*, 2019, 176, 107305, ISSN 1359-8368, https://doi.org/10.1016/j.compositesb.2019.107305.
11. Hasan, K. M, F.; Horváth, P. G.; Bak, M.; Alpar, T. A state-of-the-art review on coir fiber-reinforced biocomposites. *RSC Adv.*, **2021**, 11. 10.1039/d1ra00231g.
12. Koley, S. K.; , Aggarwal, L.; Dr. Ravinder Singh Joshi, R. S.; Singh, B. J. A Review on Progress of Bagasse and Coir Fibre Composites and Their Mechanical Performances,

IOSR J. of Mech. and Civil Eng. (IOSR-JMCE), **2017**, 14(3), 68-72 e-ISSN: 2278-1684,p-ISSN: 2320-334X.

13. Prakash, S. Om Sahu, Parul Madhan, Mohankumar Johnson Santhosh, A. A Review on Natural Fibre-Reinforced Biopolymer Composites: Properties and Applications, *Int. J. of Polym. Sci.*, **2022,** 7820731. https://doi.org/10.1155/2022/7820731
14. Prasad, N.; Agarwal, V.; Sinha, S. Hybridization effect of coir fiber on physico-mechanical properties of polyethylene-banana/coir fiber hybrid composites. *Sci. and Eng. of Compos. Mater.*, **2018**, *25*(1), 133-141. https://doi.org/10.1515/secm-2015-0446

CHAPTER 3

Preparation and Characterization of DPM Fiber Reinforced Composites

3.1 Introduction

Environmental concerns have raised awareness of the manufacturing of "green" items using natural materials [1]. One such effective substance that substitutes synthetic materials is natural fibers [2]. Natural fibers are widely available, and as a result, their application in composite materials is rising steadily [1]. The benefits of employing plant fibers include their low cost, low weight, biodegradability, good comparative mechanical characteristics, reduced tool wear during the machining process, and ease of recycling, making them environmentally benign [2,4]. The typical sources of natural fibers are different parts of plants such as leaves, fruits, seeds, grasses, silks, forests, lobes, and stems [5]. The utilization of natural fibers in polymer matrix composites has garnered a lot of attention and finds use in a wide range of industries. Natural fibers are being used more frequently in a variety of industries, including construction, furniture, packaging, and automobiles [2].

Natural fibers can be combined with a thermosetting or thermoplastic polymer matrix to create composites. The composite with thermosetting polymer matrix exhibits fragility and incapability of being repaired. Numerous thermoplastic-based composites provide great resistance to impact loading, the ability to thermoform and shape at high temperatures, the possibility of thermal joining and repair, as well as the ability to be recycled [6]. Thermoplastic composites are widely used due to their acceptable mechanical characteristics and production advantages [4].

Natural fiber reinforced composites are already well-established, and several types of natural fibers have been used in the creation of composites such as jute [7], kenaf [8], hemp [9], corn [10], pineapple [11], coir [12], bamboo [13], rice husk [14]. Due to concerns about sustainability, researchers have recently focused on using agricultural wastes and forest residues. Agricultural wastes and plant leftovers have similar structures and chemical contents, which makes them viable reinforcement materials for plastic.

In this study, date palm mat (DPM) fibers were combined with thermoplastics to create composites as reinforcing materials. Date palm trees (Phoenix sylvestris Roxb), also known locally as Khejur, grow naturally or are farmed in Bangladesh's southwestern areas. This tree generates a lot of agricultural waste, which is primarily utilized as fuel in homes. The aim of this study is to prepare and evaluate the physical, mechanical, thermal and biodegradation

performance of short DPM fiber reinforced polymer composites by the variation of different weight proportions of fibers.

3.2 Experimental

3.2.1 Materials

High density polyethylene (HDPE), and polystyrene (PS) were used as polymer matrix. HDPE, and PS were purchased from Saudi Polymers Company, Saudi Arabia, and Chi Mei Corporation, Taiwan respectively. DPM fibers were amassed from local area of Jashore, Bangladesh.

3.2.2 Fabrication of Composite

The polymer matrix granules were ground using a grinding machine in order to properly mix the polymeric matrix and fibers. The DPM fibers were chopped into small pieces (2-3 mm) with the help of hand scissors. The composites were fabricated by compression moulding technique. Measured amount of DPM fiber and polymer matrix were taken in a blender for proper mixing according to table 3.1. The mixed fibers and polymer matrix were poured into the mould (12x15 cm^2). The moulds were pressed (Paul Otto Weber Press Machine) at a fixed temperature and 200 kN pressure for 5 min. The temperature was maintained 160^0C, and 210^0C for HDPE, and PS respectively. The moulds were chilled for 5 min at room temperature and 200 kN pressure. Finally, the composites were lifted out from the mould. The composites were cut to specimens for mechanical properties following ASTM standard method.

Table 3.1: Fiber and polymer matrix content percentages in the composite samples

Fiber Content (wt%)	Polymer matrix (HDPE/PS) (wt%)
0	100
5	95
10	90
15	85
20	80
25	75

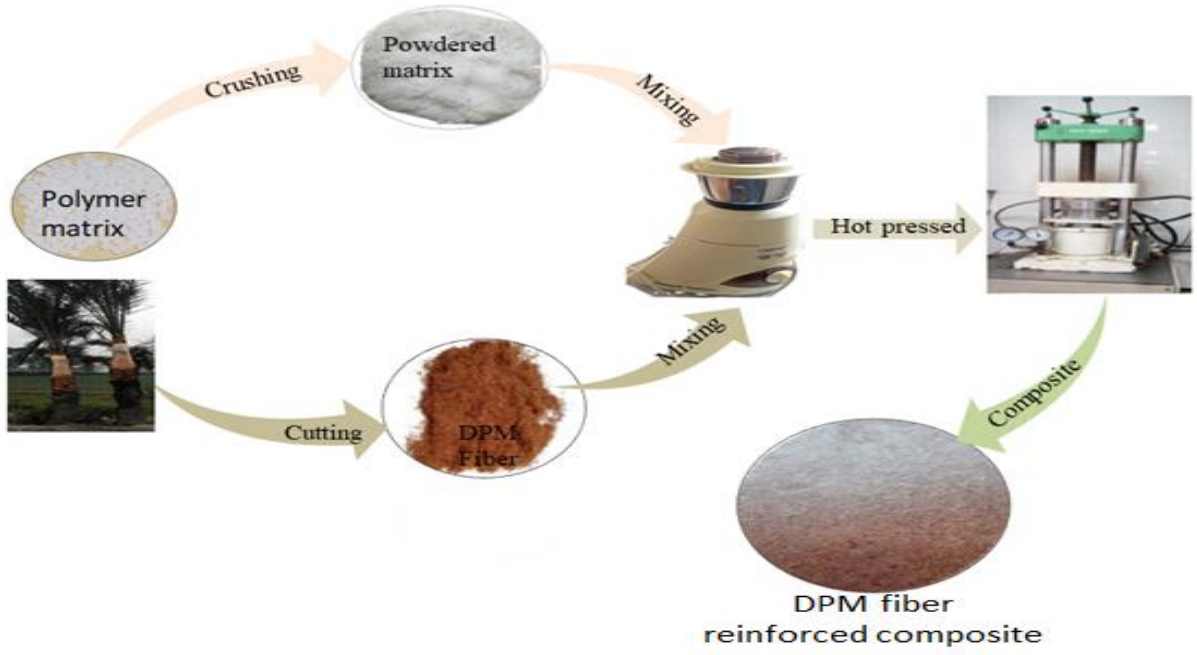

Figure 3.1: Schematic diagram of composite preparation

3.2.3 Bulk Density of the composites

Bulk density of the prepared composites was calculated by measuring the weight and dimensions of the samples utilizing the following equation 3.1. The average results for five composite samples were stated.

$$D = \frac{Weight\ of\ the\ composite}{(Length \times Width \times Height)\ of\ the\ composite} \quad (3.1)$$

3.2.4 Water Uptake of the Composites

Water uptake tests of the composites were conducted to investigate the effect of water on the composites with various amount of fiber content. Water uptake of the composites was conducted according to ASTM D570-99. With the purpose of measuring the water absorption capacity, the composite samples were dried in an oven for a specific temperature and time and then cooled in

a desiccator. The weight of the samples were taken and immersed in distilled water for 24 hours. The samples were drawn from the water, wiped dry using a cloth to eliminate any remaining water, and weighed. Three samples were tested to get an average result. The percentage of water uptake was determined by utilizing the following equation 3.2.

$$\text{Increase in weight, \%} = \frac{(W - W_0)}{(W_0)} \times 100 \quad (3.2)$$

where, W is the wet weight and W_0 is the conditioned weight of the composites.

3.2.5 Mechanical Properties

The tensile properties test was carried out to ascertain the tensile strength of the composite samples. The samples were cut in accordance with the ASTM D 882-02. The test was conducted via universal strength tester (model 1410 Titans, capacity 5 kN, England) with a constant crosshead speed of 10 mm/min. Bending strength (three point bending) of the composites were also performed following ASTM D7900. Five measurements in each composition of the composite samples were taken and the average values were reported.

3.2.6 FTIR Spectroscopy

FTIR spectra were captured for composite samples. The functional group of the composites was determined from FTIR spectra. The composites' FTIR spectra were recorded using a Frontier FT-IR/NIR spectrometer (Perkin Elmer, USA) with a wavelength range of 4,000-650 cm^{-1}.

3.2.7 Thermal Analysis

The thermogravimetric (TGA) and differential scanning calorimetry (DSC) analysis of the composite samples were performed by a NETZSCH instrument (STA 449 F3, Jupiter) in a temperature range 30-900^{0}C at nitrogen atmosphere. The heating rate was 10^{0}C/min.

3.2.8 SEM Analysis

The morphology of the fracture surfaces of the tensile samples were examined by using a field emission scanning electron microscope (JEOL JSM-7600F). The samples were cut into a small

portion, mounted onto holders using carbon tape and coated with gold. Samples were focused onto the surfaces and examined with different magnification.

3.2.9 Degradation by Soil Burial

The composites were covered up in a flower pot containing soil with moisture level at least 30%. The test samples were removed from the soil at intervals of 1 month. The samples were washed and oven dried at 80^0C for 6 h. The degradation was determined by measuring the tensile strength of the specimen.

3.3 Results and Discussion

3.3.1 Bulk Density of the Composites

The influence of various wt% of DPM fibers on the bulk density of the composites is illustrated in figures 3.2 and 3.3. The bulk density of short DPM fiber reinforced polymer composites decreases with the increase of fiber content. The density decreases from 0.8919 g/cm^3 to 0.7825 g/cm^3 for DPM fiber reinforced HDPE composites. In the case of DPM fiber reinforced PS composites the density drops from 1.6805 g/cm^3 to 1.5338 g/cm^3.). The bulk density of jute fiber reinforced LDPE composites decreases with the increase of jute fiber [17]. When more fibers are added in the polymer matrix of the composites lead improper mixing of fibers and polymer matrix. This may cause the decreasing trend of the bulk density of the composites with the increasing of fiber content [18].

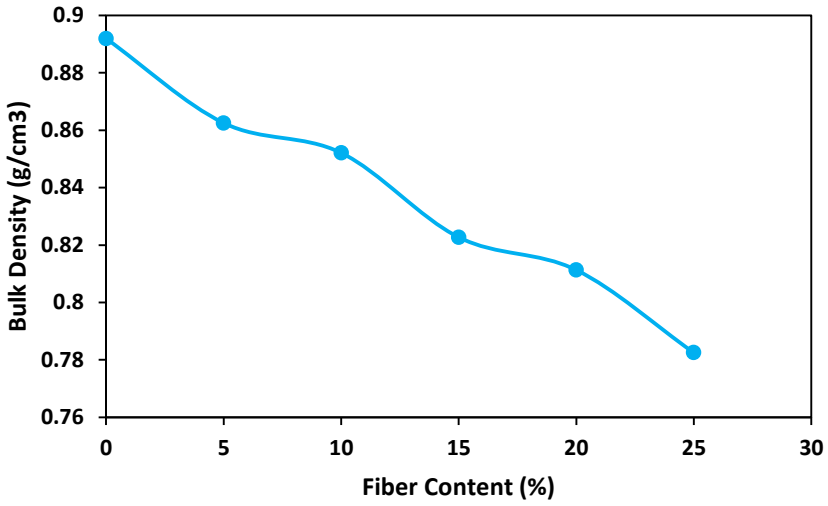

Figure 3.2: Bulk density of the DPM fiber reinforced HDPE composites at various fiber contents

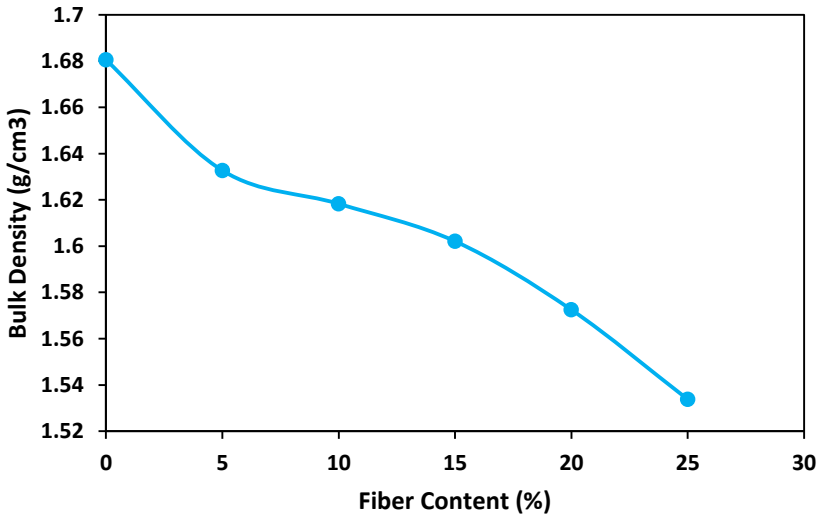

Figure 3.3: Bulk density of the DPM fiber reinforced PS composites at various fiber contents

3.3.2 Water Absorption of the composites

The consequence of various wt% of fiber content on water uptake behavior of the short DPM fiber reinforced polymer composites is presented in figures 3.4 and 3.5. It is evident from the figure that the amount of water uptake of the composites gradually increases with increasing

fiber content. Among the tested samples, the composite with 5% fiber content exhibits lowest water absorption while the composite with 25% fiber content exhibits highest amount of water absorption. Natural fibers are hydrophilic by nature, having a lot of hydroxyl groups and forming hydrogen bonds with water [19]. In the case of natural fiber composites, water molecules are absorbed through three mechanisms: diffusion of water into the polymer chain micro-gaps, water absorbed by the capillary phenomenon into the micro-gaps, and voids or defects in the fiber and matrix interfaces [2]. Das et al. [3] have reported that the water uptake of the coir fiber reinforced epoxy composites raised with increasing fiber length and fiber content. Kumari et al. [4] prepared polyester and poly lactic acid composites with sisal fiber where they also found an increase in water absorption of the composites with the increase of fiber loading. Similar findings were found for the prepared short DPM fiber reinforced polymer composites.

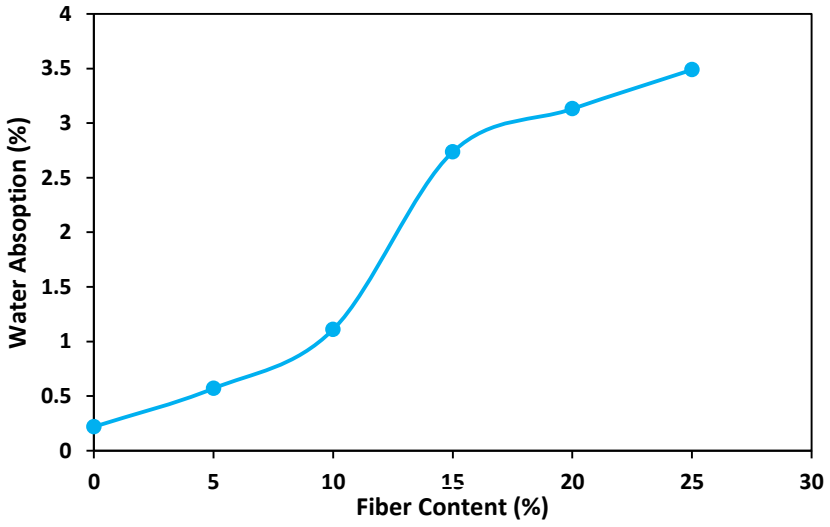

Figure 3.4: Water absorption of DPM fiber reinforced HDPE composites at various fiber contents

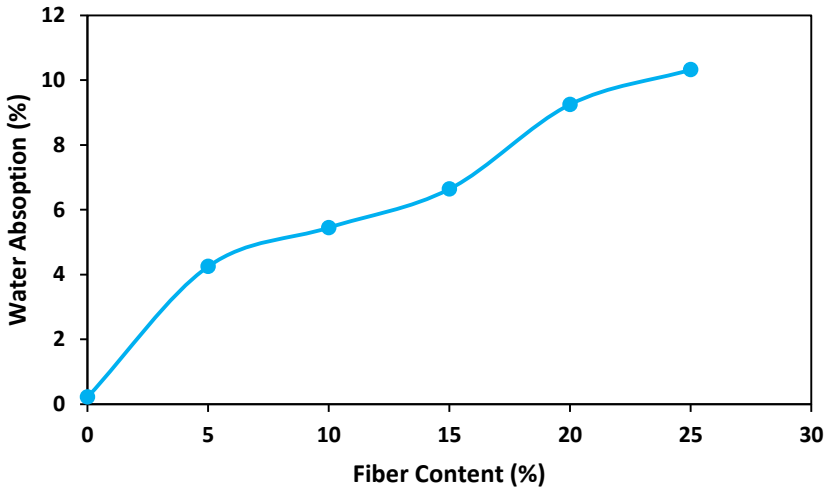

Figure 3.5: Water absorption of DPM fiber reinforced PS composites at various fiber contents

3.3.3 Mechanical Properties

Figures 3.6 and 3.7 show the consequence of the variation of fiber content on the tensile strength of the composites. As seen in the figure, the tensile strength first declines from 0 to 5% fiber content. Then the tensile strength increases with the increasing fiber content from 5 to 10%. The maximum tensile strength was found 21.09 MPa for 10% DPM fiber reinforced HDPE composites in the case of DPM fiber reinforced HDPE composites. Among the DPM fiber reinforced polystyrene composites, the highest tensile strength was around 39.07 MPa which was obtained for the composites with 10% fiber content. The tensile strength of the composites declined when the fiber percentage exceeded above 10%. This reduction in tensile strength with increment of fiber content may be owing to inadequate fiber-matrix adhesion, and debonding took place throughout tensile strength measurement. Debonding of the fiber-matrix can lead to voids which make defects to proliferate throughout the void containing areas. Furthermore, the tensile strength of the composites was impacted by the uneven dispersion of the fibers in the composites [23]. Zadeh et al. [24] have reported that the improved tensile strength for 10% date palm leaf fiber reinforced recycled blend of LDPE, HDPE and PP. The findings from our experiments are in agreement with their results.

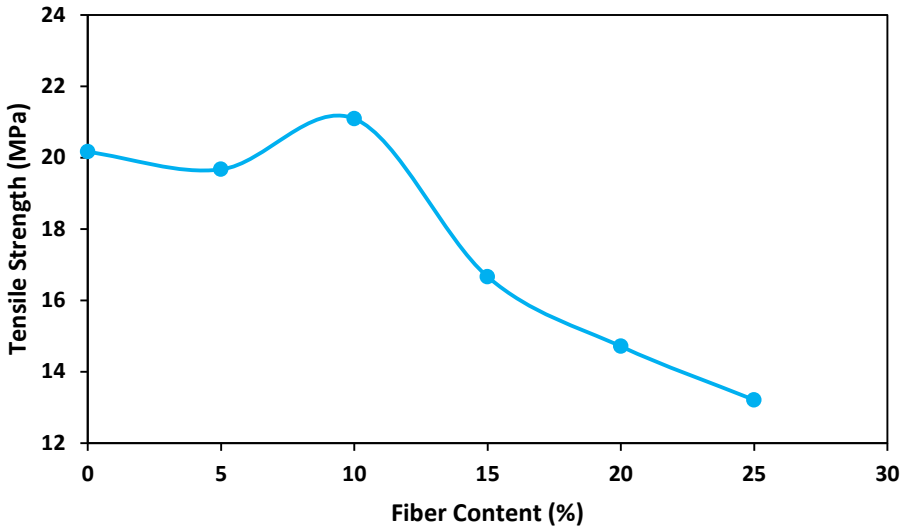

Figure 3.6: Tensile strength of DPM fiber reinforced HDPE composites at various fiber contents

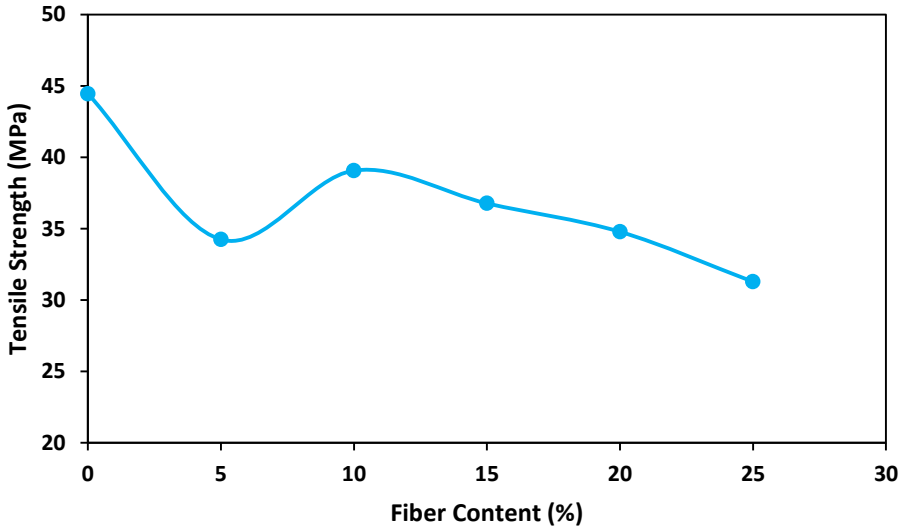

Figure 3.7: Tensile strength of DPM fiber reinforced PS composites at various fiber contents

The elongation at break specifies the toughness of the composites. Figures 3.8 and 3.9 illustrate the elongation at break of different wt% of fiber content composites. It is concluded that the addition of 5 to 25% by weight of short DPM fiber has slightly decreased the elongation at break of short DPM fiber reinforced composites compared to 100% polymer matrix (0% fiber content).

The fibers existing in the composites do not show elasticity or flexibility to the composites causing the reduction of elongation at break with increasing fiber content. In addition, the rigidity and toughness of the composites increases on the other hand ductility reduces [25]. Rahman et al. [26] used jute fiber as reinforcement for the preparation of polypropylene and linear low density composites. The fiber content of the composites was 10, 20 and 30%. They reported that the elongation at break of the composites decreased with the increasing fiber content. Huq et al. [27] prepared short jute fiber (5-30%) reinforced polypropylene composite. In their study, the elongation at break of those composites decreased gradually with the increase of fiber loading. Similar findings were observed for the prepared short DPM fiber reinforced HDPE and PS composites.

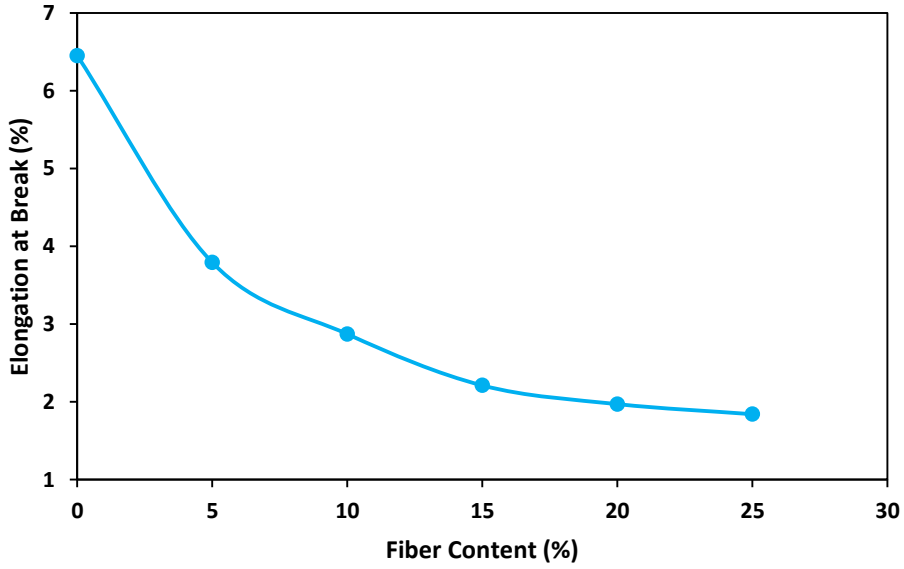

Figure 3.8: Elongation at break of DPM fiber reinforced HDPE at various fiber contents

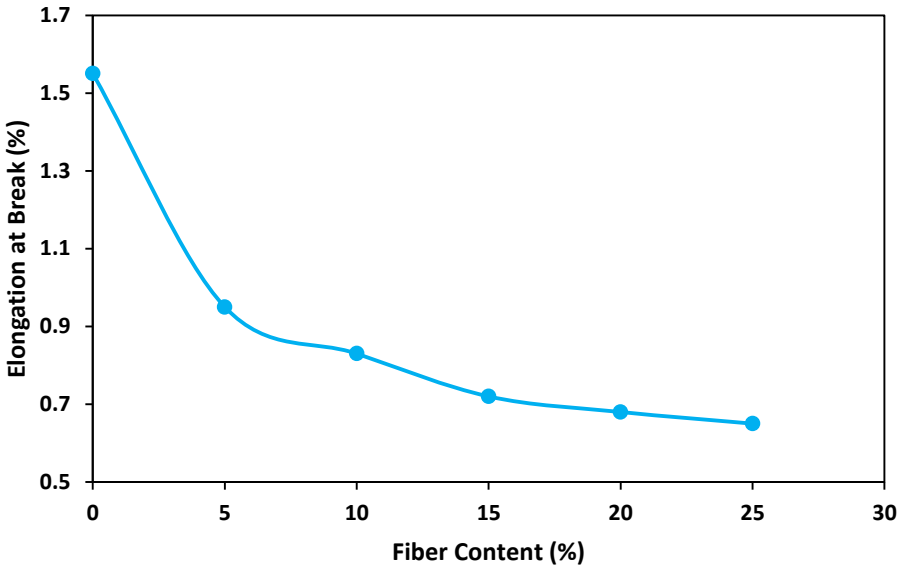

Figure 3.9: Elongation at break of DPM fiber reinforced PS at various fiber contents

The bending strength for different wt% of fiber contents is presented in figures 3.10 and 3.11. From the figure it is shown that bending strength reduced with 5% fiber content. Then bending strength improved for 10% fiber content and again reduced for 15 to 25% short DPM fiber reinforced composites. DPM fiber reinforced HDPE composites with a 10% content were found to have a maximum bending strength of 22.37 MPa. Among the composites made with DPM fiber and polystyrene, the maximum bending strength was found 47.38 MPa. The lessening in bending strength of the composites containing 15 to 25% fibers directs the reduced fiber-matrix interaction.

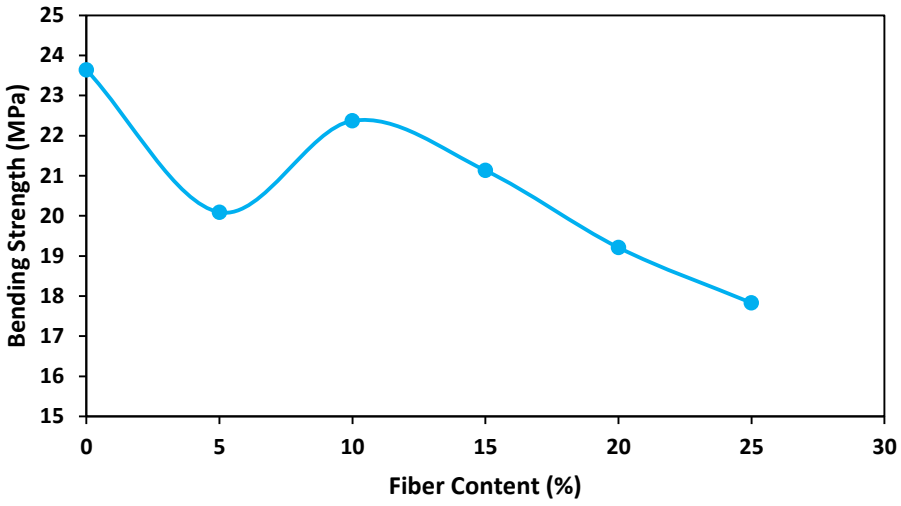

Figure 3.10: Bending strength of DPM fiber reinforced HDPE at various fiber contents

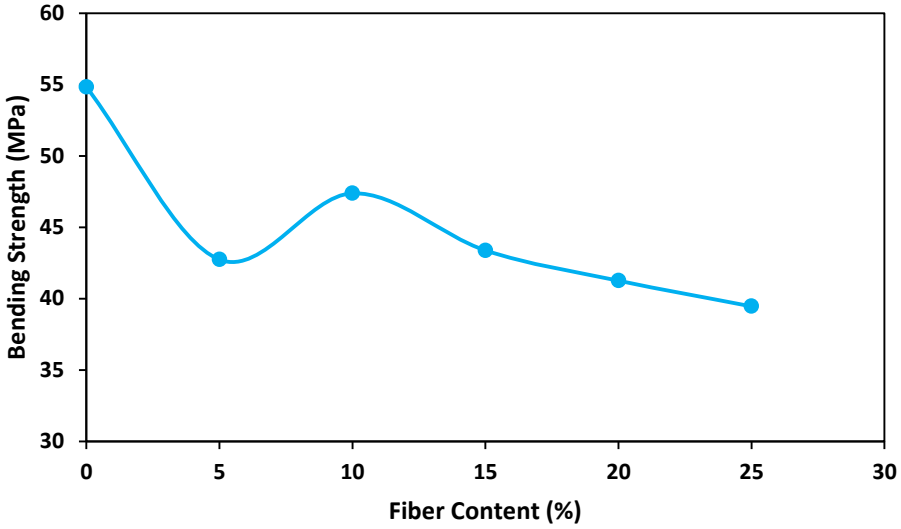

Figure 3.11: Bending strength of DPM fiber reinforced PS at various fiber contents

3.3.4 FTIR Spectroscopy

The FTIR spectra were obtained for 100% HDPE, 100% PS and 10% short DPM fiber reinforced composites and shown in figures 3.12 and 3.13. The FTIR spectra of 10% DPM fiber and 90%

HDPE composite indicate four peaks at 1740, 1607, 1372 and 1046 cm^{-1} and these peaks are not present in 100% HDPE. The absorbance peaks at 2915, 1462 and 718 cm^{-1} was observed for both 100% HDPE and 10% DPM fiber and 90% HDPE composites. The peak at 2915 cm^{-1} observed for the C-H stretching vibration [28]. The absorption band at 1740 cm^{-1} indicates the C=O stretching from the lignin and hemicellulose [29]. The peak 1607 cm^{-1} indicates C=C stretching in aromatic [30]. The peak at 1462 cm^{-1} refers to the $-CH_2$ group [30] and 1372 cm^{-1} indicates bending vibrations of the -CH group. The peak at 1046 cm^{-1} detects for C=O and -OH stretching vibrations of the polysaccharides in cellulose [29]. The peak 718 cm^{-1} corresponds to the rocking vibration of $-CH_2$ group [28].

In the case of 100% PS, the peak at 2923cm^{-1} corresponds to H-C-H asymmetric and symmetric stretch signifying the presence of alkane group. The peak at around 1600 cm^{-1}, indicates N-H bend of amides and H-C-H bend of alkane respectively [31]. The peak 1470cm^{-1} directs to aromatic C-C stretching and the peaks between 1000 cm^{-1} to 650 cm^{-1} attribute to the aromatic C-H bending vibrations [32]. For short DPM fiber reinforced PS composites, the peak at 3331cm^{-1} may relate to hydrogen bonded O-H stretching vibrations which is absent in the 100% polystyrene. The peaks at 1250 cm^{-1} and 1027 cm^{-1} resemble to the C-O stretch of the acetyl group, existing in lignin and hemicellulose [33]. Besides, the characteristic peaks of polystyrene matrix also found for the composites.

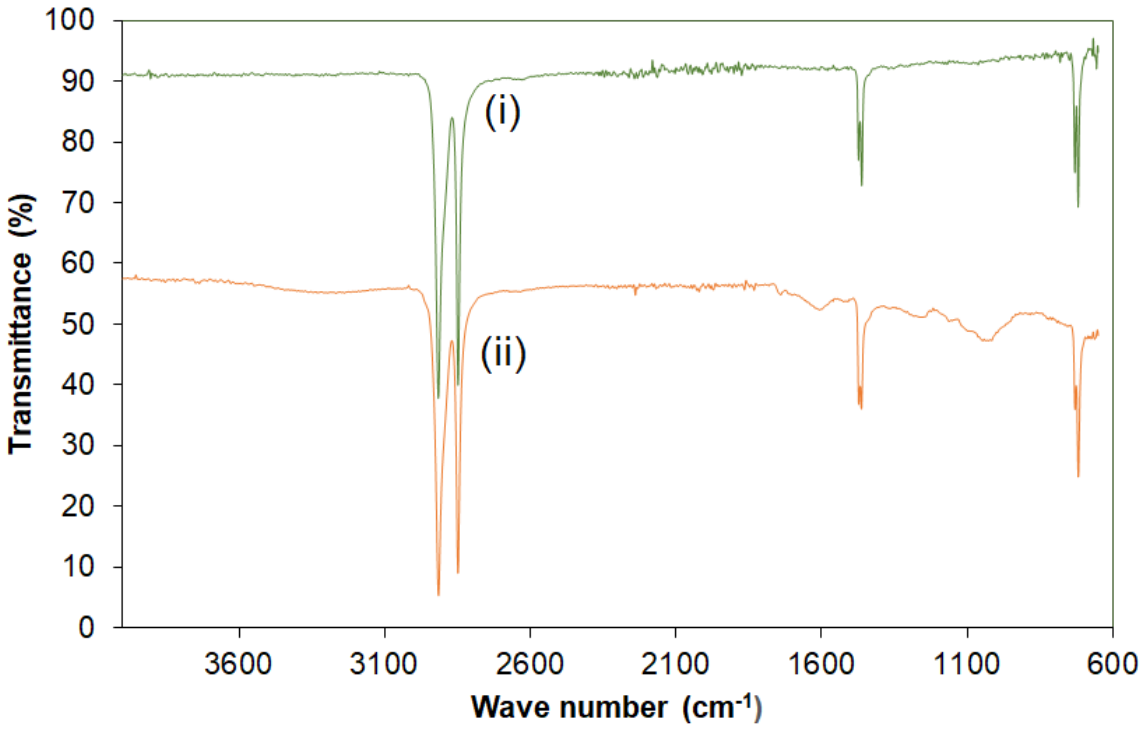

Figure 3.12: ATR-FTIR spectra of (i) 100% HDPE; (ii) 10% DPM fiber and 90% HDPE composite

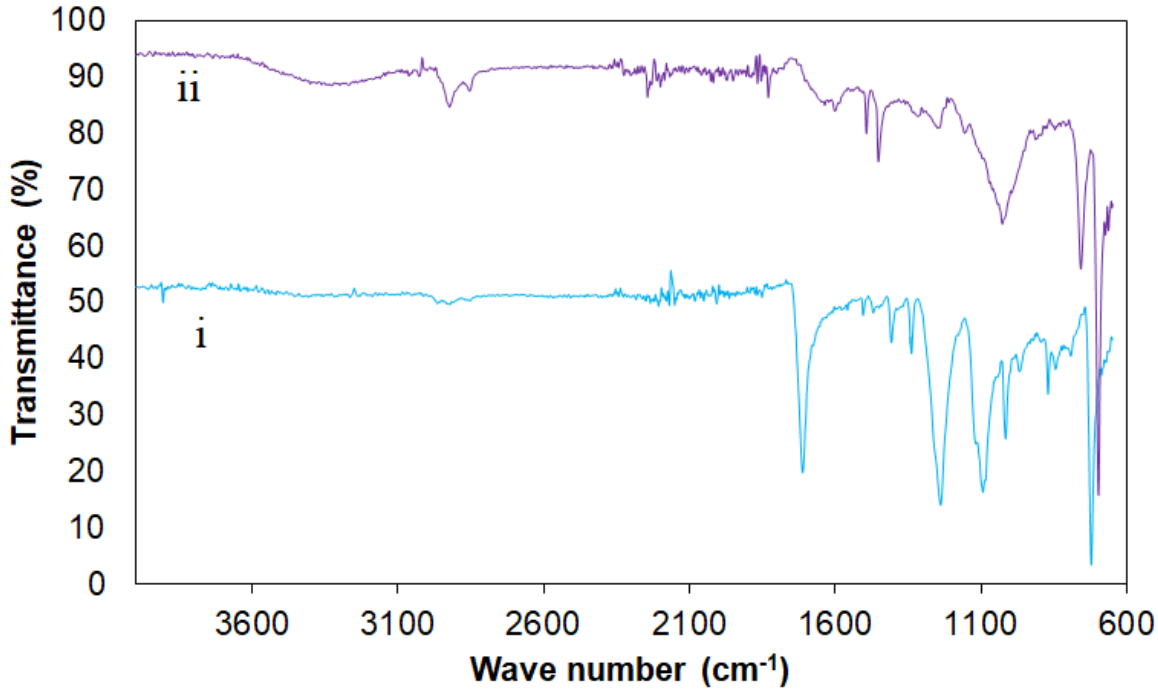

Figure 3.13: ATR-FTIR spectra of (i) 100% PS; (ii) 10% DPM fiber and 90% PS composite

2.3.5 Thermal Properties

Thermal analysis of 100% HDPE, 100% PS and optimized 10% DPM fiber reinforced composites were carried out to study their thermal stability. The TGA and DSC curves are displayed in figures 3.14-3.17. The TGA gives information about the mass change of composite samples as a function of temperature. The mass change in composites happens as a result of the breakdown of cellulose, hemicellulose, and lignin constituents throughout heating. Higher decomposition temperatures signify more thermal stability. The TGA results show that the 100% HDPE composite undergoes thermal degradation beginning at 428.7^0C and with a total mass change of 97.68%. On the other hand, the degradation of 10% DPM fiber reinforced HDPE composites start at 403.5^0C and 89.37% mass change is completed at about 500^0C. The degradation of the composite takes place earlier than 100% HDPE. The thermal degradation of the composites decreased with adding fibers. For 100% HDPE and 10% DPM fiber reinforced HDPE composite, the percentage of the residual mass at the finish of the heating process was 3.57 and 7.99 respectively. The DSC curves of 100% HDPE and 10% DPM fiber HDPE composite showed peaks of melting at 140.9and 141.1^0C respectively. The melting temperature of the composites increased slightly, this is due to the presence of DPM fiber. The DSC result of DPM fiber-HDPE composite revealed that the composite is thermally slightly more stable than HDPE due to high melting temperature.

From the figure it is clear that 100% PS started to degrade at 353.7 ^{0}C with 95.89% of mass change whereas 10% DPM fiber reinforced PS composite began to degrade at 363.0 ^{0}C. The percentage of residual mass provides the thermal stability of the composites. The higher the percentage of residual mass is the indication of improved thermal stability of the composites [34]. The percentage of the residual mass at the end of the heating process 6.74 and 7.15 was found for 100% PS and 10% DPM fiber reinforced PS composite respectively. It can be concluded from the TGA curves that 10% DPM fiber reinforced PS composite is more thermally stable than 100% PS. In case of DSC curve, a sharp endothermic peak was observed at 418.3^0C for 100% PS and at 414.7^0C for 10% DPM fiber reinforced PS composites. These endothermic peaks are corresponded to the melting process of the composite samples. In fact, the presence of the peak in the DSC curve of polystyrene was reported at almost same temperature [35].

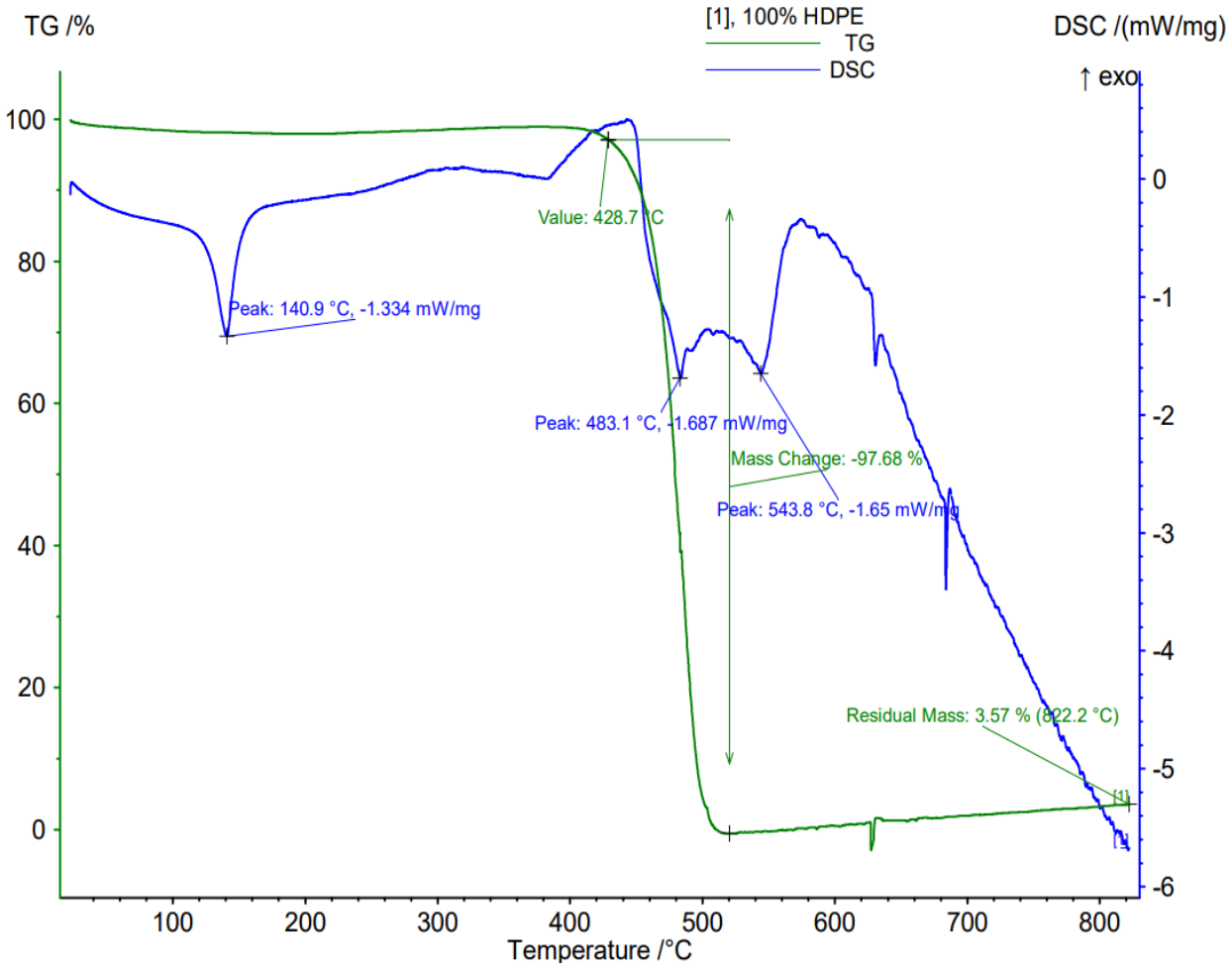

Figure 3.14: TGA and DSC of 100% HDPE

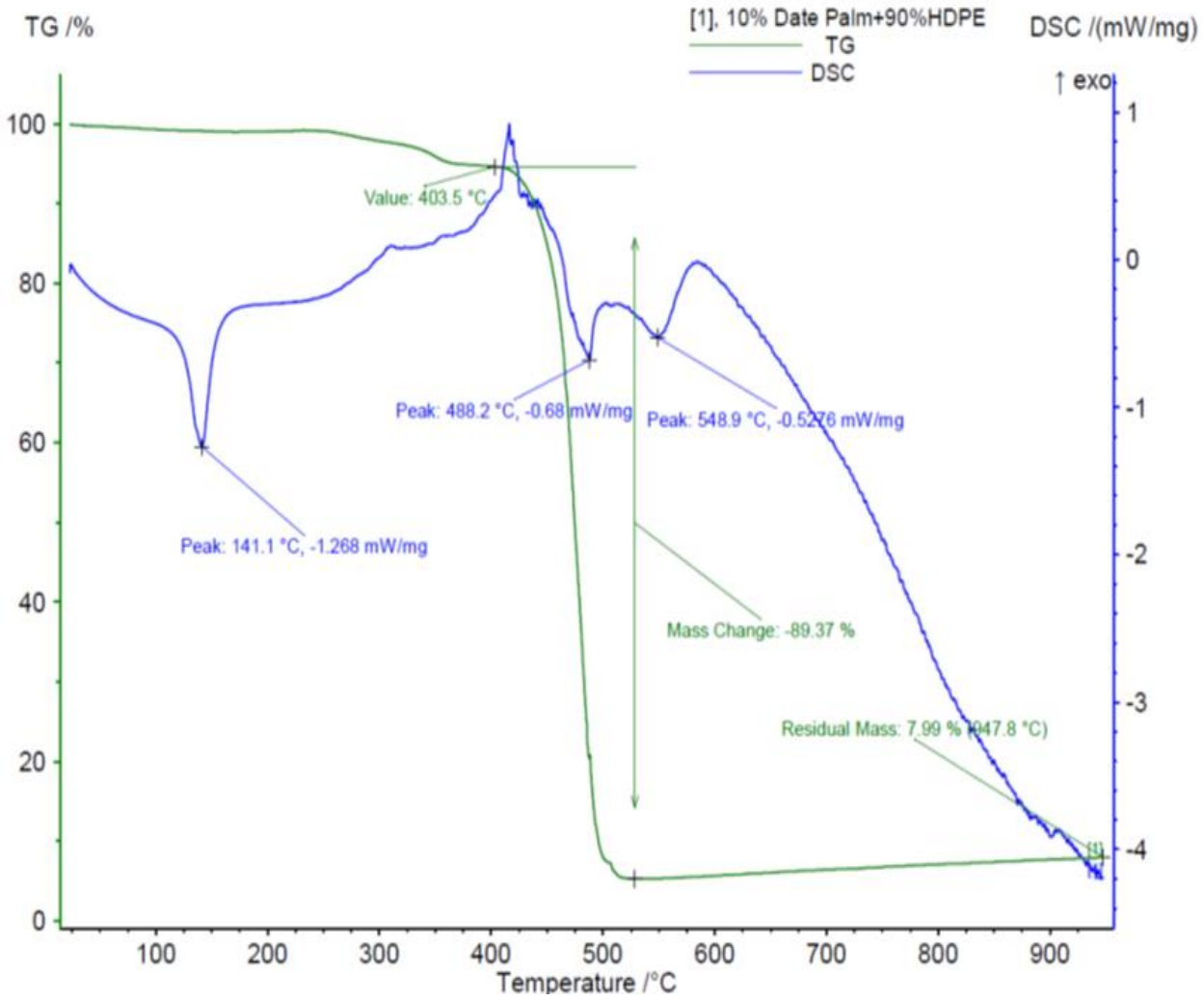

Figure 3.15**:** TGA and DSC of 10% DPM fiber and 90% HDPE composite

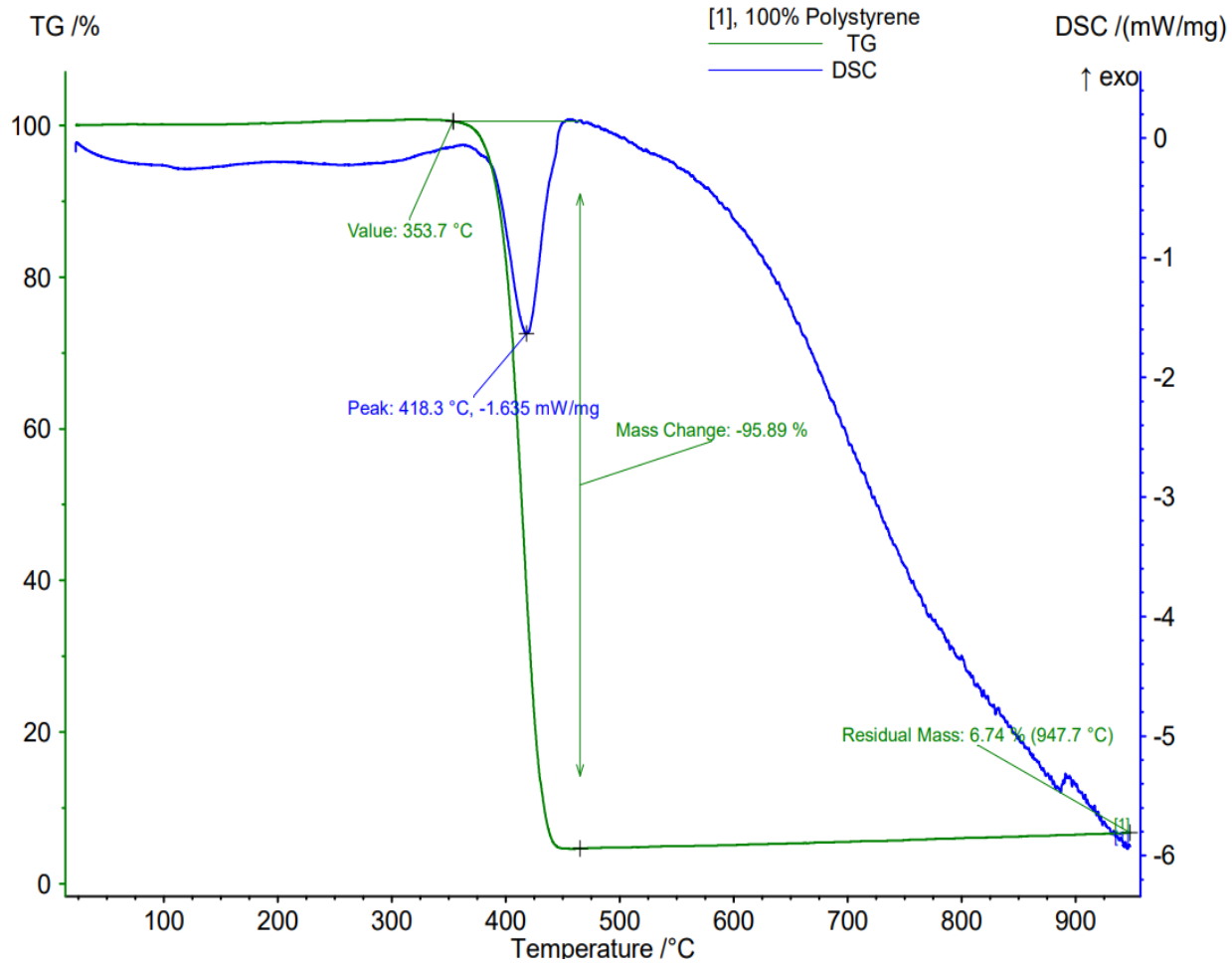

Figure 3.16: TGA and DSC of 100% PS

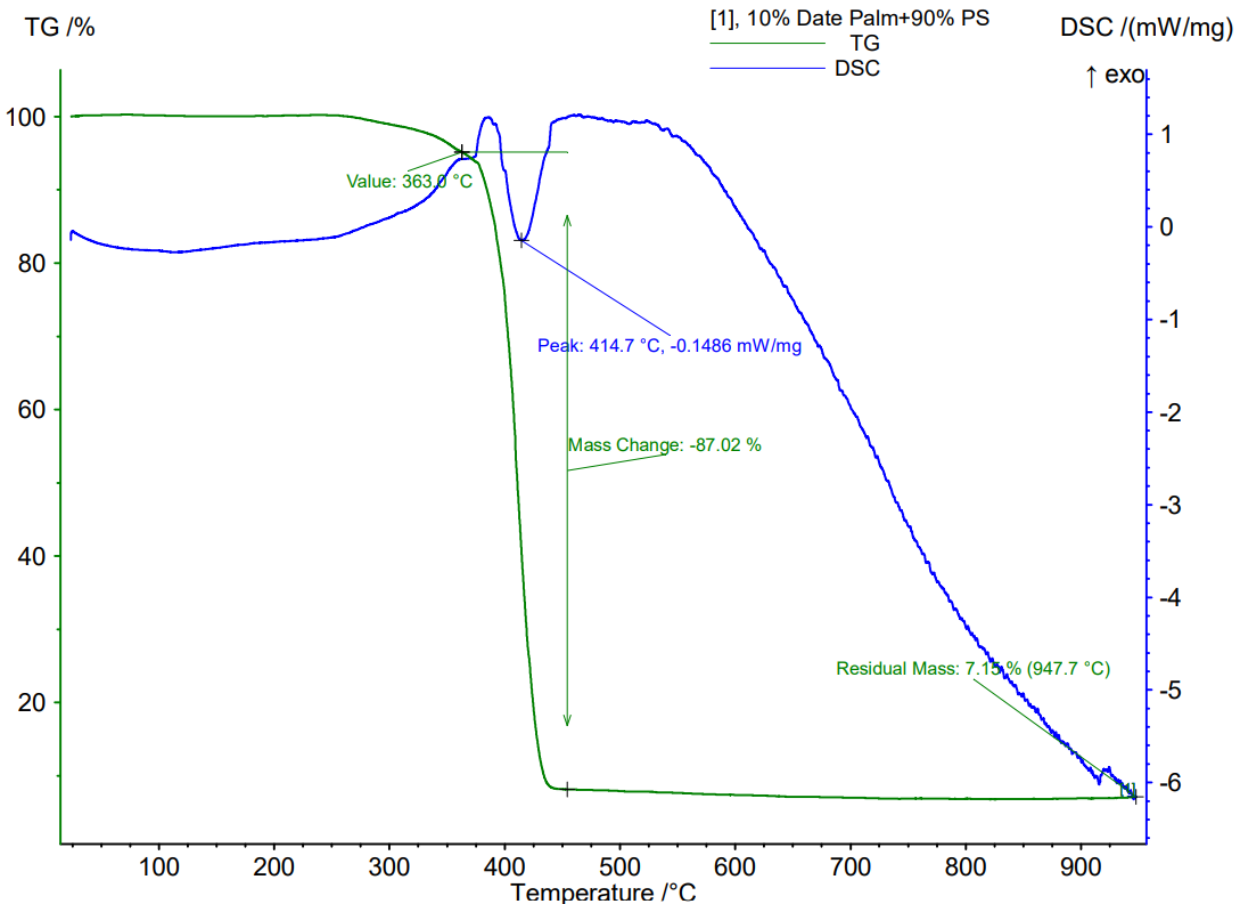

Figure 3.17: TGA and DSC) 10% DPM fiber and 90% PS composite

3.2.6 Morphological Analysis

Scanning Electron Microscope (SEM) analysis is an efficient tool to observe the surface morphology of natural fiber reinforced polymeric composite materials. The surface morphology of the tensile fracture surfaces of the 10% and 25% DPM fiber reinforced composites were inspected and the SEM micrographs in different magnitude are presented in figures 3.18 and 3.19. It can be seen from the figure that the 10% DPM fiber composite showed better fiber-matrix sticking together between fibers and HDPE matrix. In the case of 25% DPM fiber composite the image shows poor interfacial bonding between the fiber and the matrix. Voids and more fiber pull-outs in the composites containing 25% DPM fiber are found and resulted low mechanical properties.

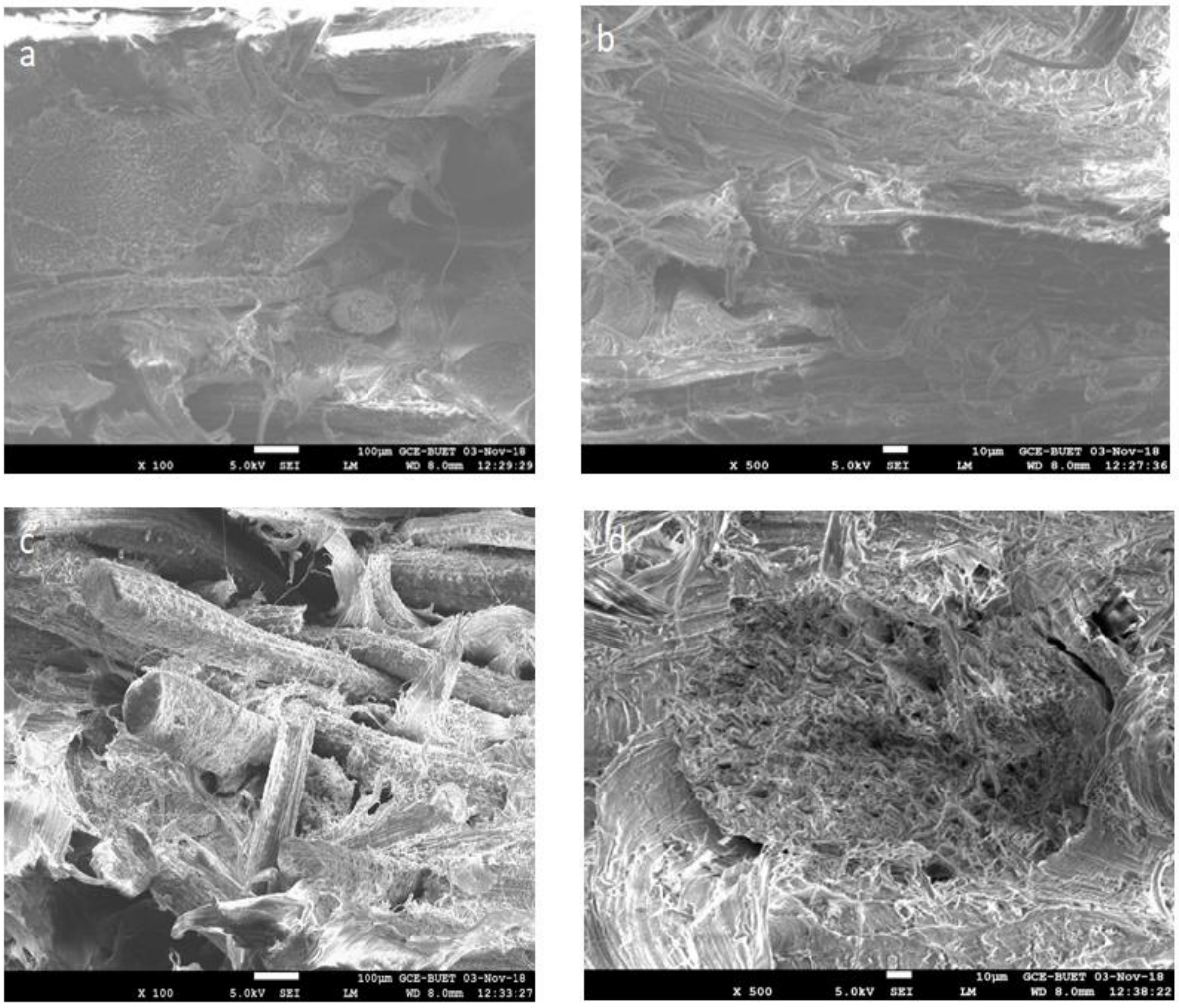

Figure 3.18: SEM micrographs of 10%DPM fiber HDPE composites (a) 100x magnification and (b) 500x magnification and25%DPM fiber HDPE composites (c) 100x magnification and (d) 500x magnification

In the micrographs, fibers are more bonded with the polystyrene matrices suggested the better fiber-matrix adhesion for the composite formulated with 10% DPM fiber and 90% PS. On the contrary, gaps, loosely bonded fibers with the matrices and fiber pull outs are observed for composite containing 25% DPM fiber and 75% PS revealed poor fiber-matrix adhesion. Easy fiber pullouts take place due to this poor fiber-matrix adhesion resulting in lower tensile strength for the 25% DPM fiber reinforced composites as compared to 10% DPM fiber reinforced composites. Sapuan et al. [36] produced short sugar palm fiber loaded high impact polystyrene composites. From the SEM image analysis, they concluded that the 40% and 50% sugar palm fiber loaded composites exhibited compacted arrangement between the fiber and matrix which caused the improvement of strength. Similar compacted arrangement between DPM fiber and polystyrene was observed for 10% DPM fiber reinforced PS composites.

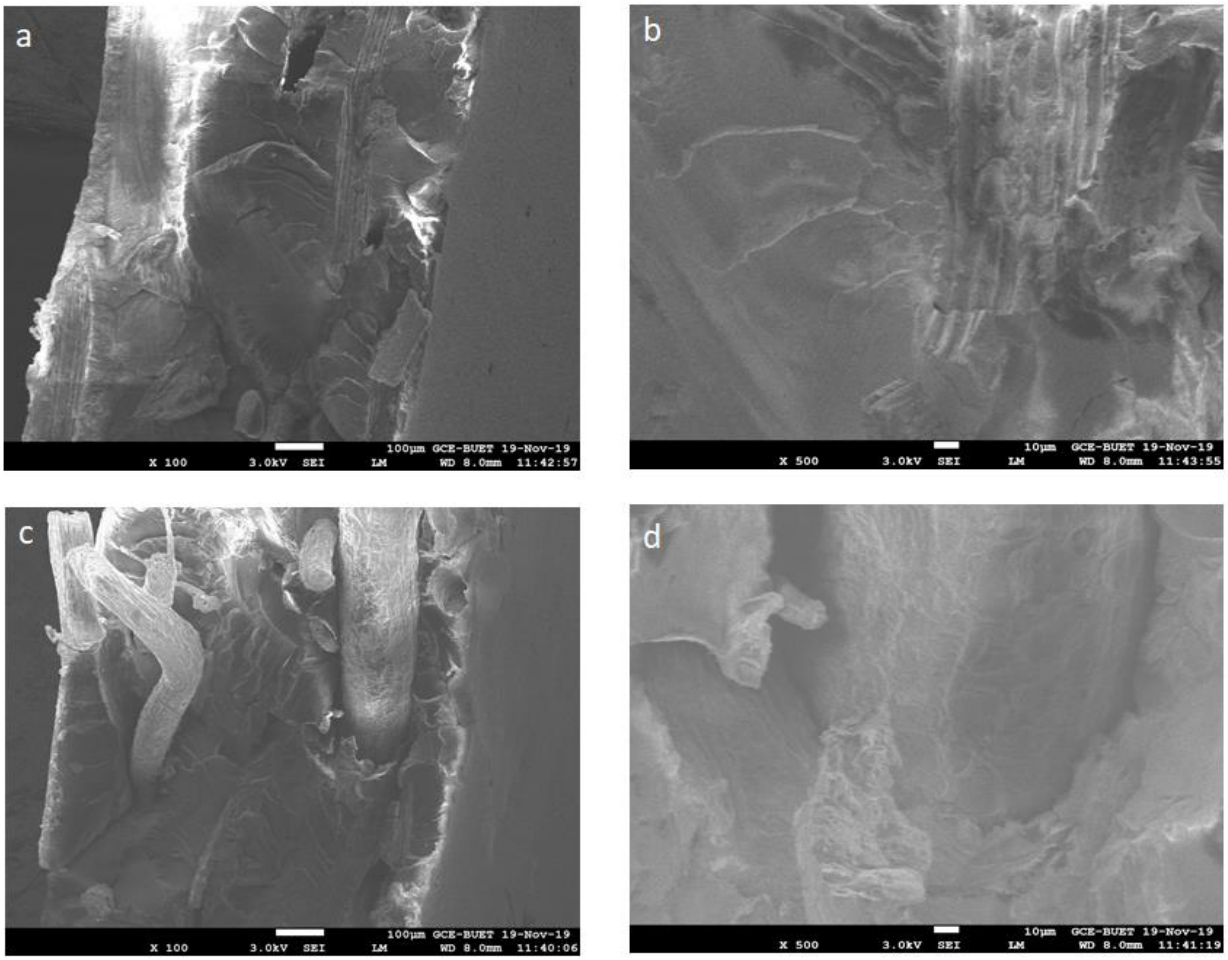

Figure 3.19: SEM micrographs of 10%DPM fiber PS composites (a) 100x magnification and (b) 500x magnification and25%DPM fiber PS composites (c) 100x magnification and (d) 500x magnification

3.3.7 Degradation by Soil Burial

Soil burial experiments of the composites were done in soil for six months. The difference in tensile strength of the composites afterward soil burial was observed. The 5%, 10%, 15%, 20% and 25% fiber reinforced HDPE composites lost 28.2%, 24.1%, 33.8%, 35.2% and 38.8% of tensile strength. The 5%, 10%, 15%, 20% and 25% fiber reinforced PS composites lost 12.2%, 10.9%, 13.8%, 18.5% and 25.1% of tensile strength. From this it is clear that 10% DPM fiber composite retained much of their tensile strength compared to other specimens. All composite samples exhibit an enlarged degradation of soil burial examinations. During soil burial process, moisture penetrated into the composites and the fibers of composite surface and interface degraded slowly causing lower strength. Strong fiber matrix adhesion was observed for 10% DPM fiber reinforced HDPE composites. This may be the cause of slower degradation of 10% DPM fiber reinforced HDPE composites [37].

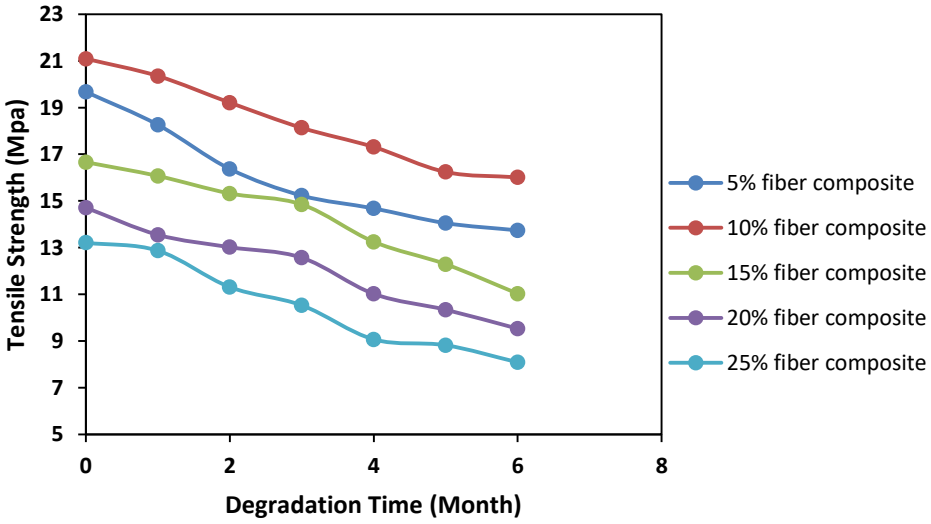

Figure 3.20: Variation of tensile strength of the buried samples of DPM fiber reinforced HDPE at various fiber contents

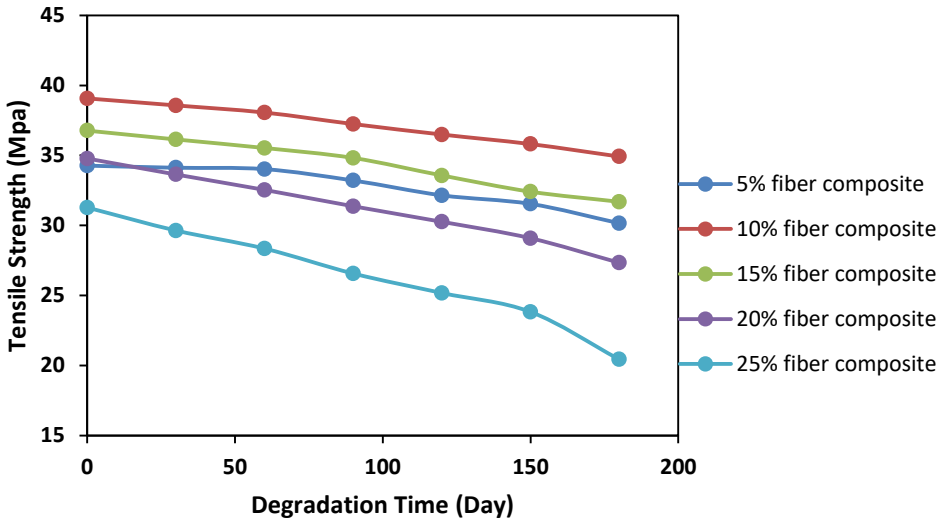

Figure 3.21: Variation of tensile strength of the buried samples of DPM fiber reinforced PS at various fiber contents

3.4 Conclusions

In this study, HDPE, PS as matrix and date palm mat fiber as reinforcement were used for the fabrication of composites by compression moulding technique. The composite samples were characterized with the help of various instrumental techniques. It can be concluded that 10% date palm mat fiber reinforced composite displays better mechanical properties than 5, 15, 20 and 25% of date palm mat fiber reinforced composites. Morphological analysis of tensile fractured surfaces of 10% date palm mat fiber reinforced HDPE and polystyrene composites shown good fiber-matrix interfacial adhesion. The incorporation of 10% DPM fiber in the polymer composites exhibits slightly higher thermal stability. The mechanical properties of the composite formed from date palm mat fiber revealed that they may be a potential choice for diversified applications.

3.5 References

1. Sudhakara, P.; Reddy, K.O.; Prasad C.V.; Jagadeesh D.; Kim H.S.; Kim B.S.; Bae S.I.; Song J.I. Studies on Borassus fruit fiber and its composites with Polypropylene. *Compos. Res.*, **2013**. 26(1), 48-53.
2. Sanjay, M.R.; Arpitha, G.R.; Naik, L.L.; Gopalakrishna, K.; Yogesha, B. Applications of Natural Fibers and Its Composites: An Overview, *Nat. Resour*. **2016**, 07, 108–114. https://doi.org/10.4236/nr.2016.73011.
3. Vignesh S.; Alagarsamy S. V.; Saravanan H. A review on natural fibre reinforced polymer composites. *Int.J. of Eng. Sci. & Res. Technol.*, **2016,** 5(10), 786-791.
4. Bhattacharjee S.; Sazzad M.H.; Islam M.A.; Ahtashom M.M.; Asaduzzaman; Miah M.Y. Effects of Fire Retardants on Jute Fiber Reinforced Polyvinyl Chloride/Polypropylene Hybrid Composites. *Int. J. of Mater. Sci. and Appl.*, **2013**, 2(5), 162-167.
5. Nguyen, T. A.; Nguyen, T. H. Study on Mechanical Properties of Banana Fiber-Reinforced Materials Poly (Lactic Acid) Composites, **2022**, Article ID 8485038 1687-806X, https://doi.org/10.1155/2022/8485038
6. Ahmed, S.; Ahsan, A.; Hasan, M. Physico-mechanical properties of coir and jute fibre reinforced hybrid polyethylene composites, *Int. J. of Aut. and Mech. Eng.*, ISSN: 2229-8649 (Print); ISSN: 2180-1606 (Online); **2017**, 14(1), 3927-3937, https://doi.org/10.15282/ijame.14.1.2017.9.0319
7. Ameer, M. H.; Nawab, Y.; Ali, Z.; Imad, A.; Ahmad, S. Development and characterization of jute/polypropylene composite by using comingled nonwoven structures, *The J. of The Tex. Inst.*, **2019**. https://doi.org/10.1080/00405000.2019.1612502
8. Mustaffa, Z.; Ragunathan, S.; Othman, N. S.; Ghani, A. A.; Mustafa, W. A.; Farhan, A. M.; Zunaidi, I.; Razlan, Z. M.; Wan W. K.; Shahriman, A. B. Fabrication and Properties of Polypropylene and Kenaf Fiber Composite, *IOP Conference Series: Mater. Sci. and Eng.*, 429, 012016, **2018**, DOI 10.1088/1757-899X/429/1/012016.
9. Vallejos, M.E.; Aguado, R.J.; Morcillo-Martín, R.; Méndez, J.A.; Vilaseca, F.; Tarrés, Q.; Mutjé, P. Behavior of the Flexural Strength of Hemp/Polypropylene

Composites: Evaluation of the Intrinsic Flexural Strength of Untreated Hemp Strands, *Polymers* **2023**, 15, 371. https://doi.org/10.3390/polym15020371

10. Kumar, N. R.; Rao, C.H. R.; P. Srikant, B.; Rao, R. Mechanical properties of corn fiber reinforced polypropylene composites using Taguchi method, *Mater. Today: Proc.*, **2015**, 2(4–5), 3084-3092, ISSN 2214-7853, https://doi.org/10.1016/j.matpr.2015.07.251.
11. Sayeed, M.M.A.; Sayem, A.S.M.; Haider, J.; Akter, S.; Habib, M.M.; Rahman, H.; Shahinur, S. Assessing Mechanical Properties of Jute, Kenaf, and Pineapple Leaf Fiber-Reinforced Polypropylene Composites: Experiment and Modelling, *Polymers*, **2023**, 15, 830. https://doi.org/10.3390/polym15040830
12. Kumar, S.; Shamprasad, M.S.; Varadarajan, Y.S.; Sangamesha, M.A. Coconut coir fiber reinforced polypropylene composites: Investigation on fracture toughness and mechanical properties, *Mater. Today: Proc.*, **2021**, 46(7), 2471-2476, ISSN 2214-7853. https://doi.org/10.1016/j.matpr.2021.01.402.
13. Sanjita, W.; Surbhi, K.; Pritesh, Y.; Halil, T.; Soydan, O.; Uday, V. Bamboo fiber reinforced polypropylene composites for transportation applications, *Front. in Mater.*, **2022**,.9, , https://www.frontiersin.org/articles/10.3389/fmats.2022.967512
14. Mahbub, H.; Reza, A.; Azman, H.; Khaliq M.; Zainoha, Z. Rice Husk Filled Polymer Composites, *Int. J. of Polym. Sci.*, Hindawi Publishing Corporation, **2015**, Article ID 501471, 1687-9422, https://doi.org/10.1155/2015/501471
15. Raghavendra, S. Mechanical Properties of Hybrid Composites with Date Palm Fibre Reinforcement, *Adv. Mater.*, **2018**, 7, 78. https://doi.org/10.11648/j.am.20180703.14.
16. Nur, H.P.; Hossain, M.A;, Sultana, S.; Mollah M. M. Preparation of Polymer Composites using Natural Fiber and their Physico-Mechanical Properties. *Bangladesh J. of Sci. and Ind. Res.*, **2010,** 45(2): 117-122.
17. Jahan, A.; Rahman, M.M.; Kabir, H.; Kabir, M. A.; Ahmed, F.; Hossain, A.M.; Gafur, M.A. Comparative Study of Physical and Elastic Properties of Jute and Glass Fiber Reinforced LDPE Composites, *Int. J. of Sci.& Technol. Res.*, **2012,** 1(10): 68-72.
18. Gennusa, M.L.; Massana P.L.; Montero, J. I.; Peña, F. J.; Rieradevall, J.; Ferrante, P.; Scaccianoce, G.; Sorrentino, G. Composite Building Materials: Thermal and

Mechanical Performances of Samples Realized with Hay and Natural Resins, *Sustainability*, **2017**. 9, 373.

19. Badaruzzaman, W.H.W.; Dabbagh, N.M.R.; Salleh, K.M.; Saharuddin, E.N.; Radzi, N.F.M.; Azham, M.A.A.; Sani, S.F.A.; Zakaria, S. Mechanical Properties and Water Absorption Capacity of Hybrid GFRP Composites, *Polymers (Basel).* **2022**, 14, 1–10. https://doi.org/10.3390/polym14071394.
20. Sanjeevi, S.; Shanmugam, V.; Kumar, S.; Ganesan, V.; Sas, G.; Johnson, D.J.; Shanmugam, M.; Ayyanar, A.; Naresh, K.; Neisiany, R.E.; Das, O. Effects of water absorption on the mechanical properties of hybrid natural fibre/phenol formaldehyde *composites, Sci. Rep.* **2021**, 11, 1–11. https://doi.org/10.1038/s41598-021-92457-9.
21. Das, G.; Biswas, S. Physical, Mechanical and Water Absorption Behaviour of Coir Fiber Reinforced Epoxy Composites Filled with Al2O3 Particulates, *IOP Conf. Ser. Mater. Sci. Eng.* **2016**, 115. https://doi.org/10.1088/1757-899X/115/1/012012
22. Kumari, Y. R.; Ramanaiah, K.; Prasad A. V. R.; Reddy, K. H.; Sanaka, S. P.; Prudhvi, A. K. Experimental investigation of water absorption behaviour of sisal fiber reinforced polyester and sisal fiber reinforced poly lactic acid composites, *Mater. Today Proc.* **2021**, 44, 935–940. https://doi.org/10.1016/j.matpr.2020.11.002.
23. Azammi, A.M. N.; Sapuan, S.M.; Ishak, M.R.; Sultan, M.T.H. Mechanical and Thermal Properties of Kenaf Reinforced Thermoplastic Polyurethane (TPU)-Natural Rubber (NR) Composites, *Fibers Polym.* **2018**, 19, 446–451. https://doi.org/10.1007/s12221-018-7737-7.
24. Zadeh, K.M.; Inuwa, I.M.; Arjmandi, R.; Hassan, A.; Almaadeed, M.Z.; Mohamad; Khanam, P.N. Effects of date palm leaf fiber on the thermal and tensile properties of recycled ternary polyolefin blend composites, *Fibers Polym.* **2017**, 18, 1330–1335. https://doi.org/10.1007/s12221-017-1106-9.
25. Chowdhury, H.; Rahman, M.M.; Uddin, M.T.; Rahman, M.M. Improvement of mechanical properties of polypropylene composite using filler, modifier and reinforcement, *J. Phys. Conf. Ser.* **2018**, 1086. https://doi.org/10.1088/1742-6596/1086/1/012003.
26. Rahaman, M. N.; Hossain, M. S.; Razzak, M.; Uddin, M.B.; Chowdhury, A.M.S.;. Khan, R.A. Effect of dye and temperature on the physico-mechanical properties of

jute/PP and jute/LLDPE based composites, *Heliyon*. **2019**, 5 e01753. https://doi.org/10.1016/j.heliyon.2019.e01753.

27. Huq, T.; Khan, A.; Hossain, F.M.J.; Akter, T.; Zaman, H.U.; Aktar, N.; Tuhin, M.O.; Islam T.; Khan, R.A. Gamma-irradiated jute/polypropylene composites by extrusion molding, *Compos. Interfaces.* **2013,** 20, 93–105,. https://doi.org/10.1080/15685543.2013.762741.
28. Sutar, H. , Sahoo C., P. , Sahu S., P. , Sahoo, S. , Murmu, R. , Swain, S. and Mishra C., S., Mechanical, Thermal and Crystallization Properties of Polypropylene (PP) Reinforced Composites with High Density Polyethylene (HDPE) as Matrix, *Mater. Sci. and Appl.s*, **2018**, 9, 502-515, doi: 10.4236/msa.2018.95035.
29. Kamarudin, S. H.; Abdullah, L. C.; Aung, M. M.; Ratnam, C. T. A study of mechanical and morphological properties of PLA based biocomposites prepared with EJO vegetable oil based plasticiser and kenaf fibres, IOP Conf. Series: *Mater. Sci. and Eng.*, **2018,** 368, doi:10.1088/1757-899X/368/1/012011
30. Singh, A. A.; Palsule, S. Composite Interfaces (2013): Jute fiber-reinforced chemically functionalized high density polyethylene (JF/CF-HDPE) composites with in situ fiber/matrix interfacial adhesion by Palsule Process, *Compos. Interfaces*, **2013,** http://dx.doi.org/10.1080/15685543.2013.813192
31. Kreutz, J.C.; de Souza, P.R.; Benetti, V.P.; Freitas, A. R.; Bittencourt, P.R.S.; Gaffo, L., Mechanical and thermal properties of polystyrene and medium density fiberboard composites, *Polimeros*, **2021,** 31, 1–7,. https://doi.org/10.1590/0104-1428.07120.
32. Chauhan, R.S.; Gopinath, S.; Razdan, P.; Delattre, C.; Nirmala, G.S.; Natarajan, R. Thermal decomposition of expanded polystyrene in a pebble bed reactor to get higher liquid fraction yield at low temperatures, *Waste Manag.* **2008,** 28**,** 2140–2145. https://doi.org/10.1016/j.wasman.2007.10.001.
33. Onifade, D.V.; Ighalo, J.O.; Adeniyi, A.G. Morphological and Thermal Properties of Polystyrene Composite Reinforced with Biochar from Plantain Stalk Fibre, *Mater. Int.* **2020**, 2, 150–156. https://doi.org/10.33263/materials22.150156
34. Muthukumar, C.; Krishnasamy. S.; Thiagamani S.M.K.; Nagarajan R.; Siengchin S., Thermal Characterization of the Natural Fiber-Based Hybrid Composites: An Overview, *Nat. Fiber-Reinforced Compos.* **2022**, 1–15. https://doi.org/10.1002/9783527831562.ch1.

35. Kurort, T.; Sekiguchi, Y.; Ogawa, T.; Sawaguchi, T.; Ikemusa, T.; Honda, T. Thermal Degradation of Polystyrene, *Nippon Kagak. Kaishi*. **1977**, 894–901. https://doi.org/10.1246/nikkashi.1977.894.
36. Sapuan, S.M.; Bachtiar, D. Mechanical Properties of Sugar Palm Fibre Reinforced High Impact Polystyrene Composites, *Procedia Chem.* **2012**, 4, 101–106. https://doi.org/10.1016/j.proche.2012.06.015.
37. Siakeng, R.; Jawaid, M.; Asim, M.; Siengchin, S. Accelerated Weathering and Soil Burial Effect on Biodegradability, Colour and Textureof Coir/Pineapple Leaf Fibres/PLA Biocomposites, *Polymers*, **2020,** 12, 458.

CHAPTER 4

Preparation and Characterization of NaOH Treated DPM Fiber Reinforced Composites

4.1 Introduction

Scientists are showing enormous potential for advancing the creation of eco-friendly, biomaterials reinforced sustainable green composites and its use in various sector such as sports, automobile, pharmaceutical, packaging, and construction [1,2]. Resources from nature are used to create green composites and natural fibers are one of them. Natural fibers have a number of advantages over synthetic fibers, such as being recyclable, being simple to manufacture and shape, and being more affordable. The use of natural fibers as reinforcing components in polymer composites is growing in popularity due to its favorable environmental advantages, ease of supply, cheaper, and biodegradability [3]. Although synthetic fibers are now the most common, natural fibers have showed encouraging outcomes when utilized to reinforce composites. Besides being pricey, synthetic fiber-reinforced polymers may be harmful to the environment. Without a doubt, natural fibers are a good choice as an alternative to synthetic fibers in polymer composites. The use of natural fibers in combination with thermoplastic materials is growing with the aim of achieving both great volume and inexpensive [4]. Cellulose, hemicellulose, and lignin are the main components of natural fibers. There are several hydrophilic groups on the surfaces of natural fibers [5]. Lignin and hemicelluloses encircle and bind the cellulose. When natural fibers are reinforced with hydrophilic matrices, the hydroxyl groups in the cellulose result hydrophilic nature of natural fibers. As a result, the interface has weak resistance to moisture absorption [6]. A number of processes, including chemical, thermal, and mechanical ones, can lessen the issues brought on by the fiber's inherent properties [7]. Among the processes, chemical modifications are widely used to improve the fiber’s interface. Activation of hydroxyl groups or introduction of new moieties may develop through chemical modifications which can result an effective interlocking between fiber and matrix. One such widely used chemical treatment is alkali treatment [6]. The bleaching activity of the alkali, which eliminates the hemicellulose, waxy material, and other impurities, causes the fibers to undergo structural changes throughout the alkali treatment [8]. As a result of the removal of impurities like hemicellulose, pectin, and lignin from the fiber cell wall's surface during alkali treatment, the adhesion between fiber and matrices is improved. This causes the improvement in the mechanical properties of the natural fiber composites [9].

The current research endeavor aims to investigate the effects of alkali treatment (NaOH) of fibers at various concentrations of 2%, 5%, and 8% on the mechanical properties of composites. DPM fibers were subjected to FTIR spectroscopy and SEM analysis on both untreated and treated fibers to examine the structural changes of fibers. NaOH treated DPM fiber reinforced HDPE composites were prepared by compression moulding technique. The mechanical, thermal and morphological properties of the DPM fiber reinforced HDPE composites were studied.

4.1 Experimental

4.2.1 Materials

HDPE was purchased from Saudi Polymers Company, Saudi Arabia. HDPE granules were ground by a grinding machine. Sodium hydroxide (NaOH) was used as received from Merck, Germany. DPM fibers were collected from the rural area of Jashore, Bangladesh. The DPM fibers were cut into 2-3mm by hand scissors.

4.2.2 Surface modification of Date Palm Mat Fiber

Different concentrations of NaOH solution (2%, 5%, and 8%) was prepared for the surface modification of DPM fiber. The DPM fibers were immersed in NaOH solution (1:20 g/ml) at room temperature for 1 h and stirred occasionally. The treated fibers were washed with distilled water until neutral and dried in an oven.

Fiber – OH + NaOH → Fiber – O – Na + H2O + impurity [10]

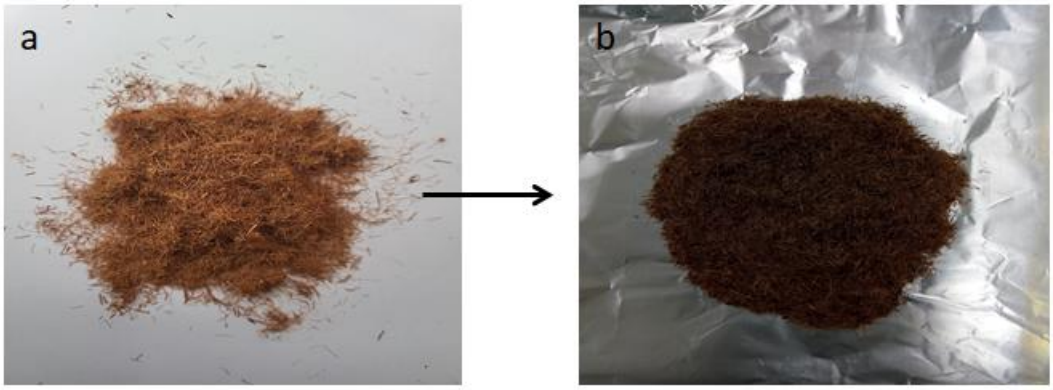

Figure 4.1: Photographs of (a) Chopped DPM fiber and (b) NaOH treated DPM fiber

4.2.3 Composite Fabrication

Compression moulding technique was used to fabricate the composites. HDPE with DPM fibers were mixed using a blender. The mixed fibers and HDPE were transferred to the mould (12x15 cm^2) and finally hot pressed (Paul Otto Weber Press Machine) at a temperature of 160^0C for 5 min maintaining a pressure of 200 kN. The moulds were cooled at room temperature and under 200 kN pressure for 5 min and removed from the mould.

4.2.4 Bulk Density of the composites

Bulk density of the composites was calculated by measuring the weight and dimensions of the samples utilizing the following equation 4.1. The average results for five composite samples were stated.

$$D = \frac{Weight\ of\ the\ composite}{(Length \times Width \times Height)\ of\ the\ composite} \quad (4.1)$$

4.2.5 Water absorption test of Composites

Water absorption tests of the composite samples were done following ASTM D570-99. The test samples were dried in an oven at 105^0C for 2h and cooled in a desiccator. The composite samples were weighed and dipped in distilled water for 24h at room temperature. The samples were withdrawn from the beaker, removed excess water with a cloth and weighed. Three composite samples were tested to get the average results. The percentage of water absorption was calculated as follows:

$$\text{Increase in weight, \%} = \frac{(\text{wet wt} - \text{conditioned wt})}{(\text{conditioned wt})} \times 100 \quad (4.2)$$

4.2.6 Mechanical Properties

Tensile properties such as tensile strength, percent elongation at break of the composites were measured using universal strength tester (model 1410 Titans, capacity 5 kN, England). The crosshead speed was 10 mm/min. The tests were carried out according to standard method (ASTM D 3039/D 3039 (M) 2002). The average values of five specimens were stated in each case. Bending strength (three point bending) of the composites was also performed following

ASTM D7900. Five measurements in each composition of the composite samples were taken and the average values were reported.

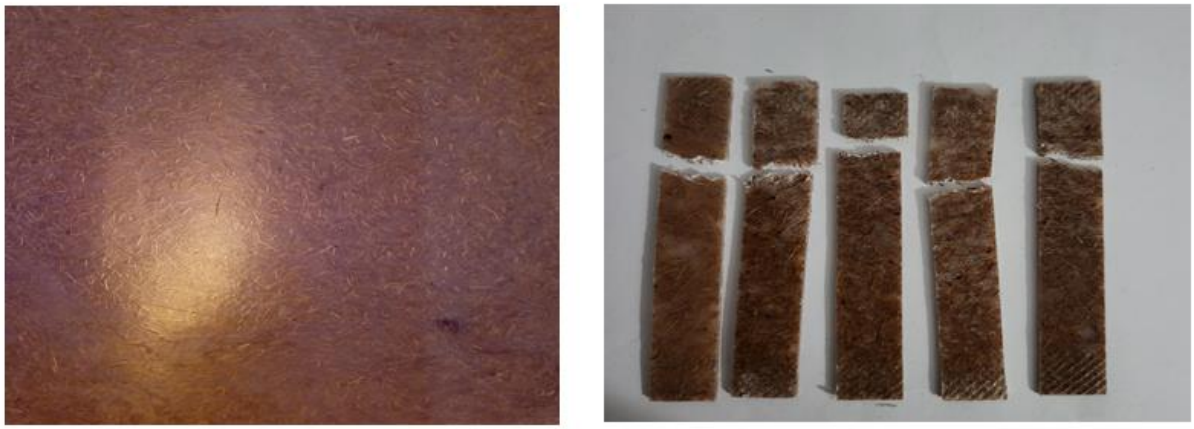

Figure 4.2: Photographs of the (a) prepared composite and (b) samples for tensile strength after testing

4.2.7 FTIR Spectroscopy

The fibers were examined by a FT-IR/NIR spectrometer (Frontier, Perkin Elmer, USA). The FTIR spectra were recorded in the region 4,000-650 cm^{-1}. FT-IR spectroscopy was used to find out the functional group of the fibers.

4.2.8 Thermal Analysis

The thermogravimetric (TGA) and differential scanning calorimetry (DSC) analysis of the composite samples were performed by a NETZSCH instrument (STA 449 F3, Jupiter) in a temperature range 30-900^{0}C at nitrogen atmosphere. The heating rate was 10^{0}C/min.

4.2.9 Surface Morphology

The raw fiber, alkali treated fiber and the fracture surfaces of the tensile specimens were examined by a field emission scanning electron microscope (JEOL JSM-7600F) operated with an accelerating voltage of 5.0 kV. The samples were cut into a small portion, mounted onto holders using carbon tape and coated with gold. The composite samples were focused onto the surfaces and observed with different magnification.

4.2.10 Soil Burial Test

The composite samples were buried in a soil containing flower pot and the moisture level was kept at least 30%. The test samples were removed from the soil at intervals of 1 month, washed with distilled water and dried at 80^0C in an oven for 6 h. The degradation was determined on the basis of measuring the tensile strength of the specimen.

4.3 Results and Discussion

4.3.1 Bulk Density of the Composites

The effect of various concentrations of NaOH on the bulk density of the composites is shown in figure 4.3. The bulk density of short DPM fiber reinforced HDPE composites increases from 2 to 5% NaOH concentration then decreases slightly at 8% NaOH concentration. The elimination of wax, fat, and other contaminations from the fiber enhanced the bulk density [11].

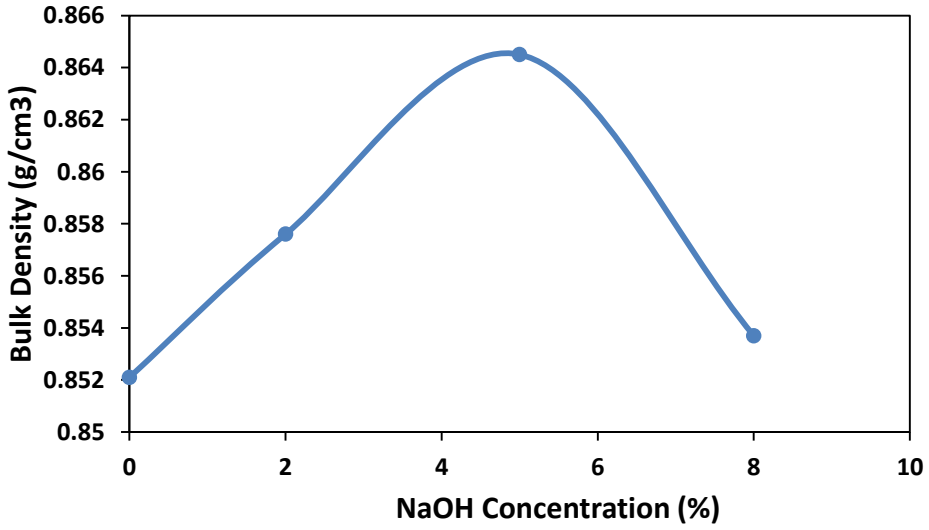

Figure 4.3: Bulk density of the DPM fiber reinforced HDPE composites at various NaOH concentrations

4.3.2 Water Absorption of the Composites:

The effect of NaOH concentration on water absorption of the composites was studied and it exposes that the water absorption of the composites decreases up to 5% NaOH concentration.

The lowest water absorption was found for 5% NaOH concentration. The main constituents of natural fibers are cellulose, hemicellulose and lignin. All of these constituents contain hydroxyl groups. This may be as a result of water molecules forming hydrogen bonds with the hydroxyl groups in the components of lignin, hemicellulose, and cellulose in raw DPM fiber. However, alkali treatment removes hemicellulose and lignin of the DPM fiber completely or partially and therefore, the internal structure becomes less hydrophilic [12]. Hence, NaOH treated DPM fiber reinforced HDPE composites absorb a reduced amount of water than raw DPM fiber reinforced HDPE composites.

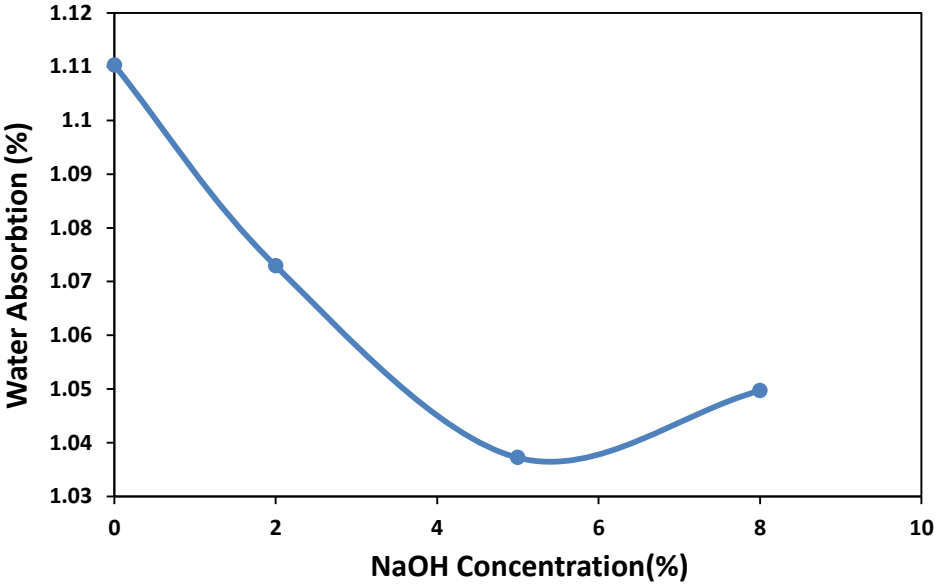

Figure 4.4: Water absorption of the DPM fiber reinforced HDPE composites at various NaOH concentrations

4.3.3 Mechanical Properties

Figure 4.5 shows the effect of the variation of NaOH concentration on the tensile strength of the composites. The graph shows that the tensile strength of the composites increased up to a 5% NaOH concentration and declined for 8% NaOH concentration. The maximum tensile strength was recorded 23.56 MPa for the composite samples at 5% NaOH concentration. 5% NaOH treated DPM fiber reinforced HDPE composites showed higher tensile strength than control (untreated composites). Hemicellulose, lignin, wax, and other surface impurities in the

fiber were eliminated as a result of the alkali treatment which caused better interaction between fiber and matrix. It also causes the fiber's surface to become rougher and improve the fiber-matrix adhesion [13].

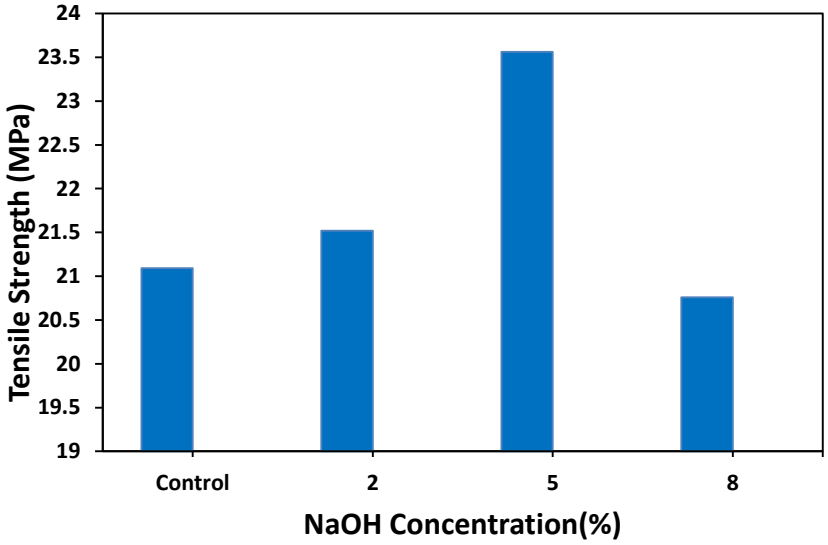

Figure 4.5: Tensile strength of DPM fiber reinforced HDPE composites at various NaOH concentrations

The effect of NaOH concentration on the elongation at break values of the composites is represented in figure 4.6. The elongation at break of composite was improved with increasing NaOH concentration up to 5 %, and then started diminishing for 8 % NaOH concentration. Dahham et al. stated that the increase in elongation at break of the NaOH treated *Cyperus Odoratus* /polypropylene composites [14]. Their findings are similar with our results.

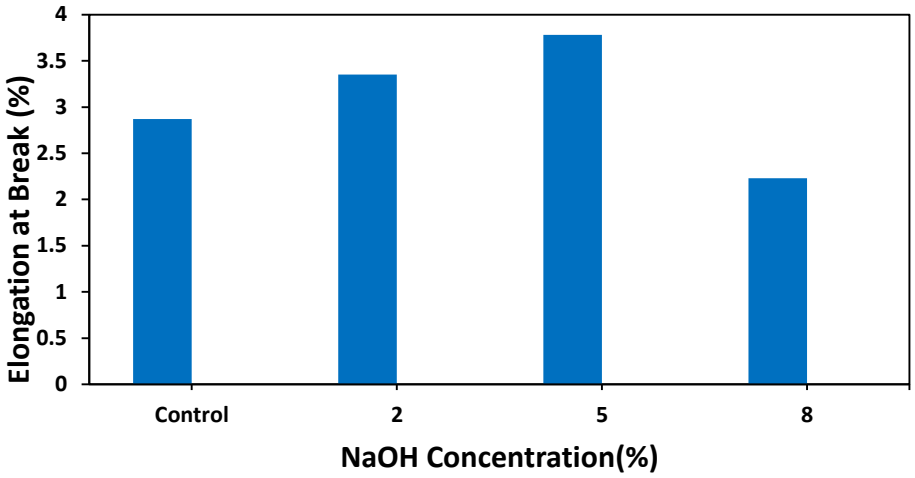

Figure 4.6: Elongation at break of DPM fiber reinforced HDPE composites at various NaOH concentrations

The effect of NaOH concentrations on the bending strength of the composite samples is illustrated in figure 4.7. It is seen from the figure that bending strength of the composites was increased with increasing NaOH concentrations. The bending strength of 5% NaOH treated DPM fiber reinforced composites enhanced by 12.92% in comparison with the control (untreated composites). This may be due to the removal of lignin, hemicellulose and other impurities during alkali treatment as a result of superior interfacial adhesion between the polymer matrix and fibers [15].

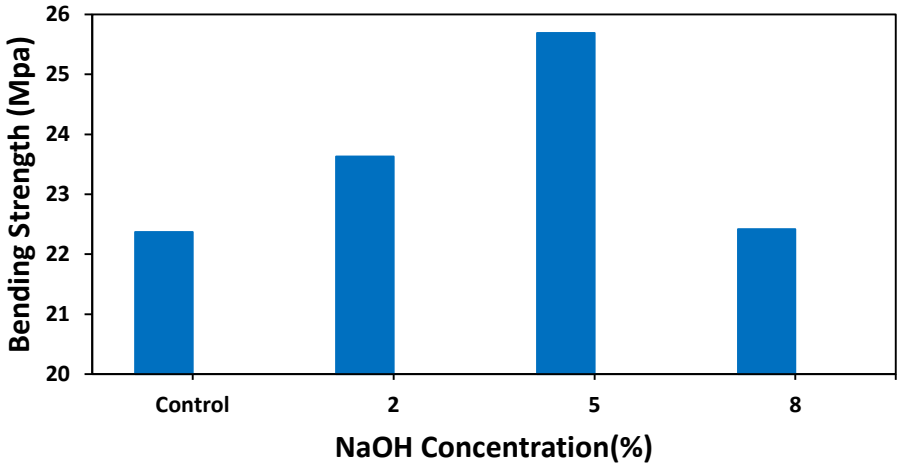

Figure 4.7: Bending strength of DPM fiber reinforced HDPE composites at various NaOH concentrations

4.3.4 FTIR Spectroscopy

The figure 4.8 shows FTIR spectra of raw DPM fiber and 5% NaOH treated DPM fiber. The absorption band at 3324 and 3327 cm^{-1} represent O–H stretching vibration of the hydroxyl groups in raw fibers and 5% NaOH treated DPM fiber respectively [16]. The peaks at 2929 and 2924 cm^{-1} indicate the C–H stretching of cellulose, hemicellulose and lignin in raw fibers and 5% NaOH treated DPM fiber respectively [17]. The absorption peak at 1728 cm^{-1} in raw DPM fiber resembles to the carbonyl (C=O) stretching vibrations of carboxyl and acetyl groups in hemicelluloses [11]. After NaOH treatment, the absorbance band at 1728 cm^{-1} is absent in the DPM fibers. The peak at 1610 and 1599 cm^{-1} is associated to absorbed water molecules in carbohydrates for raw fibers and 5% NaOH treated DPM fiber respectively [18]. The peak at 1508 and 1507 cm^{-1} signifies the C=C stretching vibration of the aromatic ring in lignin for raw fibers and 5% NaOH treated DPM fiber respectively [19]. The peak at 1423 cm^{-1} indicates CH_2 symmetric bending in hemicellulose [20] which is absent in 5% NaOH treated DPM fiber. The absorption peak at 1239cm^{-1} is resulting from the vibration and stretching of C–O, ascribed the existence of acetyl group in lignin and hemicellulose [21]. The peak at 1032 and 1029 cm^{-1} corresponds to the C-O stretching vibrations of the polysaccharide in cellulose for raw fibers and 5% NaOH treated DPM fiber respectively [22].

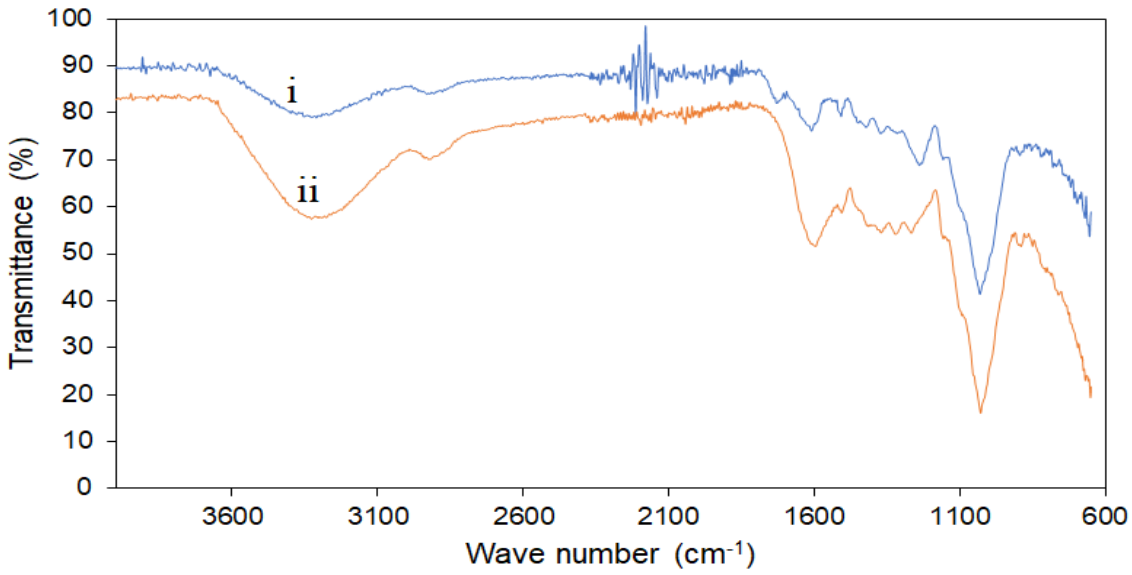

Figure 4.8: ATR-FTIR spectra of (i) raw DPM fiber; (ii) 5% NaOH treated fiber

4.3.5 Thermal Analysis

Thermal analysis of 10% DPM fiber reinforced HDPE (control), and 5%NaOH treated DPM fiber reinforced composites were examined to determine their thermal stability. In figure, the TGA and DSC curves are shown. The TGA results show that the untreated DPM fiber reinforced HDPE composites undergoes thermal degradation beginning at 403.5 ^{0}C and with a total mass change of 97.62%. On the other hand, the degradation of 5% NaOH treated DPM fiber reinforced HDPE composites takes place in two stages. In the first stage, the degradation starts at 280.0 ^{0}C and in the second stage, the degradation start at 425.8 ^{0}C with a total 97.62% mass change. For untreated DPM fiber and 5% NaOH treated DPM fiber reinforced HDPE composites, the percentage of the residual mass at the finish of the heating process was 7.99 and 2.38 respectively. The DSC curves of untreated DPM fiber and 5% NaOH treated DPM fiber reinforced HDPE composites showed peaks of melting at 141.1 and 160.3 ^{0}C respectively. The melting temperature of the composites increased, this is due to the presence of DPM fiber. 5% NaOH treated DPM fiber reinforced composites is thermally more stable than untreated DPM fiber due to high melting temperature.

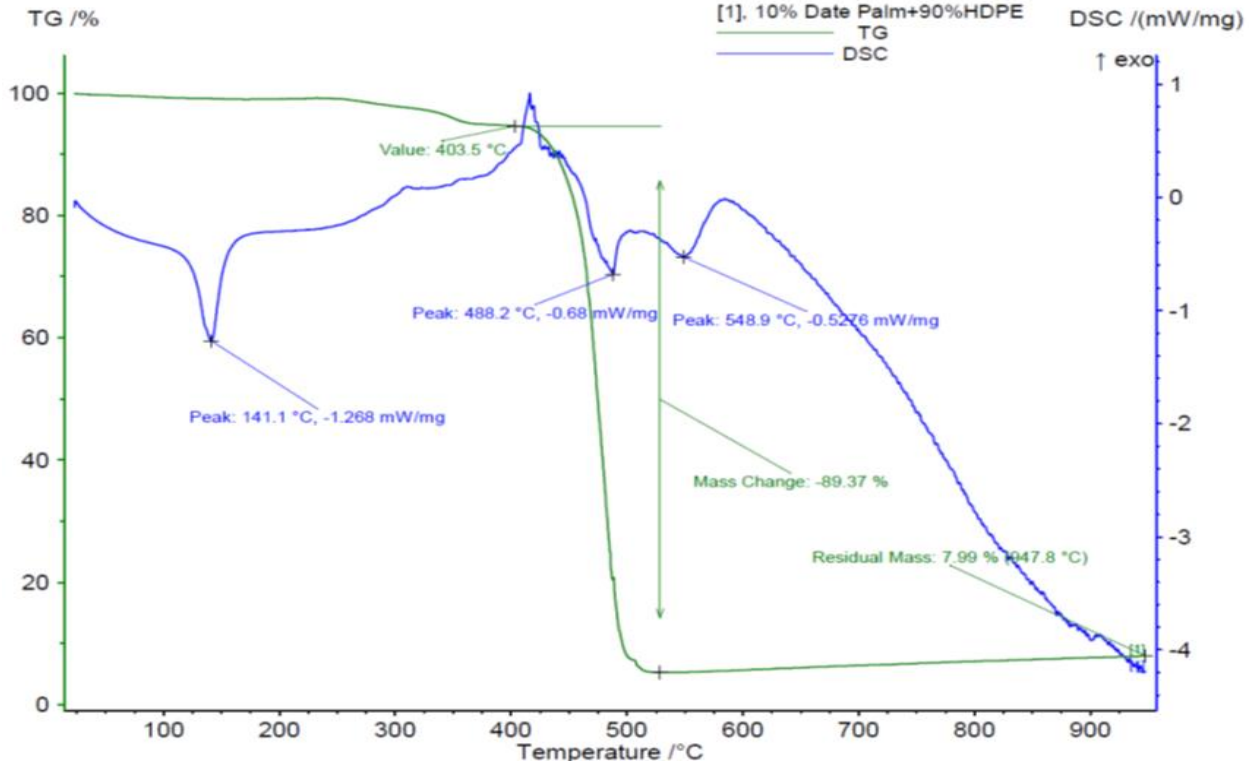

Figure 4.9: TGA and DSC of untreated DPM fiber reinforced HDPE composite

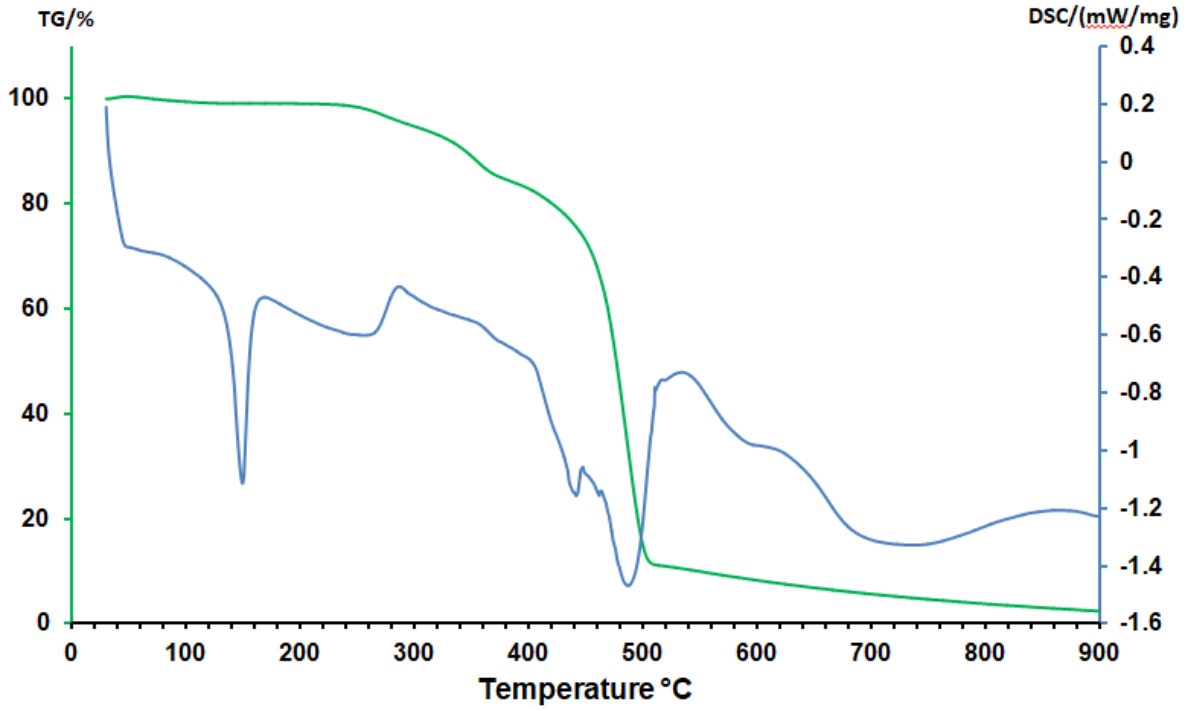

Figure 4.10: TGA and DSC of 5% NaOH treated DPM fiber reinforced HDPE composite

4.3.6 Morphological Analysis

Figure 4.11 shows that the impurities such as lignin and hemicelluloses were present on the surface of the raw fibers which were removed as a result of the alkali treatment. A rough surface was observed for the alkali treated fiber.

The surface morphology of the tensile fracture surfaces of the untreated DPM fiber reinforced composites and 5% NaOH treated DPM fiber reinforced composites were examined and the SEM micrographs in different magnitude are presented in figure 4.12. It can be seen from the figure that superior fiber-matrix interaction between fibers and HDPE matrix was observed for 5% NaOH treated DPM fiber whereas voids and loosely bonded fiber matrix adhesion was found for untreated DPM fiber reinforced composites.

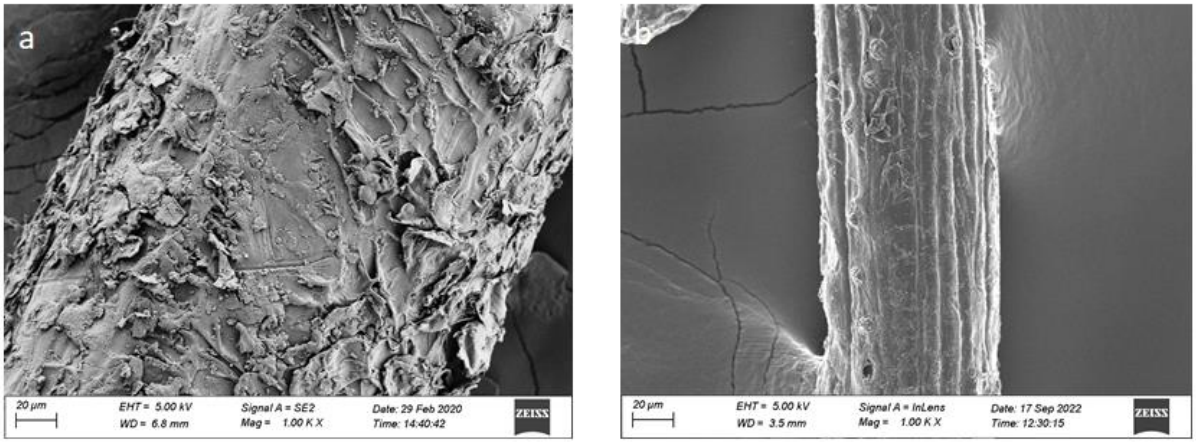

Figure 4.11: SEM micrographs of (a) raw fiber and (b) 5% NaOH treated DPM fiber

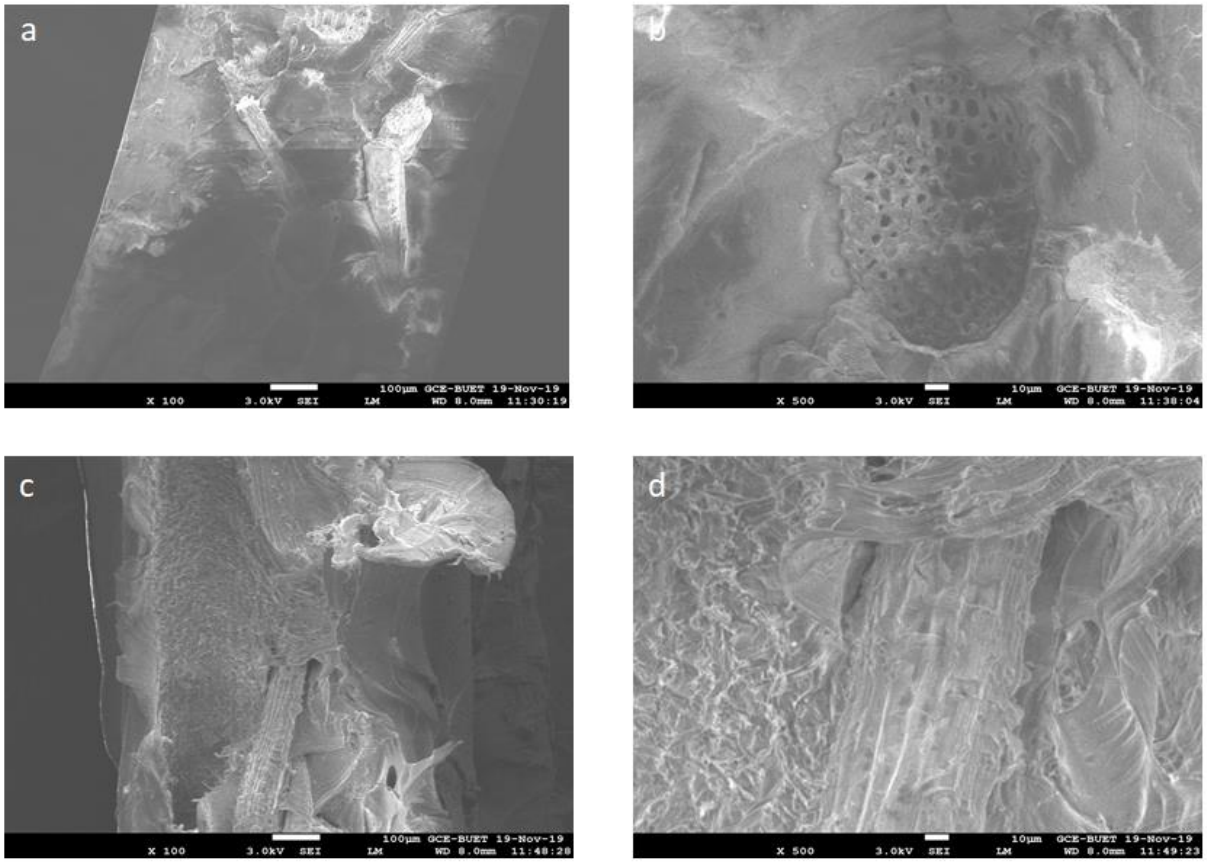

Figure 4.12: SEM micrographs of 5% NaOH treated DPM fiber composite (a) 100x magnification and (b) 500x magnification and untreated DPM fiber composites (c) 100x magnification and (d) 500x magnification

4.3.7 Degradation by Soil Burial

Soil burial tests of the composites were done in soil for six months. The difference in tensile strength of the composites afterward soil burial is presented in figure. Figure clearly shows that the tensile strength of the composites decreases with time. 5% NaOH treated DPM fiber reinforced HDPE composites lost 21.56% of tensile strength whereas untreated DPM fiber reinforced HDPE composites lost 24.1% of tensile strength. 5% NaOH treated DPM fiber reinforced HDPE composites retained much of their tensile strength compared to untreated DPM fiber reinforced HDPE composites. Alkali treatment reduced the hydrophilic character of the fiber [12] which is the reason for less water absorption and alkali treated composites show lower reduction in tensile strength compared to untreated composites.

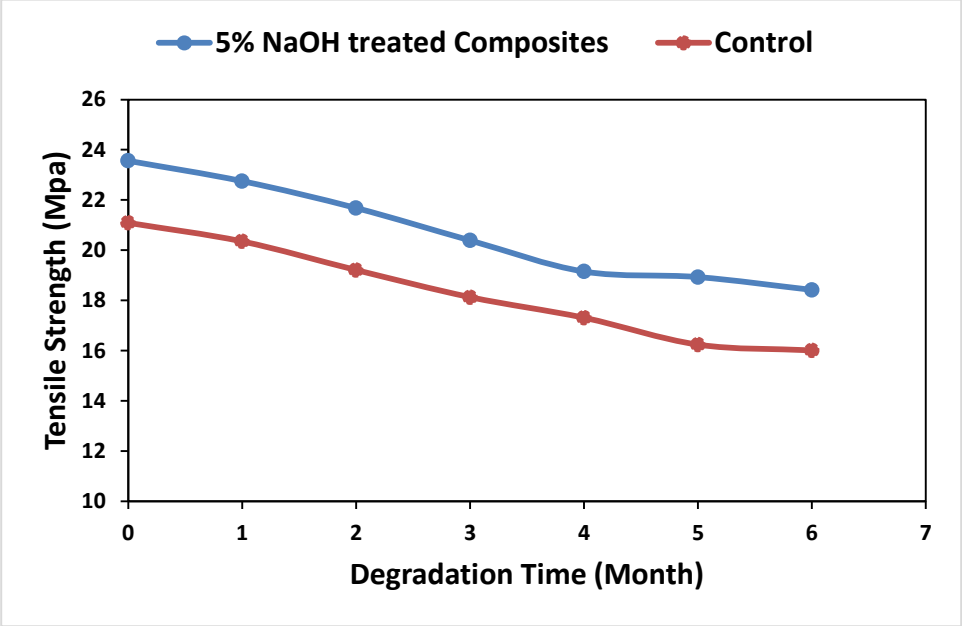

Figure 4.13: Variation of tensile strength of the buried composite samples

4.4 Conclusions

The composites with alkali-treated fiber reinforcement displayed enhanced mechanical characteristics than untreated composites. The enhancement in mechanical properties was highest for the composites fabricated with treated fibers at 5% NaOH concentration. The removal of amorphous components from the fiber is assumed to have improved fiber matrix adhesion, as shown by FTIR investigations. The surface morphology of the composites reveals that the treated DPM fiber reinforced HDPE composites had more fiber matrix

bonding interaction than those in the untreated DPM fiber reinforced HDPE composites. The composites' characteristics suggest that the produced new composites could be employed for interior and outdoor applications.

4.5 References

1. Malik, K.; Ahmad, F.; Gunister, E. A Review on the Kenaf Fiber Reinforced Thermoset Composites. *Appl Compos Mater*. **2021**, 28, 491–528. https://doi.org/10.1007/s10443-021-09871-5
2. Chowdhury, M.N.K.; Beg, M.D.H.; Khan, M.R. Copper nanoparticle in cationized palm oil fibres: physico-chemical investigation. *Colloid Polym Sci*. **2015**, 293, 777–786. https://doi.org/10.1007/s00396-014-3462-y
3. Mousa, S.; Alomari, A.S.; Vantadori, S.; Alhazmi, W.H.; Abd-Elhady, A.A.; Sallam, H.E.D.M. Mechanical Behavior of Epoxy Reinforced by Hybrid Short Palm/Glass Fibers. *Sustainability* **2022**, *14*, 9425. https://doi.org/10.3390/su14159425
4. Gift, M. D. M.; Mantri, S.; Raviteja, S.; Rinawa, M. L.; Patel, D. R.; Nagaraju, V.; Seikh, A. H.; Khan, S. M. A.; Christopher, D. Mechanical Behaviour of Alkali-Treated Fabric-Reinforced Polymer Matrix Composites, *Adv. in Polymer Tech.* Hindawi, **2022,** 1833955SN - 0730-6679. https://doi.org/10.1155/2022/1833955
5. Wang, X.; Chang, L; Shi, X.; Wang, L. Effect of Hot-Alkali Treatment on the Structure Composition of Jute Fabrics and Mechanical Properties of Laminated Composites. *Materials* (Basel). **2019**, 12(9):1386. doi: 10.3390/ma12091386. PMID: 31035442; PMCID: PMC6539758
6. Rajesh, G.; Prasad, A.V. R. Tensile Properties of Successive Alkali Treated Short Jute Fiber Reinforced PLA Composites, *Procedia Mater. Sc.*, **2014,** 5, 2188-2196, ISSN 2211-8128, https://doi.org/10.1016/j.mspro.2014.07.425
7. Ed-Dariy, Y.; Lamdour, N.; Cherradi, T.; Rotaru, A.; Barbuta, M.; Mihai, P. Effect of alkali treatment of Jute fibers on the compressive strength of normal-strength concrete members strengthened with JFRP composites, *J. of Appl.Sci. and Eng.*, **2020**, 23, 4, 677--685, ISSN 1560-6686. https://doi.org/10.6180/jase.202012_23(4).0012.
8. Singh, J.I.P.; Singh, S.; Dhawan, V. Effect of alkali treatment on mechanical properties of jute fiber-reinforced partially biodegradable green composites using

epoxy resin matrix. *Polym. and Polym. Compos*., **2020**, 28(6), 388-397. doi:10.1177/0967391119880046

9. Ariawan, D.; Rivai, T. S.; Surojo, E.; Hidayatulloh, S.; Akbar, H. I; Prabowo, A. R. Effect of alkali treatment of Salacca Zalacca fiber (SZF) on mechanical properties of HDPE composite reinforced with SZF, *Alexandria Eng. J.*, **2020**, 59(5), 3981-3989, ISSN 1110-0168. https://doi.org/10.1016/j.aej.2020.07.005.
10. Prasad, G. L. S. R.; Kumar, M.V.H.S.; Rajesh, G. Effect of Fiber Loading and Successive Alkali Treatments on Tensile Properties of Short Jute Fiber Reinforced Polypropylene Composites, *Int. J. of Eng. Sci. Inven.*, **2014,** 3(3), 30-34.
11. Ganesan M.; Nallathambi, G. Alkali-treated coir fibrepith composite for waste water treatment, *J. of Ind. Tex.*, **2022**, Vol. 51(1S) 749S–768S, DOI: 10.1177/15280837211014247
12. Diaw, I.; Faye, M.; Bodian S.; Sambou, V. Effects of Chemical Treatment on the Physical Properties of Typha, *Fluid Dynam. & Mater. Proc.*, **2022**, 18(5) 1409–1418. https://doi.org/10.32604/fdmp.2022.021968
13. , Alauddin, A; R. A. Rashid S.B.M.; Husin, H.B.; Shueb, M. I. Performance of Polylactic Acid Natural Fiber Biocomposite, *Int. J. of Appl. Chem.*. **2016,** 12 (1) , 72-77, ISSN 0973-1792
14. Dahham, O. S.; Noriman, N. Z.; Marwa R. H.; Al-Samarrai, N.; Idrus, S. Z. S.; Shayfull Z.; Adam, T.; Mohammed M. The Influences NaOH Treatment on Polypropylene/Cyperus Odoratus (PP/CY) Composites: Tensile and Morphology, IOP Conf. Series: *J. of Phys. Conf. Series* 1019, **2018,** 012057 doi :10.1088/1742-6596/1019/1/012057
15. Archana, D. P.; Reddy, J.; Paruti, H. N.; Basavaraju, Mechanical Characterization of Biocomposites Reinforced with Untreated and 4% NaOH-Treated Sisal and Jute Fibres, *Adv. in Mater. Sci. and Eng.*, **2022**. https://doi.org/10.1155/2022/7777904
16. Salem, T.F.; Seha, T.; Oyku, A. A.; and Umit, T. Enhancement of mechanical, thermal and water uptake performance of TPU/jute fiber green composites via chemical treatments on fiber surface, *e-Polymers*, **2020**, 20(1), 133-143 https://doi.org/10.1515/epoly-2020-0015.

17. Noranizan I.; Ahmad, I. "Effect of Fiber Loading and Compatibilizer on Rheological, Mechanical and Morphological Behaviors, *Open J. of Polym.r Chem.*, **2012**, 2, 31-41. DOI:10.4236/ojpchem.2012.22005.
18. Zaini, L.; Jonoobi, M.; Tahir P.; Karimi, S. Isolation and Characterization of Cellulose Whiskers from Kenaf (Hibiscus cannabinus L.) Bast Fibers, *J. of Biomater.s and Nanobiotechnol.*, **2013**, 4 (1), 37-44. doi: 10.4236/jbnb.2013.41006.
19. Zhou, G.; Taylor, G.; Polle, A. FTIR-ATR-based prediction and modelling of lignin and energy contents reveals independent intra-specific variation of these traits in bioenergy poplars. *Plant Meth.*, **2011**, 7, (9). https://doi.org/10.1186/1746-4811-7-9.
20. Manap, N.; Jumahat, Rahman A.; N. A.; Rahman, N. A. A. NaOH treated Kenaf/Glass hybrid composite: The effects of nanosilica on longitudinal and transverse tensile properties, *J. of Phys. Conf. Ser.* 1432, **2020**, 012046, doi:10.1088/1742-6596/1432/1/012046.
21. Vijay, R.; Vinod, A.; Singaravelu, D. L.; Sanjay, M.R.; Siengchin, S. Characterization of chemical treated and untreated natural fibers from Pennisetum orientale grass- A potential reinforcement for lightweight polymeric applications, *Int. J. of Lightwei. Mater. and Manuf.*, **2021**, 4(1), 43-49, ISSN 2588-8404, https://doi.org/10.1016/j.ijlmm.2020.06.008.
22. Al Abdallah, H.; Abu-Jdayil, B.; Iqbal, M.Z. The Effect of Alkaline Treatment on Poly(lactic acid)/Date Palm Wood Green Composites for Thermal Insulation. *Polymers*. **2022**; 14(6), 1143. https://doi.org/10.3390/polym14061143.

CHAPTER 5

Preparation and Characterization of ZnO NPs Loaded DPM Fiber Reinforced Composites

5.1 Introduction

Composite materials have attracted a lot of interest because of their multipurpose characteristics, which enable a wide range of applications in several sectors. These materials are used in a variety of sectors, including those in the packaging, aircraft, automobile, sports, and furniture industries. Polymer matrix is used to create a variety of composite materials due to their flexibility, low cost, and simplicity of manufacture. These composites are made using synthetic polymers, which are made from petroleum sources. The primary drawback of these polymers is that they are not biodegradable, which rises the quantity of waste that is disposed of in landfills and contributes to pollution. The usage of conventional composite materials is constrained by governments' laws. Researchers have been focusing on environmentally friendly materials in recent decades to lessen their impact. Natural fibers can be obtained from renewable sources in a sustainable manner. They are prospective substitute materials for synthetic fibers in the composites sector because of their eco-friendliness, affordability, renewability, and abundance. The use of natural fibers, including flax, jute, sisal, ramie, coconut coir, pineapple leaf fiber, kenaf, bamboo fiber, and rice husk, has improved as a result of researchers' increasing efforts [1,2].

The key drawbacks of natural fibers in corresponding composites are their comparatively high moisture absorption and poor compatibility with the matrix. Natural fibers can easily create cavities in composites that can weaken the material's mechanical characteristics [3]. The incorporation of nanofillers in the composite is one of the likely ways to improve the compatibility with the matrix of the composites [4]. Researchers are attempting to create a polymer-based composite with improved qualities by adding a number of reinforcements or nanofiller to polymeric material [5]. Nanofillers form chemical bonds or entangle mechanically with the polymer matrix in order to improve the characteristics of the composites [4]. Nanofillers are chemically active due to their huge surface areas, which facilitates easier interaction with the matrix [6]. Nanofillers typically contain inorganic materials, but occasionally organic ones. The mechanical, thermal, and water absorption characteristics can be significantly enhanced by the use of a little amount of these fillers [7]. Numerous nanofillers, such as montmorillonite, silica, calcium carbonate, and aluminum oxide, have been shown to effectively enhance the mechanical, thermal, electrical, gas barrier, and refractory properties of polymer matrix composites. ZnO nanoparticles have received a

lot of interest among different inorganic fillers because of its distinctive physical characteristics, inexpensive price, and extensive use [8]. The introduction of nanoparticles as a result of advances in nanoscience has added a new dimension to the area of composite material [4]. Researchers are constantly looking for ways to build strong, versatile, cost-effective nanocomposites for innovative material applications, such as aircraft, automotive, sensors, conductors, and petroleum refineries [9].

In this section of present study, a new sustainable composite is developed with ZnO nanoparticles, DPM fiber and HDPE. Considering this, ZnO nano particles have been synthesized and characterized. Therefore, our study focus on the fabrication of DPM fiber reinforced HDPE composites with the incorporation of ZnO nanoparticles and to understand the effect of ZnO nanoparticles on the physical, mechanical, thermal and morphological properties of the DPM fiber reinforced HDPE composites.

5.2 Experimental

5.2.1 Materials

HDPE was purchased from Saudi Polymers Company, Saudi Arabia. HDPE granules were ground by a grinding machine. DPM fibers were collected from the rural area of Jashore, Bangladesh. The DPM fibers were cut into 2-3mm by hand scissors.

5.2.2 Preparation of ZnO nanoparticles

At first, two separate solutions were prepared by dissolving zinc acetate dehydrate and KOH in methanol. KOH solution was added drop by drop into the zinc acetate dehydrate solution with constant stirring at 52°C for 2 hours resulting white colored solution. The white solution was centrifuged, washed and dried [10].

Figure 5.1: Image of prepared ZnO nanoparticles

5.2.3 Composite Fabrication

Compression moulding technique was used to fabricate the composites. HDPE, DPM fibers and ZnO nanoparticles (1 to 7%) were mixed using a blender. The mixture was transferred to the mould (12x15 cm^2) and finally hot pressed (Paul Otto Weber Press Machine) at a temperature of 160^0C for 5 min maintaining a pressure of 200 kN. The moulds were cooled at room temperature and under 200 kN pressure for 5 min and removed from the mould.

5.2.4 Bulk Density of the composites

Bulk density of the composites was calculated by measuring the weight and dimensions of the samples utilizing the following equation 5.1. The average results for five composite samples were stated.

$$D = \frac{Weight\ of\ the\ composite}{(Length \times Width \times Height)\ of\ the\ composite} \quad (5.1)$$

5.2.5 Water absorption test of Composites

Water absorption tests of the composite samples were done following ASTM D570-99. The test samples were dried in an oven at 105^0C for 2h and cooled in a desiccator. The composite samples were weighed and dipped in distilled water for 24h at room temperature. The samples were withdrawn from the beaker, removed excess water with a cloth and weighed. Three

composite samples were tested to get the average results. The percentage of water absorption was calculated as follows:

$$\text{Increase in weight, \%} = \frac{(\text{wet wt} - \text{conditioned wt})}{(\text{conditioned wt})} \times 100 \qquad (5.2)$$

5.2.6 Mechanical Properties

Tensile properties such as tensile strength, percent elongation at break of the composites were measured using universal strength tester (model 1410 Titans, capacity 5 kN, England). The crosshead speed was 10 mm/min. The tests were carried out according to standard method (ASTM D 3039/D 3039 (M) 2002). Bending strength (three point bending) of the composites were also performed following ASTM D7900. Five measurements in each composition of the composite samples were taken and the average values were reported.

5.2.7 FTIR Spectroscopy

The composites were examined by a FT-IR/NIR spectrometer (Frontier, Perkin Elmer, USA). The FTIR spectra were recorded in the region 4,000-650 cm^{-1}. FT-IR spectroscopy was used to find out the functional group of the fibers.

5.2.8 Thermal Analysis

The thermogravimetric (TGA) and differential scanning calorimetry (DSC) analysis of the composite samples were performed by a NETZSCH instrument (STA 449 F3, Jupiter) in a temperature range 30-900^{0}C at nitrogen atmosphere. The heating rate was 10^{0}C/min.

5.2.9 Surface Morphology

Surface morphology and elemental analysis of the synthesized ZnO nanoparticles were investigated by FESEM coupled with Energy dispersive X-ray spectroscopy (EDX). The fracture surfaces of the tensile specimens were examined by a field emission scanning electron microscope (JEOL JSM-7600F) operated with an accelerating voltage of 5.0 kV. The samples were cut into a small portion, mounted onto holders using carbon tape and coated with gold. Samples were focused onto the surfaces and examined with different magnification.

5.2.10 Soil Burial Test

The composite samples were buried in a soil containing flower pot and the moisture level was kept at least 30%. The test samples were removed from the soil at intervals of 1 month, washed with distilled water and dried at 80^0C in an oven for 6 h. The degradation was determined on the basis of measuring the tensile strength of the specimen.

5.3 Results and Discussion

5.3.1 Surface Morphology and EDX of ZnO Nanoparticles

SEM analysis was carried out to examine the surface morphology of produced ZnO nanoparticles. SEM micrograph of ZnO nanoparticles exposes that the nanoparticles have a spherical shape. The SEM micrograph evidently demonstrates that the particles sizes range from 13 nm to 34 nm. The results of the EDX investigation support the presence of ZnO nanoparticles. The ZnO nanoparticles have 71.22% zinc and 18.87% oxygen according to the elemental analysis.

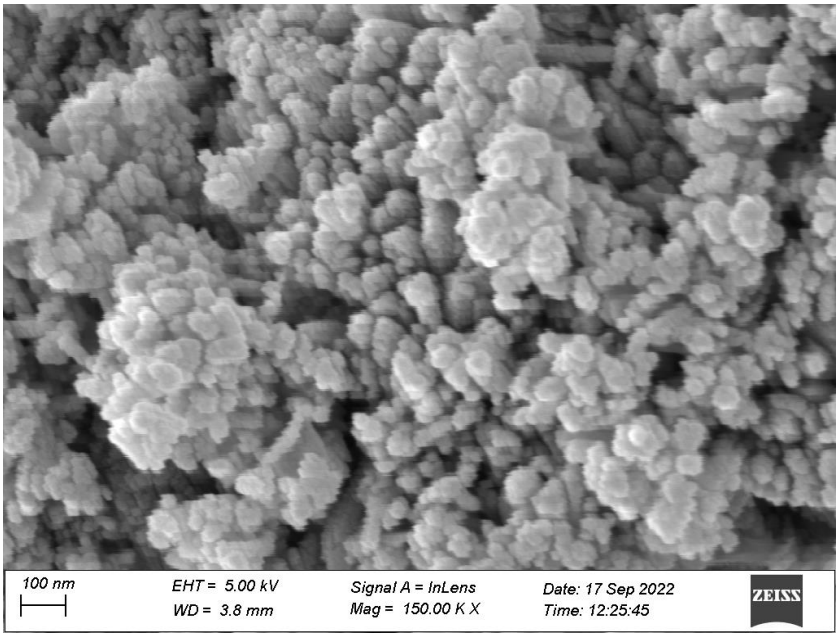

Figure 5.2: SEM micrograph of ZnO nanoparticles

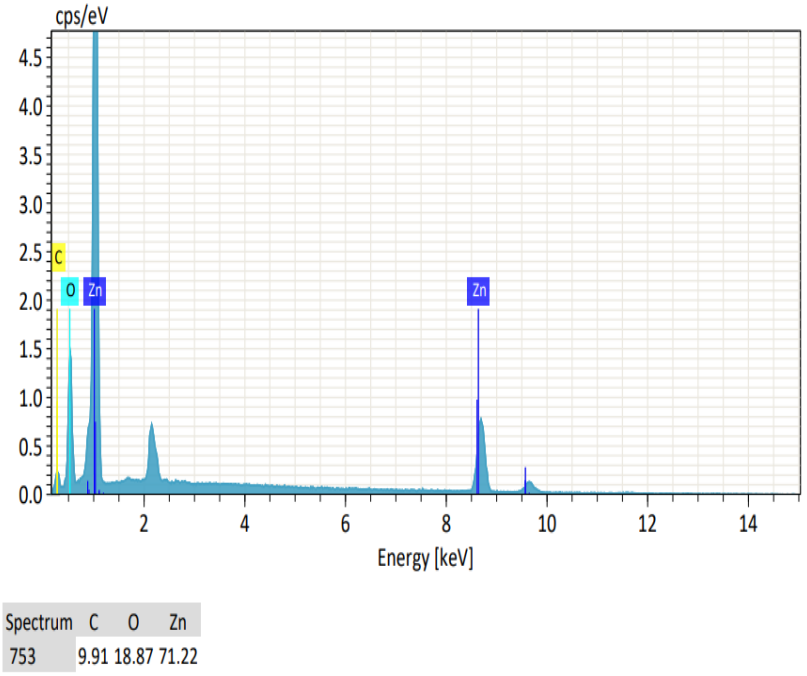

Figure 5.3: EDX spectrograph of ZnO nanoparticles

5.3.2 Bulk Density of the Composites

The effect of various quantities of ZnO nanoparticles on the bulk density of the composites is displayed in figure 5.4. The bulk density of short DPM fiber reinforced HDPE composites increases with increasing quantity of ZnO nanoparticles. There are more amount of denser ZnO nanoparticles present at greater nanoparticles weight percentages in the composites. As a result, the composites with increasing ZnO nanoparticles exhibit higher density [4].

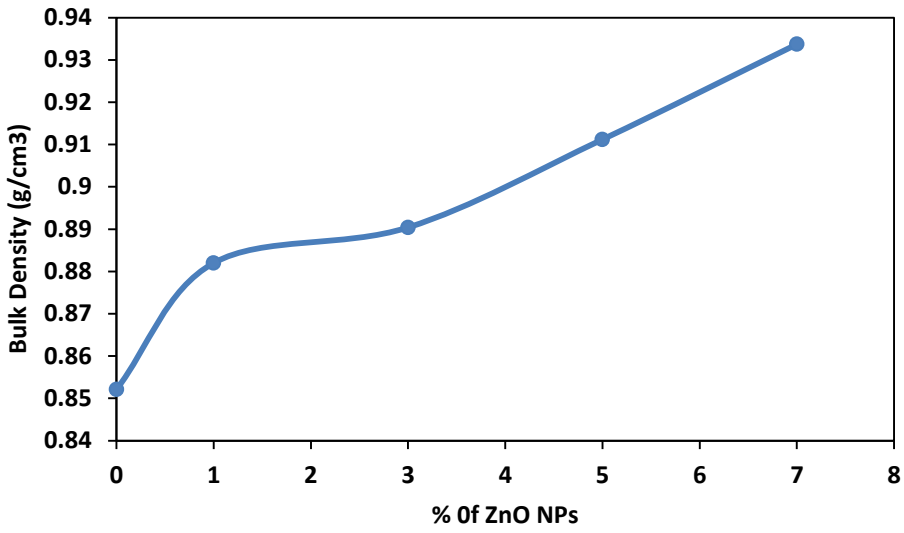

Figure 5.4: Bulk density of the DPM fiber reinforced HDPE composites at various percent of ZnO NPs

5.3.3 Water Absorption of the Composites:

The effect of ZnO nanoparticles on water absorption of the composites was studied and it reveals that the water absorption of the composites with ZnO nanoparticles declines. However, the incorporation of ZnO nanoparticles into the DPM fiber reinforced HDPE composites shows reduced amount of water absorption than the composites without ZnO nanoparticles. ZnO nanoparticles filled the voids in the composites, reducing the amount of empty spaces for water absorption [11]. This may also be as a result of ZnO nanoparticles on the surface of the composites which cause less penetration of water and reduced water absorption. Bose et al. prepared nano ZnO filled glass fiber reinforced epoxy composites and found that nano ZnO filled glass fiber reinforced epoxy composites absorb less water than the neat composite [12]. Their findings are similar to our results.

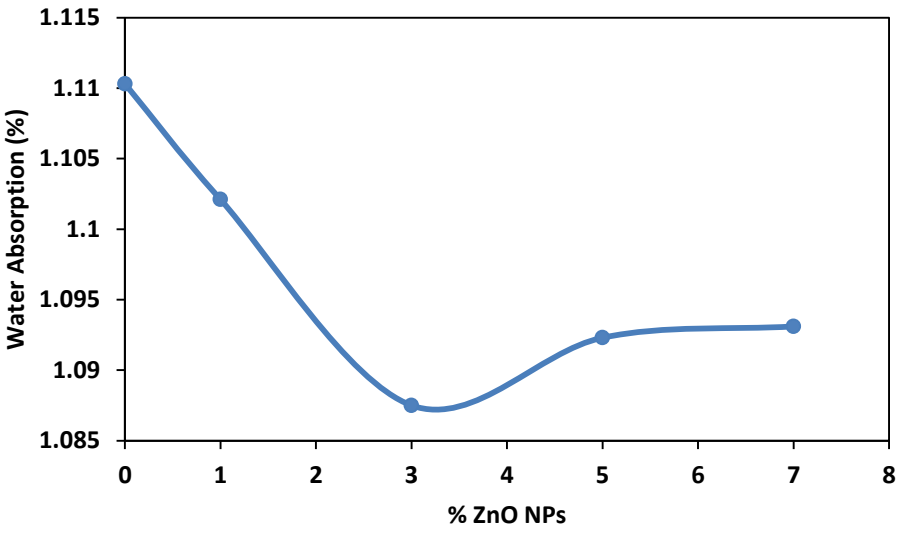

Figure 5.5: Water absorption of the DPM fiber reinforced HDPE composites at various percent of ZnO NPs

5.3.4 Mechanical Properties

Figure 5.6 shows the effect of the variation of ZnO nanoparticles on the tensile strength of the composites. From the graph it is concluded that the tensile strength of the composite samples increased up to a 3% ZnO nanoparticles and decreased from 5 to 8% ZnO nanoparticles. The highest tensile strength was 22.71 MPa for the composites containing 3% ZnO nanoparticles. The incorporation of 3% ZnO nanoparticles in the composites the tensile strength increased by 7.7% compared to composites without filler. As a consequence of the better interaction between the ZnO nanoparticles and matrix, the values of tensile strength of composites increase with the addition of ZnO nanoparticles. The interaction between the particles becomes more intense at higher percent of ZnO nanoparticles. As a result, aggregates of nanofillers are created and may be the reason for the reduction in tensile strength of the composites at higher percent of ZnO nanoparticles [4].

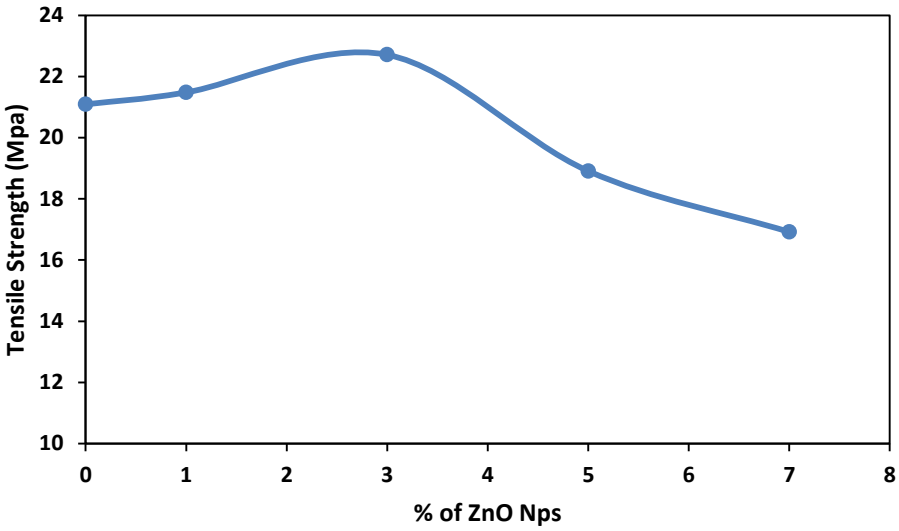

Figure 5.6: Tensile strength of the DPM fiber reinforced HDPE composites at various percent of ZnO NPs

Figure 5.7 illustrates the effect of the variation of ZnO nanoparticles on the elongation at break of the composites. The elongation at break of the composites gradually decreased with increasing amount of ZnO nanoparticles. The inclusion of ZnO nanoparticles boosted the composite's stiffness but did not increase its elasticity or overall flexibility. The reduction in flexibility of the composites was owing to a lack in adhesion of foreign particle surfaces in the matrix which resulted to a poor load transfer from the matrix to the fibers. This is in line with the findings of Hassana et al. [13].

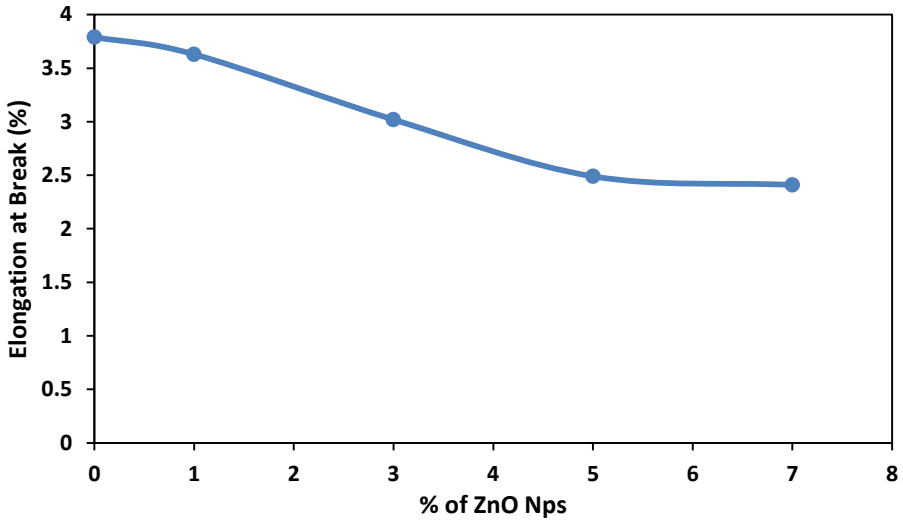

Figure 5.7: Elongation at break of the DPM fiber reinforced HDPE composites at various percent of ZnO NPs

Figure 5.8 elucidates the effect of the variation of ZnO nanoparticles on the bending strength of the composites. The graph displays that the bending strength of the composites increased up to a 3% ZnO nanoparticles and dropped from 5 to 8% ZnO nanoparticles. The maximum bending strength 25.32 MPa was noticed for the composite samples containing 3% ZnO nanoparticles. The incorporation of 3% ZnO nanoparticle was noticed to increase the bending strength of the composite when compared to 0%, 1%, 5%, and 7%. Improved compatibility produced by the addition of ZnO nanoparticles which can strengthen the interaction between fiber and matrix. This outcome demonstrates that voids of the composite can be filled by adding ZnO nanoparticles to the composite.

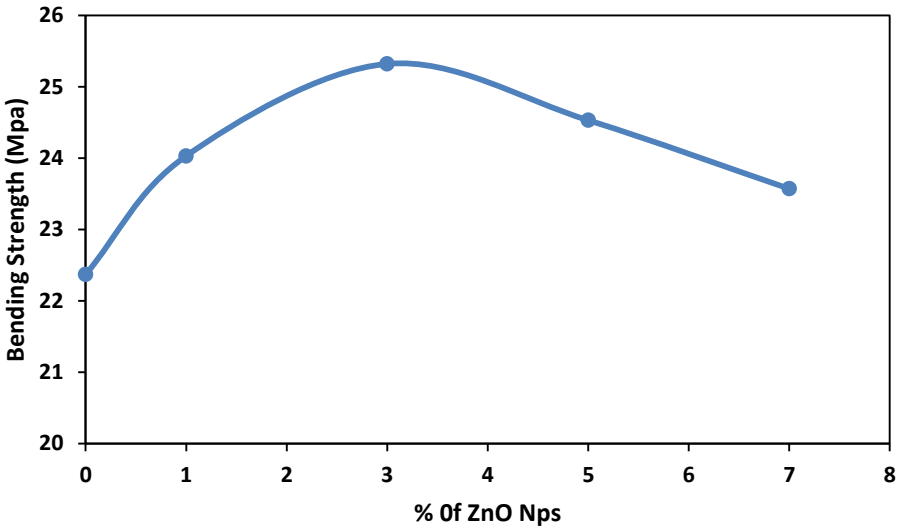

Figure 5.8: Bending strength of the DPM fiber reinforced HDPE composites at various percent of ZnO NPs

5.3.5 FTIR Study

The FTIR spectra were recorded for 0% ZnO nanoparticles containing DPM fiber reinforced HDPE and 3% ZnO nanoparticles containing DPM fiber reinforced HDPE composites and presented in figure 5.9. Additional functional group was not found since chemical bonds were not formed during the fabrication of the composites. Both composites showed peaks in the same region. The peaks 3400-3200 cm^{-1} correspond to O–H stretching vibration of the hydroxyl groups. The peak at 2915 cm^{-1} observed for the C-H stretching vibration [14]. The absorption band at 1740 cm^{-1} indicates the C=O stretching from the lignin and hemicellulose [15]. The peak 1607 and 1595 cm^{-1} indicate C=C stretching in aromatic [16]. The peak at 1462 and 1372 cm^{-1} refers to the bending vibration of $-CH_2$ group and bending vibrations of the -CH group respectively [17]. The peak at 1077 and 1046 cm^{-1} detects for C-O stretching vibrations [18]. The peak 718 cm^{-1} corresponds to the rocking vibration of $-CH_2$ group [19].

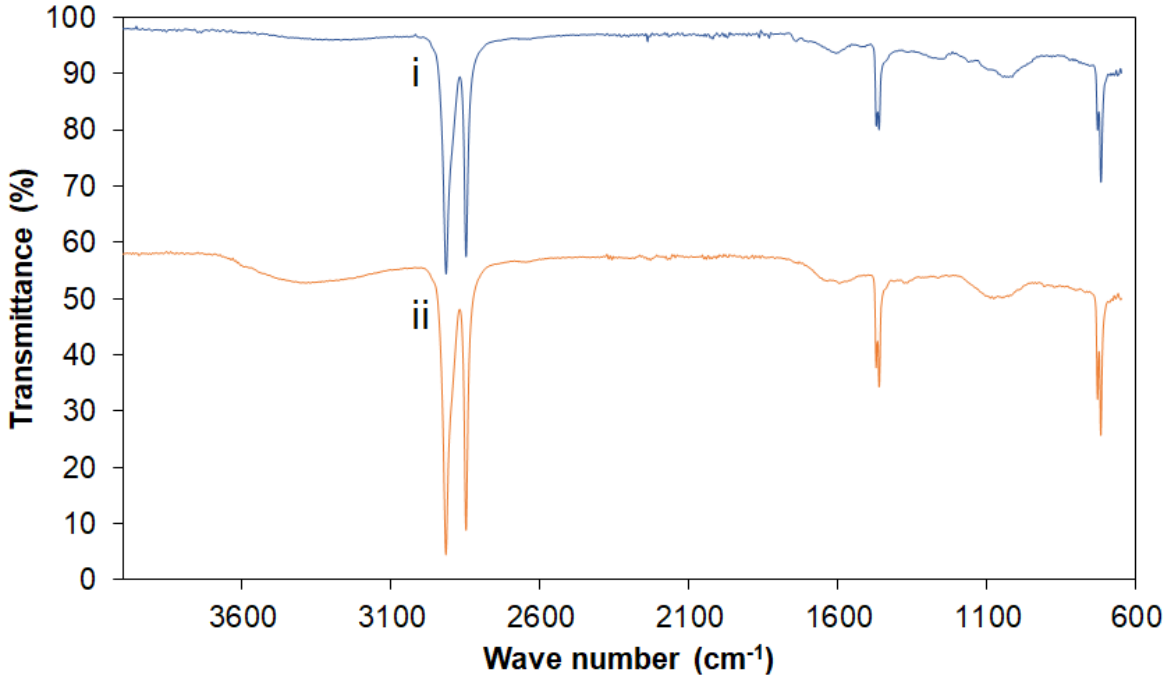

Figure 5.9: ATR-FTIR spectra of (i) 0% ZnO NPs composite; (ii) 3% ZnO NPs composite

5.3.6 Thermal Properties

To investigate the thermal stability of the composites, thermal analyses of 0% ZnO NPs composite, and optimum 3% ZnO NPs composites were performed. The TGA results show that the degradation of 0% ZnO NPs composites start at 403.5 ^{0}C and 89.37% mass change is completed at about 500^{0}C. Conversely, the 3% ZnO NPs composites start to degrade at 407.1 ^{0}C with a total mass change 97.6%. The thermal degradation of the composites increased with the incorporation of ZnO nanoparticles. For 0% ZnO NPs composite, and 3% ZnO NPs composites, the percentage of the residual mass at the finish of the heating process was 7.99 and 2.4% respectively. The DSC curves of 0% ZnO NPs composite, and 3% ZnO NPs composites showed peaks of melting at 141.1 and 152.1 ^{0}C respectively. The melting temperature of the composites increased, this is owing to the presence of ZnO nanoparticles. The DSC result of optimum 3% ZnO NPs composites showed that the composite is thermally slightly more stable.

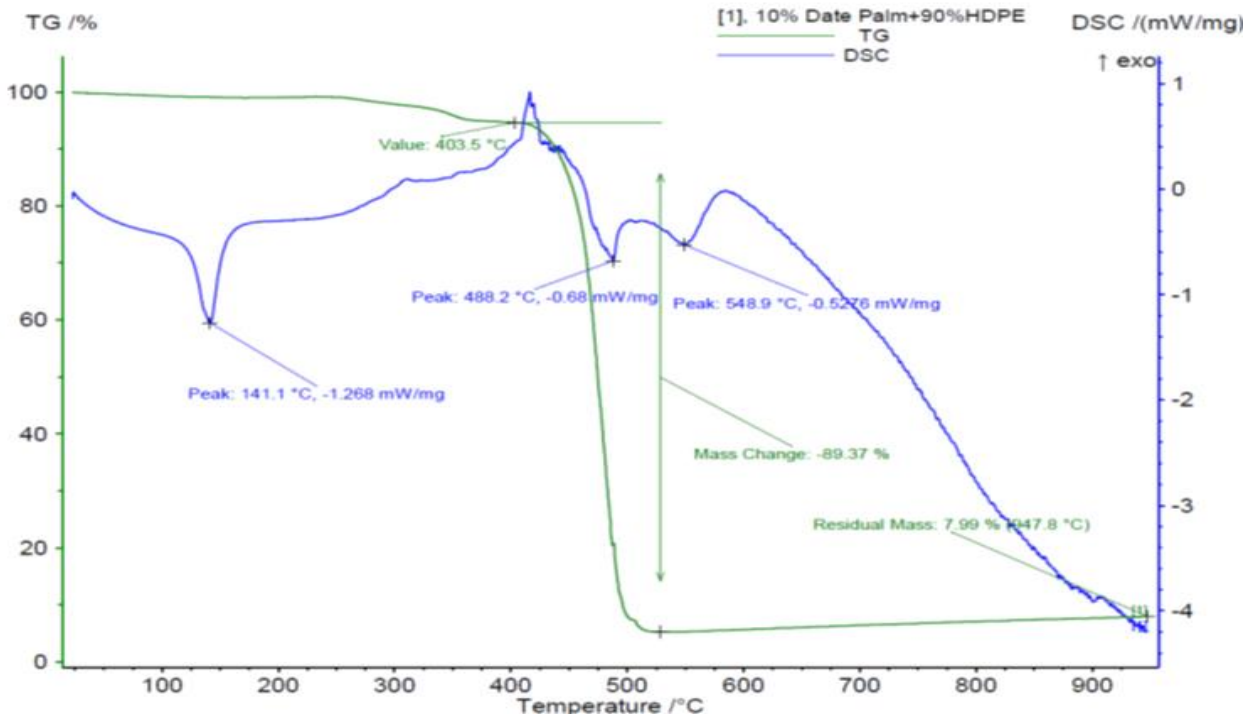

Figure 5.10: TGA and DSC of 0% ZnO NPs composites

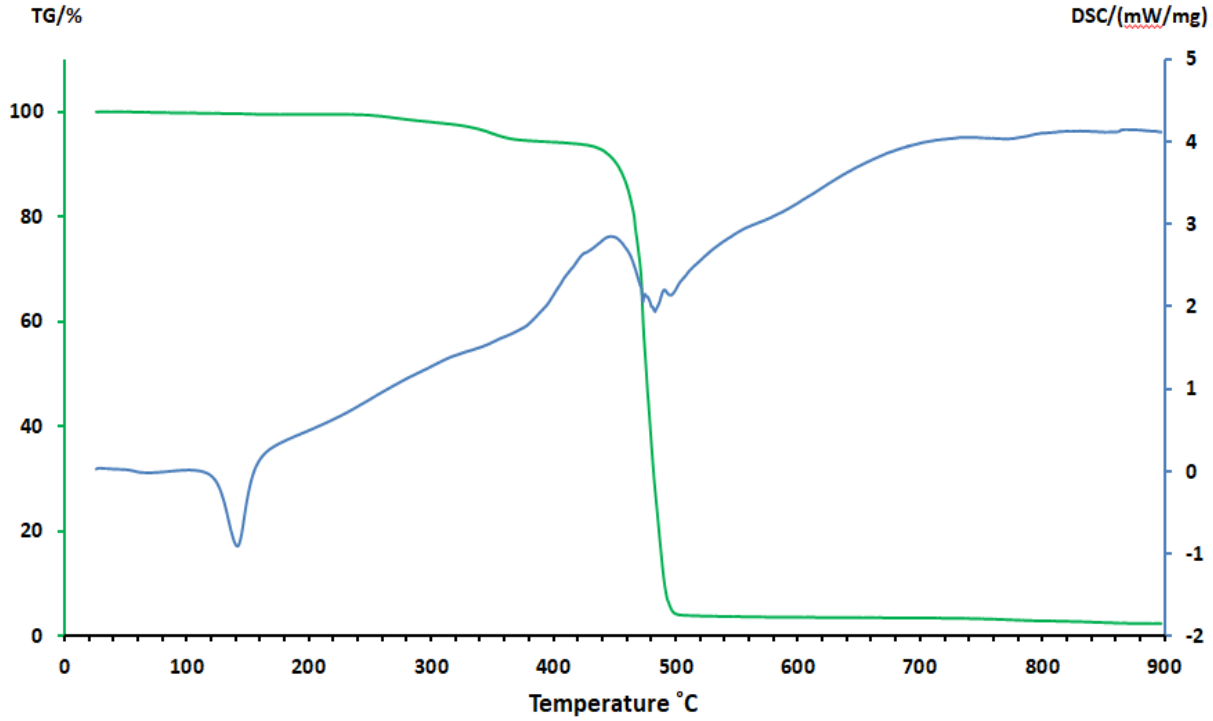

Figure 5.11: TGA and DSC of 3% ZnO NPs composites

5.3.7 Surface Morphology

The surface morphology of the tensile fracture surfaces of the 3% ZnO loaded and 0% ZnO loaded DPM fiber reinforced composites were studied, and SEM micrographs of various magnifications are shown in the figure 5.12. In the micrograph, more voids and loosely bonded fibers was observed for the composites without ZnO nanoparticles while better interaction between fiber and matrix was found for 3% ZnO loaded DPM fiber reinforced HDPE composites. Using ZnO nanoparticles are anticipated to fill the composite's voids and empty spaces and enhance its mechanical, physical, and thermal properties as seen by SEM micrographs.

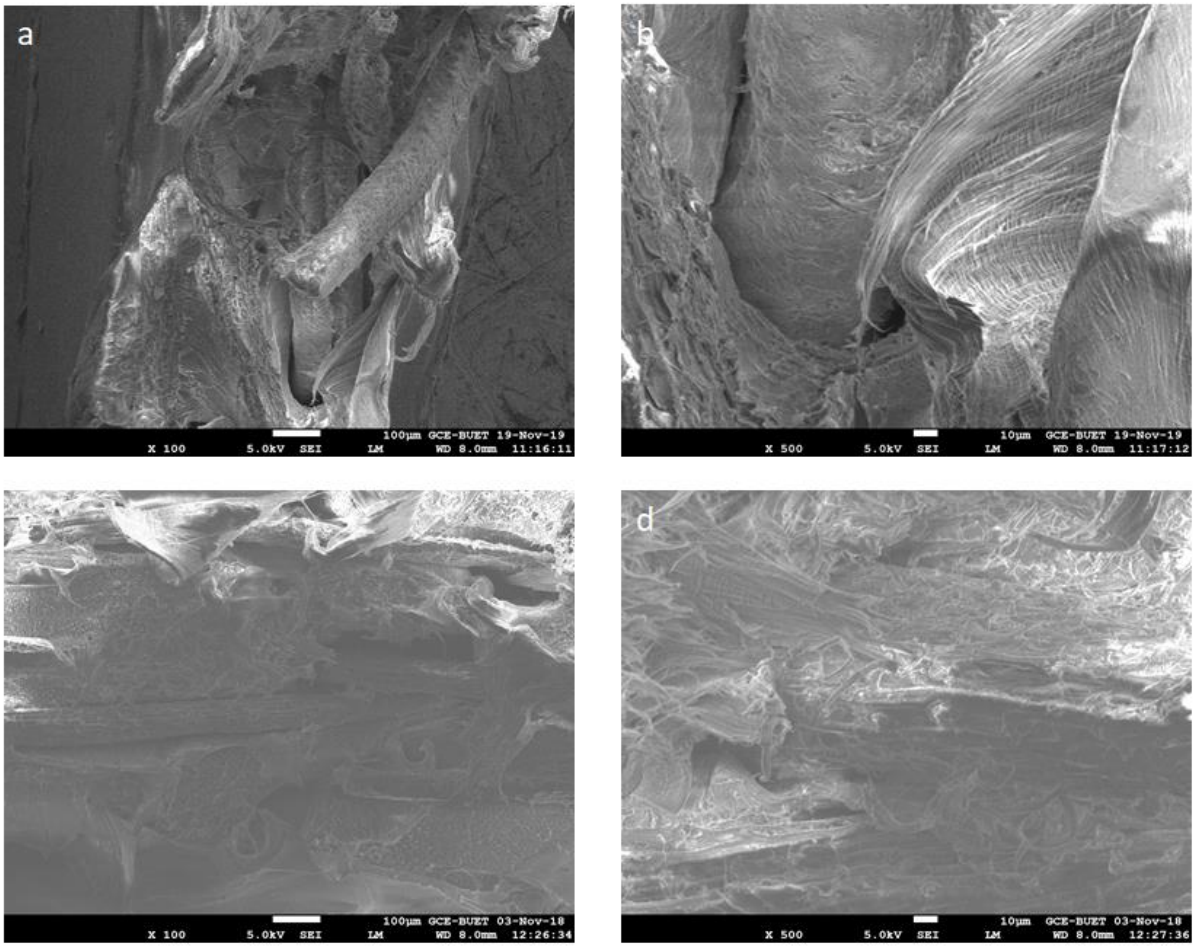

Figure 5.12: SEM images of 3% ZnO NPs composite (a) 100x magnification and (b) 500x magnification and 0% ZnO NPs composites (c) 100x magnification and (d) 500x magnification

5.3.8 Degradation by Soil Burial

Soil burial experiments of the composites were done in soil for six months. The variation in tensile strength of the composites afterward soil burial is presented in figure 5.13. It can be seen from the figure that the tensile strength of the composites decreases with time. DPM fiber reinforced HDPE composites (0% ZnO nanoparticles) lost 24.1% of tensile strength whereas 3% ZnO nanoparticles filled DPM fiber reinforced HDPE composites lost 22.2% of tensile strength. 3% ZnO nanoparticles loaded DPM fiber reinforced HDPE composites retained much of their tensile strength compared to DPM fiber reinforced HDPE composites without fillers. The interruption of hydrogen bonds in the fiber structure caused by the addition of nanoparticles to DPM fiber can cause to lose their empty spaces, crystallize more quickly, depolymerize more quickly, and become more hydrophobic, which reduces the composites' ability to absorb water and become less biodegradable. On the other hand, DPM fiber reinforced HDPE composites without fillers contains greater gaps, which is disclosed in the composite as well as allows water molecules to cause the degradation of the composites [20].

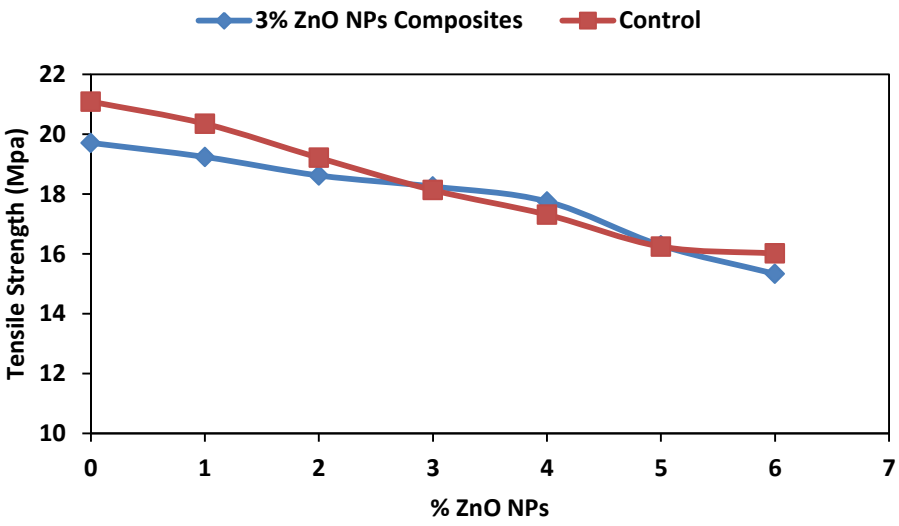

Figure 5.13: Variation of tensile strength of the buried composite samples

5.4 Conclusion

The preparation and characterization of the DPM fiber reinforced HDPE composites by incorporating ZnO nanoparticles was successfully accomplished, which had an impact on their mechanical properties. The tensile strength and bending strength of the composites were increased by adding ZnO nanoparticles. The highest mechanical properties were observed at 3% ZnO nanoparticles. Morphological analysis of the composites containing 3% ZnO nanoparticles showed better compatibility which also supported better mechanical performances. 3% ZnO nanoparticles filled DPM fiber reinforced HDPE composites exhibited a reduced amount of water absorption. The thermal stability of the composites increased due to the incorporation of ZnO nanoparticles. The biodegradability of the composites was decreased by adding ZnO nanoparticles. The results of the newly developed composites indicate that it may find potential applications in numerous fields.

5.5 References

1. Sanivada, U.K.; Mármol, G.; Brito, F.P.; Fangueiro, R. PLA Composites Reinforced with Flax and Jute Fibers-A Review of Recent Trends, Processing Parameters and Mechanical Properties. *Polymers* (Basel). **2020**, 15, 12(10):2373. doi: 10.3390/polym12102373. PMID: 33076571; PMCID: PMC7602707.
2. Faruk, O.; Bledzki, A. K.; Fink, H.-P.; Sain M. Progress Report on Natural Fiber Reinforced Composites, *Macromol. Mater. Eng.* **2014**, 299, 9–26 https://doi.org/10.1002/mame.201300008
3. Mohammed, M.; Rozyanty, R.; Mohammed, A. M.; Osman, A. F.; Adam, T.; Dahham, O. S. Hashim, U.; Noriman, N. Z.; Betar, B. O. Fabrication and characterization of zinc oxide nanoparticle-treated kenaf polymer composites for weather resistance based on a solar UV radiation, *BioRes*. **2018**, 13(3), 6480-6496. DOI:10.15376/BIORES.13.3.6480-6496
4. Thipperudrappa, S.; Hiremath, A.; Nagaraj, B. K. Synergistic effect of ZnO and TiO2 nanoparticles on the thermal stability and mechanical properties of glass fiber-reinforced LY556 epoxy composites, *Polym. Compos.*. 2**021**, 1–14, https://doi.org/10.1002/pc.26193

5. Gbadeyan, O. J.; Linganiso L. Z.; Deenadayalu N. Influence of Loading Nanoclay on Properties of the Polymer-based Composite. Nanoclay - Recent Advances, New Perspectives and Applications. *IntechOpen*, **2022**. http://dx.doi.org/10.5772/intechopen.108478
6. Cazan, C.; Enesca, A.; Andronic, L. Synergic Effect of TiO2 Filler on the Mechanical Properties of Polymer Nanocomposites. *Polymers* **2021**, 13, 2017. https://doi.org/10.3390/polym13122017
7. Devnani, G.L. Sinha, S. Effect of nanofillers on the properties of natural fiber reinforced polymer composites, *Mater. Today: Proc.*, **2019**, 18(3), 647-654, ISSN 2214-7853. https://doi.org/10.1016/j.matpr.2019.06.460.
8. Adlie, T.A.; Ali, N.; Huzni, S.; Ikramullah, I.; Rizal, S. Impact of Zinc Oxide Addition on Oil Palm Empty Fruit Bunches Foamed Polymer Composites for Automotive Interior Parts. *Polymers*, **2023**, 15, 422. https://doi.org/10.3390/polym15020422
9. Sanusi, O. M.; Benelfellah, A.; Hocine, N. A. Clays and carbon nanotubes as hybrid nanofillers in thermoplastic-based nanocomposites – A review, *Appl. Clay Sci.*, **2020**, 185, 105408, ISSN 0169-1317, https://doi.org/10.1016/j.clay.2019.105408.
10. Khan, M.Z.H., Das P. P.; Abdullah, M. One step synthesis of ZnO nanoparticles with zinc acetate dehydrates and potassium, *Int. J. Nanomanufacturing*, **2020**, 16(1), 89-96.
11. Devi R. R.; Maji, T. K. Effect of Nano-ZnO on Thermal, Mechanical, UV Stability, and Other Physical Properties of Wood Polymer Composites, *Ind. & Eng. Chem. Res.*, **2012,** 51(10), 3870-3880, DOI: 10.1021/ie2018383.
12. Bose, K. J. C.; Thiagarajan, A.; Venkatesh, D. N.; Velmurugan, K. Effects of ZnO nano reinforcements in the polymer matrix on the GFRP composites fabricated through VARTM, *Mater.Today: Proc.*, **2019,** 19(2), 721-725, ISSN 2214-7853, https://doi.org/10.1016/j.matpr.2019.08.081.
13. Hassana, D. J.; Ali, N. A.. Evaluation of Mechanical Properties for Epoxy reinforced with palm oil /Zinc oxide composites. *Iraqi J. of Phys.*, **2022**, 20(2), 26–37. https://doi.org/10.30723/ijp.v20i2.978
14. Martínez, K. I.; González, R. Soto J. J.; Rosales, I. Characterization by FTIR spectroscopy of degradation of polyethylene films exposed to CO2 laser radiation and domestic composting, *J. of Phys. Conf. Ser.* 1723, **2021**, 012038, doi:10.1088/1742-6596/1723/1/012038

15. Saddem, M.; Koubaa, A.; Riedl, B. Properties of High-Density Polyethylene-Polypropylene Wood Composites. *IntechOpen*. **2022**, doi: 10.5772/intechopen.101282.
16. Nawab, Y.; Gideon, R., Atalie, D. Mechanical and Water Absorption Properties of Jute/Palm Leaf Fiber-Reinforced Recycled Polypropylene Hybrid Composites, 1687-*Int. J. of Polym. Sci.*, **2022**, 4408455, 9422. https://doi.org/10.1155/2022/4408455
17. Menta, V.G.K.; Tahir, I.; Abutunis A. Effects of Blending Tobacco Lignin with HDPE on Thermal and Mechanical Properties. *Materials (Basel*). **2022**, 23, 15(13):4437. doi: 10.3390/ma15134437. PMID: 35806561; PMCID: PMC9267181
18. Aftab, H.; Rahman, G. M. S.; Kamruzzaman, M.; Khan, M. A.; Ali, M. F.; Mamun, M. A. A.. Physico-Mechanical Properties of Industrial Tea Waste Reinforced Jute Unsaturated Polyester Composites. *J. of Eng. Adv.*, **2022**, 3(02), 42–49. https://doi.org/10.38032/jea.2022.02.001
19. Sutar, H. ; Sahoo C., P.; Sahu, S. P.; Sahoo, S.; Murmu, R.; Swain, S.; Mishra C., S. Mechanical, Thermal and Crystallization Properties of Polypropylene (PP) Reinforced Composites with High Density Polyethylene (HDPE) as Matrix, *Mater. Sci. and Appli.*, **2018**, **9**: 502-515, doi: 10.4236/msa.2018.95035.
20. Xie, Q.; Li, F.; Li, J.; Wang, L.; Li, Y.; Zhang, C.; Xu, J.; Chen, S. A new biodegradable sisal fiber–starch packing composite with nest structure, *Carbohyd. Polym.***,** **2018**, 189, 56-64, ISSN 0144-8617, https://doi.org/10.1016/j.carbpol.2018.01.063.

CHAPTER 6

Preparation and Characterization of Gamma Irradiated DPM Fiber Reinforced Composites

6.1 Introduction

Composites are formed of two or more materials that, when combined, give rise to a substance with physical or chemical properties that are markedly distinct from those of the individual materials [1]. Polymer composites are now widely used in a variety of specialized fields due to their excellent and distinctive combination of physical and mechanical characteristics, including civil construction, chemical equipment and machinery construction, electrical and electronic equipment, the automotive and marine industries, aircrafts etc. Numerous studies have been conducted on synthetic fiber-reinforced with synthetic matrix materials. The inability of the fibers to degrade is a drawback of employing synthetic fiber reinforced composites. Composites comprised of natural fibers as reinforcing agent and thermoplastic polymers as matrix are being explored more and more frequently as a result of rising environmental awareness [2,3]. Therefore, the creation of natural fiber reinforced polymer composites has garnered a lot of attention in the field of composite research recently [4]. The primary natural reinforcements now employed in the composites sector include jute, flax, hemp, sisal, and kenaf [5].

Natural fibers offer a number of benefits, including affordability, light weight, processing flexibility, low energy usage, renewability, and strong biodegradability. Furthermore, natural fibers contain hydroxyl and other polar groups in their constituents causing high moisture absorption. As a result, they show low compatibility with hydrophobic polymer matrices and have poor adhesion at the fiber-matrix interface that significantly limits their use as reinforcing materials in polymers [4,6]. The most often utilized method for increasing compatibility of natural fibers and matrices is chemical treatment. In some cases, it is not possible to produce natural fiber composites on a huge amount through chemical treatment. Environmental issues increase the stress on composite researchers to use sustainable modifications of composites with the purpose of improving performance of composites. In contrast, during the last few decades, the researchers have shifted its preference toward the modification of natural fibers via gamma radiation [5]. Gamma radiation induced composites has a number of benefits, such as uninterrupted operation, a short curing period, reduced environmental pollution, curing at room temperature, more flexible design via process control, etc [7].

In the current investigation, gamma radiation was applied to the composites to enhance their mechanical properties. The use of gamma radiation in composites is not new, but the preparation of gamma irradiated DPM fiber reinforced polymer composites is a new work. The effect of gamma radiation on the physical, mechanical, thermal and biodegradation behavior of the DPM fiber reinforced polymer composites was investigated.

6.2 Experimental

6.2.1 Materials

HDPE, and PS were purchased from Saudi Polymers Company, Saudi Arabia, and Chi Mei Corporation, Taiwan respectively. DPM fibers were collected from the local area of Jashore, Bangladesh. The DPM fibers were cut into 2-3mm by hand scissors.

6.2.2 Composite Fabrication

Compression moulding technique was used to fabricate the composites. Measured amount of HDPE and PS were mixed with DPM fibers using a blender. The mixed fibers and polymer matrix were transferred into the mould (12x15 cm^2) and finally hot pressed (Paul Otto Weber Press Machine) at a temperature fixed temperature for 5 min maintaining a pressure of 200 kN. The moulds were cooled at room temperature and 200 kN pressure for 5 min and removed from the mould.

6.2.3 Gamma Radiation

The optimized composite samples were subjected to gamma radiation to enhance their mechanical characteristics. Composite samples were sealed in an airtight plastic bag. 90 kCi Cobalt 60 was served as radiation source. Composites were subjected to various gamma radiation doses (2.5, 5.0, and 7.5 KGy) at room temperature with a dose rate 350 krad/h.

6.2.4 Bulk Density of the composites

Bulk density of the composites was calculated by measuring the weight and dimensions of the samples. The average results for five composite samples were stated.

6.2.5 Water absorption test of Composites

Water absorption tests of the composite samples were done following ASTM D570-99. The test samples were dried in an oven at 105^0C for 2h and cooled in a desiccator. The composite samples were weighed and dipped in distilled water for 24h at room temperature. The samples were withdrawn from the beaker, removed excess water with a cloth and weighed. Three composite samples were tested to get the average results.

6.2.6 Mechanical Properties

Tensile properties such as tensile strength, percent elongation at break of the composites were measured using universal strength tester (model 1410 Titans, capacity 5 kN, England). The crosshead speed was 10 mm/min. The tests were carried out according to standard method (ASTM D 3039/D 3039 (M) 2002). The average values of five specimens were stated in each case. Bending strength (three point bending) of the composites were also performed following ASTM D7900. Five measurements in each composition of the composite samples were taken and the average values were reported.

6.2.7 FTIR Spectroscopy

The non-irradiated and gamma irradiated composites were inspected by a FT-IR/NIR spectrometer (Frontier, Perkin Elmer, USA). The FTIR spectra were recorded in the region 4,000-650 cm^{-1}. FT-IR spectroscopy was used to find out the functional group of the composites.

6.2.8 Thermal Analysis

The thermogravimetric (TGA) and differential scanning calorimetry (DSC) analysis of the composite samples were performed by a NETZSCH instrument (STA 449 F3, Jupiter) in a temperature range 30-900^0C at nitrogen atmosphere. The heating rate was 10^0C/min.

6.2.9 Surface Morphology

The fracture surfaces of the tensile specimens were examined by a field emission scanning electron microscope (JEOL JSM-7600F) operated with an accelerating voltage of 5.0 kV. The samples were cut into a small portion, mounted onto holders with the help of carbon tape and coated with gold. Samples were focused onto the surfaces and observed with different magnification.

6.2.10 Soil Burial Test

The composite samples were buried in a soil containing flower pot and the moisture level was kept at least 30%. The test samples were lifted out from the soil at intervals of 1 month, cleaned with distilled water and dried at 80^0C in an oven for 6 h. The degradation was determined by measuring the tensile strength of the composite samples.

6.3 Results and Discussion

6.3.1 Bulk Density of the Composites

The optimized composites (10% DPM fiber reinforced HDPE and PS) were exposed to gamma radiation at various doses (2.5-7.5 kGy). The effect of gamma radiation on the bulk density of the composites is illustrated in figure 6.1 and 6.2. The bulk density of the gamma irradiated composites increased. The highest value was found for the composites at 5 kGy radiation dose.

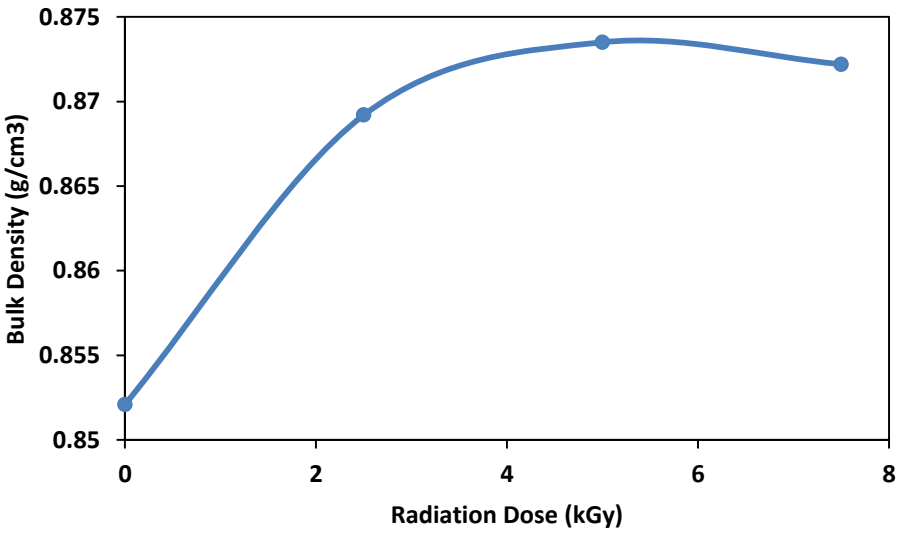

Figure 6.1: Bulk density of the DPM fiber reinforced HDPE composites at various radiation doses

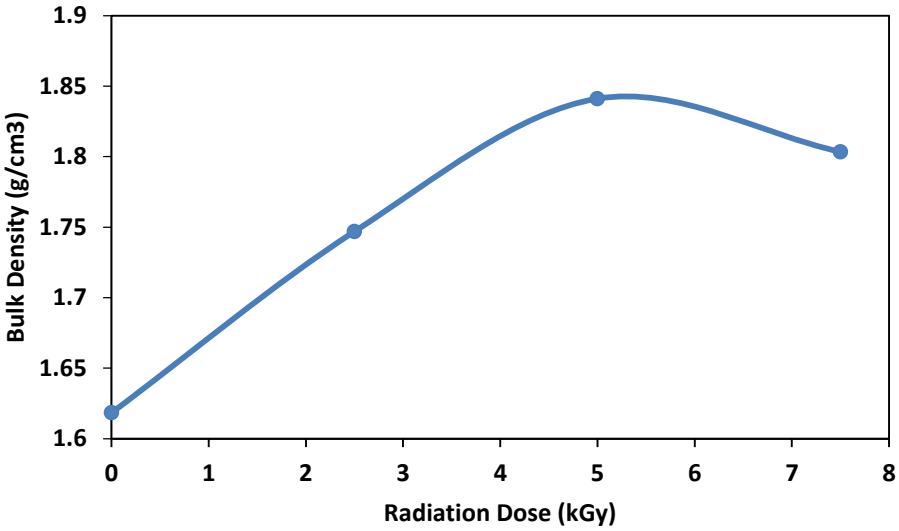

Figure 6.2: Bulk density of the DPM fiber reinforced PS composites at various radiation doses

6.3.2 Water Absorption of the composites

The effect of gamma radiation on the water absorption of the composites is represented in figures 6.3 and 6.4. The results show that the water absorption of the gamma irradiated composites decreased when compared to non-irradiated composites. Similar findings were found in agreement with the work conducted by Zaman et al. [8]. The hydrophilic properties of the natural fibers are the reason of the water absorption. The voids and micro cracks in the composites also trap water molecules. The hydroxyl groups in natural fibers are the causes of water absorption. Gamma radiation reduced the hydroxyl groups in the fibers through the removal of moisture and by crosslinking processes, reduced the amorphous portions while increasing the crystalline region [9].

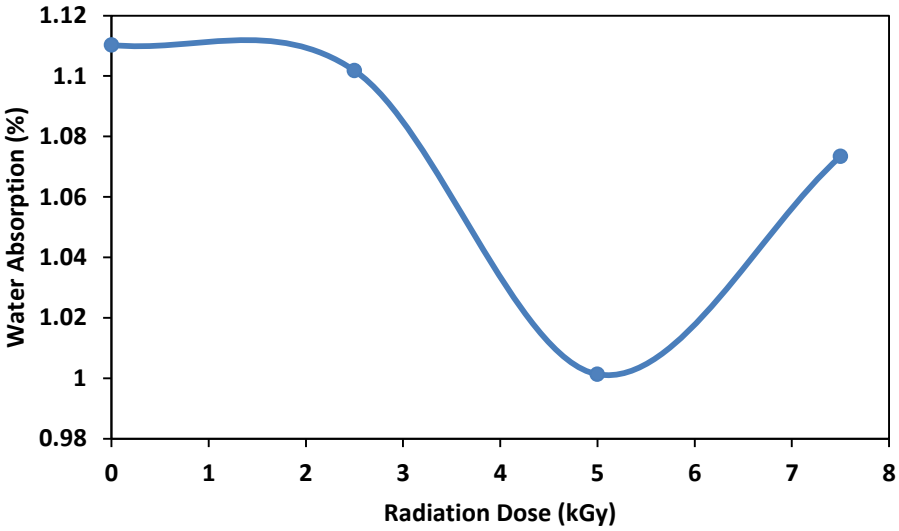

Figure 6.3: Water absorption of DPM fiber reinforced HDPE composites at various radiation doses

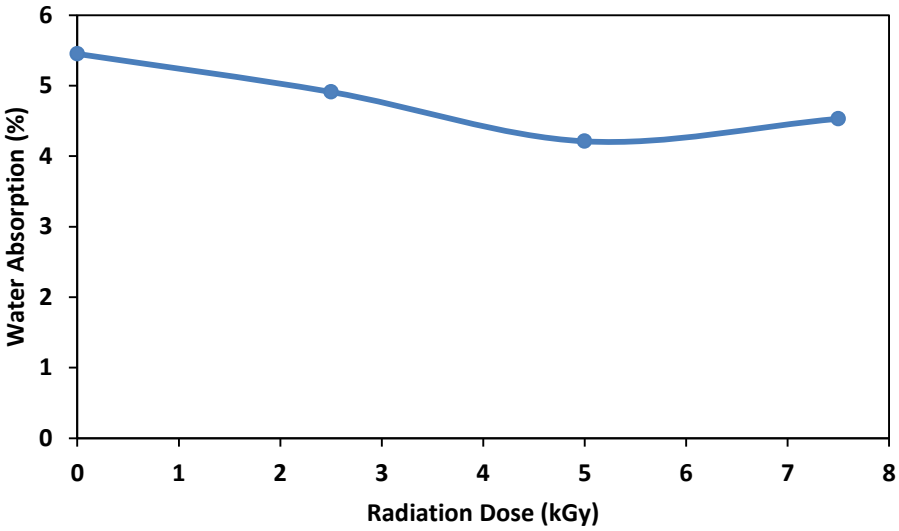

Figure 6.4: Water absorption of DPM fiber reinforced PS composites at various radiation doses

6.3.3 Mechanical Properties

The optimized composites (10% DPM fiber reinforced HDPE and PS) were exposed to gamma radiation at various doses (2.5-7.5 kGy). The effect of gamma radiation on the tensile strength of the composites is depicted in figures 6.5 and 6.6. It is clear that gamma radiation

significantly raises the tensile strength up to a certain dose. Nevertheless, the tensile strength of the composites decreases as the dose is increased beyond 5 kGy. The maximum tensile strength was observed 27.06 and 43.81 MPa at 5 kGy radiation dose for DPM fiber reinforced HDPE and PS composites respectively. The graph clearly indicate that the bending strength of the composites show an increasing trend from 2.5 to 5.0 kGy, followed by a decline in values up to 7.5 kGy dosage. The maximum bending strength was found 27.73 and 54.33 MPa at 5 kGy radiation dose for DPM fiber reinforced HDPE and PS composites respectively.

On exposure to gamma radiation photo cross-linking and photo degradation are the two opposite phenomena happen concurrently [10]. This increment in tensile and bending strength may be owing to the cross-linking of neighboring chains and consequently, better adhesion between the fiber and matrix on exposure to the gamma radiation causing the composites' more ordered polymeric structure [11]. The moisture content, which can be reduced by gamma radiation and raise the tensile strength, is one of the key barriers to improve the mechanical characteristics of the composites [12]. The degradation of the cellulose backbone caused by gamma radiation may be the cause of decreasing tensile properties of the composites. Azim et al. investigated mechanical properties of jute fiber reinforced polyester composites and noticed that under gamma radiation the tensile and bending strength of the composites raised from 2.5 to 5.0 kGy, whereas increasing radiation dose up to 9 kGy showed a decreased trend [5].

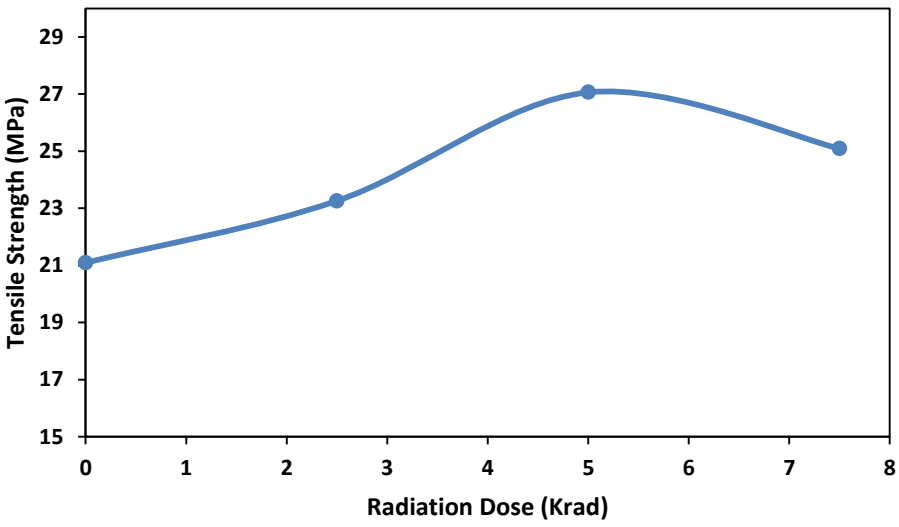

Figure 6.5: Tensile strength of DPM fiber reinforced HDPE composites at various radiation doses

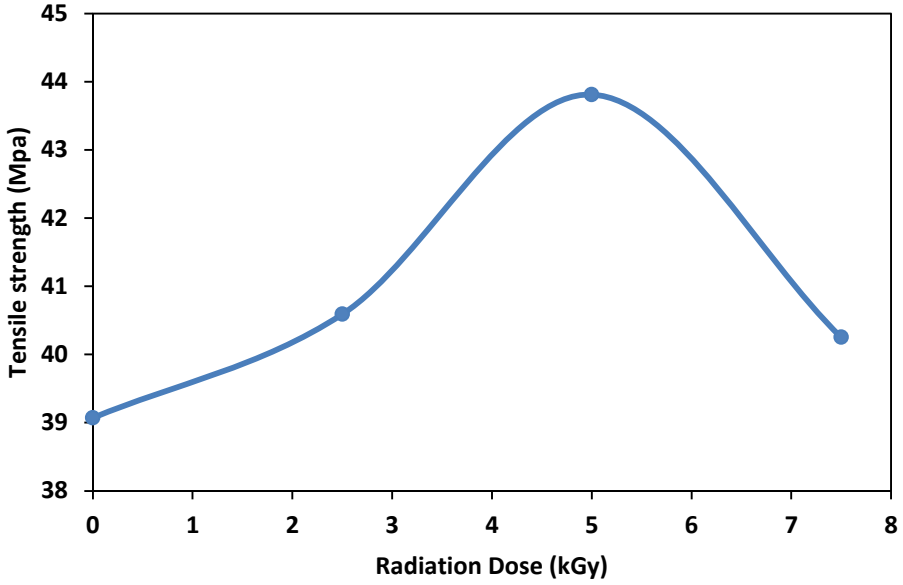

Figure 6.6: Tensile strength of DPM fiber reinforced PS composites at various radiation doses

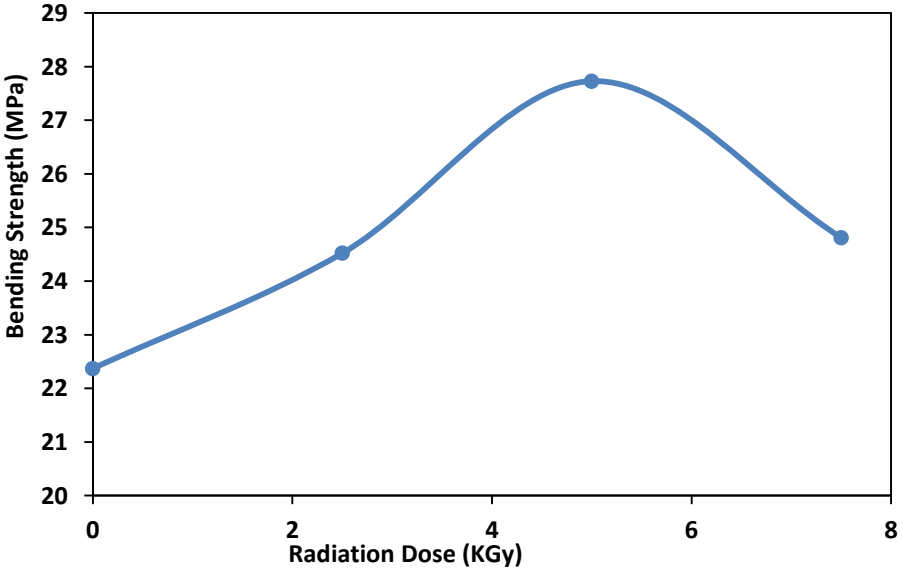

Figure 6.7: Bending strength of DPM fiber reinforced HDPE composites at various radiation doses

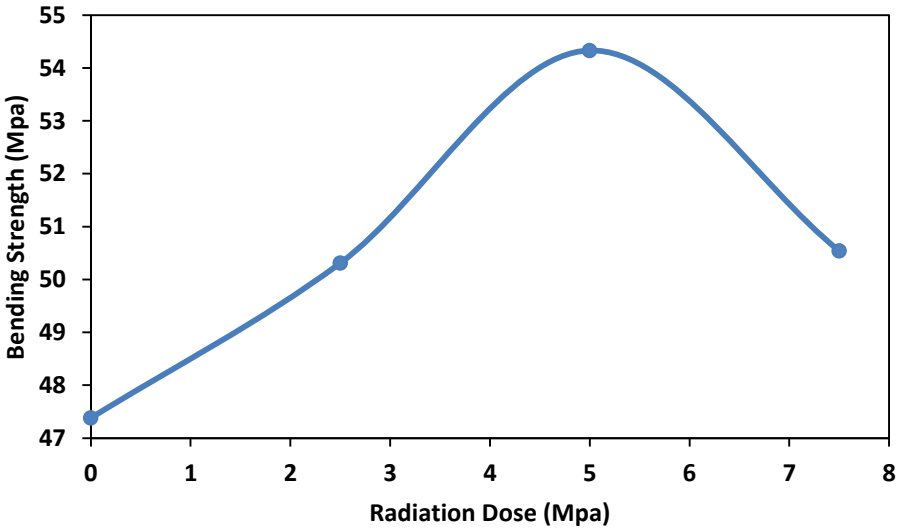

Figure 6.8: Bending strength of DPM fiber reinforced PS composites at various radiation doses

Figures 6.9 and 6.10 depict the impact of gamma radiation on the elongation at break of the composites. The graph shows that the elongation at break of the DPM fiber reinforced HDPE composites decreased up to a certain radiation dose and then increases slightly. The elongation at break of the DPM fiber reinforced PS composites initially dropped and subsequently slightly increased. The increased crosslinking between the molecules may result in increased crystallinity, which would then limit the segmental movement of the polymeric chains, causing lower elongation at break value of the composites [10].

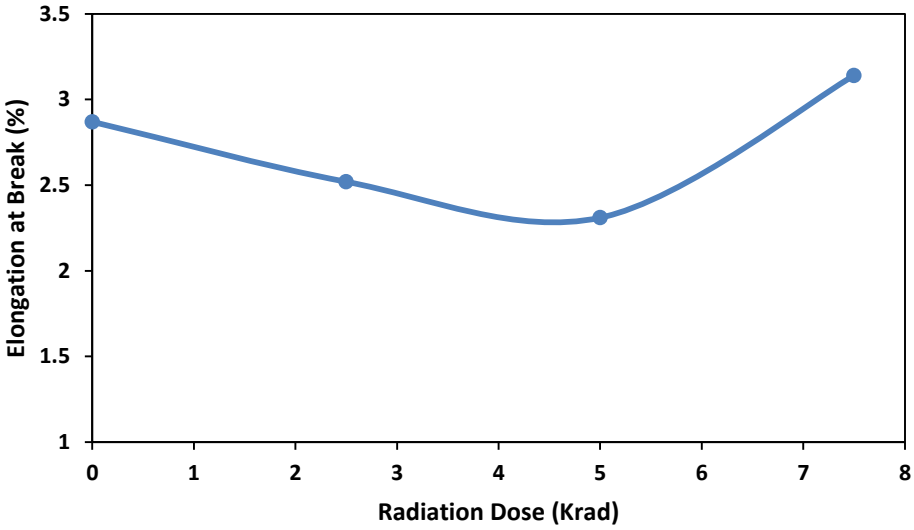

Figure 6.9: Elongation at break of DPM fiber reinforced HDPE composites at various radiation doses

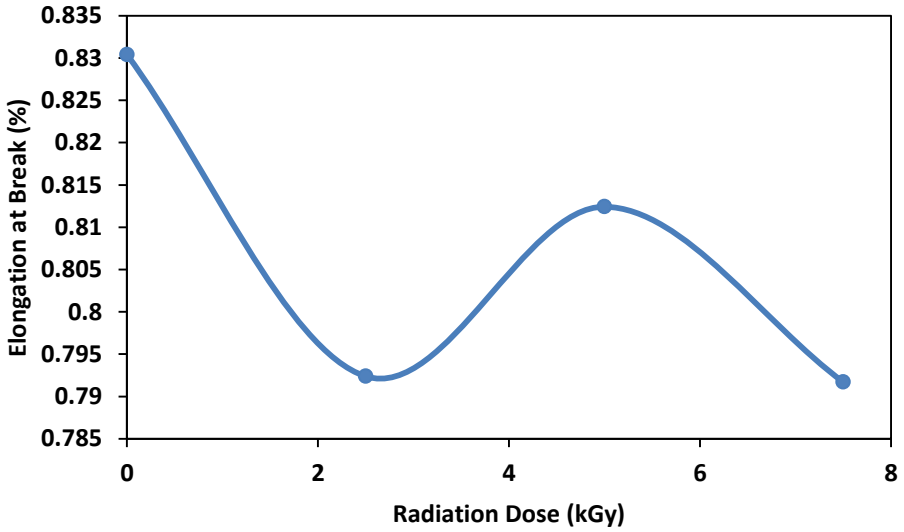

Figure 6.10: Elongation at break of DPM fiber reinforced PS composites at various radiation doses

6.3.4 FTIR Study

The FTIR spectra for non-irradiated and gamma irradiated composites are depicted in figures 6.11 and 6.12. Both non-irradiated and gamma irradiated HDPE matrix based composites displayed same peaks with a very little displacement. The peak at 2915 cm^{-1} observed for the C-H stretching vibration [13]. The absorption band at 1740 cm^{-1} specifies the C=O stretching from the lignin and hemicellulose [14]. The peak 1607 cm^{-1} directs C=C stretching in aromatic [15]. The peak at 1462 cm^{-1} refers to the $-CH_2$ group [16] and 1372 cm^{-1} indicates bending vibrations of the -CH group. The peak at 1046 cm^{-1} detects for C=O and -OH stretching vibrations of the polysaccharides in cellulose [16]. The peak 718 cm^{-1} corresponds to the rocking vibration of $-CH_2$ group [15].

Similar peaks noticed for both non-irradiated and gamma irradiated DPM fiber reinforced PS composites. The peak at 3331 cm^{-1} may relate to hydrogen-bonded O-H stretching vibrations [17]. The peak at 2923 cm^{-1} resembles to H-C-H asymmetric and symmetric stretch signifying the presence of alkane group. The peak at around 1600 cm^{-1}, specifies N-H bend of amides and H-C-H bend of alkane respectively [18]. The peak 1470cm^{-1} directs to aromatic C-C stretching and the peaks between 1000 cm^{-1} to 650 cm^{-1} attribute to the aromatic C-H bending vibrations [18]. The peaks at 1250 cm^{-1} and 1027 cm^{-1} resemble to the C-O stretch of the acetyl group, existing in lignin and hemicellulose [17].

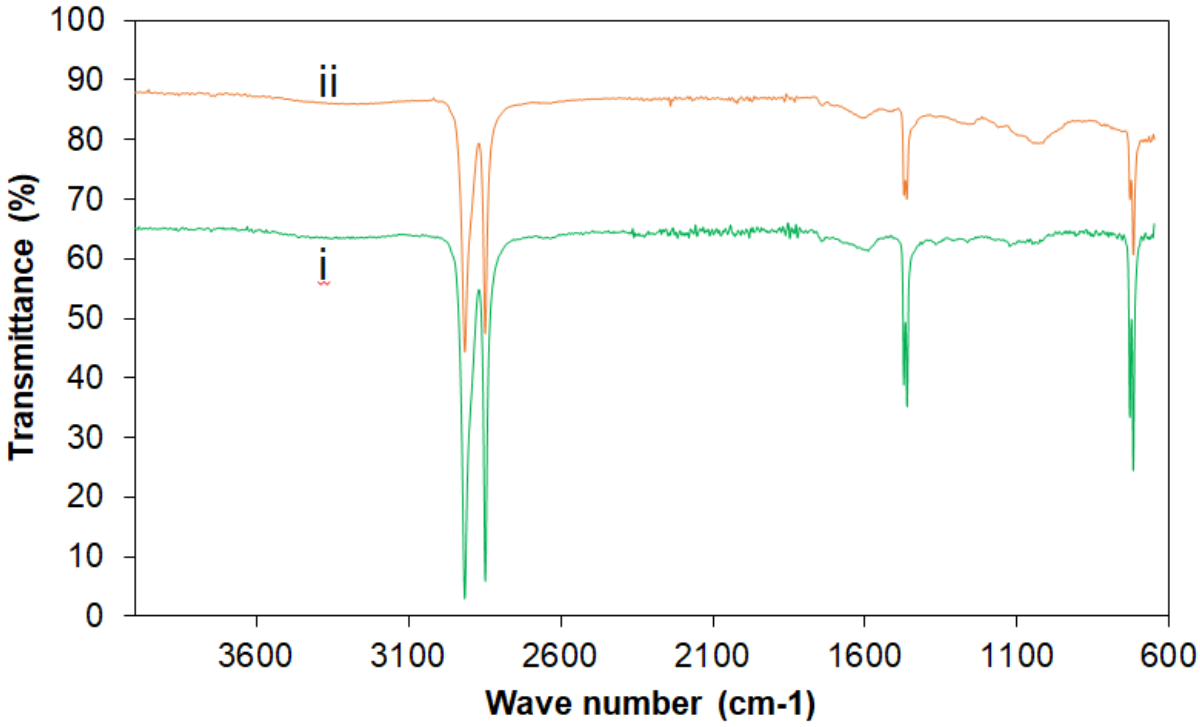

Figure 6.11: ATR-FTIR spectra of (i) gamma irradiated DPM fiber reinforced HDPE composites; (ii) non-irradiated DPM fiber reinforced HDPE composite

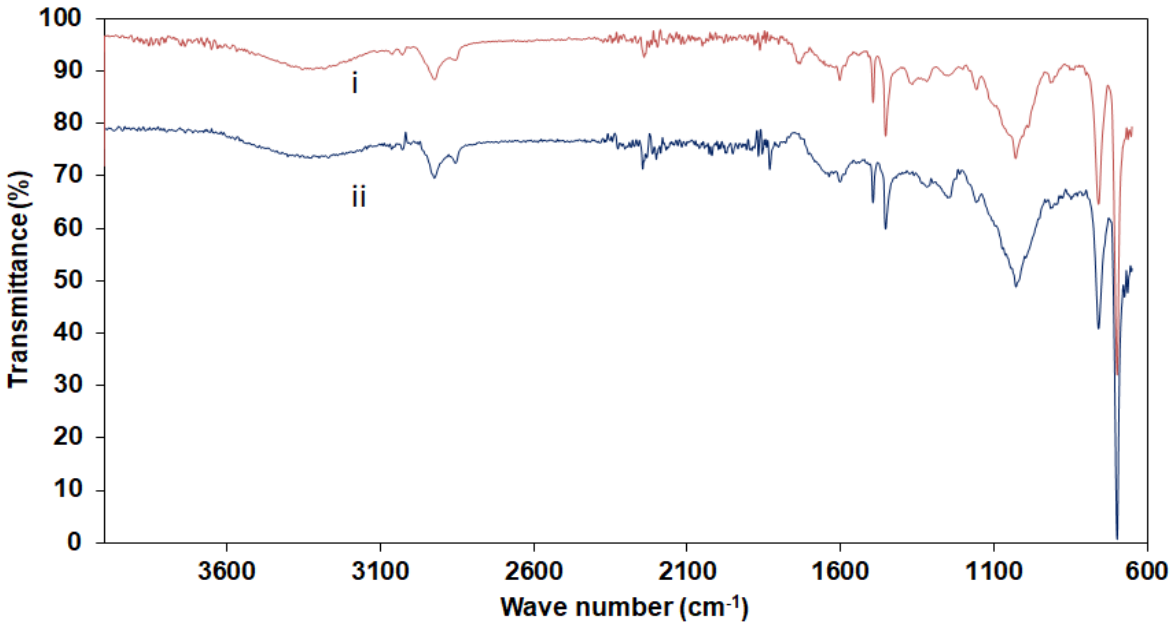

Figure 6.12: ATR-FTIR spectra of (i) gamma irradiated DPM fiber reinforced PS composites; (ii) non-irradiated DPM fiber reinforced PS composite

6.3.5 Thermal Properties

Thermal analysis of non-irradiated and gamma irradiated composites were carried out to study their thermal stability. The TGA and DSC curves are displayed in figures 6.13-6.16. The TGA results show that the non-irradiated DPM fiber reinforced HDPE composite undergoes thermal degradation beginning at 403.5^{0}C and 89.37% mass change is completed at about 500^{0}C. On the other hand, the degradation of gamma irradiated DPM fiber reinforced HDPE composites start at 405.0^{0}C and a total 96.82% mass change is completed at about 500^{0}C. For non-irradiated and gamma irradiated DPM fiber reinforced HDPE composites, the percentage of the residual mass at the finish of the heating process was 7.99 and 3.18 respectively. The DSC curves of non-irradiated and gamma irradiated DPM fiber reinforced HDPE composites showed peaks of melting at 141.1 and 174.5^{0}C respectively. The melting temperature of the composites increased, this may be due to the application of gamma radiation. The DSC result of gamma irradiated DPM fiber-HDPE composite revealed that the composite is thermally slightly more stable than non-irradiated composite due to high melting temperature.

From the figure it is clear that non-irradiated DPM fiber reinforced PS composite started to degrade at 363.0 ^{0}C whereas gamma irradiated DPM fiber reinforced PS composite began to degrade at 367.3 ^{0}C. It can be concluded from the TGA curves that gamma irradiated DPM fiber reinforced PS composite is more thermally stable than non-irradiated DPM fiber reinforced PS composite. In case of DSC curve, a sharp peak was observed at 414.7 ^{0}C for non-irradiated composites and 379.3 ^{0}C at for and gamma irradiated DPM fiber reinforced PS composites.

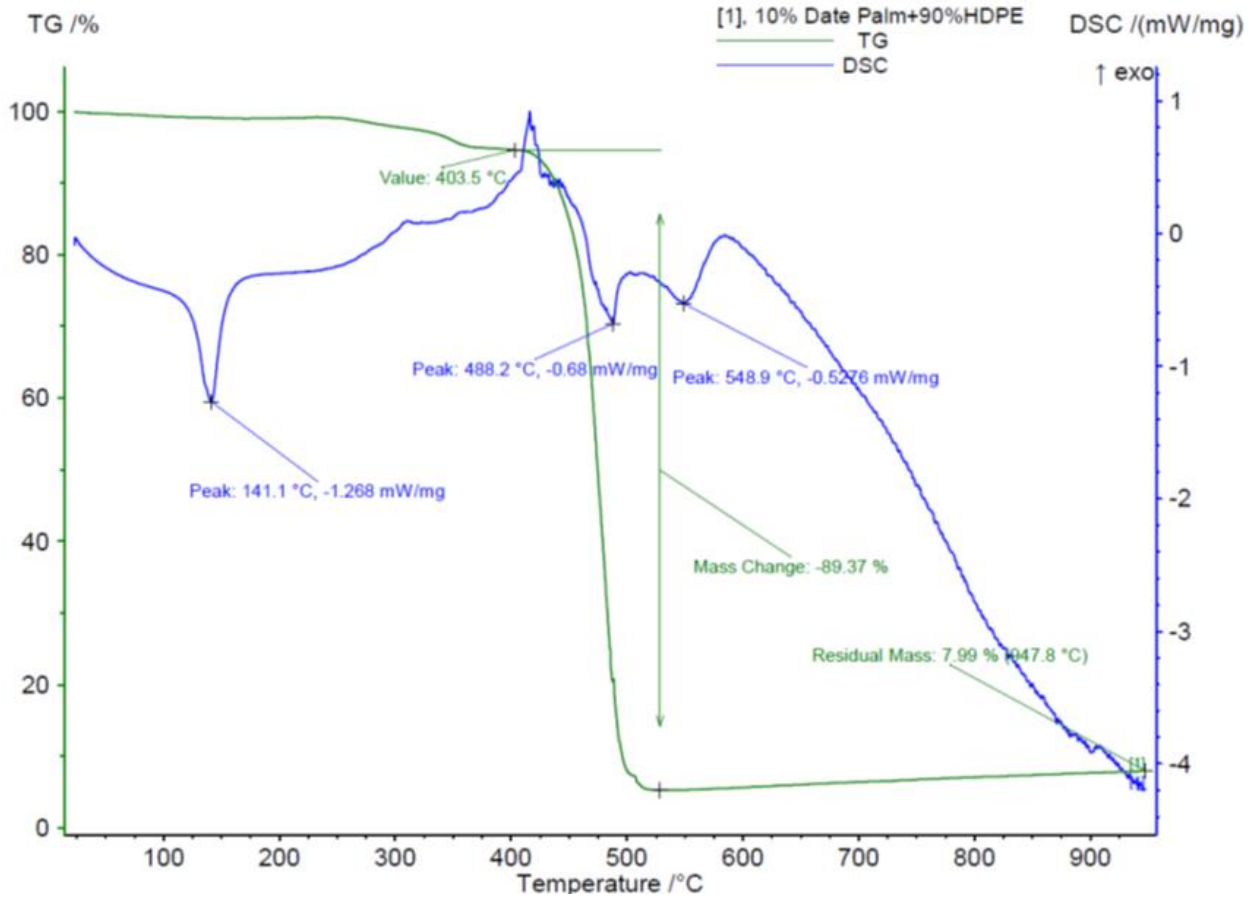

Figure 6.13: TGA and DSC of non-irradiated DPM fiber reinforced HDPE composite

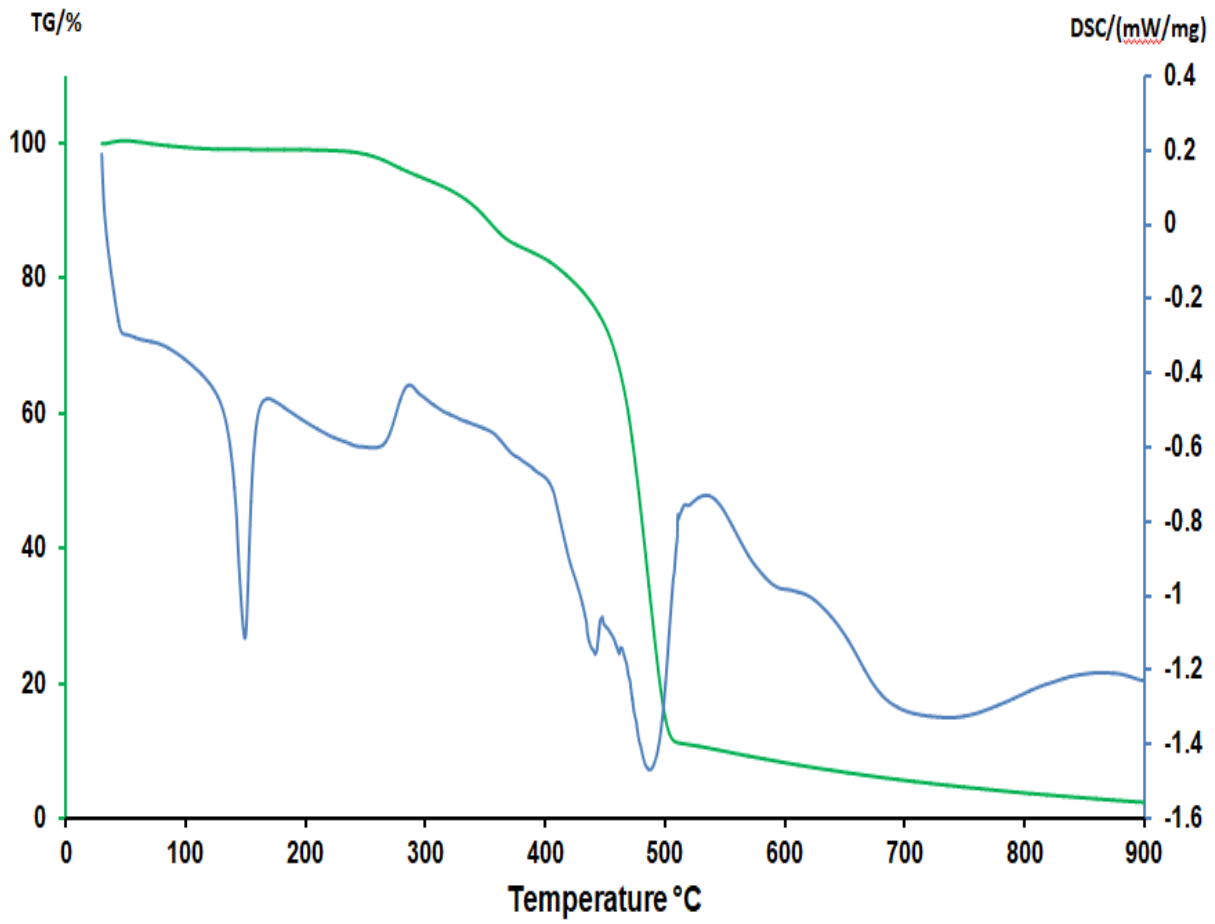

Figure 6.14: TGA and DSC gamma irradiated DPM fiber reinforced HDPE composites

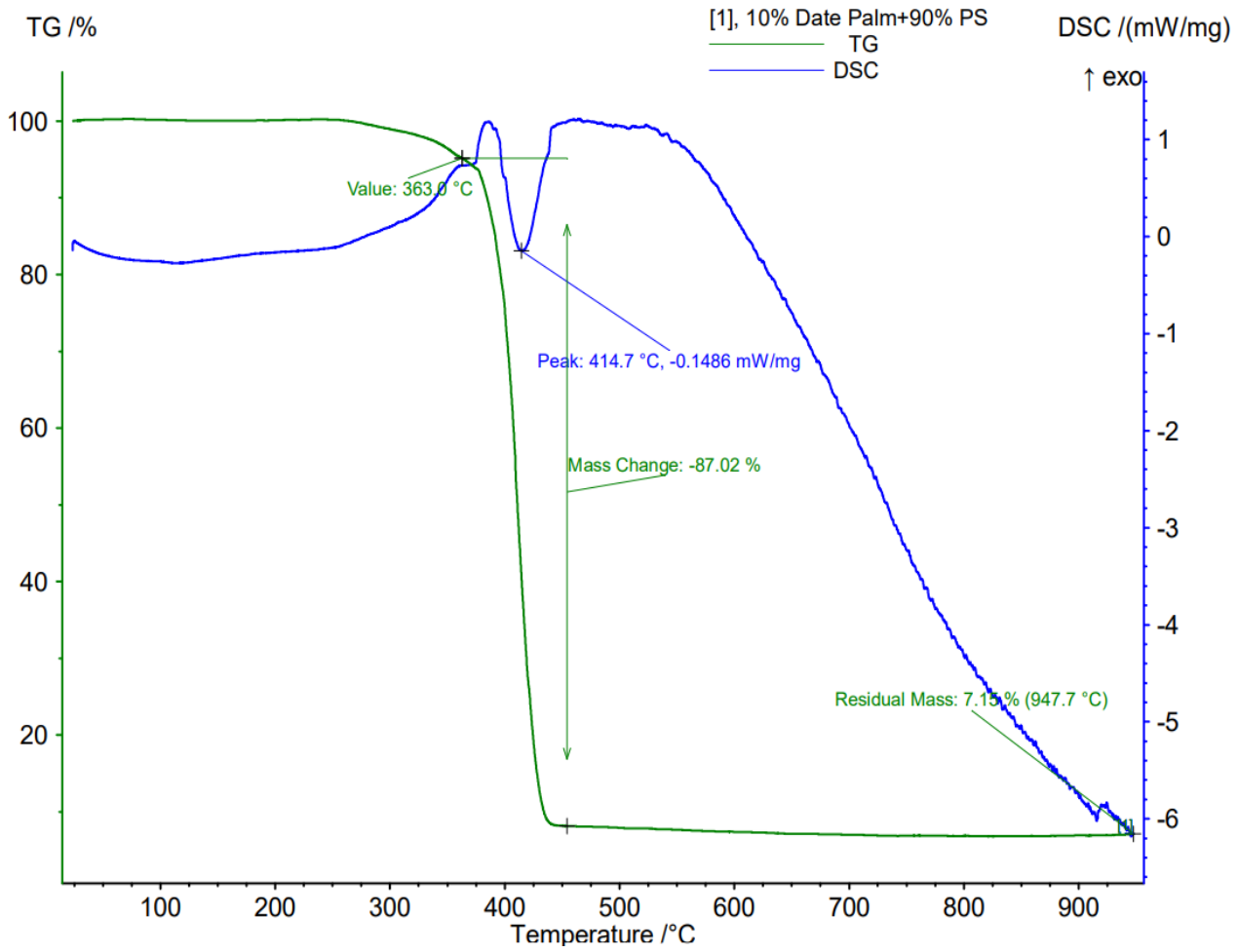

Figure 6.15: TGA and DSC non-irradiated DPM fiber reinforced PS composite

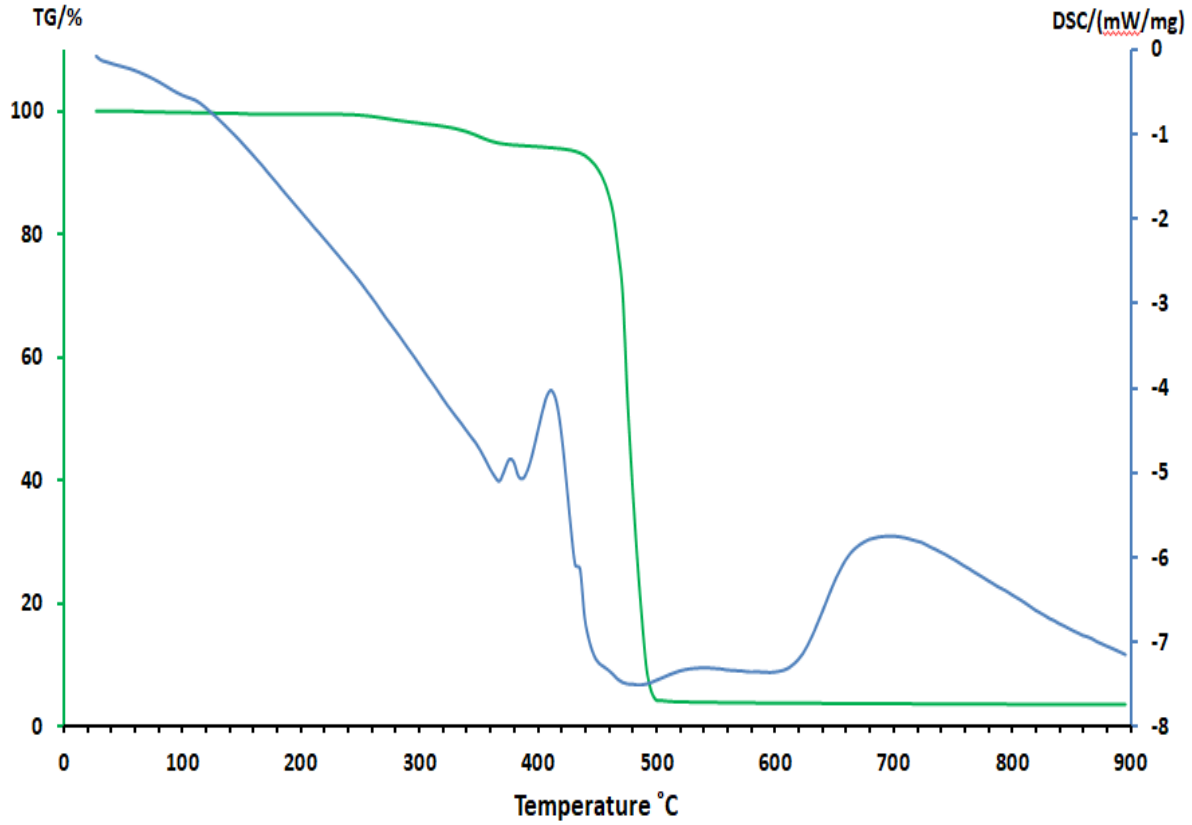

Figure 6.16: TGA and DSC gamma irradiated DPM fiber reinforced PS composites

6.3.6 Morphological Analysis

The surface morphology of the tensile fracture surfaces of the non-irradiated DPM fiber reinforced composites and gamma irradiated DPM fiber reinforced composites were examined and the SEM micrographs in different magnitude are displayed in figures 6.17 and 6.18. SEM micrographs of the fracture surfaces suggested that superior fiber-matrix interaction between fibers and polymer matrix was observed for gamma irradiated DPM fiber reinforced composites whereas voids and loosely bonded fiber-matrix adhesion was found for non-irradiated DPM fiber reinforced composites. The mechanical properties stated in this experiment also supported by SEM micrographs. Overall, the visual representation is unambiguous, exposing the composites' interfacial features and providing an explanation for why gamma-irradiated composites exhibited higher mechanical properties than non-irradiated composites.

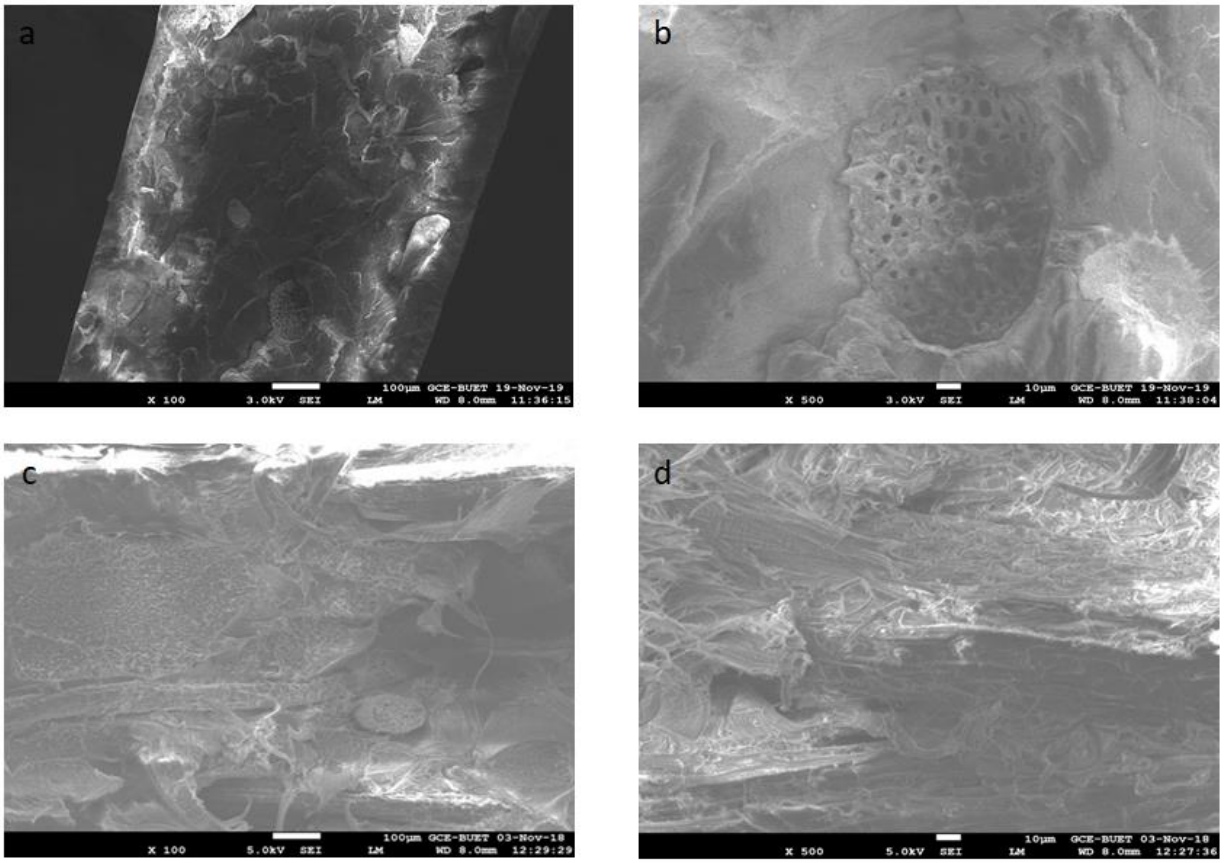

Figure 6.17: SEM micrographs of gamma irradiated (5kGy) DPM fiber HDPE composites (a) 100x magnification; (b) 500x magnification and non-irradiated DPM fiber HDPE composites (c) 100x magnification; (d) 500x magnification

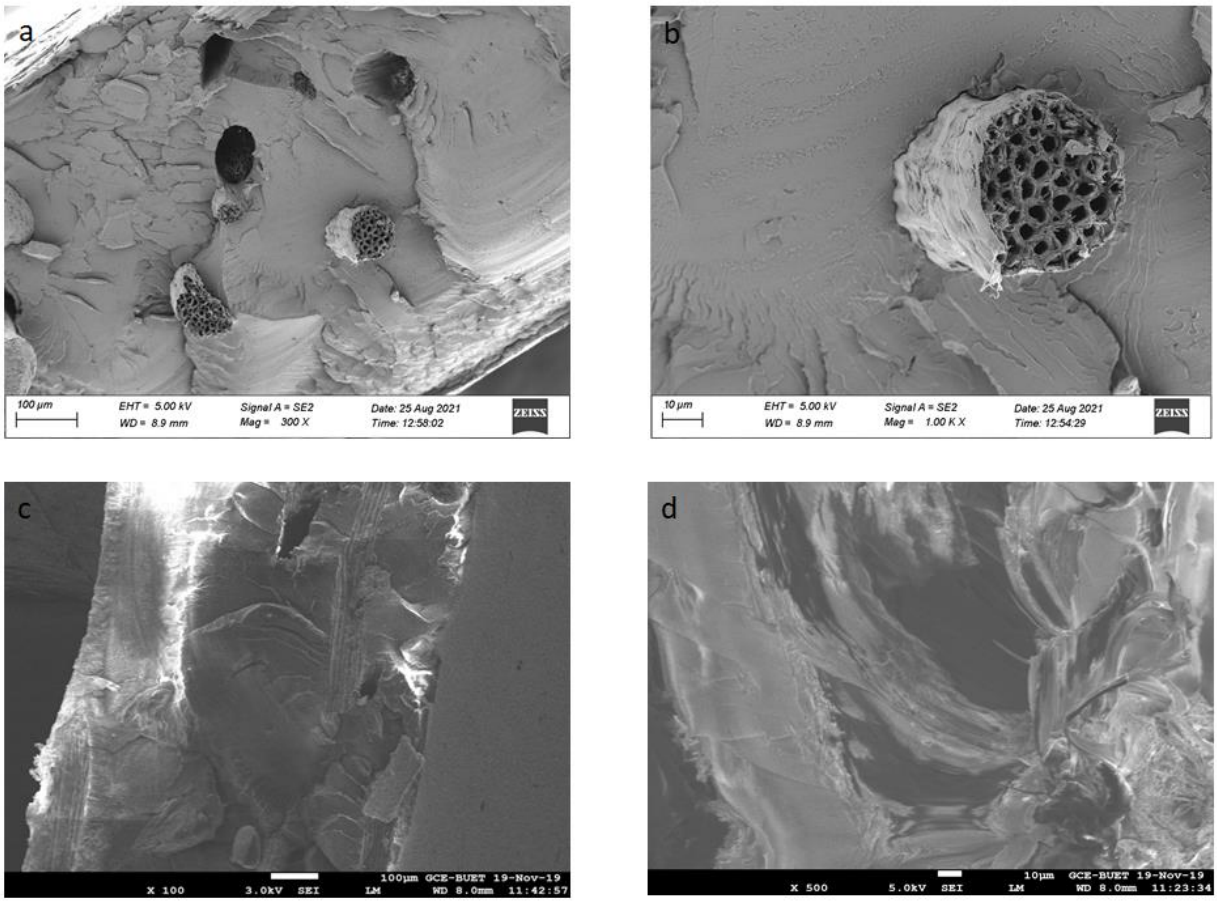

Figure 6.18: SEM micrographs of gamma irradiated (5kGy) DPM fiber PS composites (a) 100x magnification; (b) 500x magnification and non-irradiated DPM fiber PS composites (c) 100x magnification; (d) 500x magnification

6.3.7 Degradation by Soil Burial

Soil burial experiments of the non-irradiated and gamma irradiated composites (5kGy) were done in soil for six months. The change in tensile strength of the composites afterward soil burial was measured and the results are shown in figures 6.19 and 6.20. The non-irradiated DPM fiber reinforced HDPE composites lost 24.1% of tensile strength whereas 16.9% decrease in tensile strength was observed for gamma irradiated DPM fiber reinforced HDPE composites. On the contrary, the non-irradiated DPM fiber reinforced PS composites lost 10.9% of tensile strength whereas 8.9% decrease in tensile strength was observed for gamma

irradiated DPM fiber reinforced PS composites. In both cases, gamma irradiated composite samples retained much of their tensile strength through soil burial test. Gamma irradiated composites' more ordered polymeric structure and reduced hydrophilic character of the fiber causing relatively less water penetration and consequently, retained much of their tensile strength compared to non-irradiated composites.

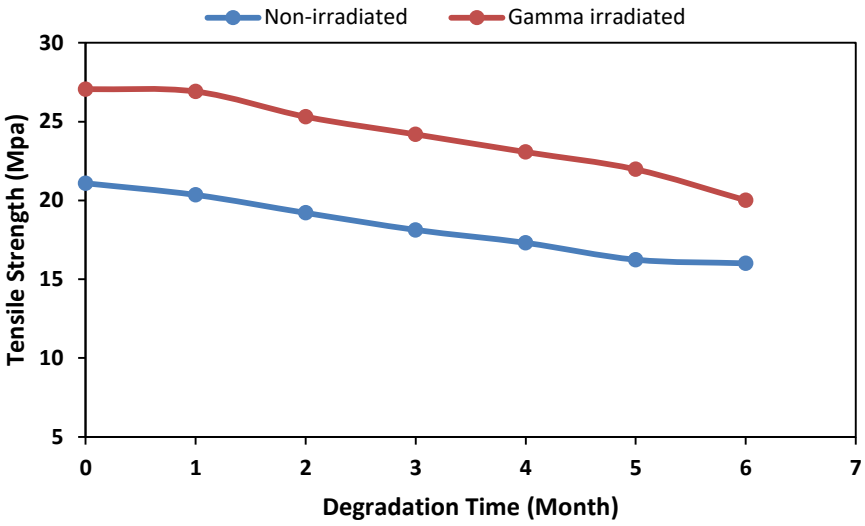

Figure 6.19: Variation of tensile strength of the buried non-irradiated and gamma DPM fiber HDPE composites

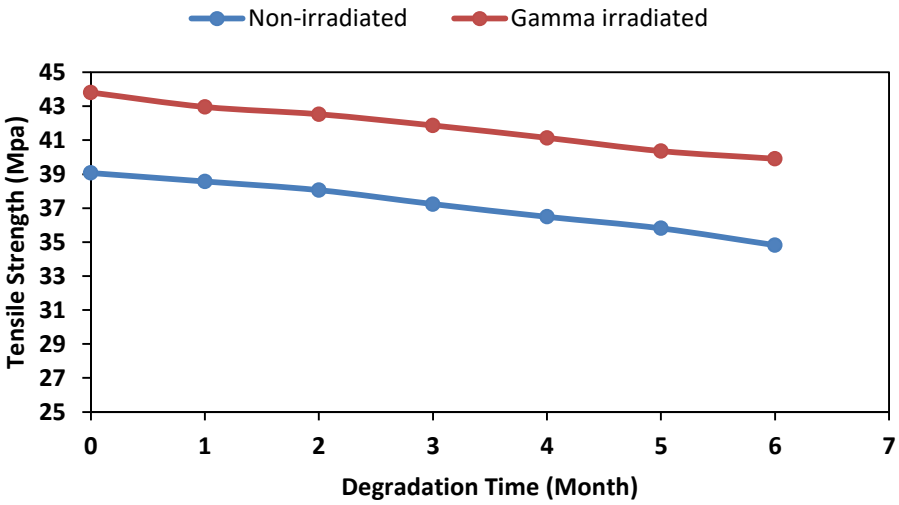

Figure 6.20: Variation of tensile strength of the buried non-irradiated and gamma DPM fiber PS composites

6.4 Conclusions

In this study, short DPM fiber reinforced composites were prepared by compression moulding technique. The composite samples were characterized with the help of various instrumental techniques. It can be concluded that composites at radiation dose 5 kGy show better mechanical properties. The gamma irradiated composites are thermally more stable than non-irradiated composites. Morphological analysis of tensile fractured surfaces of composites at radiation dose 5 kGy shown good fiber-matrix interfacial adhesion compared to non-irradiated composites. The mechanical properties of the composites formed from DPM fiber revealed that they may be a potential choice for diversified applications.

6.5 References

1. Raghavendra, S. B. S.; Vinod, B.; Sudev, L. J. Effect of Gamma Irradiation on Mechanical Properties of Natural Fibers Reinforced Hybrid Composites, IJSTE – *Int. J. of Sci. Technol. & Eng.* , **2015**, 2(4), ISSN (online): 2349-784X.
2. Verma, D.; Gope, P.C.; Maheshwari, M.K.; Sharma, R.K. Bagasse Fiber Composites-A Review, *J. Mater. Environ. Sci.*, **2012**, 3(6), 1079-1092, ISSN : 2028-2508.
3. Rahman, A.N.M.; Alimuzzaman, S.; Khan, R.A.; Hossen, J. Evaluating the performance of gamma irradiated okra fiber reinforced polypropylene (PP) composites: comparative study with jute/PP. *Fash. Text.* **2018**, 5, 28 https://doi.org/10.1186/s40691-018-0148-y
4. Zhu, J., Xiong, J., Hu, X. et al. Mechanical Properties and Wettability of Bagasse-reinforced Composite. *J. Wuhan Univ. Technol.-Mat. Sci.*, **2019**, 34, 312–316. https://doi.org/10.1007/s11595-019-2053-7
5. Azim, A. Y.M. A.; Alimuzzaman S.; Sarker F. Optimizing the Fabric Architecture and Effect of γ-Radiation on the Mechanical Properties of Jute Fiber Reinforced Polyester Composites, *ACS Omega* **2022**, 7, 12, 10127–10136, https://doi.org/10.1021/acsomega.1c06241
6. Shah, S. S. M.; Munirah, N. R.; Noriman, N. Z. The influences of filler loading on tensile properties and water absorption properties of carbonized sugarcane bagasse

filled high density polyethylene (HDPE) composite, *IOP Conf. Ser.: Mater. Sci. Eng*. **2020,** 932 012026, DOI 10.1088/1757-899X/932/1/012026

7. Shubhra, Q.T.H.; Alam, A.K.M.M. Effect of gamma radiation on the mechanical properties of natural silk fiber and synthetic E-glass fiber reinforced polypropylene composites: A comparative study, *Rad. Phys. and Chem.y*, **2011**, 80(11), 1228-1232, ISSN 0969-806X, https://doi.org/10.1016/j.radphyschem.2011.04.010.
8. Zaman, H. U.; Khan, A. H.; Hossain, M. A.; Khan, M. A.; Khan, R. A. Mechanical and Electrical Properties of Jute Fabrics Reinforced Polyethylene/Polypropylene Composites: Role of Gamma Radiation, *Polym.-Plas. Technol. and Eng.*, **2009**, 48(7), 760-766, DOI: 10.1080/03602550902824655.
9. Amir, S.M.M.; Sultan, M.T.H.; Jawaid, M.; Shah, A.U.M.; Hamdan, A.; Mohd, S.; Salleh, K.A.M. Water Absorption Associated with Gamma Irradiation on Kevlar/Oil Palm EFB Hybrid Composites, *Int. J. of Rec. Technol. and Eng.*, **2019**, 8(1S5), ISSN: 2277-3878.
10. Motaleb, K.Z.M.A.; Milašius, R.; Ahad, A. Influence of gamma radiation on mechanical properties of jute fabric-reinforced polymer composites, *Fibers.* **2020**, 8. https://doi.org/10.3390/FIB8090058.
11. Amir, S.M.M.; Sultan, M.T.H.; Jawaid, M.; Safri, S.N.A.; Shah, A.U.M.; Yusof, M.R.; Naveen, J.; Mohd, S.; Salleh, K.A.M.; Saba, N. Effects of layering sequence and gamma radiation on mechanical properties and morphology of Kevlar/oil palm EFB/epoxy hybrid composites, *J. Mater. Res. Technol.* **2019**, 8, 5362–5373. https://doi.org/10.1016/j.jmrt.2019.09.003.
12. Ndiaye, D.; Tidjani, A. Physical changes associated with gamma doses on wood/polypropylene composites, *IOP Conf. Ser. Mater. Sci. Eng.* **2014**, 62. https://doi.org/10.1088/1757-899X/62/1/012025.
13. Sutar, H. ;Sahoo C., P. ; Sahu S.; P. , Sahoo, S. , Murmu, R. , Swain, S. and Mishra C., S., Mechanical, Thermal and Crystallization Properties of Polypropylene (PP) Reinforced Composites with High Density Polyethylene (HDPE) as Matrix, *Mater. Sci. and Appli.*, **2018**, 9, 502-515, doi: 10.4236/msa.2018.95035.
14. Kamarudin, S. H.; Abdullah, L. C.; Aung, M. M.; Ratnam, C. T. A study of mechanical and morphological properties of PLA based biocomposites prepared with

EJO vegetable oil based plasticiser and kenaf fibres, *IOP Conf. Series: Mater. Sci. and Eng.*, **2018**, 368, doi:10.1088/1757-899X/368/1/012011

15. Singh, A. A.; Palsule, S. Composite Interfaces (2013): Jute fiber-reinforced chemically functionalized high density polyethylene (JF/CF-HDPE) composites with in situ fiber/matrix interfacial adhesion by Palsule Process, *Compos. Interf.*, **2013**, http://dx.doi.org/10.1080/15685543.2013.813192
16. Onifade, D.V.; Ighalo, J.O.; Adeniyi, A.G. Morphological and Thermal Properties of Polystyrene Composite Reinforced with Biochar from Plantain Stalk Fibre, *Mater. Int.* **2020**, 2, 150–156. https://doi.org/10.33263/materials22.150156
17. Kreutz, J.C.; de Souza, P.R.; Benetti, V.P.; Freitas, A. R.; Bittencourt, P.R.S.; Gaffo, L., Mechanical and thermal properties of polystyrene and medium density fiberboard composites, *Polimeros*, **2021**, 31, 1–7,. https://doi.org/10.1590/0104-1428.07120.
18. Chauhan, R.S.; Gopinath, S.; Razdan, P.; Delattre, C.; Nirmala, G.S.; Natarajan, R. Thermal decomposition of expanded polystyrene in a pebble bed reactor to get higher liquid fraction yield at low temperatures, *Waste Manag.* **2008**, 28, 2140–2145. https://doi.org/10.1016/j.wasman.2007.10.0001.

CHAPTER 7

Preparation and Characterization of Fire Retardant Additives Loaded DPM Fiber Reinforced Composites

7.1 Introduction

Polymer composites reinforced with natural fiber have received considerable attention in different fields of industrial applications owing to ecological and economical benefits over the traditional composites. The utilization of natural fibers has offered many advantages such as light weight, renewability, high specific strength, easy availability, low cost, biodegradability, less damage to equipment during processing and free from toxic byproducts [1,2,3]. Polymer composites reinforced with natural fiber have been used in many applications especially in disposable accessories, packaging, civil infrastructure, insulation, aircraft, spacecraft, and automotive industry [4,5].

Composites made of thermoplastic resin are widely used because of their favorable production characteristics and good mechanical properties [6]. High Density Polyethylene (HDPE) and Polystyrene (PS), two common thermoplastics, have some particularly notable properties. HDPE has low density, low melting temperature, and relatively good mechanical properties [7]. HDPE polymer is used for a variety of things, including food storage containers, bottle caps, and pipes for moving hazardous waste and potable water [8]. PS exhibits excellent mechanical capabilities as well as dimensional stability, electrical insulation, anticorrosive properties, transparency, and ease of processing [9, 10]. Thus, PS is employed in a variety of applications, including those related to refrigerator liners, home appliances, food packaging, vending cups, cousion materials during the transportation of products, the automobile, and the engineering sectors [10, 11, 12]. However, the use of these composite materials has significantly amplified the risk of fire due to their capability of catching fire and possible escape of toxic byproducts and fire accident resulted serious damages to people's lives and of belongings [13,14]. Therefore, it is required to improve the fire retardancy of the polymer composites reinforced with natural fiber to achieve the demand for wider applications.

Ribeiro et al. prepared jute fiber reinforced epoxy composites and investigated their flame retardancy. They noticed that the addition of jute fiber had no influence on the fire [15]. Zaman et al. studied chemical and flame resistance of jute fiber reinforced unsaturated polyester composites. They stated that the composites exhibited better mechanical and flame resistance properties [16]. Bhattacharjee et al. [17] made jute fiber reinforced polyvinyl

chloride/polypropylene hybrid composites and examined their flame retardancy. They used aluminium trihydrate and zinc borate with antimony trioxide as fire retardant additives and found improved fire resistance properties over the virgin matrix. Starch/plant fiber composites with foam structure were prepared by Cui et al. [18] and magnesium hydroxide was used as fire retardant additive. They found that magnesium hydroxide improved the fire retardancy of the composites. To obtain the desired fire resistance, fire retardants are physically mixed or chemically included into the composites.

The goal of this study was to investigate the effect of monosodium phosphate (MSP), monoammonium phosphate (MAP) and magnesium hydroxide (MH) as fire retardants on the mechanical properties (including tensile strength, bending strength, elongation at break) and fire retardant properties of the date palm mat fiber reinforced composites.

7.2 Experimental

7.2.1 Materials

In this work, high density polyethylene (HDPE) and polystyrene (PS) were used as polymeric matrix and DPM fibers are chosen as reinforcement. HDPE and PS were purchased from Saudi Polymers Company, Saudi Arabia and Chi Mei Corporation, Taiwan respectively. DPM fibers were collected from Jashore, Bangladesh. Monosodium phosphate (MSP), monoammonium phosphate (MAP) and magnesium hydroxide (MH) were used as fire retardant additives which are bought from Sigma-Aldrich. MSP, MAP and MH were used as received. HDPE and PS were grinded in a grinding machine in order to get a good mixture of polymer matrix, fiber and additives. . Fibers were chopped into 2-3 mm in length.

7.2.2 Methods

7.2.1 Preparation of Composite

The composites were prepared by compression moulding technique. Required amount of polymer matrix, fiber and fire retardant additives according to table 7.1 were dry blended in a blender and poured inside of the mould (12x15 cm^2). The moulds were placed in a compression moulding machine (Paul Otto Weber Press Machine). A pressure 200 kN

applied, the temperature is 160^0C for HDPE and and 210^0C for PS and hot pressed for 5 min. followed by cooling to room temperature at 200 kN. After curing, the composites were cut according to ASTM standard method.

Table 7.1: Sample code and compositions of the composites

Sample code	Compositions
HDPEF1	Matrix(HDPE) + Fiber(10%)
HDPEFMSP2	Matrix(HDPE) + Fiber(10%) + Monosodium Phosphate (10%)
HDPEFMAP3	Matrix(HDPE) + Fiber(10%) + Monoammonium Phosphate (10%)
HDPEFMH4	Matrix(HDPE) + Fiber(10%) + Magnesium Hydroxide (10%)
PSF5	Matrix(PS) + Fiber(10%)
PSFMSP6	Matrix(PS) + Fiber(10%) + Monosodium Phosphate (10%)
PSFMAP7	Matrix(PS) + Fiber(10%) + Monoammonium Phosphate (10%)
PSFMH8	Matrix(PS) + Fiber(10%) + Magnesium Hydroxide (10%)

7.2.2 Bulk Density

Bulk density of the composites was determined by measuring the weight and dimensions of the samples using the following equation 7.1. The average results for five composite samples were stated.

$$Density\ (g/cm^3) = \frac{Weight\ of\ the\ composite\ (g)}{(Length \times Width \times Height)\ of\ the\ composite} \quad (7.1)$$

7.2.3 Mechanical Properties Analysis

Tensile properties of the composites were examined using universal strength tester (model 1410 Titans, capacity 5 kN, England). The crosshead speed was 10 mm/min and a gauge length of 50 mm. The tests were performed according to standard method ASTM D 882-02. Bending strength (three point bending) of the composite samples was also done following ASTM D7900. In each case, the average results of five samples were presented.

7.2.4 Fire Retardant Properties Study

Fire Retardant Properties tests on DPM fiber reinforced polymer composites were performed following ASTM D635 for horizontal UL-94 and ASTM D3801 for vertical UL-94. The test samples were fixed in horizontal and vertical directions through a stand. In order to fire the sample, a Bunsen burner is used. The sample was exposed to fire. The required time for burning was calculated using a stop watch. Five replicate samples were tested to get an average value. The burning rate of the composites was calculated by following the equation 7.2.

$$\text{Burning rate (mm/min)} = 60 \times \frac{\text{Length of the sample burnt (mm)}}{\text{Burning time of the sample (S)}} \quad (7.2)$$

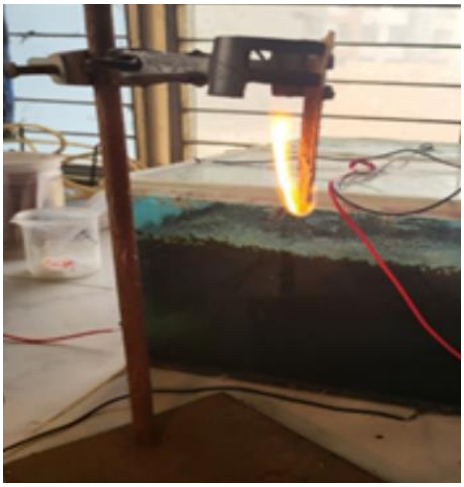

Figure 7.1: Photographs of fire retardant properties test

7.3 Results and Discussion

7.3.1 Bulk Density

The density of the composite material becomes more significant in applications where weight is a consideration in addition to their flame retardant properties. The effect of fire retardant additives on the bulk density of the composites is demonstrated in figure 7.2. The bulk density of composites decreases with the incorporation of fire retardant additives. The highest density is 1.6138 g/cm^3 found for the composite PSF5. Among three types of fire retardant additives, MAP loading composites exhibited the highest density. However, MSP loading composites exhibited the lowest density. This may be due to the development of a weak interface between the composite phases and formation of voids or gaps [19].

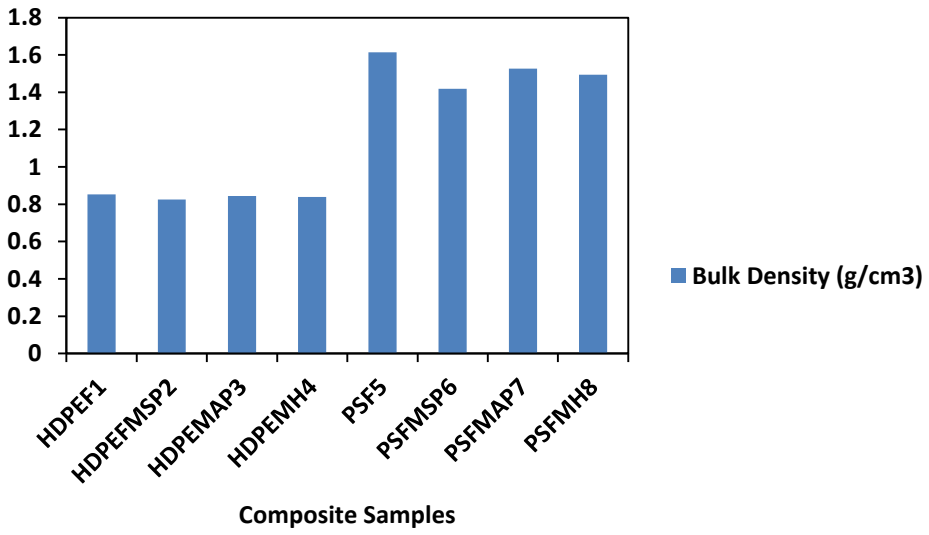

Figure 7.2: Effect of fire retardant additives on the bulk density of the composites

7.3.2 Mechanical Properties of the Composites

The mechanical properties such as tensile strength, bending strength, and elongation at break of the prepared composites were determined. The obtained results from the mechanical tests are presented below in the figures 7.3 and 7.4. Among the HDPE matrix based composites, HDPEF1 shows higher tensile strength, bending strength, and elongation at break 21.09 MPa, 22.37 MPa, and 2.87% respectively. In the case of PS matrix based composites, PSF5 shows higher tensile strength, bending strength, and elongation at break 39.07 MPa, 47.38 MPa, and 0.83% respectively. With the incorporation of fire retardant additives, the composites exhibited a reduction of tensile strength, bending strength, and elongation at break. The addition of MAP in the DPM fiber reinforced PS composites showed higher tensile strength and bending strength when compared to the composites with MSP and MH. The PSF5 (DPM fiber reinforced PS) composites are superior to HDPEF1 (DPM fiber reinforced HDPE). Generally, a reduction of mechanical properties was observed when fire retardant additives are incorporated into the polymer composites [20]. Bhattacharjee et al. [17] prepared fire retardant composites and found that the tensile strength and bending strength of the composites decreased with the addition of fire retardant additives.

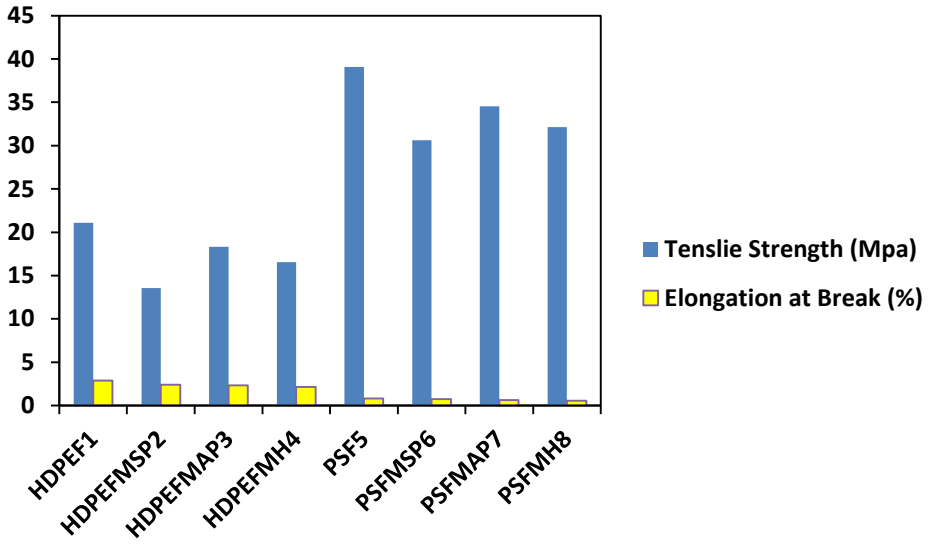

Figure 7.3: Tensile strength, and elongation at break of the composites

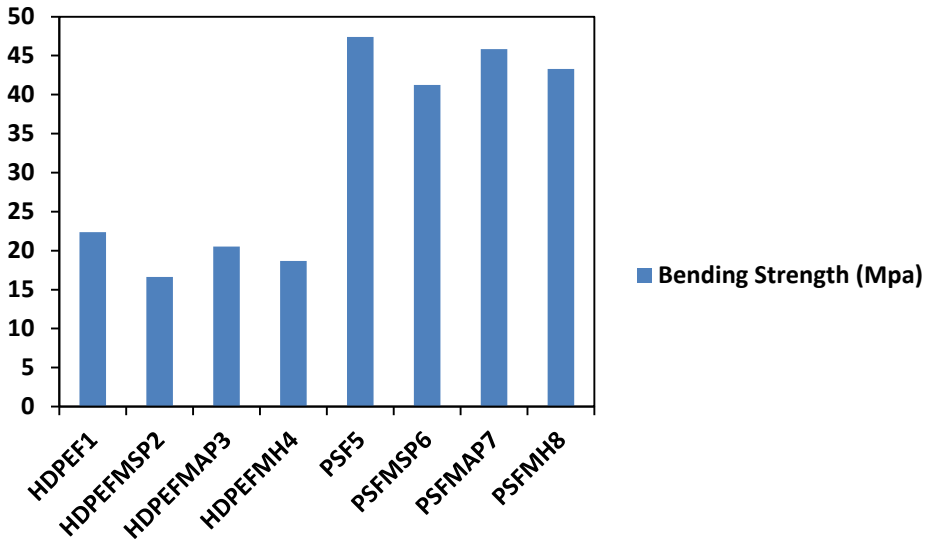

Figure 7.4: Bending Strength and elongation at break of the composites

7.3.3 Fire Retardant Properties

Fire retardant properties were conducted to assess the effect of additives on the polymer composites. Figure 7.5 -7.7 show the results of the studied parameters throughout fire retardant property measurements. The incorporation of fire retardant additives in the composites results a significant increase in ignition time, horizontal and vertical total firing time. From the results, the ignition time of the composites using MAP was twice to the

composites without fire retardant additives. This indicated that the addition of fire retardants slowed down the burning. The PS based composites burn quickly as compared to HDPE based composites. The addition of fire retardants; i.e. MSP, MAP, and MH, into DPM fiber reinforced HDPE and PS composites increase the total firing time of the composites. Among these three types of fire retardants, the incorporation of MAP remarkably enhanced fire retardancy of the composites.

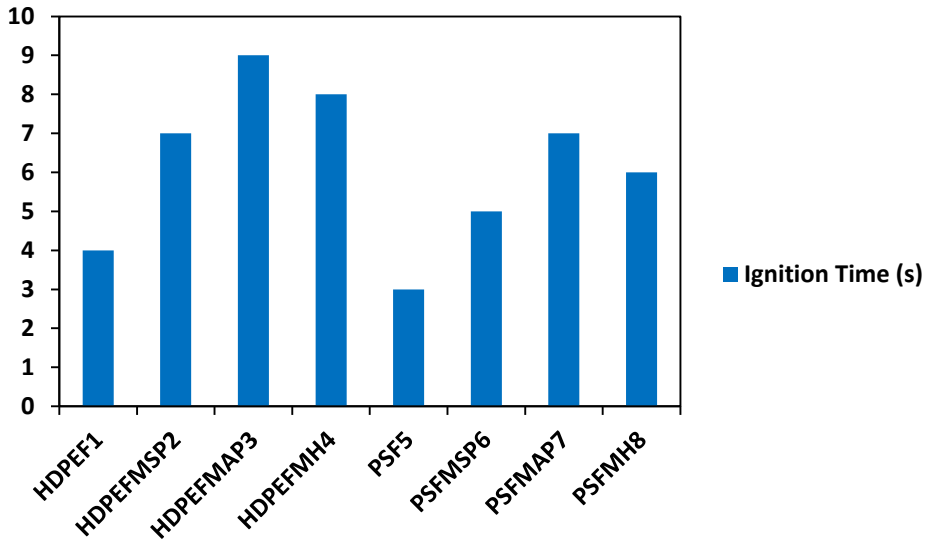

Figure 7.5: Ignition time of the composites

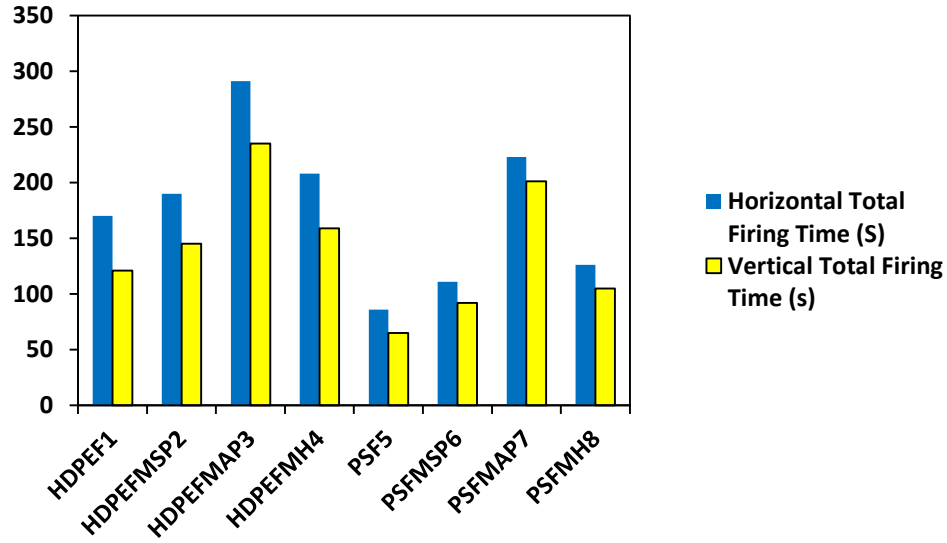

Figure 7.6: Horizontal and vertical total firing time of the composites

The results of horizontal and vertical burning rate of the prepared composite are shown in figure 7.7. The PSF5 (DPM fiber reinforced PS composite) presented the highest burning rate. On the other hand, the incorporation of fire retardant additives; i.e. MSP, MAP, and MH into DPM fiber reinforced HDPE and PS composites reduced the burning rate of the composite. This recommended that fire retardant additives improved fire retardancy of the composites. Among these three types of fire retardants, MAP exhibited the maximum enhancement of fire retardancy of the composites. However, MSP exhibited the lowest improvement of fire retardancy of the composites. On the basis of the combustion results, the fire-retardancy order of the composites was HDPEFMAP3> PSFMAP7> HDPEFMH4> HDPEFMSP2> HDPEF1> PSFMH8> PSFMSP6> PSF5.

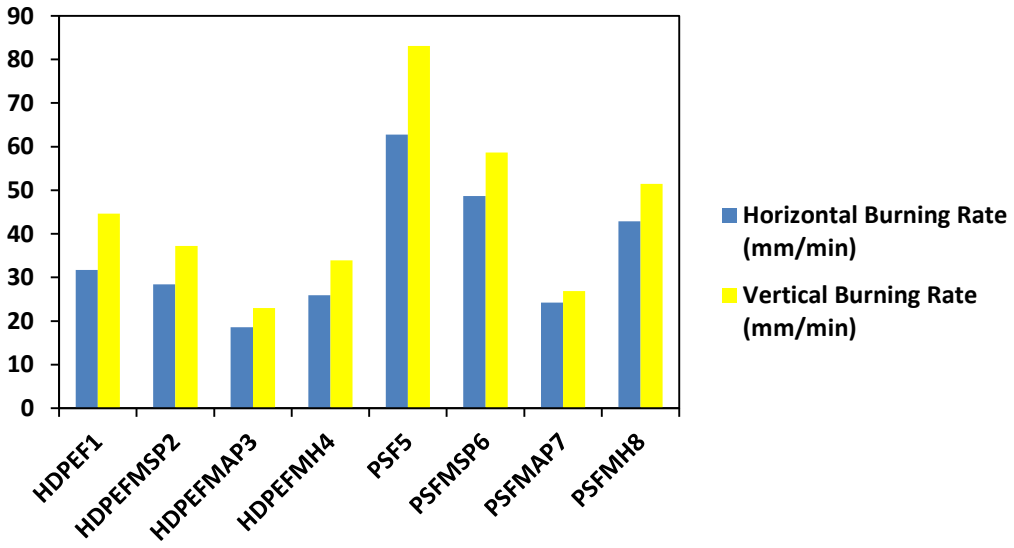

Figure 7.7: Horizontal and vertical burning rate of the composites

7.4 Conclusions

The effect of incorporation of fire retardant additives i.e. MSP, MAP and MH on the mechanical and fire retardant properties of the DPM fiber reinforced composites were studied. The composites were prepared by compression molding technique. The presence of fire retartands in composites showed lower mechanical properties. However, the incorporation of fire retardant additives in the composites improved the fire resistant properties. It can be concluded from the study that monoammonium phosphate showed remarkable fire retardant properties compared to others.

7.5 References

1. Jeencham, R.; Suppakarn, N.; Jarukumjorn, K.; Effect of Flame Retardants on Flame Retardant, Mechanical, and Thermal Properties of Sisal Fiber/Polypropylene Composites, *Compos. Part B*, **2013**, doi: http://dx.doi.org/10.1016/j.compositesb.2013.08.012
2. Izhar, T.; Nuraiti, T.; Jiat, C. C.; Lutpi. N. A. "A Study of Fire Retardant Effect in Natural Fiber Composite Panels with Magnesium Hydroxide and Zinc Borate as Additives." *Appl. Mechan. and Mater.*, **2015,** 815, 148–52. https://doi.org/10.4028/www.scientific.net/amm.815.148.
3. Sanjay, M. R.; Arpitha, G. R.; Naik, L. L.; Gopalakrishna, K.; Yogesha, B. Applications of Natural Fibers and Its Composites: An Overview, *Natur. Resour.*, **2016**, 7, 108-114. http://dx.doi.org/10.4236/nr.2016.73011
4. Bazan, P.; Salasińska, K.; Kuciel, S. Flame retardant polypropylene reinforced with natural additives, *Ind. Crops and Prod.*, **2021**, 164, 113356, ISSN 0926-6690, https://doi.org/10.1016/j.indcrop.2021.113356.
5. Shi, X.-H.; Li, X.-L.; Li, Y.-M.; Li, Z.; Wang, D.-Y. Flame-retardant strategy and mechanism of fiber reinforced polymeric composite: A review, *Compos. Part B: Eng.*, **2022,** 233, 109663, ISSN 1359-8368, https://doi.org/10.1016/j.compositesb.2022.109663.
6. Arnab, R.; Mandal, A.; Mitra, B.; Jacobson, R.E.; Roger, R.; Banerjee, A.N.J. Short jute fiber-reinforced polypropylene composites: Effect of compatibilizer. *J. of Appl. Polym. Sci.*, **1998.** 69. 329 - 338. 10.1002/(SICI)1097-4628(19980711)69:2<329::AID-APP14>3.0.CO;2-R
7. Haibin N.; Pillay, S.; Lu, N.; Shaik Z.; Yongzhe, Y. Natural fiber-reinforced high-density polyethylene composite hybridized with ultra-high molecular weight polyethylene. *J. of Compos. Mater.*, **2019**, 5, 3. 002199831882271. 10.1177/0021998318822716.
8. Shaari, N. Z. K.; Taha, A. R.; Hanipah, S. H. Composite from high density polyethylene (HDPE) reinforced with rice husks (Oryza sativa): Preparation and mechanical property, *Malays. J of Chemi. Eng. & Technol.*, **2020**, 3(2) 25–29, https://doi.org/10.24191/mjcet.v3i2.10941

9. Kreutz, J. C.; de Souza, P.R.; Benetti, V. P.; Freitas, A. R.; Bittencourt, P. R. S.; Gaffo. L. Mechanical and thermal properties of polystyrene and medium density fiberboard composites, *Polímeros*, **2021**, 31(2), e2021013, https://doi.org/10.1590/0104-1428.07120
10. Chen, Q.; Xie, Z.; Xu, X.; Xu, W.; Huang, Y.; Zhang, Y. Preparation and properties of polystyrene composites modified by macromolecular antioxidant, *J of Phys. Conf. Ser.* 1605, **2020**, 012169, doi:10.1088/1742-6596/1605/1/012169
11. Mondal, S.; Mudila, H.; Prasher, P.; Kumar, U.; Kadyan, N.; Bishnoi, A.; Kaur N.; Silmana, S. Modification of Polystyrene Based Composites for Environment Sustainability: A Review, *J. of Phys.: Conf. Ser.* 1531, **2020**, 012107 IOP Publishing doi:10.1088/1742-6596/1531/1/012107
12. Kouadio, K. C.; Traoré, B.; Kaho, S. P.; Kouakou, C. H.; Emeruwa, E. Influence of a Mineral Filler on the Fire Behaviour and Mechanical Properties of a Wood Waste Composite Material Stabilized with Expanded Polystyrene, *Open J. of Appl.Sci.,* **2020**, 23, 834-843 DOI: 10.4236/ojapps.2020.1012059
13. Giri, R.; Nayak L.; Rahaman M. Flame and fire retardancy of polymer-based composites, Mater. Res. Innov., **2020**. https://doi.org/10.1080/14328917.2020.1728073
14. Shen, J.; Liang, J.; Lin, X.; Lin, H.; Yu, J.; Wang, S. The Flame-Retardant Mechanisms and Preparation of Polymer Composites and Their Potential Application in Construction Engineering. *Polymers*, **2022**, 14, 82. https://doi.org/ 10.3390/polym1401008
15. Ribeiro, A.; Mariot, H.; Angioletto, E.; Noni, A. D.; Ribeiro, A.; Mariot, H.; Angioletto , E.; Junio A. D. N. "Fire exposure behavior of epoxy reinforced with jute fiber applied to ceramic tiles for a ventilated facade system," *Mater. Res.*, **2019,** 22, 1, e20180885,.http://dx.doi.org/10.1590/1980-5373-MR-2018-088
16. Zaman, S. U.; Shahid, S.; Shaker, K.; Nawab, Y.; Ahmad, S.; Umair, M.; Khaliq, Z.; Azam F. Development and characterization of chemical and fire resistant jute/unsaturated polyester composites, *The J. of The Tex. Ins.*, **2021.** https://doi.org/10.1080/00405000.2021.1889131
17. Bhattacharjee, S.; Sazzad, M, H.; Islam, M. A.; Ahtashom, M M.; Asaduzzaman, Miah, M. Y. Effects of Fire Retardants on Jute Fiber Reinforced Polyvinyl

Chloride/Polypropylene Hybrid Composites. *Int. J. of Mater. Sci. and Appl.*. **2013,** 2(5), 162-167. doi: 10.11648/j.ijmsa.20130205.13

18. Cui, J.-F.; Li, F.-Y.; Li, J.-Y.; Li, J.-F.; Zhang, C.W.; Chenab S.; Suna, X. Effects of magnesium hydroxide on the properties of starch/plant fiber composites with foam structure, *RSC Adv*. **2019**, 9, 17405–17413, DOI: 10.1039/c9ra01992h
19. Hidalgo-Salazar, M. A.; Muñoz, M. F.; Mina, J. H. Influence of Incorporation of Natural Fibers on the Physical, Mechanical, and Thermal Properties of Composites LDPE-Al Reinforced with Fique Fibers, *Int. J. of Polym. Sci.*, **2015**, Article ID 386325, 8 pages http://dx.doi.org/10.1155/2015/386325].
20. Jeencham, R.; Suppakarn, N.; Jarukumjorn, K. Effect of Flame Retardants on Flame Retardant, Mechanical, and Thermal Properties of Sisal Fiber/Polypropylene Composites, *Compos. Part B* **2013**, doi: http://dx.doi.org/10.1016/j.compositesb.2013.08.012

CHAPTER 8

Preparation and Characterization of DPM Fiber Reinforced PLA Composites

8.1 Introduction

Composite materials have drawn a lot of interest because of their adaptable qualities, which enable numerous applications in a vast array of sectors. These materials are used in a variety of sectors, including the aerospace, automotive, sports, furniture, construction, medical, and packaging industries. Polymer matrix composites are used to create a variety of composite materials due to their flexibility, low cost, and simplicity of manufacture. Petroleum resources are employed to create the synthetic polymers that are utilized in the preparation of these composites. The primary drawback of these polymers is that they are not biodegradable, which rises the amount of waste that is disposed of in landfills and contributes to pollution. Researchers have been searching for environmentally friendly materials throughout the current decades. Consequently, there has always been concern in the manufacture of green composites [1,2]. Concerns about the environment have led to a greater focus on natural fiber-reinforced polymer composites. Polymer matrix based composites with natural fibers such as coir, banana, jute, and sisal present a desirable and sustainable substitute to glass fibers. Natural fibers are substituting synthetic fibers due to advantages like low cost, low density, easily available, eco-friendly, nontoxicity, high flexibility, renewability, biodegradability, high specific strength and stiffness, and simplicity of processing [3]. Natural fibers have attracted attention as a reinforcing material in a polymer matrix due to these qualities.

Some environmental concerns for example waste formation, gathering in disposal systems and reproduction were restricted the usage of numerous non-biodegradable polymers [4]. So much emphasis has been placed on using biodegradable polymers as a matrix in composites. These biodegradable plastics have attracted a lot of interest because they break down through the activity of living beings though traditional polymers do not [5]. Hence, research has been conducted to search biodegradable polymers in place of non-biodegradable polymers. Polylactic acid (PLA) is one of the biodegradable polymer matrices. PLA is aliphatic polyester which is thermoplastic polymer made mostly from naturally occurring resources such sugar cane, sugar beet, cassava, and maize [6].

In this study, DPM fibers as reinforcing materials were combined with PLA to produce biodegradable composites. The goal of this study is to fabricate and assess the physical,

mechanical, thermal and biodegradation performance of short DPM fiber reinforced PLA composites by varying different weight proportions of fibers.

8.2 Experimental

8.2.1 Materials

Polylactic acid (PLA) was used as polymer matrix. PLA was acquired from Sigma-Aldrich. DPM fibers were amassed from local area of Jashore, Bangladesh.

8.2.2 Fabrication of Composite

PLA granules were ground by a grinding machine so that PLA and fibers can mix thoroughly. The DPM fibers were cut into small pieces (2-3 mm) by a hand scissor. The composites were prepared by compression moulding technique. Measured amount of DPM fiber and PLA were taken in a blender for proper mixing according to table 8.1. The mixed fibers and PLA were transferred into the mould (12x15 cm^2). The moulds were pressed (Paul Otto Weber Press Machine) at 180^0C and 200 kN pressure for 5 min. The moulds were cooled for 5 min at room temperature and 200 kN pressure. Lastly, the composites were taken out from the mould and stored in desiccator. The composites were cut to specimens for mechanical properties following ASTM standard method.

Table 8.1: Fiber and PLA content percentages in the composite samples

Fiber Content (wt%)	PLA (wt%)
0	100
5	95
10	90
15	85
20	80
25	75

8.2.3 Bulk Density of the composites

Bulk density of the composites was determined by measuring the weight and dimensions of the samples using the following equation 8.1. The average results for five composite samples were stated.

$$D = \frac{Weight\ of\ the\ composite}{(Length \times Width \times Height)\ of\ the\ composite} \quad (8.1)$$

8.2.4 Water Uptake of the Composites

Water uptake tests of the composites were performed to investigate the effect of water on the composites with various amount of fiber content. Water uptake of the composites was conducted according to ASTM D570-99. With the purpose of measuring the water absorption capacity, the composite samples were dried in an oven for a specific temperature and time and then cooled in a desiccator. The weight of the samples were taken and immersed in distilled water for 24 hours. The samples were drawn from the water, wiped dry using a cloth to eliminate any remaining water, and weighed. Three samples were tested to get an average result. The percentage of water uptake was determined by utilizing the following equation 8.2.

$$\text{Increase in weight, } \% = \frac{(W - W_0)}{(W_0)} \times 100 \quad (8.2)$$

where, W is the wet weight and W_0 is the conditioned weight of the composites.

8.2.5 Thickness Swelling of the Composites

The composite samples were immersed in water to evaluate thickness swelling. The initial thickness and thickness after 24 hours immersion in water of the samples were measured. The percentage of thickness swelling was calculated following the equation 8.3 [7].

$$\% TS = \frac{T_f - T_i}{T_i} \times 100 \quad (8.3)$$

where T_i and T_f initial thickness and final thickness after immersion in water.

8.2.6 Mechanical Properties

The tensile properties test was carried out to ascertain the tensile strength of the composite samples. The samples were cut in accordance with the ASTM D 882-02. The test was conducted via universal strength tester (model 1410 Titans, capacity 5 kN, England) with a constant crosshead speed of 10 mm/min. Bending strength (three point bending) of the composites were also performed following ASTM D7900. Five measurements in each composition of the composite samples were taken and the average values were reported.

8.2.7 FTIR Spectroscopy

FTIR spectra were recorded for composite samples. The functional group of the composites was determined from FTIR spectra. The composites' FTIR spectra were recorded using a Frontier FT-IR/NIR spectrometer (Perkin Elmer, USA) with a wavelength range of 4,000-650 cm^{-1}.

8.2.8 Thermal Analysis

The thermogravimetric (TGA) and differential scanning calorimetry (DSC) analysis of the composite samples were performed by a NETZSCH instrument (STA 449 F3, Jupiter) in a temperature range 30-900^{0}C at nitrogen atmosphere. The heating rate was 10^{0}C/min.

8.2.9 SEM Analysis

The morphology of the fracture surfaces of the tensile samples were examined by using a field emission scanning electron microscope (JEOL JSM-7600F). The samples were cut into a small portion, mounted onto holders using carbon tape and coated with gold. Samples were focused onto the surfaces and examined with different magnification.

8.2.10 Degradation by Soil Burial

The composites were covered up in a flower pot containing soil with moisture level at least 30%. The test samples were removed from the soil at intervals of 1 month. The samples were cleaned and oven dried at 80^{0}C for 6 h. The degradation was determined on the basis of weight of the specimen. Equation 8.4 was used to calculate the percentage of weight loss.

$$\%\, Weight\ loss = \frac{W_f - W_i}{W_i} \times 100 \qquad (8.4)$$

Where W_i and W_f were the initial and final weight after drying respectively.

8.3 Results and Discussion

8.3.1 Bulk Density of the Composites

The effect of various wt% of DPM fibers on the bulk density of the composites is shown in figure 8.1. The bulk density of short DPM fiber reinforced PLA composites drops with the

rise of fiber content. The density of the composites decrease from 1.4789 to 1.2035 g/cm^3. Ramanaiah et al. [8] prepared borassus seed shoot fiber reinforced polyester composites and examined their physical and mechanical properties. They found that the density of borassus seed shoot fiber reinforced polyester composites decreased with increasing fiber content. The results are similar with our findings. The polymer matrix of composites becomes improperly mixed with the fibers, with an increase in fiber content which may result in a declining trend in the bulk density of composite materials.

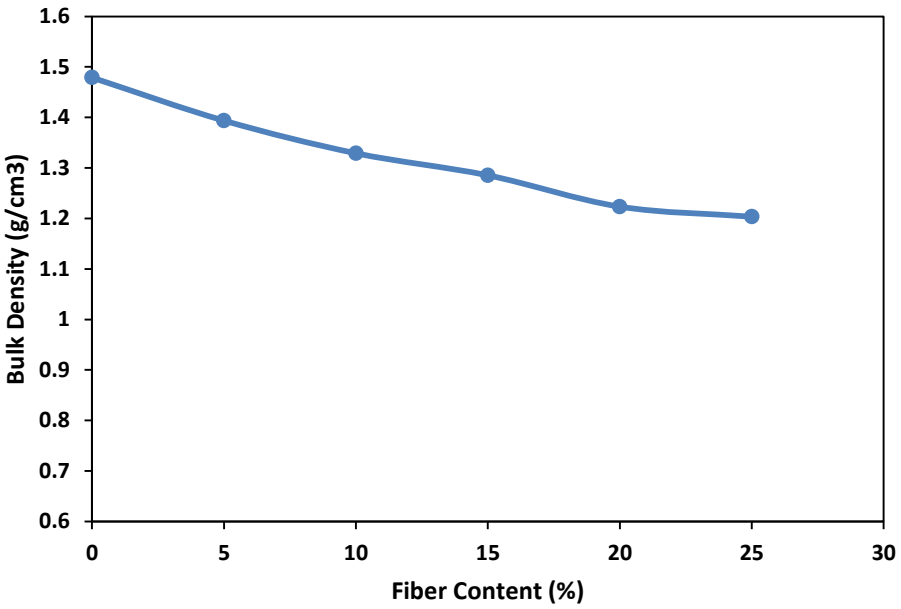

Figure 8.1: Bulk density of the DPM fiber reinforced PLA composites at various fiber contents

8.3.2 Water Absorption of the composites

Water absorption is an important parameter and used to measure durability of composites. Figure 8.2 shows how the short DPM fiber reinforced PLA composites respond to different fiber content weight percentages in terms of water uptake behavior. The graph clearly shows that as the fiber content increases, the composites' water absorption gradually rises. The composite with 5% fiber content shows the lowest amount of water absorption among the examined samples, whereas the composite with 25% fiber content shows the largest amount. Natural fibers are hydrophilic, which contain several hydroxyl groups and may establish hydrogen bonds with water. More fibers in the composites led to greater water absorption. As

a result, 25% fiber content composite had the maximum level of water absorption. Manpreet et al. [9] concluded that 5% pineapple fiber reinforced HDPE composites absorbed lowest amount of water which is in agreement with our results.

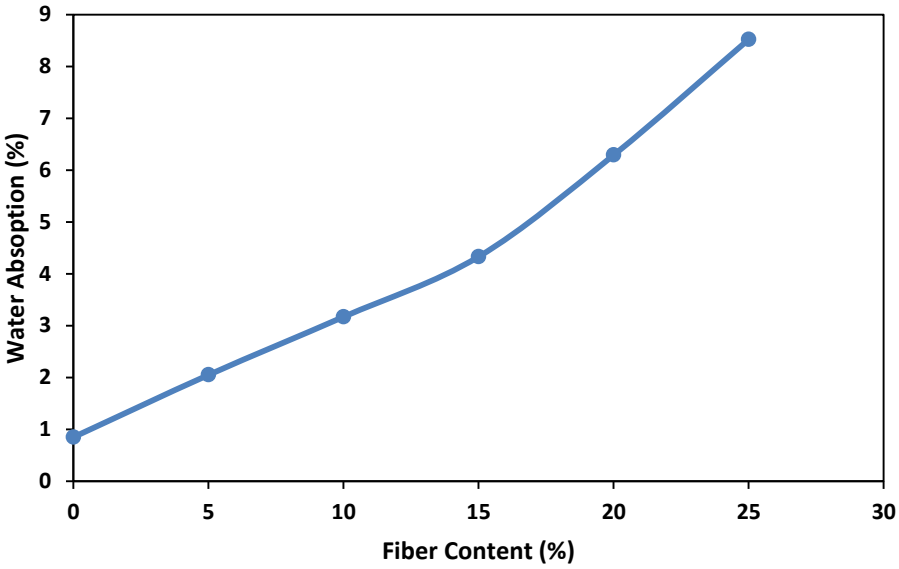

Figure 8.2: Water absorption of the DPM fiber reinforced PLA composites at various fiber contents

8.3.3 Thickness Swelling of the Composites

Thickness swelling test of the composites was performed in order to evaluate variations in the dimensional stability of the composites. The thickness swelling of the composites is depicted in figure 8.3. The findings demonstrated a similar pattern with water absorption, where the thickness swelling of the composites had increased with increasing fiber content. The composite with 25% fiber content displayed the maximum value of thickness swelling which was 5.33%. The hydrophilic cellulosic fibers in the composites start to swell when it is in contact with water. Das et al. fabricated waste newspaper reinforced unsaturated polyester composites and found that the thickness swelling of the composites increased with increasing fiber content [10].

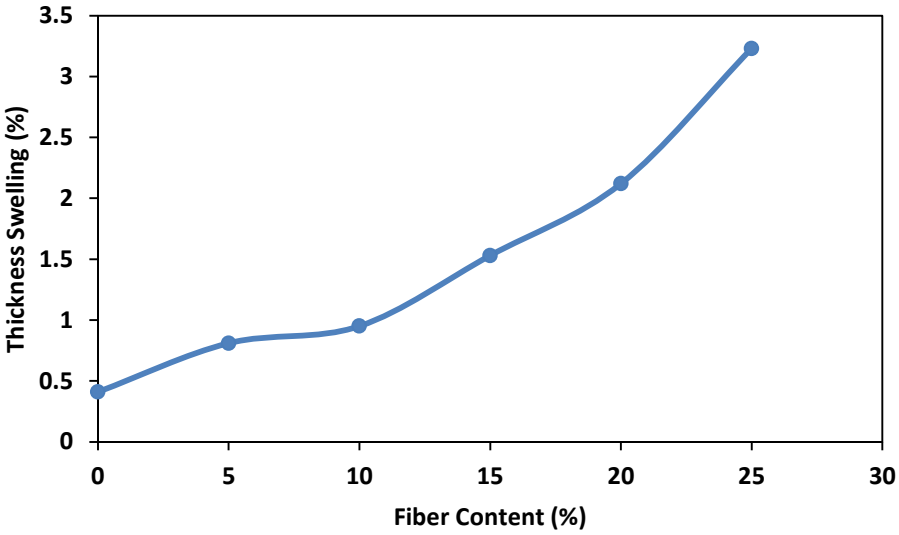

Figure 8.3: Thickness swelling of the DPM fiber reinforced PLA composites at various fiber contents

8.3.4 Mechanical Properties

The impact of changing the fiber content on the composites' tensile strength is depicted in figure 8.4. The figure demonstrates that the tensile strength begins to decrease from 0 to 5% fiber content. When the fiber percentage rises from 5% to 10%, then the tensile strength increases. The maximum tensile strength for 10% DPM fiber reinforced HDPE composites was 21.09 MPa. When the fiber percentage increased above10%, the composites' tensile strength decreased. This decrease in tensile strength with increasing fiber content may be caused by poor fiber-matrix adhesion and debonding that occurred during tensile strength measurement. Debonding of the fiber matrix can result in voids, which cause faults to spread throughout the void-containing sections. The uneven distribution of the fibers inside the composites also had an effect on their tensile strength.

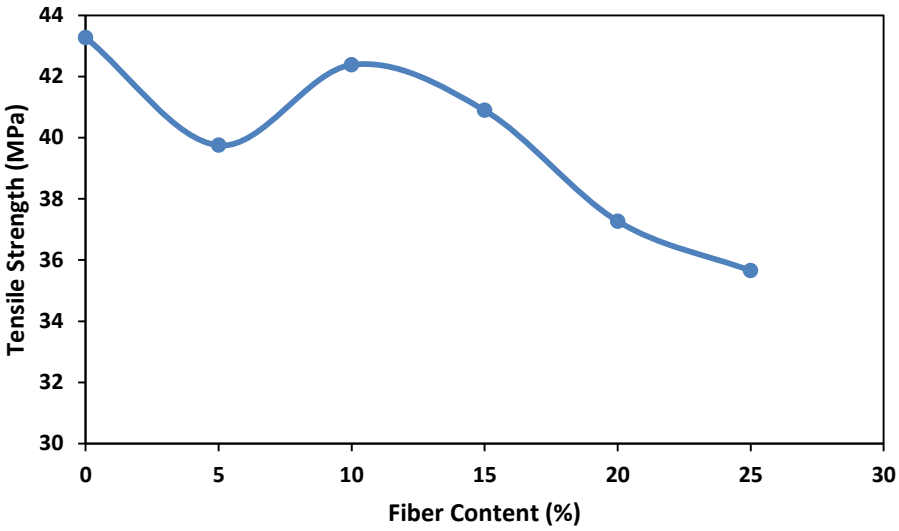

Figure 8.4: Tensile strength of DPM fiber reinforced PLA composites at various fiber contents

Figure 8.5 shows the elongation at break for composites with various weight percentages of fiber. It is clear that the elongation at break of short date palm mat fiber reinforced PLA composites has been somewhat reduced when compared to 100% PLA. When the amount of fiber increases, the elongation at break of the composites decreases because the fibers present in the composites do not exhibit elasticity or flexibility. Moreover, the composites' toughness and rigidity both rise, while their ductility declines. [11].

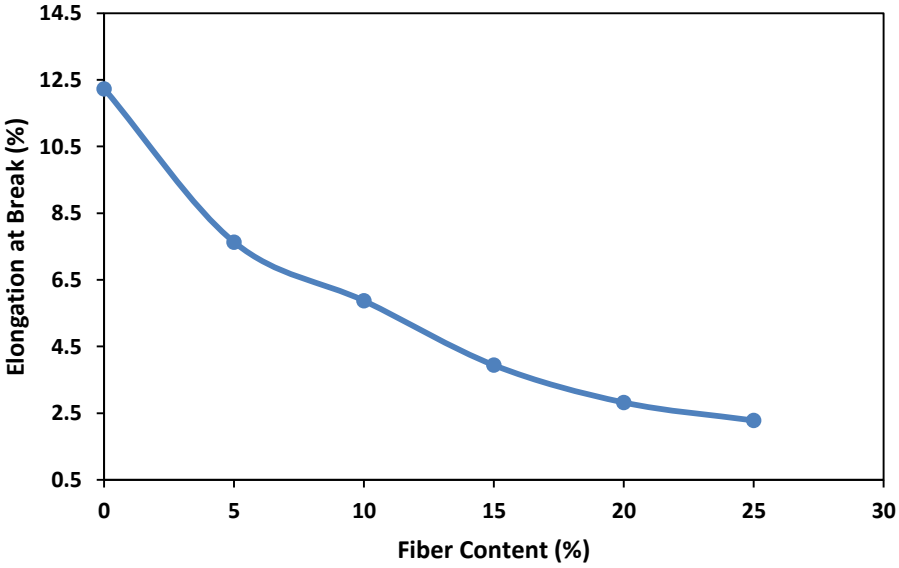

Figure 8.5: Elongation at break of DPM fiber reinforced PLA at various fiber contents

Figure 8.6 displays the bending strength of the composites for various weight percentages of fiber. According to the figure, bending strength decreased by 5% fiber content. When the fiber content was 10%, the bending strength increased, and when the DPM fiber content was 15% to 25%, the strength decreased once again. A maximum bending strength of MPa was discovered for 10% DPM fiber reinforced PLA composites. Poor fiber-matrix interaction is caused a reduction in the bending strength of composite materials with 15 to 25% fiber content.

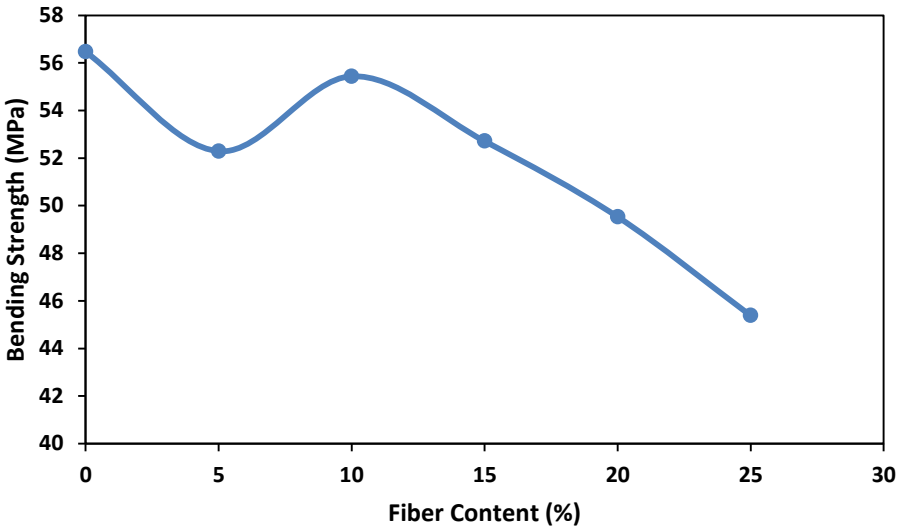

Figure 8.6: Bending strength of DPM fiber reinforced PLA at various fiber contents

8.3.5 FTIR Study

The FTIR spectra of 100% PLA, and 10% short DPM fiber reinforced PLA composites are displayed in figure 8.7. The PLA exhibits typical peaks at 1746, 2995, 2946, and 1080 cm-1 for C=O, -CH_3 asymmetric, -CH_3 symmetric, and C-O, respectively. For DPM fiber reinforced PLA composites, the peak at 1452 and 1363 cm^{-1} correspond to -CH_3 asymmetric and -CH_3 symmetric bending vibrations [12]. The peaks 3400-3200 cm^{-1} resemble to O–H stretching vibration of the hydroxyl groups [13] which is absent in 100% PLA. Additionally, the composites showed the distinctive peaks of the PLA matrix.

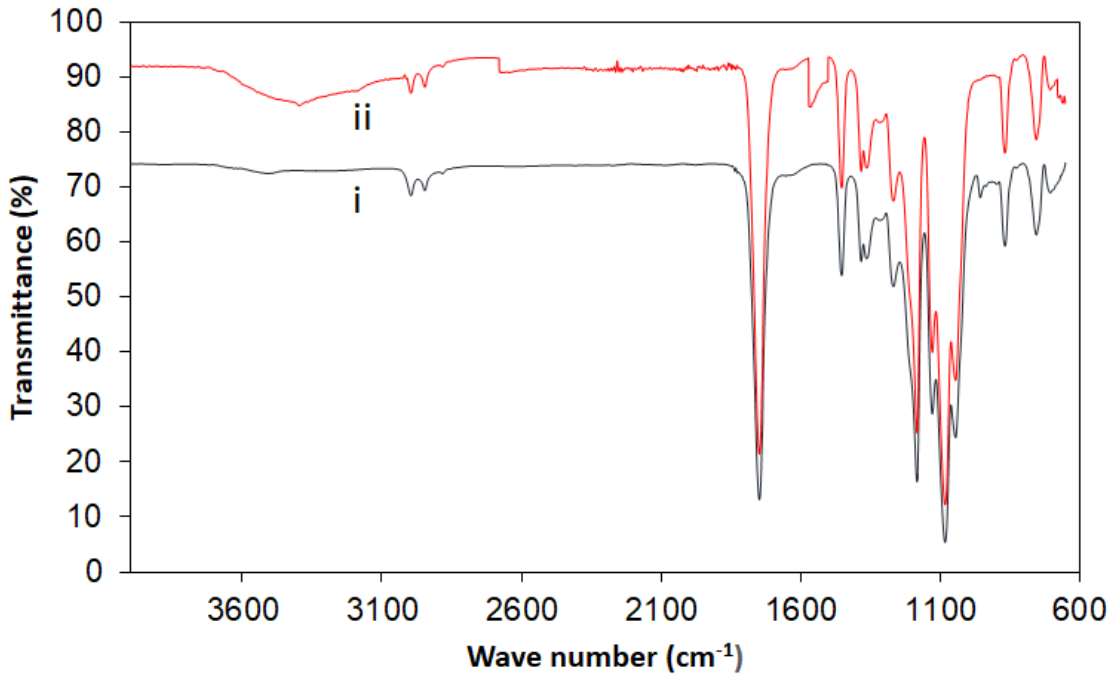

Figure 8.7: ATR-FTIR spectra of (i) 100% PLA; (ii) 10% DPM fiber and 90% PLA composite

8.3.6 Thermal Properties

Thermal analysis was conducted to investigate the thermal stability of 100% PLA and optimized 10% DPM fiber reinforced PLA composites. The figures 8.8 and 8.9 show the TGA and DSC curves. The TGA results show that the 100% PLA composite undergoes thermal degradation beginning at 410^0C and with a total mass change of 97.6% while the degradation of 10% DPM fiber reinforced PLA composites start at 300.8^0C and a total 97.8% mass change is completed at the end of the process. In both cases, degradation completed within 500 ^{0}C. The degradation of the composite takes place earlier than 100% PLA. The thermal degradation of the composites decreased with adding fibers. For 100% PLA and 10% DPM fiber reinforced PLA composite, the percentage of the residual mass at the finish of the heating process was 2.4 and 2.2 respectively. The DSC curves of 100% PLA and 10% DPM fiber reinforced PLA composite showed peaks of melting at 134.1and 124.8^0C respectively.

The melting temperature of the composites decreased slightly, this is due to the presence of DPM fiber.

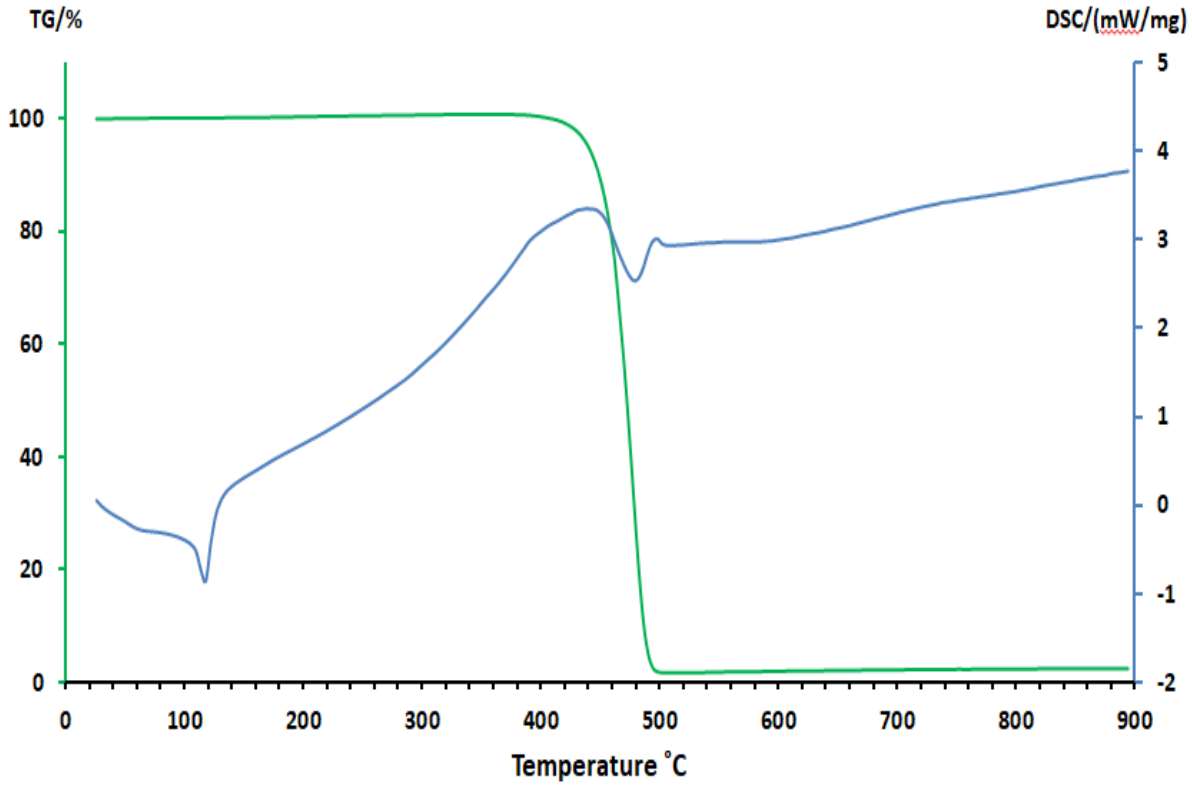

Figure 8.8: TGA and DSC of 100% PLA

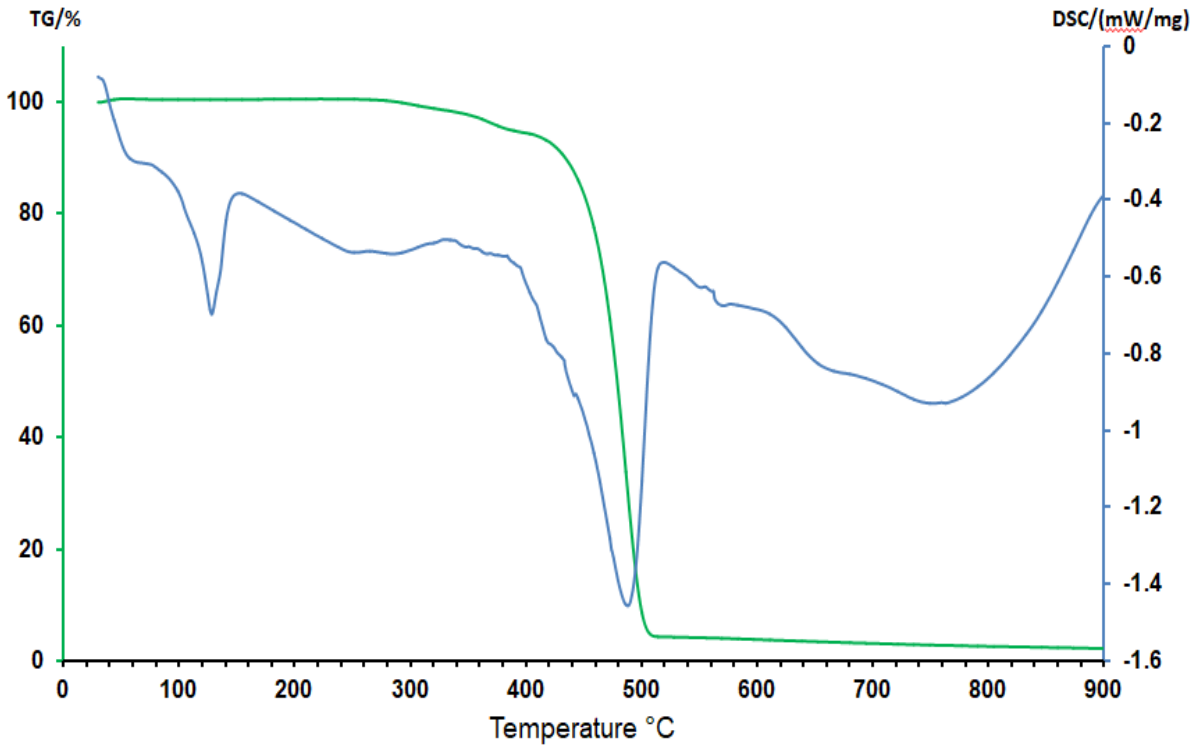

Figure 8.9: TGA and DSC of 10% DPM fiber and 90% PLA composite

8.3.7 Morphological Analysis

Scanning Electron Microscope (SEM) analysis is an efficient tool to observe the surface morphology of natural fiber reinforced polymeric composite materials. The tensile fracture surfaces of the 10% and 25% DPM fiber reinforced PLA composites were examined and the SEM micrographs in different magnitude are displayed in figure 8.10. As seen in figure, 10% DPM fiber reinforced PLA composite showed improved fiber-matrix interaction between fibers and PLA matrix. On the contrary, voids and loosely bound fibers were observed for 25% DPM fiber reinforced PLA composites indicating poor fiber-matrix adhesion and resulted low mechanical properties of the composites.

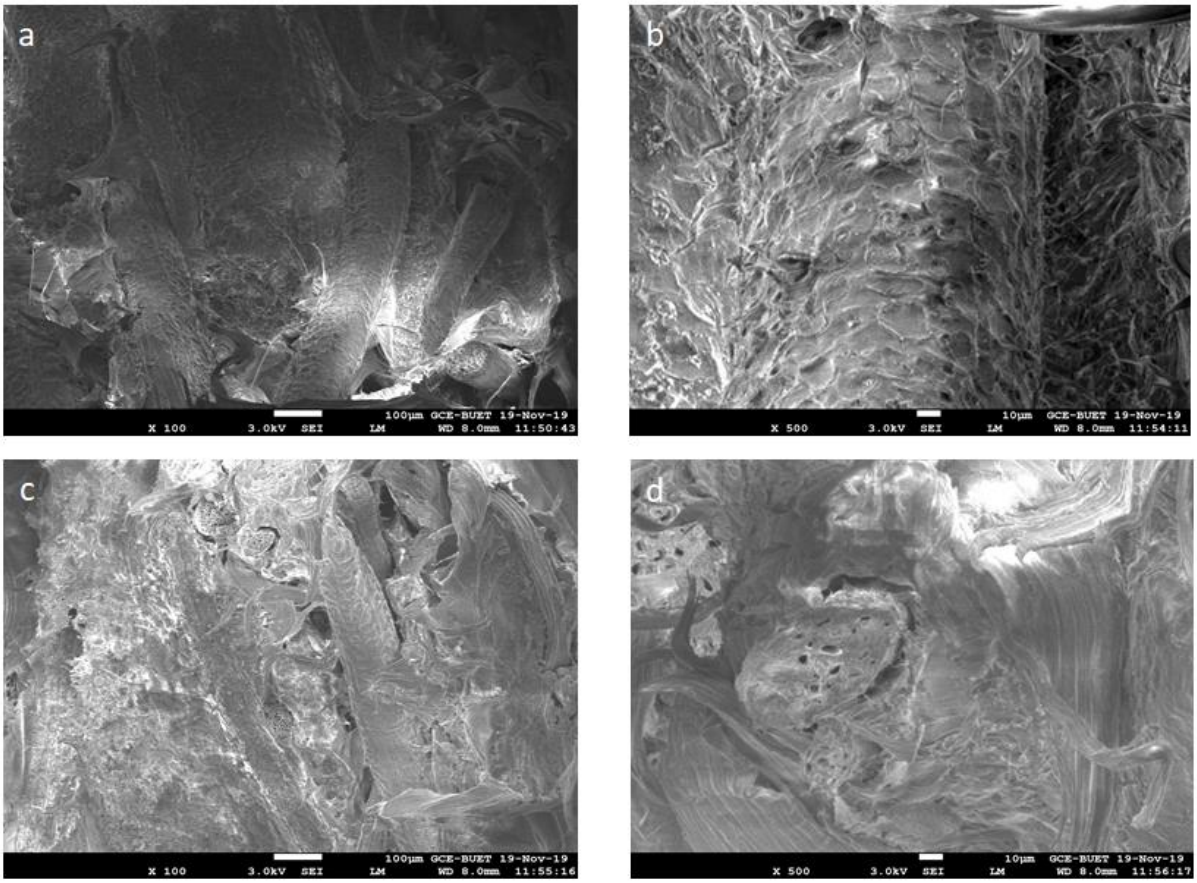

Figure 8.10: SEM images of 10% DPM fiber PLA composite (a) 100x magnification and (b) 500x magnification and 25% DPM fiber PLA composites (c) 100x magnification and (d) 500x magnification

8.3.8 Degradation by Soil Burial

Soil burial test was used to examine the biodegradation of the composites. The test was conducted on DPM fiber reinforced PLA composites. Soil burial experiments of the composites were done in soil for three months. The figure clearly shows that the weight loss increases with increasing time and fiber content. After three months, the composites with 5% fiber shows 4.38% weight loss whereas 25% fiber content composites shows 13.49% weight loss. Both PLA and natural fibers have a hydrophilic character [14]. During soil burial process, the fibers in the composite surface and interface absorb moisture easily and weaken the bond between fiber and matrix causing degradation.

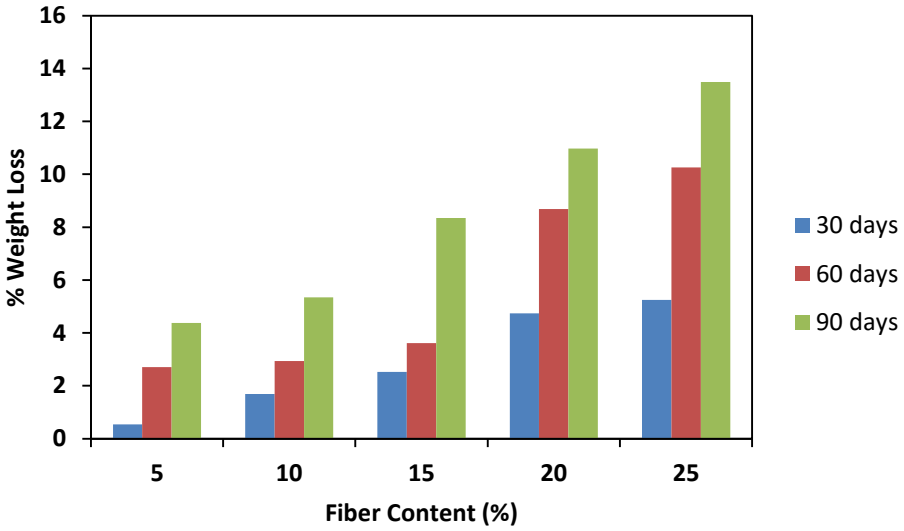

Figure 8.11: Variation of weight loss of the buried composite samples

8.4 Conclusions

In this section, short DPM fiber reinforced PLA composites were successfully prepared by compression moulding technique. The effects of fiber content on the physical, mechanical and thermal properties were studied. The analysis shows that the incorporation of 10% DPM fiber enhances mechanical properties than 5, 15, 20 and 25% of DPM fiber reinforced composites. Morphological analysis of tensile fractured surfaces of 10% DPM fiber reinforced PLA composites also revealed good fiber-matrix interfacial adhesion. The mechanical characteristics of the composites made from date palm mat fiber suggested that they would be a viable option for a variety of applications.

8.5 References

1. Sanivada, U.K.; Mármol, G.; Brito, F.P.; Fangueiro, R. PLA Composites Reinforced with Flax and Jute Fibers—A Review of Recent Trends, Processing Parameters and Mechanical Properties. *Polymers*, **2020**, 12, 2373. https://doi.org/10.3390/polym12102373
2. Song, X.; Zou, T.; Zhang, Y.; Li, Y.; Wang, P. The Mechanical Properties of Jute/PLA Composites Combining Nano Polymerized Styrene Butadiene Rubber

Modified by Coupling Agents, *J. of Natur. Fib.*, **2023**, 20(1), 2157921. https://doi.org/10.1080/15440478.2022.2157921

3. Yasir, N.; Rotich G.; Desalegn, A.; Mechanical and Water Absorption Properties of Jute/Palm Leaf Fiber-Reinforced Recycled Polypropylene Hybrid Composites, *Int. J. of Polym. Sci.*, **2022,** 4408455, , 1687-9422, https://doi.org/10.1155/2022/4408455
4. Jha, K.; Kataria, R.; Verma, J.; Pradhan. S. Potential biodegradable matrices and fiber treatment for green composites: A review[J]. *AIMS Mater. Sci.*, **2019**, 6(1): 119-138. doi: 10.3934/matersci.2019.1.119
5. Jagadeesh, D.; Kanny, K.; Prashantha, K. A review on research and development of green composites from plant protein-based polymers, *Polym. Compos.*, **2015**, https://doi.org/10.1002/pc.23718
6. Li, X.; Lin, Y.; Liu, M.; Meng, L.; Li, C.; A review of research and application of polylactic acid composites, *J. of Appl. Polym. Sci.*, **2022**, https://doi.org/10.1002/app.53477
7. Adekomaya O.; Adama, K. Investigating water absorption and thickness swelling tendencies of polymeric composite materials for external wall application in refrigerated vehicles, *Niger. J. of Technol. (NIJOTECH)*, **2018**, 37(1), 167 – 172, Print ISSN: 0331-8443, Electronic ISSN: 2467-8821, http://dx.doi.org/10.4314/njt.v37i1.22
8. Ramanaiah, K.; Prasad, A. V. R.; Reddy, K. Effect of fiber loading on mechanical properties of borassus seed shoot fiber reinforced polyester composites, *J. of Mater. and Environm. Sci.*, **2012**, 3, 374- 378.
9. Bahra, M. S.; Gupta, V.K.; Aggarwal, L. Effect of Fibre Content on Mechanical Properties and Water Absorption Behaviour of Pineapple/HDPE Composite, *Mater. Today: Proc.*, **2017**, 4(2), Part A, 3207-3214, ISSN 2214-7853, https://doi.org/10.1016/j.matpr.2017.02.206.
10. Das, S. Mechanical and water swelling properties of waste paper reinforced unsaturated polyester composites, *Cons. and Build. Mater.*, **2017**, 138, 469-478, ISSN 0950-0618. https://doi.org/10.1016/j.conbuildmat.2017.02.041.
11. Chowdhury, H.; Rahman, M.M.; Uddin, M.T.; Rahman, M.M. Improvement of mechanical properties of polypropylene composite using filler, modifier and

reinforcement, *J. Phys. Conf. Ser.* 1086, **2018.** https://doi.org/10.1088/1742-6596/1086/1/012003.

12. Woei C.B.; Ibrahim, N.; Yunus, W.; Hossain., M. Effects of Graphene Nanopletelets on Poly(Lactic Acid)/Poly(Ethylene Glycol) Polymer Nanocomposites. *Polymers*. **2013**, 6. 93-104. 10.3390/polym6010093.
13. Martínez, K. I.; González, R.; Soto J. J.; Rosales, I. Characterization by FTIR spectroscopy of degradation of polyethylene films exposed to CO2 laser radiation and domestic composting, *J. of Phys.: Conf. Ser.* 1723, **2021**. 012038, IOP Publishing, doi:10.1088/1742-6596/1723/1/012038
14. Ejaz, M.; Azad, M.; Rehman S. A.; Afaq, S.; Jung-Il, S.. Mechanical and Biodegradable Properties of Jute/Flax Reinforced PLA Composites. *Fibers and Polym.*. **2020**. 21, 2635-2641. DOI:10.1007/s12221-020-1370-y

CHAPTER 9

Preparation and Characterization of DPM and PPF Fiber Reinforced Hybrid Composites

9.1 Introduction

Hybrid composite materials are made by combining two or more different types of fibers in single matrix phase or single reinforcing phase with multiple matrix phases or multiple reinforcing and multiple matrix phases. The mechanical properties of hybrid composites depend on the fiber length, fiber orientation, weight fraction of the reinforcement, interaction between fiber and matrix [1]. Polymer composite materials are being used in aerospace, automotive, marine, infrastructure, military, leisure boats, aircraft industry and sport equipment. Present day industry takes an interest in environment friendly polymer composite materials, due to economic and ecological reasons. Natural fibers are renewable and obtained from natural resources possessing several advantages [2]. Natural fiber composites combine plant-derived fibers with a plastic binder. The natural fiber component may be wood, sisal, hemp, coconut, cotton, luffa, flax, jute, abaca, banana leaf fibers, bamboo, wheat straw or other fibrous material [3]. The primary advantages of natural fibers are low density, low cost, biodegradability, acceptable specific properties, less wear during processing and low energy consumption during extracting as well as manufacturing composites and wide varieties of natural fibers are locally available [4]. The most important matters in the development of natural fiber reinforced composites are (i) surface adhesion characteristics of the fibers, (ii) thermal stability of the fibers, and (iii) dispersion of the fibers in the case of thermoplastic composites [5]. The developed composite exhibits superior mechanical properties than the parent constituents [6]. The presence of fiber or other reinforcement in a thermoplastic matrix increases the composite strength. Polyethylene and polypropylene are well suited for use as matrix material. HDPE has very low glass transition temperature associated with a good retention of mechanical properties including flexibility and impact resistance at low temperatures and easily molded [7]. Several studies on the hybrid composites like Jute/sisal and epoxy, bamboo and glass fiber reinforced epoxy, banana/ pineapple and epoxy, banana fiber reinforced polypropylene, Glass-Hemp-Banana Fiber Reinforced Polymer Composites showed better mechanical properties [8-12].

Date palm (*Phoenix sylvestris*) and Palmyra palm (*Borassus flabellifer*) trees are plentifully available in Bangladesh. Date Palm mat and Palmyra Palm fruit fibers are considered as an agricultural waste in Bangladesh. It is evident from the literature that no work has been

reported on the utilization of date palm mat and Palmyra Palm fruit fibers reinforcement in HDPE hybrid composites fabrication. These new renewable and green source of reinforcement in composite materials which can be cheap and ecological. The aim of this study is to use of the date palm mat and Palmyra Palm fruit fiber as a potential reinforcing material in thermoplastic composite. In this study, date palm mat (DPM) and Palmyra Palm fruit (PPF) fibers reinforced HDPE hybrid composites were prepared. The physical, mechanical, thermal, morphological and degradation properties of the hybrid composites were studied and these new composites may find diversified applications like door panels, seat backs, headliners, package trays, dashboards, and interior parts of automotive [13], furniture, building and construction industries [14] etc.

9.2 Experimental

9.2.1 Materials

HDPE was purchased from Saudi Polymers Company, Saudi Arabia. HDPE has density 0.946g/cm^3 and melt index 0.18g/10 min. HDPE granules were grinded to 200-250 µm by a grinding machine for proper mixing between fibers and matrix. Date Palm mat fibers (*phoenix Sylvestris*) and Palmyra Palm (*Borassus flabellifer*) fruit fibers were collected from the rural area of Jashore, Bangladesh. The DPM and PPF fibers were cut into 2-3mm using hand scissors.

9.2.2 Hybrid Composite Fabrication

Composites were prepared by compression moulding technique. DPM and PPF fibers were weighed at a ratio (50:50) and mixed thoroughly. The fibers and HDPE were mixed in a blender according to the table 9.1. The mixture of fiber and HDPE were poured into the mold (12×15 cm^2) and finally hot pressed (Paul Ottoo Weber Press Machine) at 160^0C for 5 minutes between two steel plates under a pressure of 200 kN. At room temperature and under 200kN pressure the moulds were cooled for 5 minutes and released from the mold. The finished hybrid composite is shown in figure 9.1. The composites were cut to prepare specimens according to ASTMD 3039/ D3039(M) (2002) standard method and shown in figure 9.1.

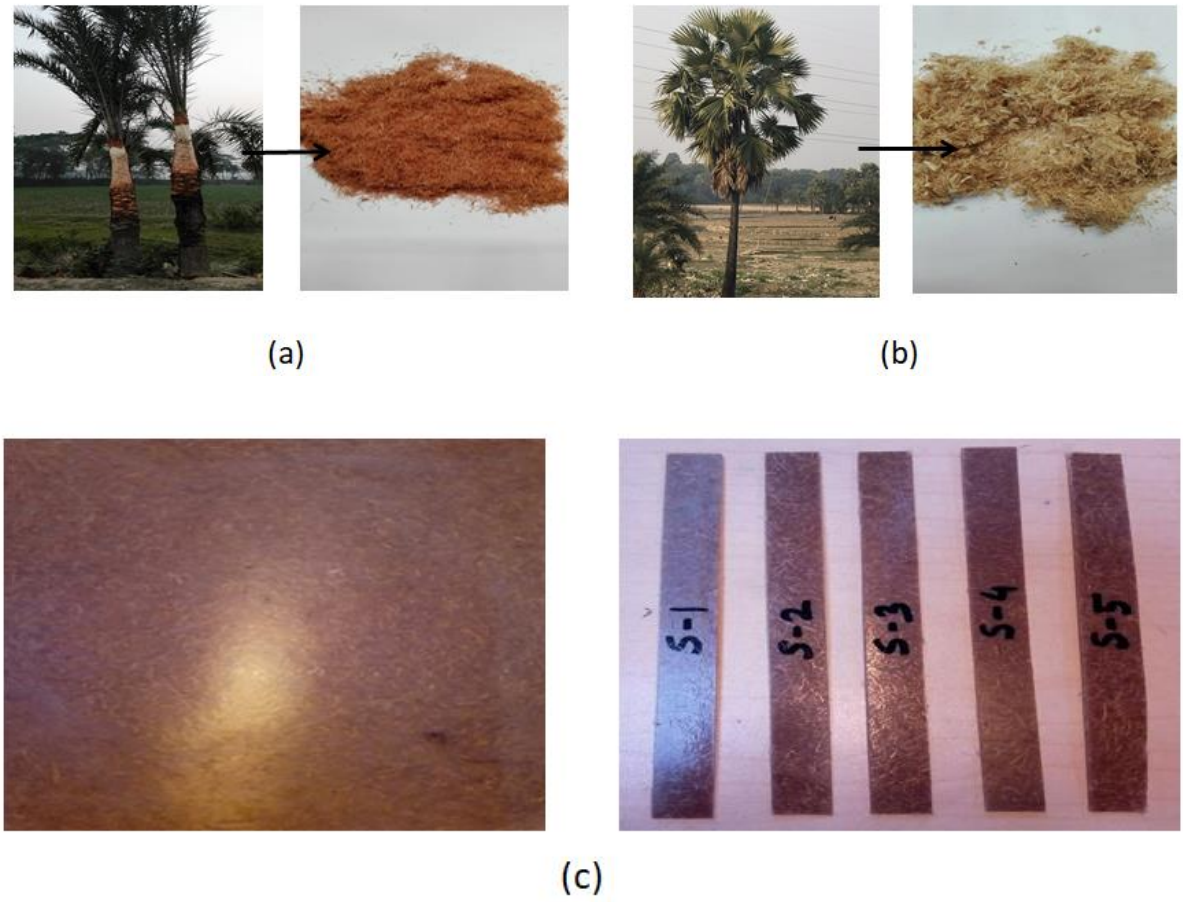

Figure 9.1: (a) DPM trees and chopped fibers; (b) PPF trees and chopped fibers and (c) finished composite sample and specimens for mechanical properties

Table 9.1: The composition of fibers and HDPE in composite samples

Fiber Content (wt%)	HDPE (wt%)
0	100
5	95
10	90
15	85
20	80
25	75

9.2.3 Bulk Density of Composites

The bulk density of the composites was determined by using the formula 9.1.

$$D = \frac{Weight\ of\ the\ composite}{(Length \times Width \times Height)\ of\ the\ composite} \quad (9.1)$$

9.2.4 Water absorption test of Composites

Water absorption tests of the composites were performed according to ASTM D570-99. Three replicate samples were employed to water absorption tests and the average results were presented. The percentage increase in weight during immersion was calculated as follows:

$$\text{Increase in weight, \%} = \frac{(\text{wet wt} - \text{conditioned wt})}{(\text{conditioned wt})} \times 100 \quad (9.2)$$

9.2.5 Mechanical Properties

Mechanical tests (tensile strength, percent elongation at break, tensile strength at break and yield strength) of the composites were carried out using universal strength tester (model 1410 Titans, capacity 5 kN, England). The tests were performed according to ASTM D 3039/D 3039 (M) (2002) standard method with a crosshead speed 10 mm/min. Bending strength (three point bending) of the composites were also performed following ASTM D7900. The average values for five samples were reported.

9.2.6 FTIR Spectroscopy

The FTIR of the composites were carried out by a FT-IR/NIR spectrometer (Frontier, Perkin Elmer, USA). The FTIR spectra were recorded in the 4,000-650 cm^{-1} region. FT-IR spectroscopy was used for the identification of functional groups of the composite samples.

9.2.7 SEM Analysis

Surface morphology of the composites were examined by a field emission scanning electron microscope (JEOL JSM-7600F). SEM analyses were done on the fracture surfaces of the tensile specimens. A small portion of the samples was taken and mounted onto holders with the help of carbon tape. Then the samples coated with gold. Samples focused onto the surfaces and examined with different magnification.

9.2.8 Thermal properties Analysis

A NETZSCH instrument (STA 449 F3, Jupiter) was employed for the thermogravimetric analysis (TGA) and differential scanning calorimetry (DSC) analysis of 100% HDPE and optimized (5% fiber content) composites.

9.2.9 Degradation of the Hybrid Composites by Soil Burial

The composite samples were buried in a flower pot soil. The moisture level of soil was kept at least 30%. The samples were withdrawn carefully at an interval of 1month period, washed with distilled water, dried at 80^0C in an oven for 6 h and cooled in a desiccator. The degradation of the hybrid composites was determined by measuring the tensile strength.

9.3 Result and Discussion

9.3.1 Bulk Density of the Composites

Figure 9.2 shows the effect of different fiber content on the bulk density of the composites. The figure indicates that the highest bulk density was found for 100% HDPE. With the increase of fiber content from 5 to 25 wt % resulted in a decrease of bulk density of the composites. This type of trend in the bulk density with the increase of fiber content of the composites was also found for jute fiber reinforced LDPE composites [15].

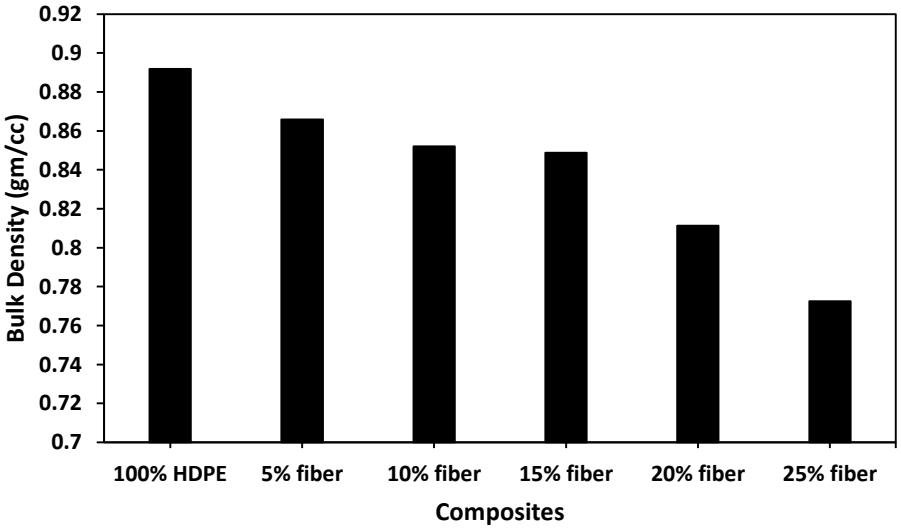

Figure 9.2: Bulk density of the composites at different fiber content

9.3.2 Water Absorption of the Composites

The effect of different fiber content on water absorption of the composites is shown in figure 9.3. It reveals that the quantity of water absorption of the composites increases with the increase of fiber content. Fibers absorb water rapidly due to its hydrophilic nature. The composites with more fiber showed more water absorption. Therefore, the 25% fiber reinforced HDPE hybrid composites showed highest quantity of water absorption.

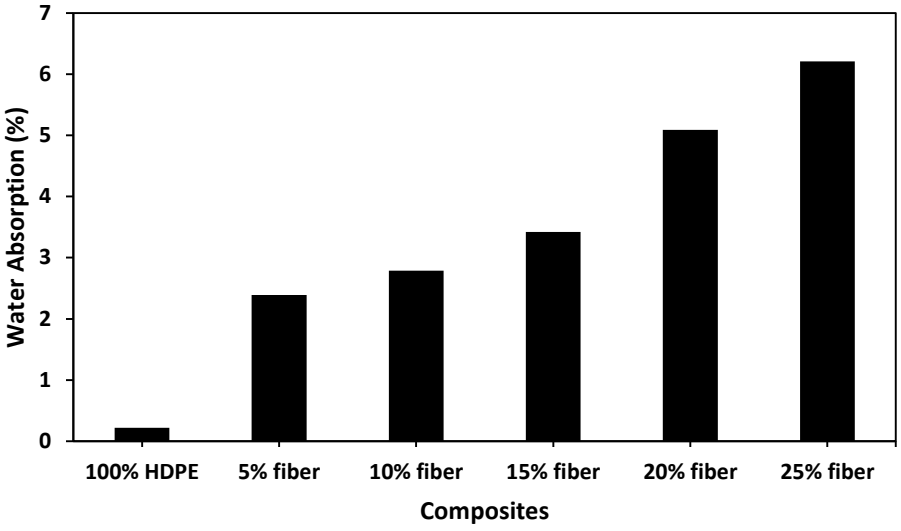

Figure 9.3: Water absorption of the composites at different fiber content

9.3.3 Mechanical Properties of the Composites

Mechanical properties such as tensile strength, elongation at break, tensile strength at break, yield strength and bending strength of the composites are shown in figures 9.4-9.8. Figure 9.4 shows the tensile strength of the hybrid composites at different fiber content. The tensile strength of 100% HDPE was found 20.16 MPa. The addition of 5 wt % fibers in HDPE increased the tensile strength than 100% HDPE. The maximum tensile strength was 24.15 MPa for 5 wt % fiber content composites due to better fiber-matrix interfacial adhesion. But the tensile strength gradually decreased for the composites containing 10 to 25% fiber. This decreased trend in tensile strength of the composites may be attributed to low fiber - matrix adhesion between fiber and HDPE with the increase of fiber content in the composite.

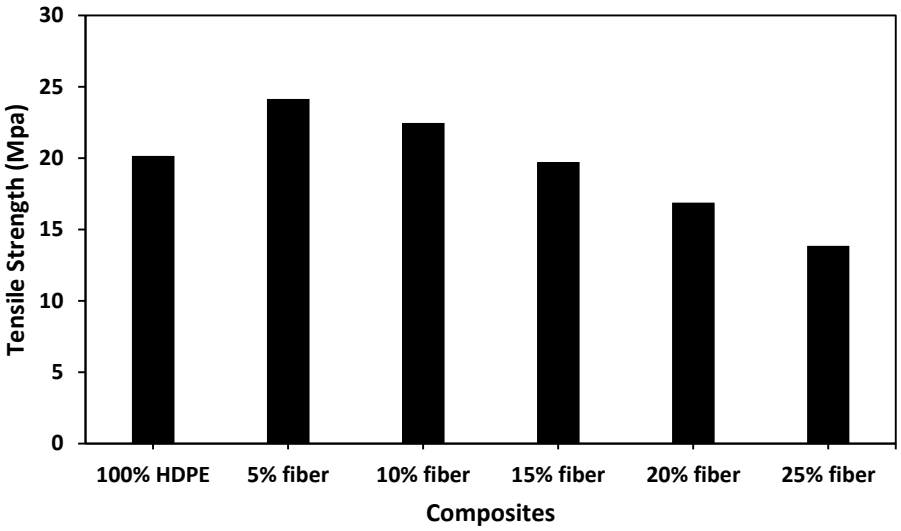

Figure 9.4: Tensile strength of the composites at different fiber content

The elongation at break of the hybrid composites for various wt% of fiber content is shown in figure 9.5. 100% HDPE presents the highest value of elongation at break. The elongation at break of the composites gradually reduced with the increase of fiber content from composites with 5 to 25% fiber content because of brittle nature of fibers reinforced composites. The fibers present in the composites do not exhibit elasticity or flexibility to the composites. That's why the elongation at break reduces with the increase of fiber content.

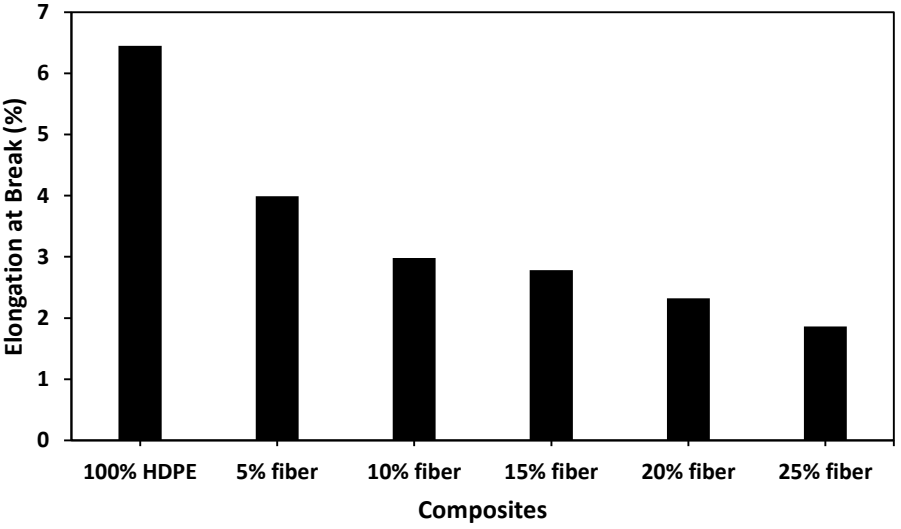

Figure 9.5: Elongation at break of the composites at different fiber content

Figure 9.6 shows the tensile strength at break of the hybrid composites at different fiber content. The maximum tensile strength at break value was found 22.07 MPa for 5% fiber content composites. Tensile strength at break reduced from composites with 10-25% fiber due to poor fiber-matrix adhesion.

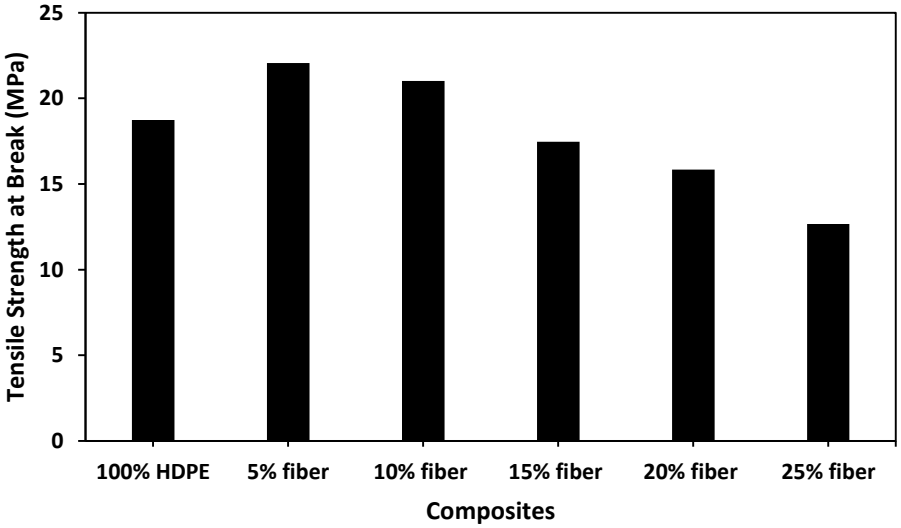

Figure 9.6: Tensile strength at break of the composites at different fiber content

Figure 9.7 shows the yield strength of the composites at different wt% of fiber content. The highest yield strength value observed 15.75 MPa by the composites with 5 % fiber loading. Yield strength value obtained for 100% HDPE is lower than 5% fiber content composites. Yield strength reduced for composites with 10-25% fibers.

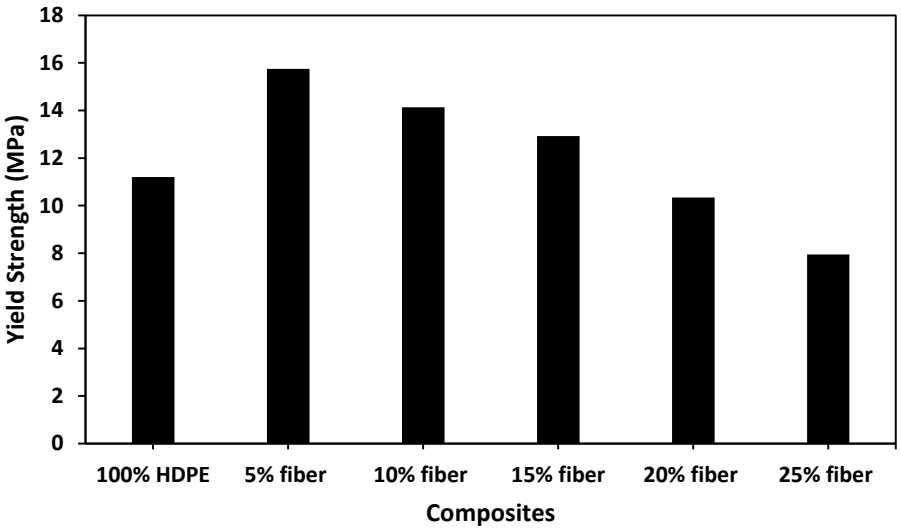

Figure 9.7: Yield strength of the composites at different fiber content

The bending strength for various wt% of fiber contents is displayed in figure 9.8. The bending strength of the hybrid composites decreased with increasing of fiber content. From the graph, it is clear that bending strength increased with 5% fiber content. Then bending strength reduced for 10 to 25% fiber content composites. Composites with 5% fiber content revealed a maximum bending strength of 26.26 MPa. The declining in bending strength of the composites containing 10 to 25% fibers directs the reduced fiber-matrix interaction.

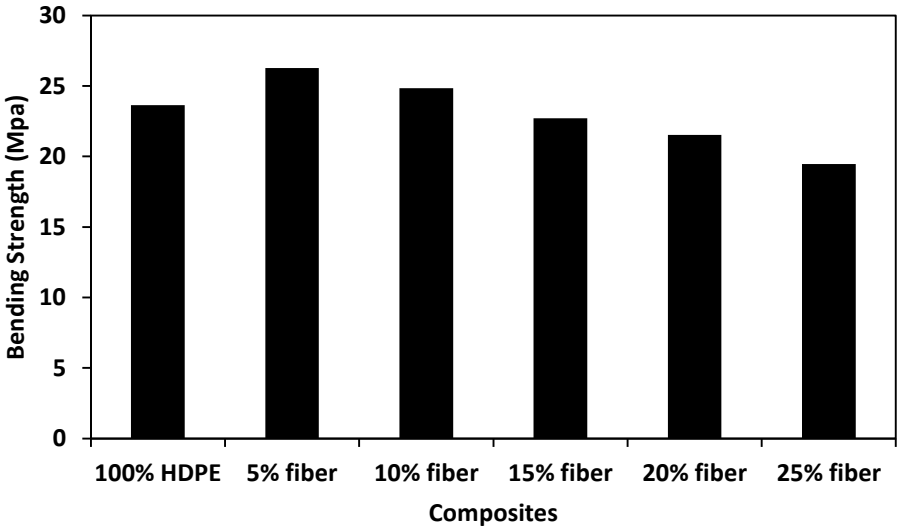

Figure 9.8: Bending strength of the composites at different fiber content

9.3.4 Degradation of the Hybrid Composites by Soil Burial

Degradation tests of the composites were carried out for up to six months. Figure 8.9 depicts the information about the degradation of the hybrid composites by soil burial. Degradation of the composites increased with time. The 5% fiber content composite lost 31.1% of tensile strength while 25% fiber content composite showed a loss of 37.8% of tensile strength. 5% fiber content composite showed more tensile strength than other composite samples. All composites express an increased degradation in the soil burial test. Moisture penetrates into the composites during soil burial tests. The fibers of composite surface and interface absorb water quickly because of hydrophilic nature and degrade slowly causing lower strength.

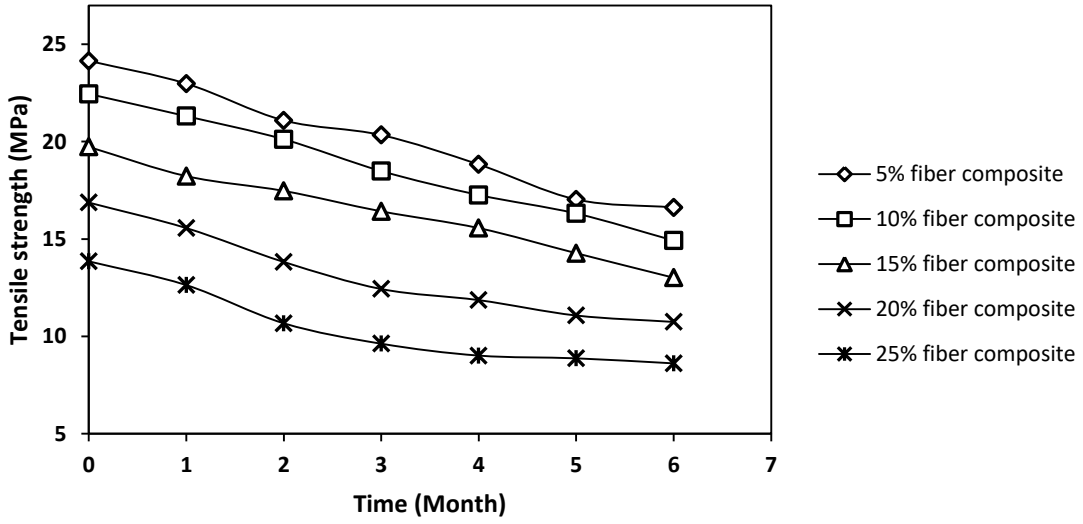

Figure 9.9: Degradation of tensile strength of the buried composite samples

9.3.5 Thermal Properties Analysis

TGA and DSC were performed to examine the thermal stability of 100% HDPE and the composites with 5% fiber. The TGA and DSC curves are shown in the figure 9.10 and 9.11. The TGA curve represents the percent mass of sample as a function of temperature. The figure 8.10 shows that 100% HDPE composite started to degrade at 428.7^0C with a mass change 97.68%. In the case of figure 8.11 the degradation of the composite started at 431.4^0C and 88.91% mass change is accomplished at about 500^0 C. The peaks of melting at 140.9 and 139.0^0 C were observed from the DSC curves of 100% HDPE and 5% fiber content

composite. There was no considerable change in thermal properties of the composites with the addition of fibers.

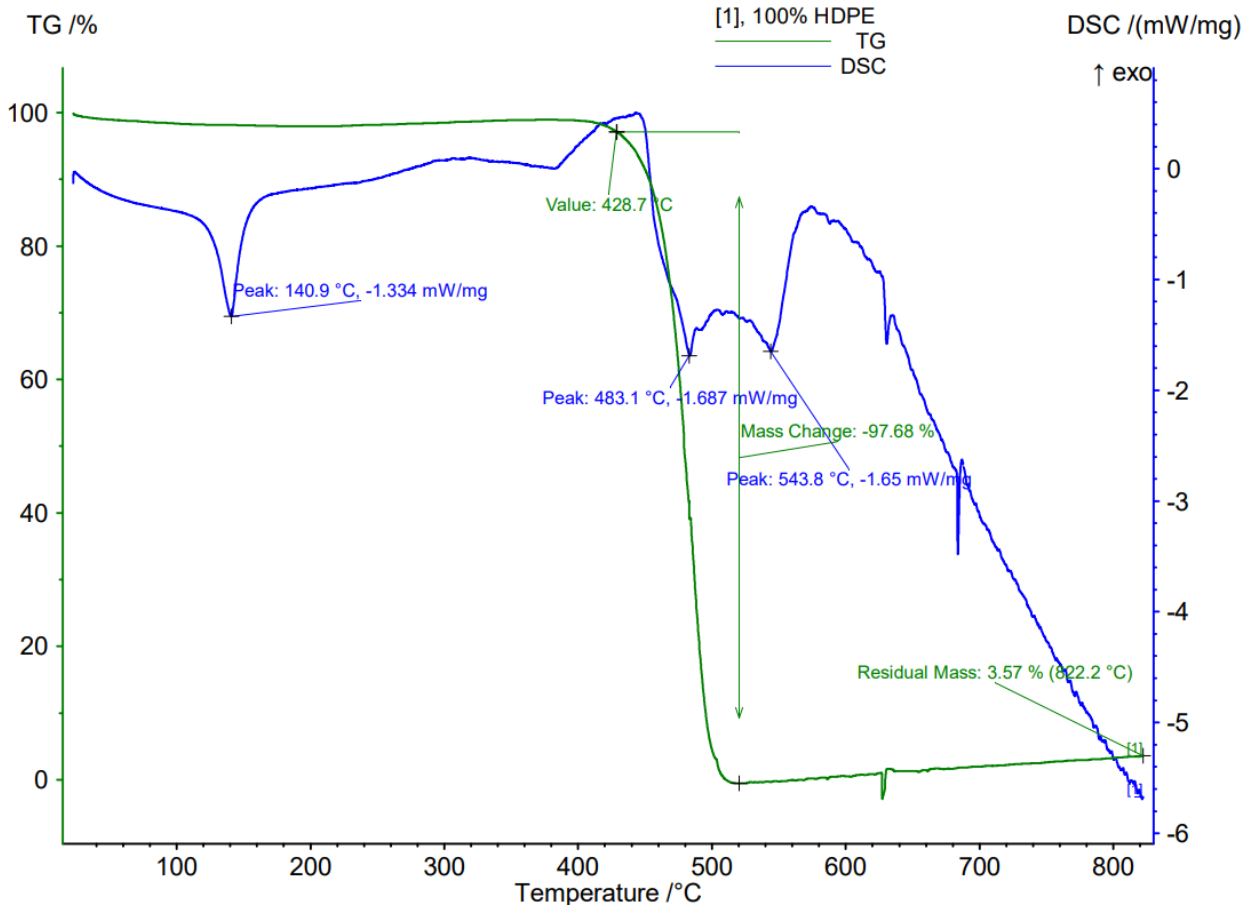

Figure 9.10: TGA and DSC of 100% HDPE

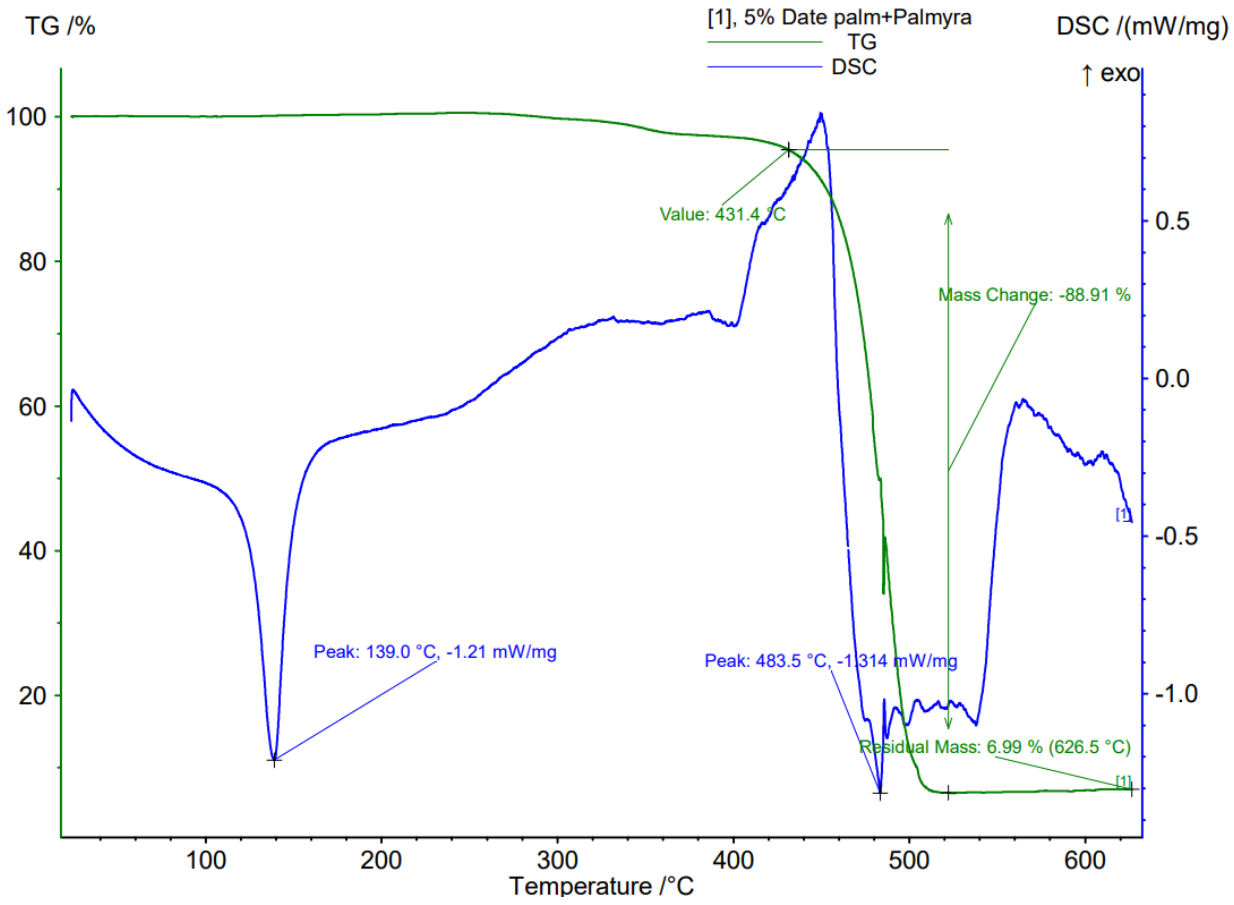

Figure 9.11: TGA and DSC of 5% fiber and 90% HDPE composite

9.3.6 FTIR Spectroscopy

The FTIR spectra of 100% HDPE and 25% fiber reinforced composites were studied and given in figure 9.12. The bands around 2915, 1462 and 718 cm^{-1} are found for both composites. The FTIR spectra of 25% fiber reinforced composite show five peaks at 3455, 1744, 1638,1258 and 1032 cm^{-1} and these are absent in 100% HDPE. The peak at 2915, 1462 and 718 cm^{-1} corresponds to the C-H stretching vibration, bending vibration of $-CH_2$ and rocking vibration of $-CH_2$ group respectively. The absorption band at 3455, 1744, 1638,1258 and 1032 indicate -OH stretching from cellulose, hemicellulose and lignin, C=O stretching from the lignin and hemicellulose, C=C stretching in aromatic, -COO vibration of acetyl

groups in hemicellulose or aryl alkyl ether compounds existing in lignin and C=O and -OH stretching vibrations of the polysaccharide in cellulose respectively.

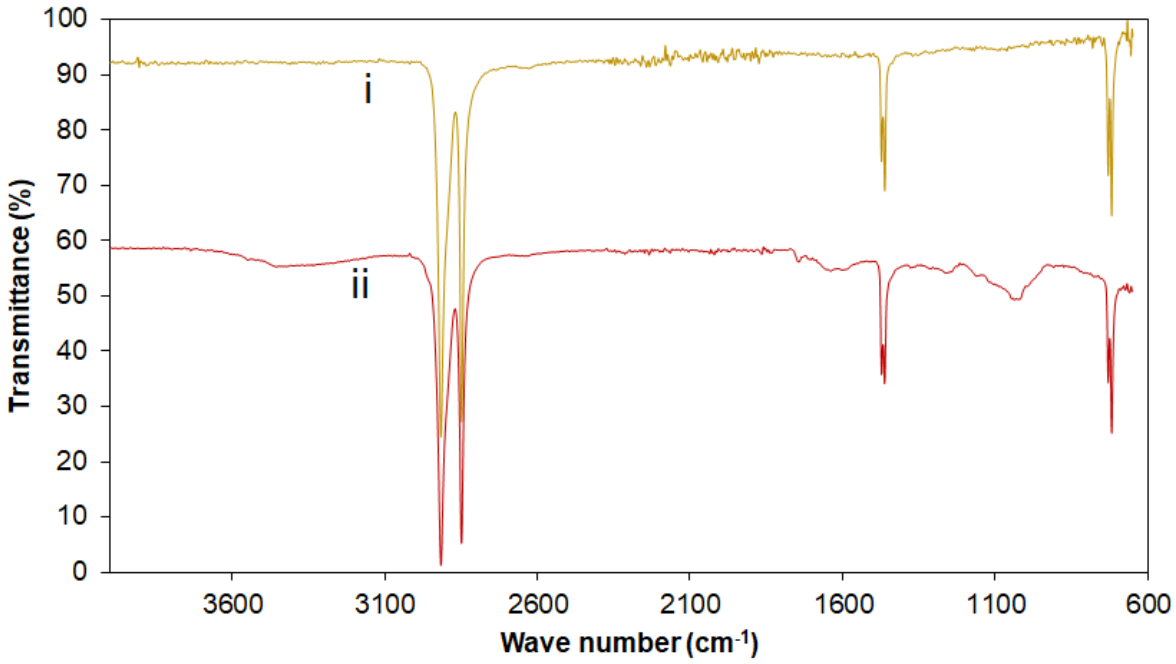

Figure 9.12: FTIR of (i) 100% HDPE and (ii) 25% fiber and 75% HDPE composite

9.3.7 SEM Analysis

The scanning electron microscopy (SEM) analysis was carried out on the fracture surfaces of 5% fiber and 90% HDPE composite and 25% fiber and 75% HDPE composite composites and the images are shown in Figure 8.13 and 8.14. SEM micrographs represent that the S1 composite showed better interfacial bonding between HDPE matrix and fibers. On the other hand, S5 composite displayed poor fiber-matrix adhesion between the matrix and the fiber. Gaps and a large extent of fiber pull-outs are observed for 25% fiber and 75% HDPE composite composites and caused low mechanical properties.

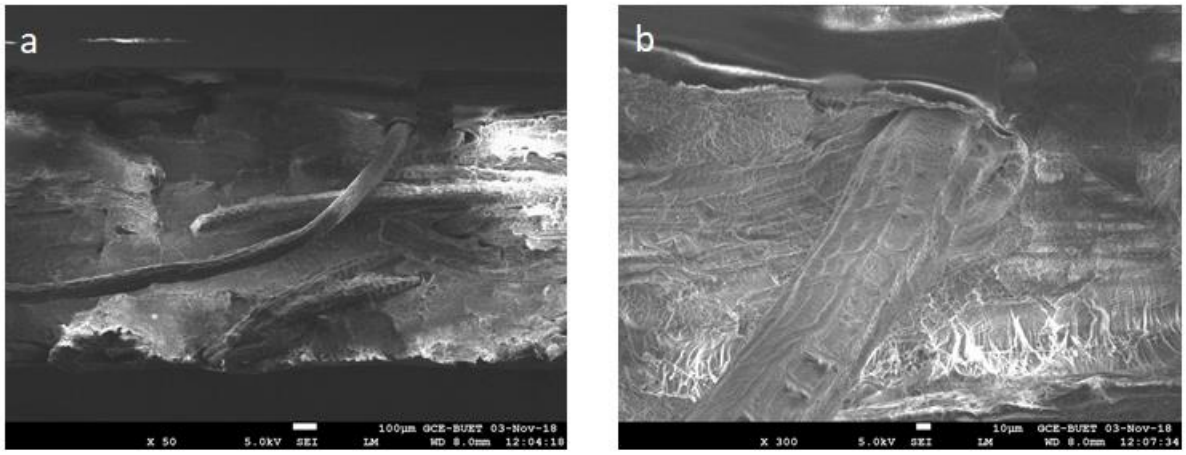

Figure 9.13: SEM images of 5% fiber and 90% HDPE composite (a) 50x magnification and (b) 300x magnification

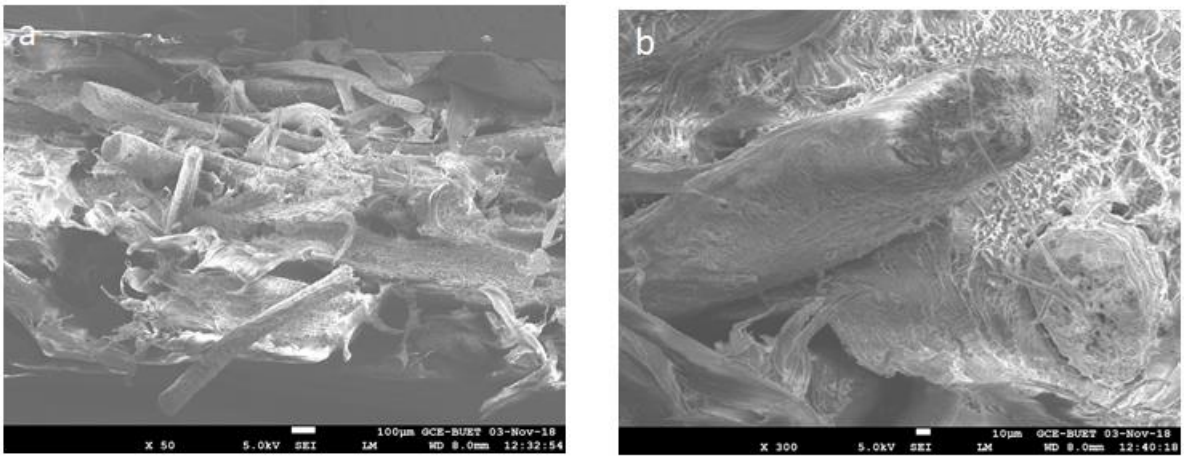

Figure 9.14: SEM images of 25% fiber and 75% HDPE composite (a) 50x magnification and (b) 300x magnification

9.4 Conclusions

DPM fiber and PPF fiber reinforced HDPE hybrid composites were fabricated by compression molding technique. It shows that the mechanical properties of hybrid composites improved at 5% fiber content and then decreased. Therefore, better mechanical properties were observed for 5% optimum fiber content. SEM images also supported good fiber-matrix adhesion with 5% fiber content. No considerable changes in thermal properties was found for

hybrid and 100% HDPE composites. The degradation rate of the composite 5% DPM and PPF fiber content was lower than other composites. These new hybrid composites may find applications in diverse field.

9.5 References

1. Madhukiran, J.; Rao, T.V.; Madhusudan, S.; Rao, R. U. Evaluation of The Mechanical Properties on Sisal-Coir Hybrid Natural Fiber Composites. *Int. J. of Eng. Res. Developm.*, **2017**, 13, 43-49.

2. Prasanna, G. V.; Subbaiah, K.V. Hardness, tensile properties and morphology of blend hybrid biocomposites. *Scholarly J. of Eng. Res.*, **2013**, 2, 21-29.

3. Tharaknath, S.; Selvakumar, S.; Purosthaman, G. Preparation and Characterization of Coir, Luffa Reinforced Polypropylene Composites. *Int.l J. of Eng. Tre. and Technol. IJETT,* **2014**, 16, 252-256.

4. Girisha, C.; Sanjeevamurthy, Srinivas, G. R. Sisal/Coconut Coir Natural Fibers – Epoxy Composites: Water Absorption and Mechanical Properties. *Int. J. of Eng. and Innov.Technol.*, **2012**, 2, 166-170.

5. Saba, N.; Tahir, P. M.; Jawaid, M. A Review on Potentiality of Nano Filler/Natural Fiber Filled Polymer Hybrid Composites, *Polymers*, **2014,** 6, 2247-2273.

6. Appusamy, A, M.; Eswaran, P.; Subramani, M.; Sadaiappan, S. Experimental studies on Mechanical properties and Characterization of Parthenium Short Fibre Reinforced Polymer Matrix Composites. *Int. J. of Eng. and Adv. Technol.*, **2018**, 8, 94-97.

7. Li.X.; Tabil. L. G.; Panigrahi, S.; Crerar, W.J. The Influence of Fiber Content on Properties of Injection Molded Flax Fiber-HDPE Biocomposites. *The Canad. Socie. for Bioeng.*, **2006**, 06, 1-10.

8. Sudhir. A.; Madhukiran, J.; Srinivasaao, R. S.; Madhusudan, S. Tensile and Flexural Properties of Sisal/Jute Hybrid Natural Fiber Composites. *Int. J. of Mod. Eng. Res.*, **2014**, 4, 29-35.

9. Rao H.R.; Indraja, Y.; Bai, G. M. Flexural Properties and Sem Analysis of Bamboo and Glass Fiber Reinforced Epoxy Hybrid Composites. *J. of Mech. and Civil Eng.*, **2014**, 11, 39-42.

10. Madhukiran, J.; Rao, S. S.; Madhusudan, S. Fabrication and Testing of Natural Fiber Reinforced Hybrid Composites Banana/Pineapple. *Int. J. of Mod. Eng. Res.*, **2013**, 3. 2239-2243.

11. Kumar, N. R.; Prasad G. R.; Rao, B. R. Investigation on Mechanical Properties of Banana Fiber Glass Reinforced Hybrid Thermoplastic Composites. *Int. J. of Eng. Res. & Technol.*, **2013**, 2, 3701-3706.

12. Bhoopathi, R.; Ramesh, M.; Rajaprasanna, R; Sasikala, G.; Deepa, C. Physical Properties of Glass-Hemp-Banana Hybrid Fiber Reinforced Polymer Composites. *Ind. J. of Sci. and Technol.*, **2017**, 10, 1-6.

13. Thiruchitrambalam, M.; Alavudeen, A,; Athijayamani, A,; Venkateshwaran, N.; Elaya Perumal, A. Improving Mechanical Properties of Banana/Kenaf Polyester Hybrid Composites Using Sodium Laulryl Sulfate Treatment. *Mater. Phys. and Mechan.*, **2009**, 8, 165-173.

14. Malathi, B.; Kumar, P. P. Experimental Investigation for Evaluation of Mechanical Properties of Rice Husk and Saw Dust Composites. *Int. J. of Trend in Res. and Develop.*, **2018**, 5, 6-10.

15. Jahan, A.; Rahman, M. M.; Kabir, H.; Kabir, M. A.; Ahmed, F.; Hossain, A. M.; Gafur, M. A. Comparative Study of Physical and Elastic Properties of Jute and Glass Fiber Reinforced LDPE Composites. *Int. J. of Scient. & Technol. Res.***2012**, 1, 68-72.

CHAPTER 10

Preparation and Characterization of CNC Reinforced Nanocomposite Films

10.1 Introduction

Biomass is playing an important role for sustainable development. The production of biomass based new materials has been paying attention due to the depletion of fossil sources and environmental issues [1,2]. Cellulose, hemicellulose, and lignin are the key components of lignocellulosic biomass. Around 35–50% cellulose is generally contained in the cell wall materialsof plant. Nanocellulose is isolated from cellulose which is a natural fiber material. The diameter of nanocellulose is generally less than 100 nm and length is several micrometers [3]. Nanocellulose is a nanomaterial that possess unique properties like low cost, renewability, biodegradability and has wide range of applications such as polymeric and paper composites, pharmaceuticals, food, energy storage, optoelectronics water purification, biomedical, 3D printing, anti-bacterial, carbon nanotubes stabilizer, electronics and tissue engineering [4,5].

Polymer blending or mixing is regarded as one of the most effective strategies for generating polymeric materials and producing products with a variety of properties. The results of the mixing approach could be customized to meet the needs that cannot be assessed using polymer alone [6]. Polyvinyl alcohol (PVA) is a polyhydroxy polymer which is semi-crystalline and water-soluble. Owing to excellent film-forming properties, hydrophilic nature, biocompatibility and biodegradability PVA is extensively used in many sectors such as textile, paper, hydrogels, membranes, tissue scaffolds, pharmaceuticals, biosensors, EMI shielding, and optoelectronics etc [7,8].

Polyvinylpyrrolidone (PVP) is an amorphous and water-soluble vinylpolymer which forms complexes with other polymers and contains highly polar side groups in the lactam rings [9]. PVP exhibits properties such as adhesion, biocompatibility, high hydrophilicity, no toxicity and solubility in water and nearly all organic solvents and used in various biomedical applications [10,11]. Polymer blending has the potential to produce products with improved properties [11,12]. In recent years blend films have received a lot of attention as a food packaging material [9]. The main disadvantage of PVA is that it suffers from suspension under physiological settings; however, blending with PVP can lessen this by connectivity by hydrogen bonds, which increases the blend's stability under physiological conditions [12]. So, PVA/PVP blend films are ideal materials for food packaging as well as controlled release of various pharmaceutical antibacterial drugs [11]. The blend of PVA and PVP has the potential

to be used in the production of biomaterials and multifunctional utilities [12]. Both PVA and PVP are water soluble, and PVP is found an excellent partner for PVA in polymer mixing due to its ability and mild electrical conductivity relevant to its personal properties [6]. The formation of intermolecular hydrogen bonding between the hydroxyl group of PVA and carbonyl group of PVP occurs through the mixing of PVA and PVP [12]. In this research, PVA/PVP mix film-based nanocomposite will be made utilizing a solution casting method to increase PVA properties.

Date palm (*Phoenix sylvestris*) trees are abundantly grown in Bangladesh and the fibers from these trees are taken into consideration as an agricultural waste [13]. Handoko et al. [14] prepared polyvinyl alcohol nanocomposites with nanocrystalline cellulose from tea waste. Oyeoka et al. [15] prepared polyvinyl alcohol/gelatin nanocomposite films with water hyacinth cellulose nanocrystals. PVP/cellulose nanocrystals composite films from commercial MCC and aerogels produced by Voronova et al. [16]. Poonguzhali et al. [17] synthesized nanocomposites based on chitosan and PVP with nanocellulose from *Hibiscus cannabinas*. Cellulose nanocrystals (CNC) reinforced PVA/starch nanocomposite films prepared by Popescu et al. [18]. Pavalayadon et al. [19] produced cellulose nanocrystals from sugarcane bagasse and coir and used those cellulose nanocrystals as reinforcing material to develop PVA nanocomposite films. Shaikh et al. [20] fabricated and characterized polyvinyl alcohol/gaur-gum nanocomposite films with cellulose nanocrystals from date palm tree trank mesh fiber. From the literature survey, to the best of our knowledge, there is no report on the production of CNC from date palm mat (DPM) fibers (*Phoenix sylvestris*) and their nanocomposites with PVA and PVP at different compositions. This work emphasizes on the utilization of DPMs as a potential source of crystalline nanocellulose. In our present study, the chemical compositions of DPM fibers are analyzed. CNC is extracted from the DPM fibers through acid hydrolysis process that are used as reinforcement to prepare a new composite film. The composite films with nanocellulose, PVA and PVP are prepared by solution casting method. The properties of nanocomposite films have been investigated by varying the percentage of nanocellulose.

9.2 Experimental

10.2.1 Materials

Date palm mat fibers (*Phoenix sylvestris*) used in this study were collected from Jashore, Bangladesh (Figure 10.1). Sodium hydroxide and sulfuric acid were purchased from Merck, Germany. Sodium chlorite was obtained from Research-Lab Fine Chem Industries, India. Acetic acid, Polyvinyl alcohol (molecular weight 89,000-98,000, 99+% hydrolyzed) and Polyvinylpyrrolidone (average molecular weight 40000) were purchased from Sigma-Aldrich. All chemicals used are of analytical grade.

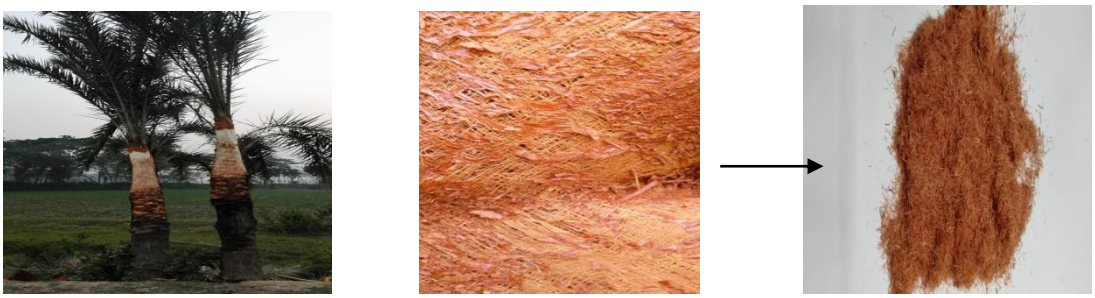

(a) (b)

Figure 10.1: Images of the (a) date palm tree (*Phoenix sylvestris*) and (b) DPM fibers

10.2.2 Analysis of Chemical Composition

The chemical compositions of DPM fibers were determined such as α - cellulose, hemicellulose, lignin, aqueous extracts, fatty and waxy matters. The chemical compositions of the fiber affect the different properties for the fabrication of fiber reinforced polymer composites. The methods for the determination of chemical compositions of DPM fibers were carried out according to Poddar et al. [21].

10.2.3 Extraction of Cellulose

At first the fibers were cut into 2-3 mm using hand scissors. The fibers were soaked to distilled water and heated at around 100^0C for 2 hours. The fibers then washed with cold distilled water and dried in air. The dried fibers (5g) were bleached by sodium chlorite (5g) in hot water (250ml) with glacial acetic acid (10ml) and heated at 80-90^0C for 1h. This process was repeated for 3 times until fiber became white and filtered. After filtration the fibers were washed for several times with distilled water and air dried. The bleached fibers were treated

with 17.5% (w/v) sodium hydroxide solution at room temperature for 2 hours and washed carefully with distilled water. Finally, the cellulose was dried in air after filtration.

10.2.4 Preparation of Crystalline Nanocellulose (CNC)

CNC was prepared by the acid hydrolysis of cellulose. The cellulose was treated with 64% (w/w) sulfuric acid at 45^0C for 1h with constant stirring. The reaction was quenched by the addition of deionized water (10 folds) and centrifuged at 9500 rpm for 20 min to remove acidic solution. The precipitate was rinsed and centrifuged with deionized water repeatedly until neutral pH. The CNC as suspension was kept in a refrigerator until further use.

10.2.5 Preparation of CNC reinforced PVA and PVA/PVP films

The solution casting method was used to prepare CNC reinforced PVA and PVA/PVP films by optimizing the concentration of raw materials. The PVA solution (2.5%) was prepared by dissolving PVA powder in deionized water at 80^0C for 2 hours and stirred with magnetic stirrer (500 rpm). CNC was dispersed in deionized water to get a suspension. After the PVA was completely dissolved, CNC (3-12%) (w/w) relative to PVA was added to the PVA solution and stirred to get a homogeneous mixing. The final mixture was sonicated for 10 minutes and casted on glass petridish to dry at room temperature. Finally, the film was removed from the petridish. In the case of PVA/PVP blend film preparation PVA and PVP were used with a weight ratio of 3:1. The prepared films (Figure 10.2) were stored in a desiccator before further characterization. The thickness of the resulting films varied from 0.18–0.27 mm.

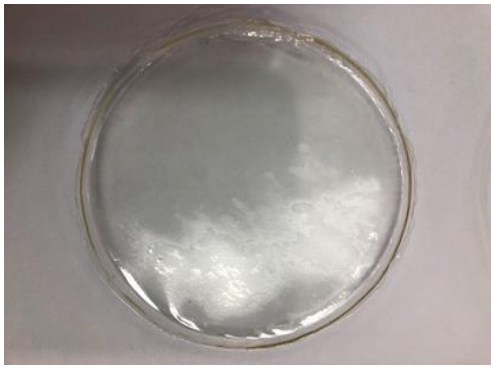

Figure 10.2 Image of prepared CNC/PVA/PVP film

10.2.6 Yield of CNC

For the determination of yield of CNC, the prepared CNC suspension was dehydrated in an oven at 50 ^{0}C until constant weight was obtained. The percent of yield of CNC was calculated utilizing the following equation 10.1 [22].

$$\text{Yield } (\%) = \frac{w_2}{w_1} \times 100\% \quad (10.1)$$

where w_2 is the weight of the dried CNC and w_1 is the weight of the raw DPM fiber.

10.2.7 Dynamic Light Scattering (DLS)

The average particle size and zeta potential of CNC were examined by DLS (Nano Zetasizer, Malvern). The CNC was dispersed in deionized water and inserted in the cuvette in order to measure particle size and zeta potential of CNC. The measurements were carried out at room temperature.

10.2.8 FTIR Analysis

The presence of functional groups was characterized by using FTIR. A FT-IR/NIR spectrometer (Frontier, Perkin Elmer, USA) was used to record the FTIR spectra of DPM fiber, cellulose, CNC and films. The FTIR spectra were recorded in the wavelength range from 4,000-650 cm^{-1}. Attenuated and total reflectance (ATR) technique was used to investigate the samples.

10.2.9 Morphological Analysis

The morphology of solid surface of CNC, 100% PVA, PVA/PVP, 3% CNC reinforced PVA/PVP and 12% CNC reinforced PVA nanocomposite films was observed by a field emission scanning electron microscope (JEOL JSM-7600F) operated with an accelerating voltage of 5.0 kV. A small portion of the fibers or nanocomposite films was mounted on a metal stub using conductive carbon tape, coated with gold and observed.

10.2.10 Tensile Properties

Tensile properties of the CNC reinforced PVA and PVA/PVP films were measured using universal strength tester (model 1410 Titans, capacity 5 kN, England) according to ASTMD 3039/D 3039M-00 (2002). The measurements were conducted at a cross head speed 10

mm/minand a gauge length of 50 mm. Five specimens in each composition were tested for an average value.

10.2.11 Water Absorption Capacity of the Films

Water absorption capacity of the CNC reinforced PVA and PVA/PVP films were carried out according to ASTM D 570-99. The test films were dried in an oven at 50^0C for 2h and cooled in a desiccator. The samples were weighed immediately. These samples were immersed in distilled water for 24 h at room temperature. The samples were taken out from the beaker, removed excess water by wiping with a cloth and weighed. Three samples were tested in each case and the results were presented as average. The water absorption capacity was calculated by following the equation 10.2:

$$\text{Water absorption capacity, \%} = \frac{(\text{Final weight} - \text{First weight})}{(\text{First weight})} \times 100 \qquad (10.2)$$

10.2.12 Density Estimation

The density of the films was calculated by measuring the weight and dimensions of the film with the help of the following equation 10.3 [23].

$$\text{Density} = \frac{Mass}{Area \times Thickness} \qquad (10.3)$$

10.3. Results and Discussion

10.3.1. Chemical Composition Analysis

The chemical compositions of DPM fibers were determined. The percentage of chemical compositions of DPM fiber is shown in Table 10.1.The chemical composition in the fiber was approximately same as that of other lignocellulosic materials and the fiber is also considered to use as a source of cellulose raw material.

Table 10.1 The chemical compositions of DPM fibers

Fiber	α-cellulose	Hemicellulose	Lignin	Aqueous extract %	Fatty and waxy	Pectic matters	References

					matters		
DPM fibers	43.99	15.78	21.74	3.18	7.26	8.05	Present work
Jute	67-71.5	13.6-20.4	12-13	-	0.5	0.2	[24]
Date palm leaf	58	-	15.3	-	-	2.3	[25]
Coconut stem fiber	46.26	18.02	22.54	5.52	5.91	1.75	[21]
Date palm stem	39.8	30.6	17.1	-	-	-	[26]
Sugarcane bagasse	35	25	22	-	-	-	[27]

10.3.2 Yield of the CNC

The use of DPM fiber as a source material for CNC isolation has not been studied. CNC was isolated from DPM fiber by acid hydrolysis and the yield was found 37.9%±0.85. Brito et al. [28] prepared cellulose nanocrystals from bamboo fiber with a yield of 30%. Xiong et al. [29] prepared nanocrystalline cellulose via acid hydrolysis from waste cotton fabrics with 21.5% yield. Xiaoshan et al. [22] isolated CNC from Pennisetum hydridum fiber and the highest yield was 43.6%.Battisti et al.[30] CNC extracted from royal palm tree fiber with 48.8% yield. Raza et al. [26] produced cellulose nanocrystals from date palm stem waste with 21.2%±0.5 yield.

10.3.3. Particle Size Analysis

DLS was utilized to measure the size distribution of CNC. Figure 10.3 shows the results of particle size distribution of CNC obtained by acid hydrolysis process. The DLS analysis revealed that the average particle size of CNC was around114.7 nm. The resulted CNC suspension from cellulose was in the nanometer range. The CNC did not show uniform

particle size distribution because of the fragmentation of the celluloses throughout acid hydrolysis process [31].

Zeta potential measurement is a characterization technique of nanocrystals for the estimation of surface charge in a colloidal solution. The Zeta potential value is the indication of the stability of the crystalline nanocellulose in suspension. The Zeta potential of CNC suspension is shown in figure 10.4. Usually, zeta potential value of lower than -30 mV and higher than 30 mV shows a stable suspension of crystalline nanocellulose.The CNC prepared from DPM fibers possess Zeta potential value of -38.6 mV. The results reveal good stability of CNCs. This may be owing to the repulsive forces are formed between anionic sulfate groups and CNC chain during the acid hydrolysis process of CNC [32].

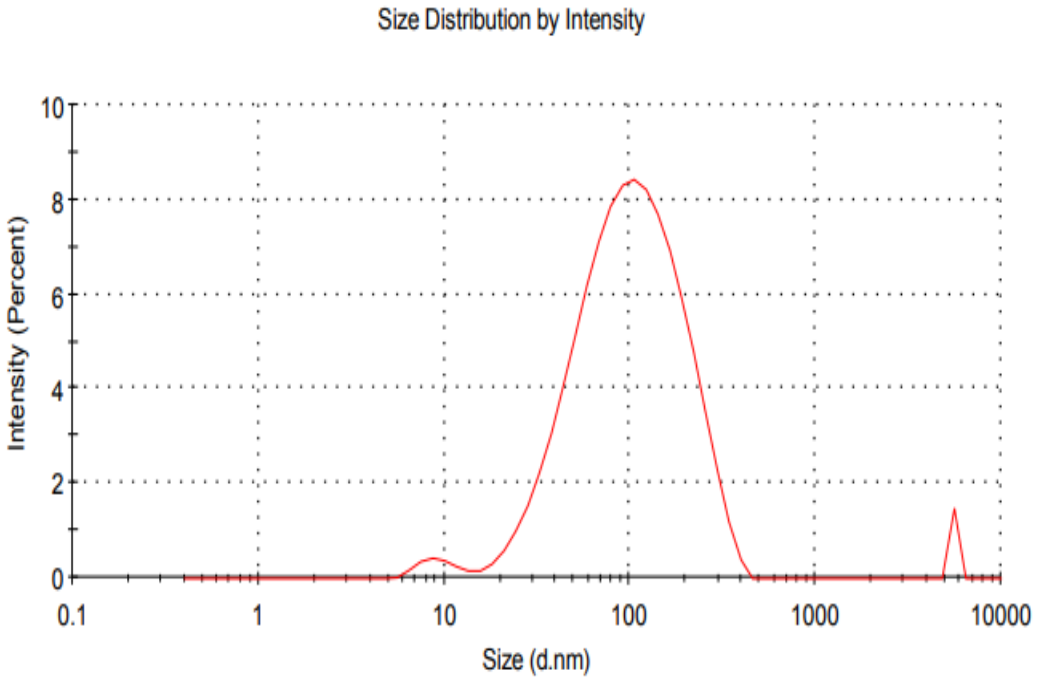

Figure 9.3: Particle size distribution of crystalline nanocellulose suspension

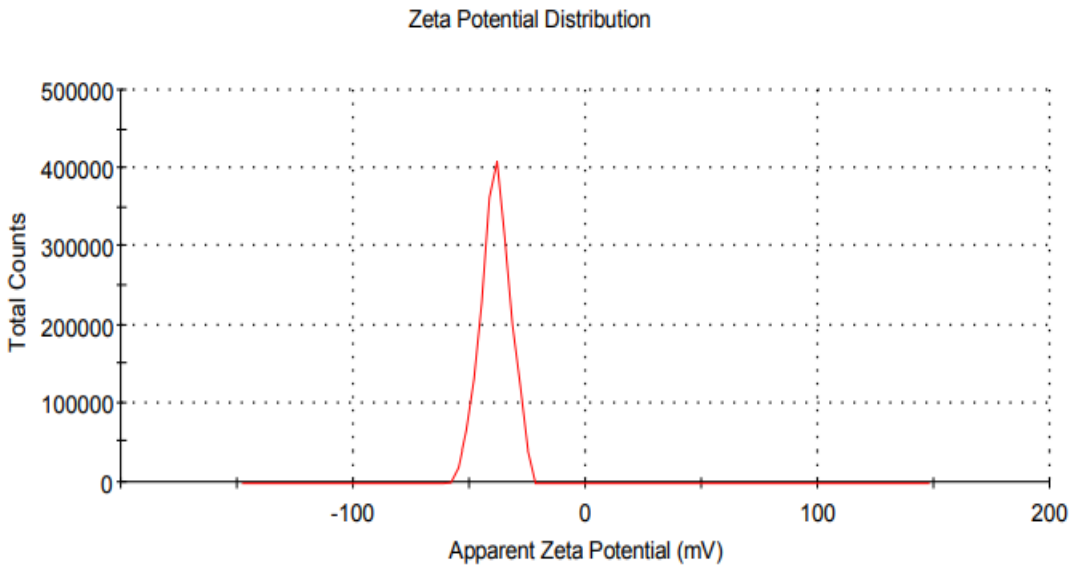

Figure 10.4: Zeta potential of crystalline nanocellulose suspension

10.3.4 FTIR Analysis

FT-IR analysis was used to identify the functional group of the raw DPM fibers, cellulose, CNC and films. The FTIR spectra of raw DPM fibers, cellulose and CNC are shown in figure 10.5. The absorption bands related to stretching and bending vibrations of different chemical compositions of fibers that is cellulose, hemicellulose, and lignin. In the raw fiber spectrum, the peaks in the range 3600-3200 cm^{-1} represents O–H stretching vibration of the hydroxyl groups in cellulose molecules and the peaks in the region 2920-2850 cm^{-1}indicates the C–H stretching of cellulose, hemicellulose and lignin [33]. The peak in the region 1700–1740cm^{-1}, particularly at 1728cm−1 refers C=O stretching of acetyl ester in hemicellulose and carbonyl aldehyde in lignin [34]. The peak at 1610 cm^{-1} is related to absorbed water molecules in carbohydrates [35]. The peak at 1508cm^{-1} represents the C=C stretching vibration of the aromatic ring in lignin [36].The peaks observed between 1370 and 1430cm^{-1}correspond to the symmetric CH_2 bending vibrations of the cellulose [37]. The absorption peak at 1239cm^{-1} is derived from the stretching of phenolic hydroxyl groups in lignin [38].The peak at 1032 cm^{-1}corresponds to the CO and OH stretching vibrations of the polysaccharide in cellulose. The peak at around 895 cm^{-1} indicates the presence of β-glycosidic linkages between

monosaccharides [39]. The peaks are around at 1239cm^{-1}, 1508cm^{-1} and1728cm^{-1}are absent in cellulose which reveals the removal of hemicellulose and lignin during cellulose extraction process. The FTIR spectrum of CNC is same as cellulose. It proves that no new bonds are formed during acid hydrolysis process.

Figure 10.6 displays the FTIR spectra of PVA, PVA/PVP, PVA/9%CNC and PVA/PVP/9%CNC films. In the case of PVA, the peaks at 3287cm^{-1}, 2940 cm^{-1}and 1087 cm^{-1} correspond to the O-H stretching, C-H stretching and C=O stretching or O-H bending [40]. In contrast to the spectra of PVA and PVA/CNC films, the peaks on PVA/CNC films show just a slight displacement. The O-H and C-H peak shifted to 3270 cm^{-1} and 2937 cm^{-1} respectively due to the presence of CNC. For PVA/PVP films, a sharp peak at 1654 cm^{-1} indicates the typical C=O stretching band [41]. The O-H stretching appears at 3286 cm^{-1}. The characteristic peak at 1291cm^{-1} relates to the C-N stretching. The C=O stretching or O-H bending peak displaced to 1090 cm^{-1} due to including PVP into PVA. The other peaks for PVA/PVP films are observed with a small shifting. The peaks on PVA/PVP/9%CNC films also exhibit a little displacement in comparison to the spectra of PVA/PVP films. The O-H stretching, C-H stretching and C=O stretching and O-H bending peaks in the PVA/PVP/CNC films shifted to 3284 cm^{-1}, 2925 cm^{-1} and 1089 cm^{-1} respectively when compared to PVA/PVP.

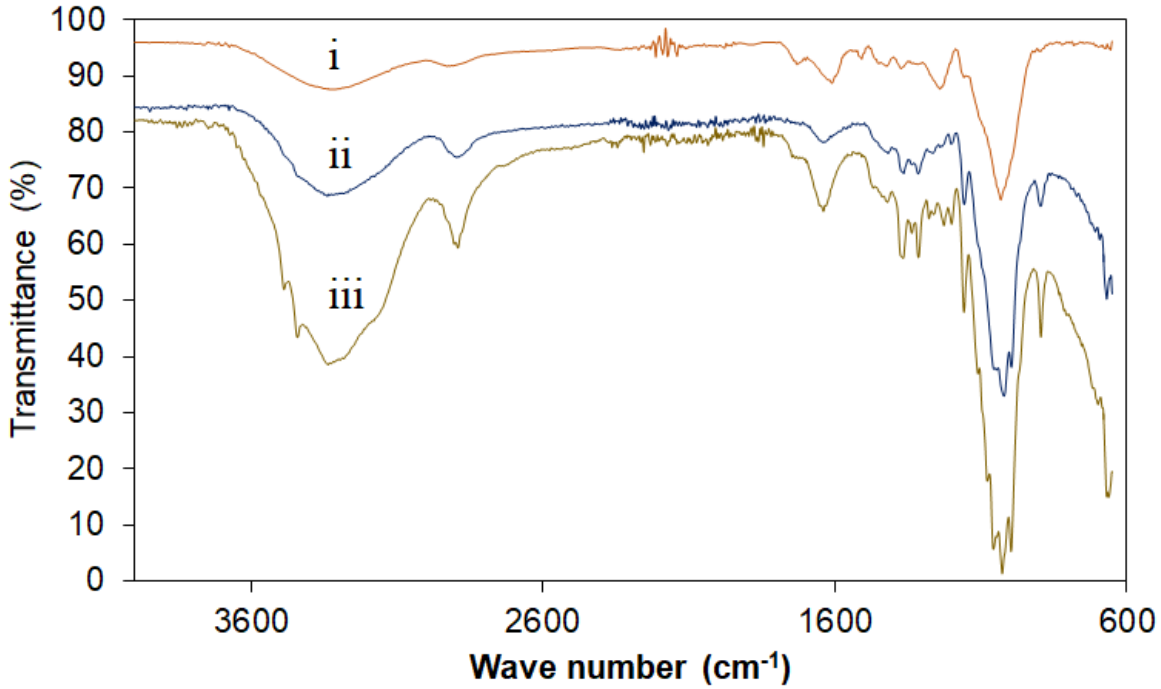

Figure 10.5: ATR-FTIR of (i) raw DPM fiber; (ii) cellulose and (iii) CNC

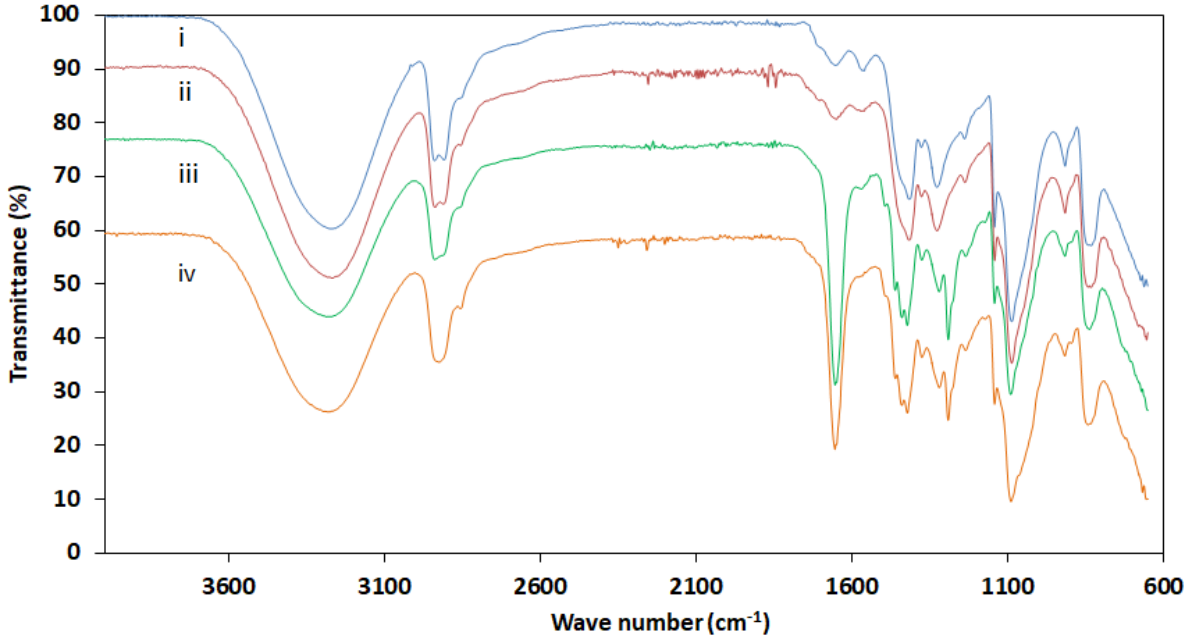

Figure 10.6: FTIR of (i) PVA; (ii) PVA/9%CNC; (iii) PVA/PVP and (iv) PVA/PVP/9%CNC films

10.3.5. Tensile Properties

CNC of DPM fiber was used to develop new nanocomposites with PVA and PVA/PVP. The influence of the addition of different percentages of CNC (0-12%) on the mechanical properties of the nanocomposite films was determined and shown in figures 10.7, 10.8 and 10.9. Neat PVA film exhibited higher tensile strength than PVA/PVP film. Soud et al. [41] showed that with the incorporation of PVP in the PVA solution the tensile strength was reduced. The mechanical properties of composite films were effectively improved by the addition of CNC as a reinforcing agent. Therefore, the additions of CNC from 3-9% into PVA /PVP matrix, the tensile strength of nanocomposite films was increased and the highest value at 9% CNC loading is 27.85 MPa (figure 10.7). The tensile strength of the PVA/CNC nanocomposite films was enhanced by 33% upon adding 9% CNC which was the highest value of 30.99 MPa. Shi et al reported that the PVA/CN nanocomposite with the addition of 9% cellulose nanocrystals extracted from kenaf fiber showed the highest tensile strength [42]. It is found from figure 10.7 that the addition of up to 9% CNC enhances the tensile strength of the nanocomposites. This is due to the well dispersion of CNC into the matrix and the formation of a network structure by hydrogen bonding interactions between CNC and PVA and PVP matrix [43]. Figure 10.7 also shows that the tensile strength of the nanocomposite films with 12% CNC reduced which may have resulted from inadequate dispersion. Inadequate dispersion is mostly caused by aggregated CNC particles, which create additional stress points in the matrix thereby reducing CNC's positive contribution to tensile strength [15].

The tensile modulus of the nanocomposite films was increased with the increasing of CNC content (figure 10.8).The composites tensile modulus achieved maximum values at 12% CNC. The incorporation of high stiffness CNCs could effectively increase the modulus of PVA even at low CNC content because the stiffness of materials is primarily dependent on the composition of the composite [44]. Asad et al. [45] also stated an increase in tensile modulus with the incorporation of CNC in PVA based films.

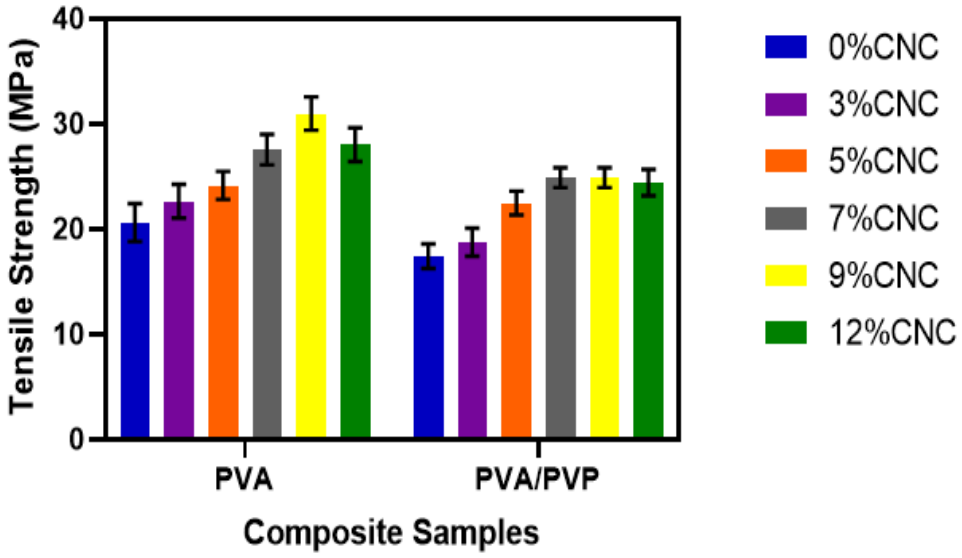

Figure 10.7: Tensile strength of the nanocomposite films at different wt. % of CNC

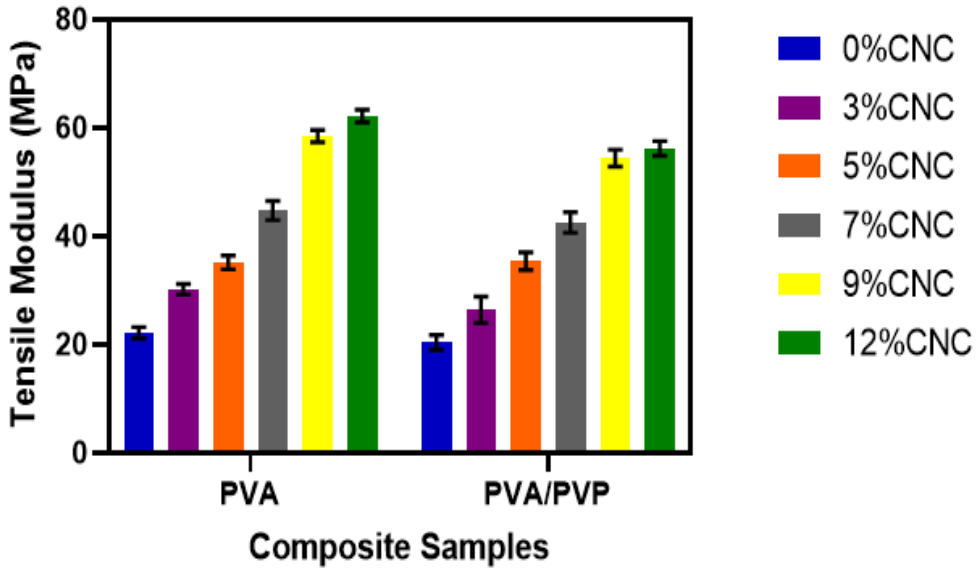

Figure 10.8: Tensile modulus of the nanocomposite films at different wt. % of CNC

The figure 10.9 presents the elongation at break of CNC reinforced PVA and PVA-PVP nanocomposite films. There is a gradual reduce in elongation at break of the nanocomposites with the increase of various ratios of CNC. Similar trend in the elongation at break with increasing CNC of the nanocomoposite films were also found for PVA/gelatin films with water hyacinth cellulose nanocrystals. This may be due to the increase of stiffness as a result

of three dimensional network structures of the nanocomposite films by the addition of CNC [15]. Huq et al. [46] also noted that the presence of nanocellulose in alginate-based films reduced their elongation at break.

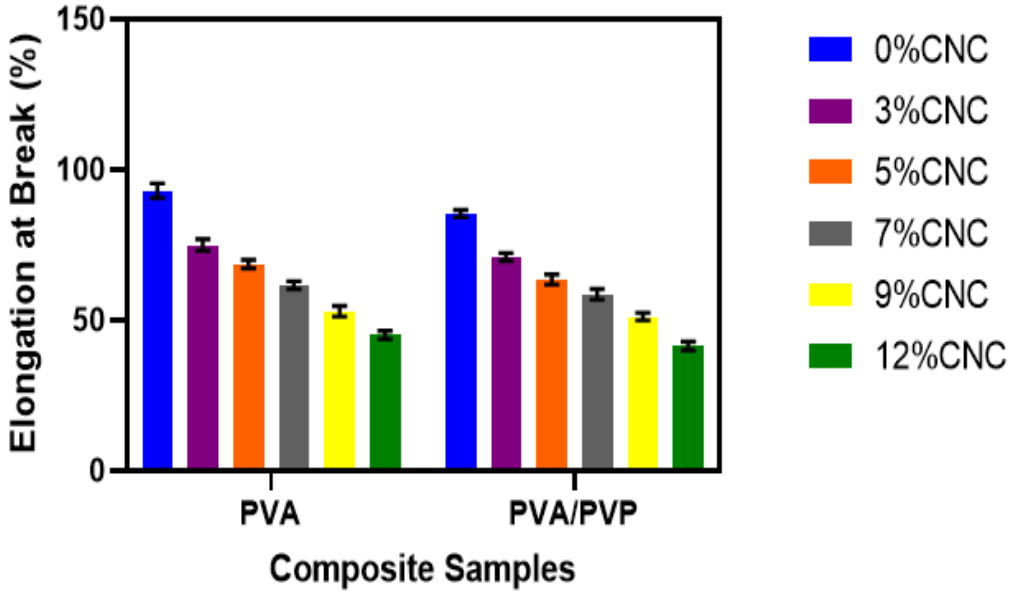

Figure 10.9: Elongation at Break of the nanocomposite films at different wt. % of CNC

The tensile properties of PVA/CNC nanocomposites and PVA/PVP/CNC nanocomposites are nearly same; however PVA/CNC nanocomposites values are slightly higher than PVA/PVP/CNC nanocomposites. Because of the blend's durability under physiological environments, PVA/PVP/CNC nanocomposites are more suitable than PVA/CNC nanocomposites for food packaging, pharmaceutical, and biomedical applications [11,12].

10.3.6 Morphological Analysis

There are three forms of nanocellulose: nanocrystalline cellulose, nanofibrillated cellulose, and bacterial nanocellulose, which are produced via acid hydrolysis, mechanical techniques, and Gluconacetobacter xylinus respectively [3]. The nanocellulose produced by acid hydrolysis is known as nanocrystalline cellulose or cellulose nanocrystals. The amorphous components are hydrolyzed and eliminated by acid during acid hydrolysis, leaving only the short-rod-like crystalline sections (high crystallinity between 54 and 88%) [3]. Figure 10.10

shows a SEM image of CNC solid surface isolated from DPM fibers. It is found from figure 10.10 that the surface of CNC has rod shaped crystalline portions. Therefore, figure 10.10 clearly indicates that acid hydrolysis of cellulose fragmented the cellulose into different rod-like crystals.

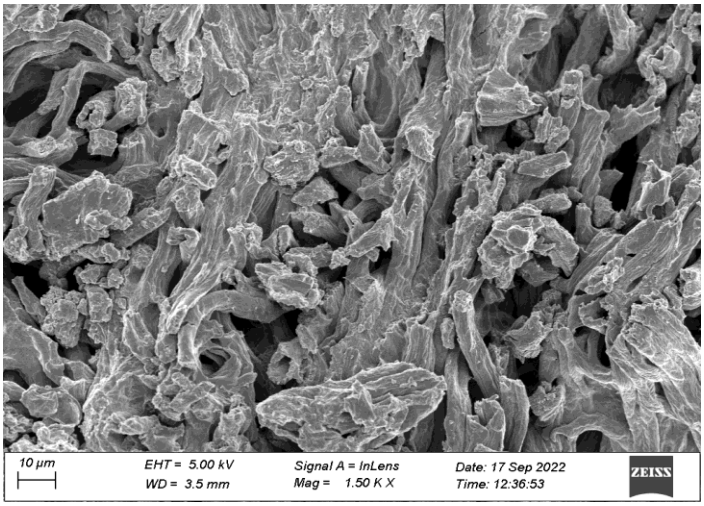

Figure 10.10: SEM micrographs of CNC from DPM fibers

The surface of the prepared nanocomposite films were examined by SEM. Figure 10.11 displays the surface micrographs of neat PVA, PVA/PVP and CNC reinforced PVA and PVA/PVP nanocomposite films. The SEM micrographs of neat PVA and PVA/PVP show a smooth surface. In the case of 3% CNC incorporation in the PVA films, the film shows a smooth surface. 3% and 9% CNC reinforced PVA films indicate proper distribution of CNC in the matrix. Larger CNC agglomeration is clearly observed for 12% CNC loading in both PVA and PVA/PVP nanocomposite films. The formation of these larger aggregates may have an effect on the mechanical performance of the nanocomposite films [47].

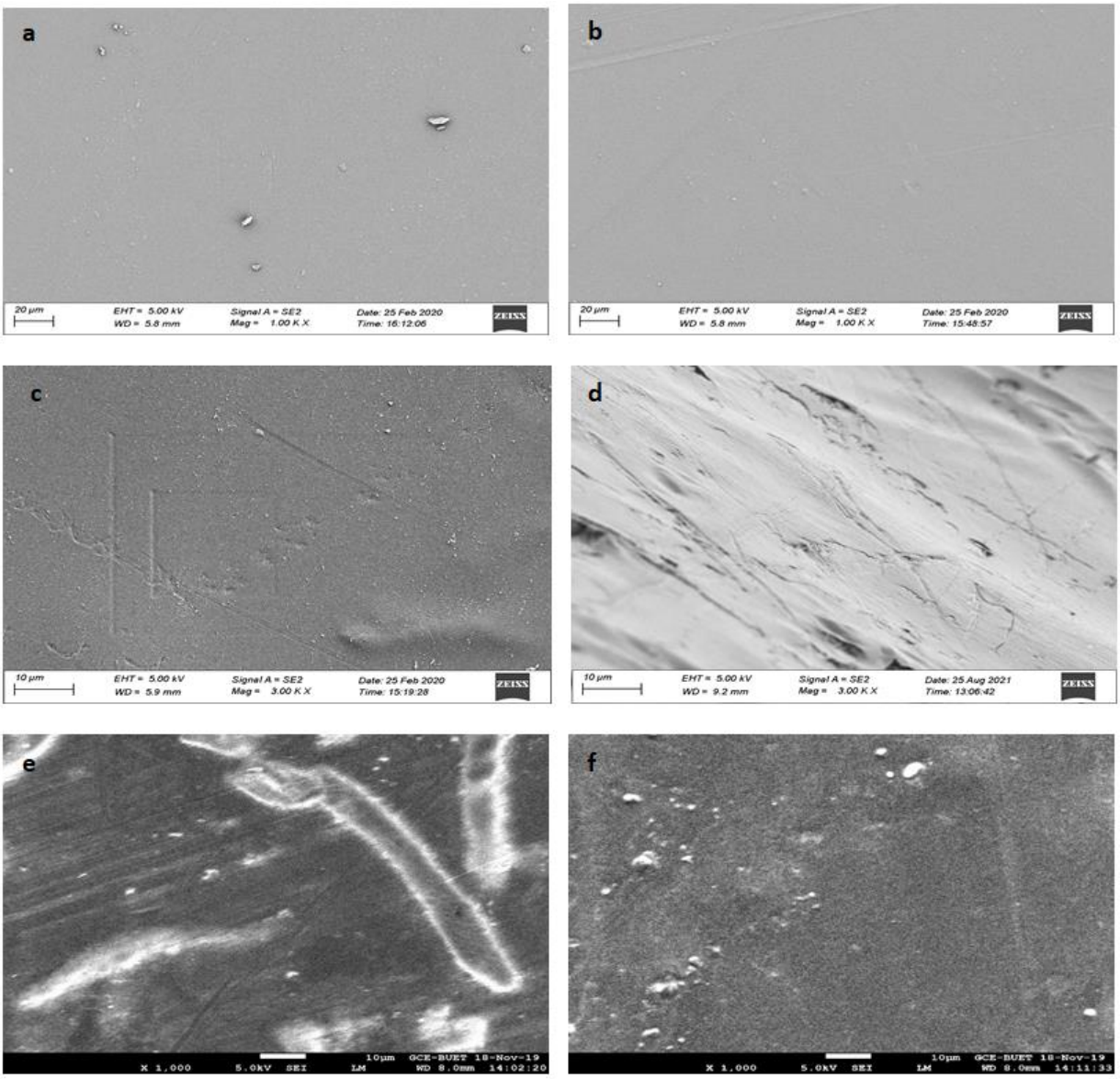

Figure 10.11: SEM micrographs of (a) neat PVA, (b) PVA/PVP, (c) 3% CNC/PVA (d) 9% CNC/ PVA (e) 12% CNC/PVA and (f) 12% CNC/PVA/PVP nanocomposite films

9.3.7 Water Absorption Capacity

The effect of different % of CNC on the water absorption capacity of the nanocomposite films is shown in figure 10.12. It is noted from the figure that PVA/PVP film shows higher water absorption capacity than neat PVA film that was 78.41 and 72.59% respectively. Helberg et al. [48] in their study reported that the water absorption capacity of PVA/PVP blend film was comparatively higher than PVA film. The results indicate that the water absorption capacity was increased with increasing amount of CNC both for PVA and PVA/PVP films. The water absorption capacity of PVA/CNC films shows 73.65 to 83.77% with CNC content 3 to 12 %. On the other hand, the water absorption capacity of PVA/PVP/CNC films shows 79.71 to 92.09% with CNC content 3 to 12 %. PVA, PVP and CNC are hydrophilic in nature [9,48]. This is because of the formation of larger aggregates, this aggregates can create voids in the nanocomposite films [49]. The presence of these voids in the nanocomposite films increase the amount of water absorption [8].

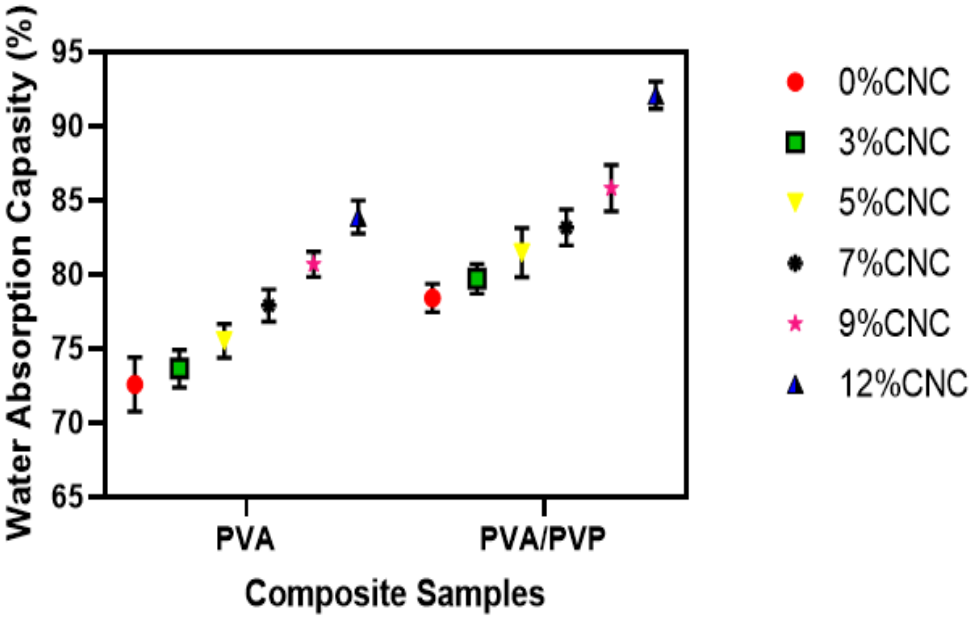

Figure 10.12: Water absorption capacity of the nanocomposite films at different wt. % of CNC

10.3.8 Density of the Films

The effect of various wt% of CNC on the density of the films is presented in figure 10.13. PVA and PVA/PVP films show comparatively higher densities than other films. The density values of the prepared nanocomposite films are almost the same. There is no significant change in densities with the addition of CNC.

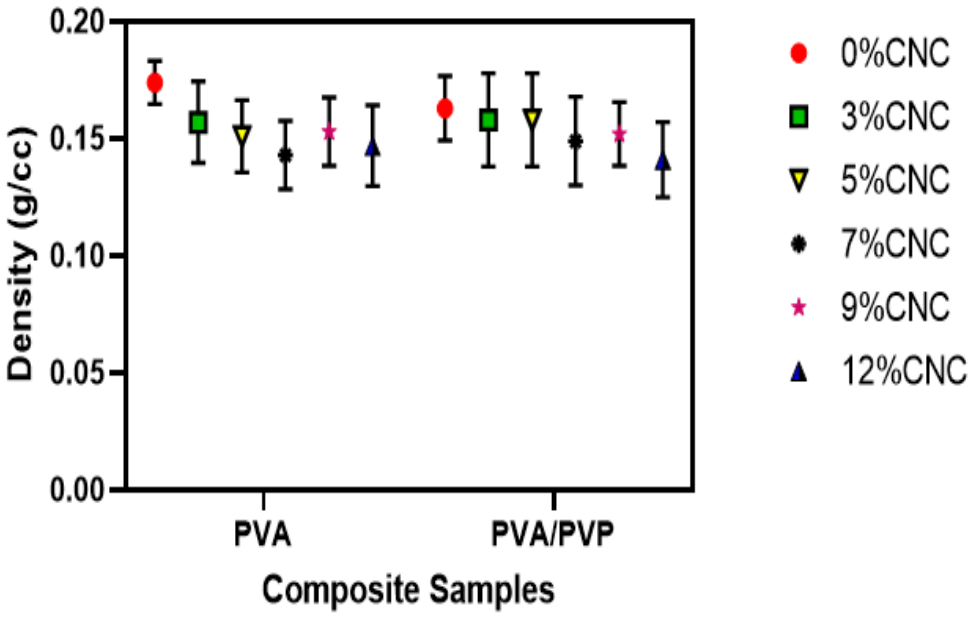

Figure 10.13: Variation of density on the CNC percentage in composite

10.4 Conclusions

The investigation was conducted to evaluate the chemical compositions of DPM fibers, isolate the CNC, and investigate the mechanical and water absorption characteristics of CNC/PVA and CNC/PVA/PVP nanocomposite films. DPM fibers can be used as source of cellulose for the preparation of CNCs and CNC reinforced PVA and PVA/PVP nanocomposite films. The average size of the CNC was 114.7 nm. The removal of hemicellulose and lignin from DPM fibers was confirmed by FTIR spectra. CNC reinforced PVA and PVA/PVP nanocomposite films were prepared by solution casting method. CNC reinforced nanocomposite films showed the best tensile strength. The addition of 9% CNCs enhanced the mechanical

properties of nanocomposites significantly. The development of acid hydrolyzed crystalline rods shaped nanocellulose was confirmed by SEM micrographs of CNC. SEM micrographs revealed a homogeneous distribution of lower CNC concentrations inside the nanocomposite films. However, the nanocomposite films with a higher concentration of CNC aggregated together to form a cluster. According to the findings date palm CNC (9%) reinforced PVA/PVP films can be considered for potential food packaging, medicinal, and biological applications.

10.5 References

1. Shen, R.; Xue, S.; Xu, Y.; Liu, Q.; Feng, Z.; Ren, H.; Zhai, H. Research Progress and Development Demand Of. *Polymers (Basel).* **2020**, 1–19.

2. Doineau, E.; Cathala, B.; Benezet, J. C.; Bras, J.; Moigne, N. Le. Development of Bio-Inspired Hierarchical Fibres to Tailor the Fibre/Matrix Interphase in (Bio)Composites. *Polymers (Basel).* **2021**, *13* (5), 1–34. https://doi.org/10.3390/polym13050804.

3. Phanthong, P.; Reubroycharoen, P.; Hao, X.; Xu, G.; Abudula, A.; Guan, G. Nanocellulose: Extraction and Application. *Carbon Resour. Convers.* **2018**, *1* (1), 32–43. https://doi.org/10.1016/j.crcon.2018.05.004.

4. Barbash, V. A.; Yashchenko, O. V.; Vasylieva, O. A. Preparation and Properties of Nanocellulose from Miscanthus x Giganteus. *J. Nanomater.* **2019**, *2019*. https://doi.org/10.1155/2019/3241968.

5. Sharma, S. K.; Sharma, P. R.; Lin, S.; Chen, H.; Johnson, K.; Wang, R.; Borges, W.; Zhan, C.; Hsiao, B. S. Reinforcement of Natural Rubber Latex Using Jute Carboxycellulose Nanofibers Extracted Using Nitro-Oxidation Method. *Nanomaterials* **2020**, *10* (4). https://doi.org/10.3390/nano10040706.

6. Tommalieh, M. J.; Awwad, N. S.; Ibrahium, H. A.; Menazea, A. A. Characterization and Electrical Enhancement of PVP/PVA Matrix Doped by Gold Nanoparticles Prepared by Laser Ablation. *Radiat. Phys. Chem.* **2021**, *179*, 109195.

https://doi.org/10.1016/j.radphyschem.2020.109195.

7. Ji, X.; Guo, J.; Guan, F.; Liu, Y.; Yang, Q.; Zhang, X.; Xu, Y. Preparation of Electrospun Polyvinyl Alcohol/Nanocellulose Composite Film and Evaluation of Its Biomedical Performance. *Gels* **2021**, *7* (4). https://doi.org/10.3390/gels7040223.

8. Ejara, T. M.; Balakrishnan, S.; Kim, J. C. Nanocomposites of PVA /Cellulose Nanocrystals: Comparative and Stretch Drawn Properties . *SPE Polym.* **2021**, *2* (4), 288–296. https://doi.org/10.1002/pls2.10057.

9. Chougale Ravindra, Sarswati, M., Sukanya, G., Shivalila, P., Soumya, Y. Tensile and Thermal Properties of Poly (Vinyl Pyrrolidone)/ Vanillin Incorporated Poly (Vinyl Alcohol) Films. *Res. J. Phys. Sci.* **2015**, *3* (8), 1–6.

10. Huang, M.; Hou, Y.; Li, Y.; Wang, D.; Zhang, L. High Performances of Dual Network PVA Hydrogel Modified by PVP Using Borax as the Structure-Forming Accelerator. *Des. Monomers Polym.* **2017**, *20* (1), 505–513. https://doi.org/10.1080/15685551.2017.1382433.

11. Mudigoudra, B. S.; Masti, S. P.; Chougale, R. B. Thermal Behavior of Poly (Vinyl Alcohol)/ Poly (Vinyl Pyrrolidone)/ Chitosan Ternary Polymer Blend Films. **2012**, *1* (9), 83–86.

12. Betti, N. A. Thermogravimetric Analysis on PVA / PVP Blend Under Air Atmosphere. *Eng. &Tech.Journal* **2016**, *34* (13), 2433–2441.

13. Khatun M, A.; S, S.; Nur H, P.; Chowdhury AM, S. Physical, Mechanical, Thermal and Morphological Analysis of Date Palm Mat (DPM) and Palmyra Palm Fruit (PPF) Fiber Reinforced High Density Polyethylene Hybrid Composites. *Adv. Mater. Sci.* **2019**, *4* (2), 1–6. https://doi.org/10.15761/ams.1000153.

14. Handoko, F.; Yusuf, Y. Synthesis and Physicochemical Properties of Poly(Vinyl) Alcohol Nanocomposites Reinforced with Nanocrystalline Cellulose from Tea (Camellia Sinensis) Waste. *Materials (Basel).* **2021**, *14* (23). https://doi.org/10.3390/ma14237154.

15. Oyeoka, H. C.; Ewulonu, C. M.; Nwuzor, I. C.; Obele, C. M.; Nwabanne, J. T.

Packaging and Degradability Properties of Polyvinyl Alcohol/Gelatin Nanocomposite Films Filled Water Hyacinth Cellulose Nanocrystals. *J. Bioresour. Bioprod.* **2021**, *6* (2), 168–185. https://doi.org/10.1016/j.jobab.2021.02.009.

16. Voronova, M.; Rubleva, N.; Kochkina, N.; Afineevskii, A.; Zakharov, A.; Surov, O. Preparation and Characterization of Polyvinylpyrrolidone/Cellulose Nanocrystals Composites. *Nanomaterials* **2018**, *8* (12). https://doi.org/10.3390/nano8121011.

17. Poonguzhali, R.; Basha, S. K.; Kumari, V. S. Synthesis and Characterization of Chitosan-PVP-Nanocellulose Composites for in-Vitro Wound Dressing Application. *Int. J. Biol. Macromol.* **2017**, *105*, 111–120. https://doi.org/10.1016/j.ijbiomac.2017.07.006.

18. Popescu, M. C.; Dogaru, B. I.; Goanta, M.; Timpu, D. Structural and Morphological Evaluation of CNC Reinforced PVA/Starch Biodegradable Films. *Int. J. Biol. Macromol.* **2018**, *116*, 385–393. https://doi.org/10.1016/j.ijbiomac.2018.05.036.

19. Pavalaydon, K.; Ramasawmy, H.; Surroop, D. Comparative Evaluation of Cellulose Nanocrystals from Bagasse and Coir Agro-Wastes for Reinforcing PVA-Based Composites. *Environ. Dev. Sustain.* **2022**, *24* (8), 9963–9984. https://doi.org/10.1007/s10668-021-01852-9.

20. Shaikh, H. M.; Anis, A.; Poulose, A. M.; Madhar, N. A.; Al-Zahrani, S. M. Date-Palm-Derived Cellulose Nanocrystals as Reinforcing Agents for Poly(Vinyl Alcohol)/Guar-Gum-Based Phase-Separated Composite Films. *Nanomaterials* **2022**, *12* (7). https://doi.org/10.3390/nano12071104.

21. Poddar, P.; Asadulah Asad, M.; Saiful Islam, M.; Sultana, S.; Parvin Nur, H.; Chowdhury, A. M. S. Mechanical and Morphological Study of Arecanut Leaf Sheath (ALS), Coconut Leaf Sheath (CLS) and Coconut Stem Fiber (CSF). *Adv. Mater. Sci.* **2016**, *1* (2), 1–4. https://doi.org/10.15761/ams.1000113.

22. Yu, X.; Jiang, Y.; Wu, Q.; Wei, Z.; Lin, X.; Chen, Y. Preparation and Characterization of Cellulose Nanocrystal Extraction From Pennisetum Hydridum Fertilized by Municipal Sewage Sludge via Sulfuric Acid Hydrolysis. *Front. Energy Res.* **2021**, *9* (November), 1–10. https://doi.org/10.3389/fenrg.2021.774783.

23. Hiremani, V. D.; Sataraddi, S.; Bayannavar, P. K.; Gasti, T.; Masti, S. P.; Kamble, R. R.; Chougale, R. B. Mechanical, Optical and Antioxidant Properties of 7-Hydroxy-4-Methyl Coumarin Doped Polyvinyl Alcohol/Oxidized Maize Starch Blend Films. *SN Appl. Sci.* **2020**, *2* (11), 1–18. https://doi.org/10.1007/s42452-020-03399-2.

24. Ekundayo, G. Reviewing the Development of Natural Fiber Polymer Composite: A Case Study of Sisal and Jute. *Am. J. Mech. Mater. Eng.* **2019**, *3* (1), 1. https://doi.org/10.11648/j.ajmme.20190301.11.

25. Pandey, S. N.; Ghosh, S. K. The Chemical Nature of Date-Palm (Phoenix Dactylifera-l) Leaf Fibre. *J. Text. Inst.* **1995**, *86* (3), 487–489. https://doi.org/10.1080/00405009508658775.

26. Raza, M.; Abu-Jdayil, B.; Banat, F.; Al-Marzouqi, A. H. Isolation and Characterization of Cellulose Nanocrystals from Date Palm Waste. *ACS Omega* **2022**, *7* (29), 25366–25379. https://doi.org/10.1021/acsomega.2c02333.

27. Rezende, C. A.; De Lima, M.; Maziero, P.; Deazevedo, E.; Garcia, W.; Polikarpov, I. Chemical and Morphological Characterization of Sugarcane Bagasse Submitted to a Delignification Process for Enhanced Enzymatic Digestibility. *Biotechnol. Biofuels* **2011**, *4* (November). https://doi.org/10.1186/1754-6834-4-54.

28. Brito, B. S. L.; Pereira, F. V.; Putaux, J. L.; Jean, B. Preparation, Morphology and Structure of Cellulose Nanocrystals from Bamboo Fibers. *Cellulose* **2012**, *19* (5), 1527–1536. https://doi.org/10.1007/s10570-012-9738-9.

29. Xiong, R.; Zhang, X.; Tian, D.; Zhou, Z.; Lu, C. Comparing Microcrystalline with Spherical Nanocrystalline Cellulose from Waste Cotton Fabrics. *Cellulose* **2012**, *19* (4), 1189–1198. https://doi.org/10.1007/s10570-012-9730-4.

30. Hafemann, E.; Battisti, R.; Marangoni, C.; Machado, R. A. F. Valorization of Royal Palm Tree Agroindustrial Waste by Isolating Cellulose Nanocrystals. *Carbohydr. Polym.* **2019**, *218*, 188–198. https://doi.org/10.1016/j.carbpol.2019.04.086.

31. Hemmati, F.; Jafari, S. M.; Taheri, R. A. *Optimization of Homogenization-Sonication Technique for the Production of Cellulose Nanocrystals from Cotton Linter*; Elsevier B.V, 2019; Vol. 137. https://doi.org/10.1016/j.ijbiomac.2019.06.241.

32. Mohaiyiddin, M. S.; Lin, O. H.; Owi, W. T.; Chan, C. H.; Chia, C. H.; Zakaria, S.; Villagracia, A. R.; Akil, H. M. Characterization of Nanocellulose Recovery from Elaeis Guineensis Frond for Sustainable Development. *Clean Technol. Environ. Policy* **2016**, *18* (8), 2503–2512. https://doi.org/10.1007/s10098-016-1191-2.

33. Reddy, K. O.; Maheswari, C. U.; Dhlamini, M. S.; Kommula, V. P. Exploration on the Characteristics of Cellulose Microfibers from Palmyra Palm Fruits. *Int. J. Polym. Anal. Charact.* **2016**, *21* (4), 286–295. https://doi.org/10.1080/1023666X.2016.1147799.

34. Ahmed, A. S.; Islam, M. S.; Hassan, A.; Mohamad Haafiz, M. K.; Islam, K. N.; Arjmandi, R. Impact of Succinic Anhydride on the Properties of Jute Fiber/Polypropylene Biocomposites. *Fibers Polym.* **2014**, *15* (2), 307–314. https://doi.org/10.1007/s12221-014-0307-8.

35. Duan, L.; Yu, W.; Li, Z. Analysis of Structural Changes in Jute Fibers after Peracetic Acid Treatment. *J. Eng. Fiber. Fabr.* **2017**, *12* (1), 33–42. https://doi.org/10.1177/155892501701200104.

36. Shahinur, S.; Hasan, M.; Ahsan, Q.; Sultana, N.; Ahmed, Z.; Haider, J. Effect of Rot-, Fire-, and Water-Retardant Treatments on Jute Fiber and Their Associated Thermoplastic Composites: A Study by Ftir. *Polymers (Basel).* **2021**, *13* (15). https://doi.org/10.3390/polym13152571.

37. Fonseca, C. S.; Scatolino, M. V.; Silva, L. E.; Martins, M. A.; Guimarães Júnior, M.; Tonoli, G. H. D. Valorization of Jute Biomass: Performance of Fiber–Cement Composites Extruded with Hybrid Reinforcement (Fibers and Nanofibrils). *Waste and Biomass Valorization* **2021**, *12* (10), 5743–5761. https://doi.org/10.1007/s12649-021-01394-1.

38. Liew, F. K.; Hamdan, S.; Rahman, M. R.; Rusop, M. Thermomechanical Properties of Jute/Bamboo Cellulose Composite and Its Hybrid Composites: The Effects of Treatment and Fiber Loading. *Adv. Mater. Sci. Eng.* **2017**, *2017*. https://doi.org/10.1155/2017/8630749.

39. Portella, E. H.; Romanzini, D.; Angrizani, C. C.; Amico, S. C.; Zattera, A. J. Influence of Stacking Sequence on the Mechanical and Dynamic Mechanical Properties of

Cotton/Glass Fiber Reinforced Polyester Composites. *Mater. Res.* **2016**, *19* (3), 542–547. https://doi.org/10.1590/1980-5373-MR-2016-0058.

40. Kharazmi, A.; Faraji, N.; Hussin, R. M.; Saion, E.; Yunus, W. M. M.; Behzad, K. Structural, Optical, Opto-Thermal and Thermal Properties of ZnS-PVA Nanofluids Synthesized through a Radiolytic Approach. *Beilstein J. Nanotechnol.* **2015**, *6* (1), 529–536. https://doi.org/10.3762/bjnano.6.55.

41. Soud, S. A.; Hasoon, B. A.; Abdulwahab, A. I.; Hussein, N. N. Synthesis and Characterization of Plant Extracts Loaded PVA / PVP Blend Films and Evaluate Their Biological Activities Synthesis and Characterization of Plant Extracts Loaded PVA / PVP Blend Films and Evaluate Their Biological Activities. **2020**, No. February 2021.

42. Shi, J.; Q.Shi, S.; H., M. B.; U.Pittman, J. A Chemical Process for Preparing Cellulosic

44. Zhou, L.; He, H.; Jiang, C.; Ma, L. I.; Yu, P. Cellulose Nanocrystals From Cotton Stalk for Reinforcement of Poly(Vinyl Alcohol) Composites. *Cellul. Chem. Technol. Cellul. Chem. Technol* **2017**, *51* (2), 109–119.

45. Asad, M.; Saba, N.; Asiri, A. M.; Jawaid, M.; Indarti, E.; Wanrosli, W. D. Preparation and Characterization of Nanocomposite Films from Oil Palm Pulp Nanocellulose/Poly (Vinyl Alcohol) by Casting Method. *Carbohydr. Polym.* **2018**, *191*, 103–111. https://doi.org/10.1016/j.carbpol.2018.03.015.

46. Huq, T.; Salmieri, S.; Khan, A.; Khan, R. A.; Le Tien, C.; Riedl, B.; Fraschini, C.; Bouchard, J.; Uribe-Calderon, J.; Kamal, M. R.; Lacroix, M. Nanocrystalline Cellulose (NCC) Reinforced Alginate Based Biodegradable Nanocomposite Film. *Carbohydr. Polym.* **2012**, *90* (4), 1757–1763. https://doi.org/10.1016/j.carbpol.2012.07.065.

47. Ching, Y. C.; Rahman, A.; Ching, K. Y.; Sukiman, N. L.; Chuah, C. H. Preparation and Characterization of Polyvinyl Alcohol-Based Composite Reinforced with Nanocellulose and Nanosilica. *BioResources* **2015**, *10* (2), 3364–3377. https://doi.org/10.15376/biores.10.2.3364-3377.

48. Lilleby Helberg, R. M.; Dai, Z.; Ansaloni, L.; Deng, L. PVA/PVP Blend Polymer Matrix for Hosting Carriers in Facilitated Transport Membranes: Synergistic Enhancement of CO2 Separation Performance. *Green Energy Environ.* **2020**, *5* (1), 59–

68. https://doi.org/10.1016/j.gee.2019.10.001.

49. Lani, N. S.; Ngadi, N.; Johari, A.; Jusoh, M. Isolation, Characterization, and Application of Nanocellulose from Oil Palm Empty Fruit Bunch Fiber as Nanocomposites. *J. Nanomater.* **2014**, *2014*. https://doi.org/10.1155/2014/702538.

CHAPTER 11

Conclusions

11.1 Conclusions

In this experimental study, date palm mat fiber reinforced thermoplastic based composites were developed by compression moulding technique. The effect of fiber content, alkaline treatment, nano filler, gamma radiation, fire retardants and crystalline nanocellulose on the physical, mechanical, thermal, morphological and biodegradation properties of the composites were stated. The following inferences are drawn on the basis of experimental findings:

- 10% DPM fiber reinforced HDPE and PS composites gave a better result than composites with 5, 15, 20 and 25% fiber content. It was therefore regarded as the optimum fiber loading.
- Alkaline treatment of the DPM fibers were carried out to improve the fiber-matrix adhesion and 5% NaOH treated DPM fiber reinforced composites showed better result than untreated composites.
- In order to enhance the mechanical properties of the composites, ZnO nanoparticles were incorporated and the composites with 3% ZnO nanoparticles presented the best results.
- Different doses of gamma radiation were used to irradiate the composite samples. The best outcome was exhibited by the composite at radiation dose 5 KGy.
- The effect of monosodium phosphate, monoammonium phosphate and magnesium hydroxide as fire retardants in the composites were investigated and the findings revealed that monoammonium phosphate showed remarkable fire retardant properties compared to others.
- For hybrid composites, the 5% fiber content composites displayed the best results. So we can conclude that better characteristics can be obtained by hybrid composite with less fiber content.
- Crystalline nanocellulose were extracted from DPM fibers and used to create nanocomposite films. The mechanical characteristics of nanocomposites were markedly improved by the inclusion of 9% CNCs. The results indicate that 9% CNC reinforced nanocomposite films may have uses in food packaging, pharmaceuticals, and biological applications.

Date Palm mat and Palmyra Palm fruit fibers are agricultural wastes. The composites and nano-composites with these fibers will therefore be economical, eco-friendly and competitive materials. The prepared composites would not only enable the exploration of new applications but also has a significant positive impact on sustainable development

LIST OF PUBLICATIONS

LIST OF PUBLICATIONS

1. **Afroza Khatun M**, Sultana S, Parvin Nur H and Sarwaruddin Chowdhury AM, **"**Physical, mechanical, thermal and morphological analysis of date palm mat (DPM) and palmyra palm fruit (PPF) fiber reinforced high density polyethylene hybrid composites", *Adv Mater Sci,* 2019 doi: 10.15761/AMS.1000153 Volume 4: 1-6

2. **Most Afroza Khatun,** Shahin Sultana, Zahidul Islam, Mohammad Shahriar Kabir, Md Sahadat Hossain, Husna Parvin Nur, A.M. Sarwaruddin Chowdhury, Extraction of crystalline nanocellulose (CNC) from date palm mat fibers and its application in the production of nanocomposites with polyvinyl alcohol and polyvinylpyrrolidone blended films, *Results in Engineering*, Volume 17, 2023, 101031, ISSN 2590-1230, https://doi.org/10.1016/j.rineng.2023.101031.

3. Most. Afroza Khatun, Shahin Sultana, Husna Parvin Nur and A. M Sarwaruddin Chowdhury, Investigation of Physico-mechanical and Thermal properties of Short Date Palm Mat (DPM) Fiber Reinforced Polystyrene Composites (Submitted)

4. Most. Afroza Khatuna, Shahin Sultana, Husna Parvin Nur and A. M Sarwaruddin Chowdhury, Investigation of Mechanical and Fire Performance of HDPE and PS based Composites with Fire Retardants (Submitted)

Conference papers

1. **Most. Afroza Khatun**, Shahin Sultana, Zahidul Islam, Md. Shahriar Kabir, Md. Shahadat Hossain, Husna Parvin Nur and A. M. Sarwaruddin Chowdhury, "Preparation and Characteriztion of Crystalline Nanocellulose (CNC) from Date Palm Mat Fibers and Their Nanocomposites with Polyvinyl Alcohol and Polyvinylpyrrolidone" International Conclave on Materials, Energy & Climate, 19-20 December,